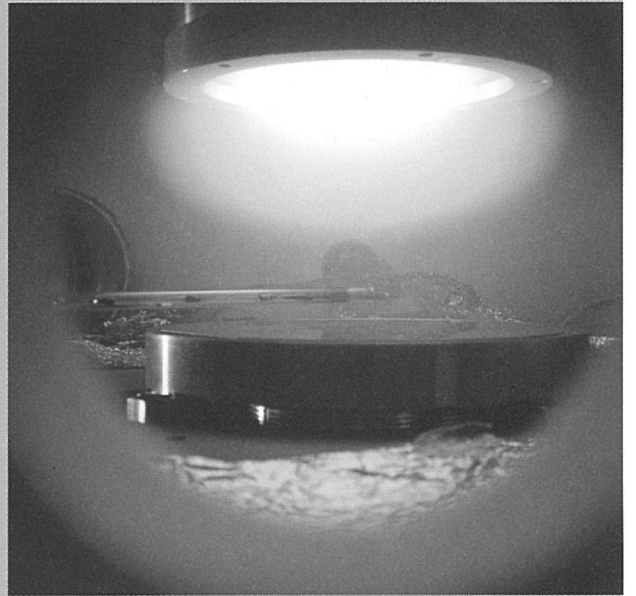
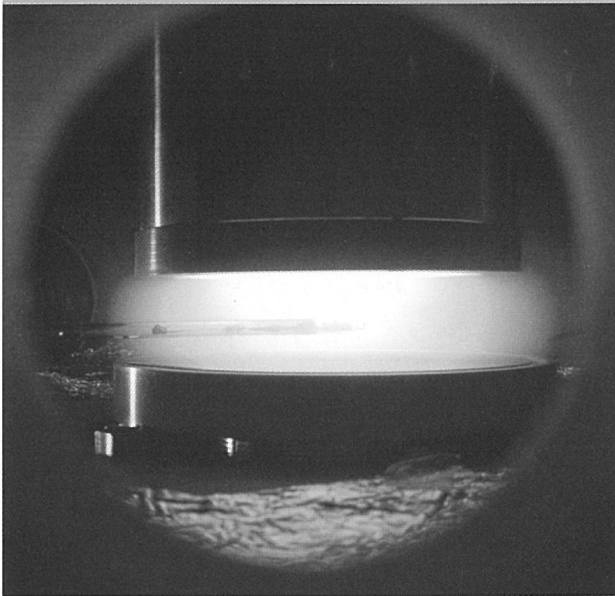


BULLETIN

OF THE AMERICAN PHYSICAL SOCIETY

61st Annual Gaseous Electronics Conference

October 13-17, 2008 • Dallas, Texas USA



THE UNIVERSITY OF TEXAS AT DALLAS

October 2008

Volume 53, No. 10

APS
physics

BULLETIN

OF THE AMERICAN PHYSICAL SOCIETY

Coden BAPSA6

Series II, Vol. 53, No. 10

Copyright 2008 by the American Physical Society

ISSN: 0003-0503

October 2008

APS COUNCIL 2008

President

Arthur Bienenstock,* *Stanford University*

President-Elect

Cherry A. Murray,* *Lawrence Livermore National Laboratory*

Vice President

Curtis G. Gallan, Jr.,* *Princeton University*

Executive Officer

Judy R. Franz,* *University of Alabama, Huntsville (on leave)*

Treasurer

Joseph W. Serene,* *Georgetown University (Emeritus)*

Editor-in-Chief

Gene D. Sprouse,* *State University of New York, Stony Brook (on leave)*

Past-President

Leo P. Kadanoff,* *University of Chicago*

General Councillors

Robert Austin, Christina Back,* Elizabeth Beise, Wendell Hill,* Katherine Freese, Ann Orel,* Marcela Carena, Richart Slusher*

Division, Forum and Section Councillors

Charles Dermer (*Astrophysics*), P. Julienne (*Atomic, Molecular & Optical Physics*), Robert Eisenberg (*Biological*), Charles S. Parmenter (*Chemical*), Arthur Epstein (*Condensed Matter Physics*), James Brassuer (*Fluid Dynamics*), Peter Zimmerman* (*Forum on Education*), Amber Stuver (*Forum on Graduate Student Affairs*), Roger Stuewer (*Forum on History of Physics*), Stefan Zollner (*Forum on Industrial and Applied Physics*), David Ernst* (*Forum on International Physics*), Philip "Bo" Hammer (*Forum on Physics and Society*), Steven Rolston (*Laser Science*), Leonard Feldman* (*Materials*), Akif Balantekin* (*Nuclear*), Janet Conrad (*Particles & Fields*), Ronald Ruth (*Physics of Beams*), David Hammer (*Plasma*), Scott Milner (*Polymer Physics*), Paul Wolf (*Ohio Section*), Heather Galloway (*Texas Section*)

**Members of the APS Executive Board*

Meetings Abstracts Coordinator:

Vinaya K. Sathyasheelappa

APS MEETINGS DEPARTMENT

One Physics Ellipse

College Park, MD 20740-3844

Telephone: (301) 209-3286

Fax: (301) 209-0866

Email: meetings@aps.org

Donna Baudrau, *Director of Meetings & Conventions*

Terri Gaier, *Assistant Director of Meetings & Conventions*

Don Wise, *Registrar*

Christine Parvez, *Meetings Program Coordinator*

International Councillor

Sabayasachi Bhattacharya

Chair, Nominating Committee

Philip Phillips

Chair, Panel on Public Affairs

Miles Klein

ADVISORS

Representatives from other Societies

Fred Dylla, *AIP*; Lila Adair, *AAPT*

International Advisors

Francisco Ramos Gómez, *Mexican Physical Society*;

Shelly Page, *Canadian Association of Physicists*

Staff Representatives

Alan Chodos, *Associate Executive Officer*; Amy Flatten, *Director of International Affairs*; Ted Hodapp, *Director of Education and Diversity*; Michael Lubell, *Director, Public Affairs*; Daniel Kulp, *Editorial Director*; Christine Giaccone, *Director, Journal Operations*; Michael Stephens, *Controller and Assistant Treasurer*

Administrator for Governing Committees

Ken Cole

Please Note: APS has made every effort to provide accurate and complete information in this *Bulletin*. However, changes or corrections may occasionally be necessary and may be made without notice after the date of publication. To ensure that you receive the most up-to-date information, please check the meeting Corrigenda distributed with this *Bulletin*.

BULLETIN

OF THE AMERICAN PHYSICAL SOCIETY

Coden BAPSA6 ISSN: 0003-0503
Series II, Vol. 53, No. 10 October 2008
Copyright 2008 by the American Physical Society

APS COUNCIL 2008

President

Arthur Bienenstock,* *Stanford University*

President-Elect

Cherry A. Murray,* *Lawrence Livermore National Laboratory*

Vice President

Curtis G. Gallan, Jr.,* *Princeton University*

Executive Officer

Judy R. Franz,* *University of Alabama, Huntsville (on leave)*

Treasurer

Joseph W. Serene,* *Georgetown University (Emeritus)*

Editor-in-Chief

Gene D. Sprouse,* *State University of New York, Stony Brook (on leave)*

Past-President

Leo P. Kadanoff,* *University of Chicago*

General Councillors

Robert Austin, Christina Back,* Elizabeth Beise, Wendell Hill,* Katherine Freese, Ann Orel,* Marcela Carena, Richart Slusher*

Division, Forum and Section Councillors

Charles Dermer (*Astrophysics*), P. Julienne (*Atomic, Molecular & Optical Physics*), Robert Eisenberg (*Biological*), Charles S. Parmenter (*Chemical*), Arthur Epstein (*Condensed Matter Physics*), James Brassuer (*Fluid Dynamics*), Peter Zimmerman* (*Forum on Education*), Amber Stuver (*Forum on Graduate Student Affairs*), Roger Stuewer (*Forum on History of Physics*), Stefan Zollner (*Forum on Industrial and Applied Physics*), David Ernst* (*Forum on International Physics*), Philip "Bo" Hammer (*Forum on Physics and Society*), Steven Rolston (*Laser Science*), Leonard Feldman* (*Materials*), Akif Balantekin* (*Nuclear*), Janet Conrad (*Particles & Fields*), Ronald Ruth (*Physics of Beams*), David Hammer (*Plasma*), Scott Milner (*Polymer Physics*), Paul Wolf (*Ohio Section*), Heather Galloway (*Texas Section*)

**Members of the APS Executive Board*

Meetings Abstracts Coordinator:

Vinaya K. Sathyasheelappa

APS MEETINGS DEPARTMENT

One Physics Ellipse

College Park, MD 20740-3844

Telephone: (301) 209-3286

Fax: (301) 209-0866

Email: meetings@aps.org

Donna Baudrau, *Director of Meetings & Conventions*

Terri Gaier, *Assistant Director of Meetings & Conventions*

Don Wise, *Registrar*

Christine Parvez, *Meetings Program Coordinator*

International Councilor

Sabayasachi Bhattacharya

Chair, Nominating Committee

Philip Phillips

Chair, Panel on Public Affairs

Miles Klein

ADVISORS

Representatives from other Societies

Fred Dylla, *AIP*; Lila Adair, *AAPT*

International Advisors

Francisco Ramos Gómez, *Mexican Physical Society*;

Shelly Page, *Canadian Association of Physicists*

Staff Representatives

Alan Chodos, *Associate Executive Officer*; Amy Flatten, *Director of International Affairs*; Ted Hodapp, *Director of Education and Diversity*; Michael Lubell, *Director, Public Affairs*; Daniel Kulp, *Editorial Director*; Christine Giaccone, *Director, Journal Operations*; Michael Stephens, *Controller and Assistant Treasurer*

Administrator for Governing Committees

Ken Cole

Please Note: APS has made every effort to provide accurate and complete information in this *Bulletin*. However, changes or corrections may occasionally be necessary and may be made without notice after the date of publication. To ensure that you receive the most up-to-date information, please check the meeting Corrigenda distributed with this *Bulletin*.

BULLETIN

OF THE AMERICAN PHYSICAL SOCIETY

Vol. 53, No. 10, October 2008

GEC Meeting 2008

TABLE OF CONTENTS

General Information.....	3
Special Sessions and Events.....	3
<i>Sessions</i>	3
Presentation Formats.....	4
GEC Student Award for Excellence.....	4
Registration.....	4
Banquet and Reception.....	4
E-mail and Other Business Services.....	4
Audio-Visual Equipment.....	4
Dining Options.....	4
Dallas Sights.....	5
Call for Nominations for GEC General and Executive Committees.....	5
<i>GEC Executive Committee</i>	6
<i>Conference Secretary</i>	6
Please Note.....	6
Sponsors and Exhibitors.....	6
Epitome.....	7
Main Text.....	10

<i>Tuesday, October 14</i>	10
<i>Wednesday, October 15</i>	43
<i>Thursday, October 16</i>	70
<i>Friday October 17</i>	85
Author Index	97
Floor Plans	At End of Issue

61st Annual Gaseous Electronics Conference

October 13-17, 2008

Dallas, Texas

GENERAL INFORMATION

Welcome to Dallas! The 61st Gaseous Electronics Conference (GEC) of the American Physical Society is being held in the Dallas/Addison Marriott Quorum by the Galleria. The GEC 2008 will highlight all of the current research in gaseous electronics. The program includes the W. Allis Plenary Lecture, Student Award for Excellence Talks, 33 invited presentations and more than 350 contributed papers presented in oral and poster sessions. The Allis Prize Plenary Lecture is awarded in even-numbered years in honor of the outstanding contributions of Will Allis to the study of ionized gases.

SPECIAL SESSIONS AND EVENTS

The GEC Executive Committee is pleased to announce that the Allis Prize Lecture will be presented by Kenneth Kulander of Lawrence Livermore National Laboratory. His talk, "The Ionization Dynamics of Atoms by Strong, Ultra-Short Laser Pulses" will be at 10:00 AM on Wednesday, October 15 in Salons A-E of the Quorum Ballroom.

The GEC will feature three parallel sessions in the mornings for the very first time this year. This was done in order to accommodate the large number of submissions and enable the conference to grow in both size and quality.

SESSIONS

Session AS	Opening Reception	Session DT2	Biological and Emerging Applications of Plasma
Session BT1	Collision Data For and From Plasma Applications	Session ET1	Dielectric Barrier Discharges and Displays
Session BT2	Plasma Aerodynamics and Propulsion I	Session ET2	Negative Ion Plasmas
Session BT3	Dusty Plasmas	Session FTP1	Poster Session I
Session CT1	Microhollow Cathode Discharges	Session GW1	Plasma Aerodynamics and Propulsion II
Session CT2	Electron/Photon Interactions with Molecules	Session GW2	Charged Particle Surface Interactions
Session CT3	Magnetically-Enhanced and Related Plasmas	Session GW3	Lasers, Breakdowns and Sparks
Session DT1	Plasma-Surface Interactions	Session HW	Allis Prize Lecture
		Session LW1	Plasma Diagnostics I
		Session LW2	Electron/Positron Atom Collisions
		Session MWP1	Poster Session II
		Session PR1	Fluorocarbon Plasmas I
		Session PR2	Ion Atom Collisions I
		Session PR3	High Pressure Discharges and Liquids
		Session QR1	Fluorocarbon Plasmas II
		Session QR2	Electron Impact Ionization of Atoms and Molecules
		Session QR3	High Pressure Glow Discharges
		Session RR1	Material Processing I
		Session RR2	Lighting Plasmas
		Session SR1	Inductively and Capacitively Coupled Plasmas
		Session SR2	Ion Atom/Molecule Collisions II
		Session TR	Banquet
		Session VF1	Glow
		Session VF2	Electron and Ion Transport in Gases
		Session VF3	Plasma Boundaries
		Session WF1	Plasma Diagnostics II
		Session WF2	Recombination and Attachment
		Session WF3	Computational Methods for Plasmas
		Session XF1	Material Processing II
		Session XF2	Capacitively-Coupled Plasmas

PRESENTATION FORMATS

Papers that have been accepted for presentation are listed in the technical program. Invited papers are allotted 25 minutes, with 5 additional minutes for questions and discussion. Oral contributed presentations are allotted 12 minutes, with 3 additional minutes for questions. Poster sessions will be provided with 48" by 96" poster boards. Presenters may mount their posters anytime in the day upon which their presentation is scheduled. Poster materials must be removed at the close of the poster session.

GEC STUDENT AWARD FOR EXCELLENCE

The GEC Executive Committee will award a \$1000 prize for the best paper presentation by a student. Students must have been nominated by their professor before being selected to present and compete for the award. Students competing for the award, in the order of their appearance in the program, are:

Sergey Belostotskiy, The University of Houston, "Laser diagnostics of high pressure microdischarge plasmas," Tuesday, October 14, 10:45 AM.

Jack Maseberg, The University of Nebraska, "Fluorescence polarization of H₂, D₂, and N₂ molecules excited by polarized electron impact," Tuesday, October 14, 11:00 AM.

Joao Santos Sousa, Universite Paris-Sud, "Atmospheric pressure generation of high fluxes of singlet oxygen for biological applications," Tuesday, October 14, 1:30 PM.

Sameer Kalghatgi, Drexel University, "Interaction of non-thermal dielectric barrier discharge plasma with DNA inside cells," Tuesday, October 14, 2:30 PM.

Kazuhiko Baba, Tohoku University, "Creation of stable plasma-liquid interfaced reactive field using Ionic liquids," Thursday, October 16, 8:45 AM.

Ola Al-Hagan, Missouri University of Science & Technology, "Atomic and molecular signatures for charged particle ionization," Thursday, October 16, 11:00 AM.

Eugene Tam, The University of Sydney, "Plasma controlled adatom delivery and (re)distribution: enabling uninterrupted low temperature growth of ultra long vertically aligned carbon nanotubes," Thursday, October 16, 2:00 PM.

REGISTRATION

The registration desk will be in the lobby of the Marriott Quorum Galleria hotel. Registration will be available from 5:00-7:15 PM on Monday afternoon and then beginning Tuesday at 7:30 AM and remaining available through most of the remainder of the conference. The on-site conference registration cost is \$450 for regular registration, \$225 for students and retirees and \$250 for a single day.

BANQUET AND RECEPTION

An opening reception will be held at 6:00 PM on Monday, October 13 poolside at the Marriott Quorum Galleria hotel. The conference banquet will be held at 7:00 PM on Thursday, October 16 in the Ballroom of the Marriott. Tickets for the banquet are \$65 and available onsite through Monday October 13th. All conference attendees and guests are encouraged to attend.

E-MAIL AND OTHER BUSINESS SERVICES

Internet access will be available in guest rooms for a fee and in the hotel business center. Services such as faxing and photocopying are also available in the hotel business center.

AUDIO-VISUAL EQUIPMENT

Each conference room will be equipped with an LCD projector and laptop. If additional equipment is required, please contact the conference secretary.

DINING OPTIONS

The Marriott Quorum sits at the edge of Addison, Texas, which has more than 170 restaurants within its 4.35 square mile border. As a result, a global variety of cuisines can easily be found within the range of the hotel's complimentary shuttle. Also, the hotel can arrange for local restaurants to deliver dinner from local restaurants to a hotel room. Additional information will be available on-site.

DALLAS SIGHTS

Dallas has something for everyone. Fans of art, food, music, rodeos, architecture, history, sports and shopping will find plenty to do in Dallas. Addison, where the hotel is located, is home to the Galleria Mall, the WaterTower Theater and The Cavanaugh Flight Museum. The hotel offers a complimentary shuttle for anything within three miles of the hotel, which includes a variety of hotels, shopping and other attractions. More information about Addison may be found at <http://www.addisontexas.net>.

Dallas is home to a variety of museums, including the Women's Museum, Hall of State, the African-American Museum, the Age of the Steam Railroad Museum, the Sixth Floor Museum, Meadows Museum of Art, the Dallas Zoo, and the Dallas Cowboys stadium.

Many museums can be found in Fair Park, which is 277-acres of land full of art deco buildings, museums, sporting facilities and amphitheatres. Two other locations worthy of note are the Dallas Arboretum and Botanical Gardens and the Old City Park. The Old City Park is a sentiment from the late 19th-century, finished with old western standards like a train depot, general store, church and schoolhouse and populated with people in character for the time.

Fair Park is also the home of the Texas State Fair, the largest such fair in the USA. This year the fair is from September 26 to October 19 and thus can be attended by GEC attendees. More information may be found at: <http://www.bigtex.com>

There are shopping options for every taste and budget, from the first Neiman Marcus store in downtown Dallas, to the vintage furniture stores, farmers markets and avant-garde boutiques of Deep Ellum.

The West End of Dallas is home to the infamous Book Depository where Lee Harvey Oswald shot President Kennedy in 1963. Today the Sixth Floor Museum examines the life, times, death and legacy of John F. Kennedy.

And naturally, fans of J.R. Ewing and his family can visit South Fork Ranch, which was featured in the show.

More information on Dallas may be found at <http://www.visitdallas.com>

CALL FOR NOMINATIONS FOR GEC GENERAL AND EXECUTIVE COMMITTEES

The GEC Executive Committee (ExComm) is the governing body of the GEC. It is the responsibility of the ExComm to oversee all aspects of the conference. This includes selection of meeting sites, budgetary decisions, selection of special topics and invited speakers, reviewing abstracts, and arranging the program. The General Committee and the ExComm meet during the GEC, and the ExComm meets again during the summer to plan the program of the next GEC. There are numerous communications between members of the ExComm (usually e-mail) during the year to ensure the successful completion of their duties. We have been fortunate over the years to have a dedicated group of volunteers who have been willing to take on these very necessary roles.

The by-laws of the Gaseous Electronics Conference describe the process whereby members of the ExComm are elected. At the GEC Business Meeting (to be held on Wednesday, October 15, at 11:00 in the Ballroom), nominations are accepted for members of the GEC General Committee (GenComm).

The GenComm consists of the ExComm and six at-large members elected at the Business Meeting. The eligible voting membership of the GEC (defined as those attending the Business Meeting) elects six at-large members. The GenComm then meets to elect new members of the ExComm.

The ExComm membership consists of the Chair, Treasurer, Past-Secretary, Secretary, Secretary-elect, past or incoming Chair, and four at-large members. The Chair is a 4-year term (1 year incoming, 2 years Chair, and 1 year past-Chair), the Secretary is a 3-year term (1 year incoming, 1 year Secretary, 1 year past-Secretary), and all other ExComm members serve 2 years. The Secretary is the person who manages the local arrangements for the meeting and is usually "recruited" and appointed to the ExComm.

The ExComm welcomes nominations, including self-nomination, for both the GenComm and the ExComm. Becoming a GenComm and/or ExComm member provides a unique opportunity to see both how the GEC is run and to influence its future direction by helping to define the programs and choosing future sites.

Please submit your nominations to the GEC Chair or any member of the ExComm. The ExComm also welcomes inquiries on hosting future GECs.

GEC 2008 EXECUTIVE COMMITTEE

Peter Ventzek, Chair, Lam Research

Bill Graham, Chair-Elect, Queen's University

Klaus Bartschat, Treasurer, Drake University

Lawrence Overzet, Secretary, The University of Texas at Dallas

Mirko Vukovic, Secretary-Elect, Tokyo Electron

Darrin Leonhardt, Past-Secretary, Fusion UV Systems

Pascal Chabert, Secretary Elect, GEC 2010 LPTP, Ecole Polytechnique

Masaru Hori, Secretary Elect, GEC 2010, Nagoya University

Matthew Goeckner, The University of Texas at Dallas

Rainer Johnsen, University of Pittsburgh

Don Madison, Missouri University of Science and Technology

Svetlana Radovanov, Varian Semiconductor

Michael Schulz, Missouri University of Science & Technology

CONFERENCE SECRETARY

Larry Overzet

The University of Texas at Dallas

800 West Campbell Road, RL10

Richardson, TX 75080

Phone: 972-883-2154

Fax: 972-883-6839

E-mail: overzet@utdallas.edu

PLEASE NOTE

The APS has made every effort to provide accurate and complete information in this *Bulletin*. However, changes or corrections may occasionally be necessary and may be made without notice after the date of publication. To ensure that you receive the most up-to-date information, please check the meeting Corrigenda distributed with this *Bulletin*.

GEC 2008 SPONSORS AND EXHIBITORS (TO PRINTING DATE)

Sponsors and Exhibitors allow the GEC Executive Committee to provide many benefits to attendees including travel assistance and decreased registration fees for junior attendees.

The GEC08 has been fortunate to receive support from the following organizations (up to the time of publication.)

The US Department of Energy

Sandia National Laboratories

Applied Materials

General Electric

IOP Publishing

Tech X Corporation

Tokyo Electron

The University of Texas at Dallas

The National Science Foundation

Hidden Analytical

The Air Force Office of Scientific Research

NorCal

Varian Semiconductor

Epitome of the 61st Gaseous Electronics Conference of the American Physical Society

**19:00 MONDAY EVENING
13 OCTOBER 2008**

AS **Opening Reception**
Poolside

**8:00 TUESDAY MORNING
14 OCTOBER 2008**

BT1 **Collision Data For and From
Plasma Applications**
Timo Gans, Stuart Loch
Salon E

BT2 **Plasma Aerodynamics and
Propulsion I**
Godfrey Mungal
Salon A-D

BT3 **Dusty Plasmas**
Addison Room

**10:00 TUESDAY MORNING
14 OCTOBER 2008**

CT1 **Microhollow Cathode Discharges**
Osamu Sakai
Salon E

CT2 **Electron/Photon Interactions with
Molecules**
*Thomas Rescigno,
Stephen Buckman*
Salon A-D

CT3 **Magnetically-Enhanced
and Related Plasmas**
Jon T. Gudmundsson
Addison Room

**13:30 TUESDAY AFTERNOON
14 OCTOBER 2008**

DT1 **Plasma-Surface Interactions**
Gilles Cartry
Salon E

DT2 **Biological and Emerging
Applications of Plasma**
Mounir Laroussi
Salon A-D

**16:00 TUESDAY AFTERNOON
14 OCTOBER 2008**

ET1 **Dielectric Barrier Discharges and
Displays**
Salon E

ET2 **Negative Ion Plasmas**
R.N. Franklin, Allan J. Lichtenberg
Salon A-D

**19:00 TUESDAY EVENING
14 OCTOBER 2008**

FTP1 **Poster Session I (19:00-21:30)**
Salon F-J

**8:00 WEDNESDAY MORNING
15 OCTOBER 2008**

GW1 **Plasma Aerodynamics
and Propulsion II**
Jean-Pierre Boeuf
Salon E

GW2 **Charged Particle Surface
Interactions**
Richard E. Palmer, Uwe Thumm
Salon A-D

GW3 **Lasers, Breakdowns and Sparks**
Addison Room

**10:00 WEDNESDAY MORNING
15 OCTOBER 2008**

HW **Allis Prize Lecture**
Kenneth Kulander
Salon A-E

11:00 WEDNESDAY MORNING
15 OCTOBER 2008

JW **Business Meeting**
Salon A-E

12:00 WEDNESDAY NOON
15 OCTOBER 2008

KW **General Committee Meeting**
Bent Tree I-II

13:30 WEDNESDAY AFTERNOON
15 OCTOBER 2008 13:30

LW1 **Plasma Diagnostics I**
Salon E

LW2 **Electron/Positron Atom
Collisions**
Oleg Zatsarinny
Salon A-D

16:00 WEDNESDAY AFTERNOON
15 OCTOBER 2008

MWP1 **Poster Session II (16:00-18:30)**
Salon F-J.

19:00 WEDNESDAY EVENING
15 OCTOBER 2008

NW **Executive Committee Meeting**
Bent Tree I-II

8:00 THURSDAY MORNING
16 OCTOBER 2008

PR1 **Fluorocarbon Plasmas I**
Kazuhiro Karahashi
Salon E

PR2 **Ion Atom Collisions I**
David Schultz, James Colgan
Salon A-D

PR3 **High Pressure Discharges and
Liquids**
Addison Room

10:00 THURSDAY MORNING
16 OCTOBER 2008

QR1 **Fluorocarbon Plasmas II**
*Tetsuya Tatsumi, Michael Gordon,
Todd Maddern, Joseph Vegh*
Salon E

QR2 **Electron Impact Ionization of
Atoms and Molecules**
N.L.S. Martin, Azzedine Bennani
Salon A-D

QR3 **High Pressure Glow Discharges**
Paul Maguire
Addison Room

13:30 THURSDAY AFTERNOON
16 OCTOBER 2008

RR1 **Material Processing I**
Salon E

RR2 **Lighting Plasmas**
J.E. Lawler
Salon A-D

16:00 THURSDAY AFTERNOON
16 OCTOBER 2008

SR1 **Inductively and Capacitively
Coupled Plasmas**
Salon E

SR2 **Ion Atom/Molecule Collisions II**
Daniel Fischer
Salon A-D

19:00 THURSDAY EVENING
16 OCTOBER 2008

TR **Banquet**
R. Heelis
Salon A-E

8:00 FRIDAY MORNING
17 OCTOBER 2008

VF1 **Gloves**
Caizhong Tian
Salon E

VF2 **Electron and Ion Transport
in Gases**
Salon A-D

VF3 **Plasma Boundaries**
Addison Room

**10:00 FRIDAY MORNING
17 OCTOBER 2008**

WF1 **Plasma Diagnostics II**
Salon E

WF2 **Recombination and Attachment**
Andreas Wolf
Salon A-D

WF3 **Computational Methods
for Plasmas**
Ikuo Sawada, Shahid Rauf
Addison Room

**13:30 FRIDAY AFTERNOON
17 OCTOBER 2008**

XF1 **Material Processing II**
Salon E

XF2 **Capacitively-Coupled Plasmas**
Thomas Mussenbrock
Salon A-D

SESSION BT1: COLLISION DATA FOR AND FROM PLASMA APPLICATIONS

Tuesday Morning, 14 October 2008; Salon E at 8:00

Natalia Babaeva, University of Michigan, presiding

*Invited Papers***8:00****BT1 1 The role of atomic and molecular collision processes in plasmas - and vice versa.***TIMO GANS, *Queens University Belfast*

A broad base of accurate data of atomic and molecular collision processes is essential for reliable modelling, simulation, and diagnostics of plasmas. This is particularly important for plasmas at elevated pressures close to atmosphere. This regime attracts rapidly growing attention due to both - promising innovative technological applications as well as new fundamental scientific phenomena. The collision dominated environment and decreasing dimensions down to microscale plasmas with extremely high surface to volume ratios significantly increase the demand for collisional deactivation and surface interaction processes. Cross sections for collisional deactivation can be determined from the effective lifetime of excited states. Direct excitation using short pulse laser systems are most reliable however limited by optical selection rules and available photon energies. Recently improved understanding of the dynamics of electron impact excitation in radio-frequency discharges allows alternative strategies using space and phase resolved optical emission spectroscopy measurements coupled with careful modelling of the population dynamics of excited states. This method based on electron impact excitation is not limited by optical selection rules and also provides access to high energetic electronic states which are not accessible with common laser systems. Data for surface interactions is inherently delicate since it strongly depends on surface properties such as coverage and temperature. Nevertheless, reliable data for recombination of radicals and metastable states, and coefficients for secondary electron emission are highly desirable for consistent modelling and simulation. An alternative approach is the active implementation of experimentally measured surface sensitive parameters such as atomic radical densities and excitation structures caused by secondary electrons. These experimentally accessible quantities can be used as fixed input parameters in improved self-consistent modelling.

*Supported by: DFG and EPSRC

8:30**BT1 2 Electron collision calculations for atomic systems and the use of this data in fusion and astrophysics modelling codes.***STUART LOCH, *Auburn University*

A brief overview will be given of the main theoretical and experimental methods used to calculate/measure electron impact ionization cross sections for use in fusion and astrophysics spectral modeling. Care must be taken when processing these cross sections into Maxwellian rate coefficients. Examples will be given showing the importance of the near threshold part of the cross section. Comparisons will be shown between data from current databases and illustrations given of how this data is commonly used in spectral modeling codes. Electron impact excitation and recombination data will also be discussed and future data needs will be highlighted.

*This work was supported by a grant from the Department of Energy and with support from the Oak Ridge National Laboratory.

*Contributed Papers***9:00****BT1 3 Time-Resolved Electron Density Measurements of Laser Produced Plasmas using X-Band Microwave Interferometry**

K. ELLEN KEISTER, JEFFREY L. PUTNEY, CLARK J. WAGNER, J. GARY EDEN, *Laboratory for Optical Physics and Engineering, University of Illinois at Urbana-Champaign* Laser produced plasma channels form a unique and significant laboratory tool for exploring the kinetics of plasma formation and decay. Using a sub-picosecond 100 GW ultraviolet laser system and a microwave interferometer operating at 9.2 GHz, time-resolved measurements are made of the electron density of the plasma. By vacuum sealing part of the interferometer, measurements are made at pressures between 10^{-2} and 10^3 Torr, and in a variety of gases,

including neon, argon, xenon, nitrogen, and oxygen. Rate constants and multiphoton ionization and excitation cross sections can be extracted from the electron density decay rates, using a simple gas kinetic model in neon. The calculated constants are consistent with existing results.

9:15**BT1 4 Radiative Losses of Solar Coronal Plasmas**

JAMES COLGAN, JOE ABDALLAH, MANOLO SHERRILL, MATT FOSTER, CHRISTOPHER FONTES, *Los Alamos National Laboratory* URI FELDMAN, *Naval Research Laboratory* A comprehensive set of calculations of the radiative losses of solar coronal plasmas is presented. The Los Alamos suite of atomic structure and collision codes is used to generate collisional data for fifteen coronal elements. These data are used in the Los Alamos plasma

kinetics code ATOMIC to compute the radiative power loss as a function of electron temperature. We investigate the sensitivity of the loss curves to the quality of the atomic data, changes in the coronal elemental abundances, and compare our results with previous work.

**SESSION BT2: PLASMA AERODYNAMICS
AND PROPULSION I**

Tuesday Morning, 14 October 2008

Salon A-D at 8:00

A. Aanesland, LPTP, Ecole Polytechnique, France,
presiding

Contributed Papers

8:00

BT2 1 Laser Induced Fluorescence Studies of NO Kinetics in Short Pulse Air and Air-Fuel Nonequilibrium Discharges*

WALTER LEMPert, MRUTHUNJAYA UDDI, IGOR ADAMOVICH, *Ohio State University* Laser Induced Fluorescence is used to measure absolute NO concentrations in air, methane-air, and ethylene-air non-equilibrium plasmas, as a function of time after initiation of a single 25 nsec discharge pulse. Peak NO density in air at 60 torr is $\sim 8.10^{12} \text{ cm}^{-3}$ occurring at $\sim 500 \mu\text{s}$ after the pulse, with decay time of $\sim 16.5 \text{ msec}$. Peak NO atom mole fraction in methane-air at $\phi=0.5$ is approximately equal to that in pure air with similar rise and decay rate. In $\phi = 0.5$ ethylene-air, the rise and decay times are also comparable to air and methane-air, but peak NO concentration is a factor of ~ 2.5 lower. Spontaneous emission measurements show that $\text{N}_2(\text{C})$ and NO (A) decay in

$\sim 25\text{ns}$ and $\sim 2.5\mu\text{s}$, respectively. Kinetic modeling calculations incorporating Boltzmann solver for EEDF, and electron impact and full air species kinetics, complemented with the GRI Mech 3.0 hydrocarbon oxidation mechanism, are compared with the experimental data using three different mechanisms. It is concluded that processes involving long lifetime ($\sim 100 \mu\text{sec}$) meta-stable states, such as $\text{N}_2(\text{X},\text{v})$ and $\text{O}_2(\text{b}^1\Sigma)$, which are formed by quenching of the metastable $\text{N}_2(\text{A})$ state by ground state O_2 , play a dominant role in NO formation.

*Support from AFOSR and NASA is acknowledged

8:15

BT2 2 Deflagration-to-detonation transition control by high voltage nanosecond discharges ANDREI STARIKOVSKII,

Drexel University ALEKSANDR RAKITIN, *NEQLab Research*

A smooth square detonation tube with a transverse size of 20 mm and a single-cell discharge chamber has been assembled to study DDT mechanisms under initiation by high-voltage nanosecond discharges. Stoichiometric propane-oxygen mixture was used at initial pressures of 0.3 and 1 bar. Two general mechanisms of DDT initiation have been observed and explained under the experimental conditions. When initiated by a spark, the mixture ignites simultaneously over the volume of the discharge channel, producing a shock wave with Mach number over 2 and a flame wave. The waves then form an accelerating complex, and, after it reaches a certain velocity, an adiabatic explosion occurs resulting in DDT. At 1 bar of initial pressure, the DDT length and time do not exceed 50 mm and 50 μs , respectively. Under streamer initiation, the mixture inside the discharge channel is excited non-uniformly. The mixture is first ignited at the hottest spot with the shortest ignition delay, which is at the high voltage electrode tip. Originating at this point, the ignition wave starts propagating along the channel and accelerates up to the CJ velocity value. The initiation energy is by an order of magnitude lower for the streamer-gradient mode when compared to the spark initiation.

Invited Papers

8:30

BT2 3 Jet Diffusion Flame Stabilization via Pulsed Plasma Forcing.*

GODFREY MUNGAL, *Stanford University*

In this work we investigate the use of high repetition rate pulsed plasma sources as a means to enhance the stability of jet diffusion flames for application to practical combustion devices. Such plasma sources have recently become popular owing to their low power requirements and their proven abilities to ignite leaner mixtures and hold stable flames. They are known to create a radical pool which can enhance combustion chemistry and thus provide increased flame stability. By first investigating a fully premixed methane/air environment we show that the resulting radical species quickly decay but leave behind a set of stable chemical species. Thus, the plasma source appears to act as a fuel reformer leading to the formation of a "cool flame" – a trailing zone of weak oxidation consisting of a slightly elevated temperature stream of products containing small amounts of hydrogen and carbon monoxide. These two key species are then directly responsible for the enhanced flame behaviors. Flame stability enhancements are shown for methane jets in co-flow and cross-flow in room temperature air, and in elevated temperature vitiated air environments. Elevated ambient temperatures deplete the hydrogen and carbon monoxide due to enhanced oxidation, so while there is an enhancement to flame stability, the beneficial effects diminish with increasing temperatures in a non-linear fashion, and ultimately, provide very limited benefits at $\sim 1000\text{K}$ ambient temperature for the present studies. The conclusions here are supported by simple plasma and chemical kinetic modeling and spectroscopic and chemiluminescence measurements.

*Supported by AFOSR MURI and STTR programs with Julian Tishkoff as Contract Monitor.

Contributed Papers

9:00

BT2 4 Simulations of Direct Current Glow Discharges in Supersonic Air Flow SHANKAR MAHADEVAN, LAXMI-NARAYAN RAJA, *The University of Texas at Austin* In recent years, there have been a significant number of computational and experimental studies investigating the application of plasma discharges as actuators for high speed flow control. The relative importance of the actuation mechanisms: volumetric heating and electrostatic forcing can be established by developing self-consistent models of the plasma and bulk supersonic flow. To simulate the plasma discharge in a supersonic air stream, a fluid model of the glow discharge is coupled with a compressible Navier-Stokes solver in a self-consistent manner. Source terms for the momentum and energy equations are calculated from the plasma model and input into the Navier-Stokes solver. In turn, the pressure, gas temperature and velocity fields from the Navier-Stokes solution are fed back into the plasma model. The results include plasma species number density contour maps in the absence and presence of Mach 3 supersonic flow, and the corresponding effect of the glow discharge on gas dynamic properties such as the gas pressure and temperature. We also examine the effect of increasing the discharge voltage on the structure of the discharge and its corresponding effect on the supersonic flow.

9:15

BT2 5 Pulse Discharge in Mixing Layer of Reacting Gases* SERGEY LEONOV, YURI ISAENKOV, *JIHT RAS* MICHAIL SHNEIDER, *Princeton University* JIHT RAS TEAM, PRINCETON UNIVERSITY TEAM, A subject of consideration is the dynamic of filamentary pulse discharge generated along contact zone of two co-flown gases. Experimental facility consists of blow-down wind tunnel PWT-50, system of the high-voltage pulse-repetitive feeding, and diagnostic equipment (schlieren device; pressure, voltage, current, radiation sensors; spectroscopic system; etc.) Typical parameters: $p=0.2\text{-}1\text{Bar}$, velocity $M=0\text{-}2$, pulse duration $\tau=0.1\text{-}1\mu\text{s}$, power release $W=20\text{-}100\text{MW}$. Recently the effect of enormously fast turbulent expansion of the post-discharge channel was observed experimentally [S. Leonov, oth., AIAA Paper 2005-0159 and S. Leonov, oth. "Physics of Plasmas," v.15, 2007]. In this paper a result of parametrical study of the mixing efficiency due to instability development are discussed. The next announced item is that the discharge position and dynamics depend on the test parameters and physical properties of gases involved. The result of interaction can be controlled by the discharge's duration and current as well as by small additives to the gas. The effects found can be applied for high-speed combustion enhancement due to mixing acceleration in multi-components flow.

*Supported by EOARD/ISTC #3793p.

SESSION BT3: DUSTY PLASMAS

Tuesday Morning, 14 October 2008

Addison Room at 8:00

S. Sen, Lancaster University, UK, presiding

8:00

BT3 1 Diffraction of Electromagnetic Waves in Dusty Magnetoplasma ANDREY YATSENKO, NIKOLAY GOROBETS, *Karazin Kharkiv National University* It is known, that the plasma in an external magnetic field (magnetoplasma) becomes anisotropy. For example, the Earth ionosphere has such properties. It's possible to present the interaction of electromagnetic waves with dusty magnetoplasma as a diffraction of electromagnetic waves on the macroscopic particles located in the anisotropic plasma. This problem solved by a method of the integral equations of macroscopic electrodynamics, constructed on the basis of Green's function for anisotropic magnetoplasma. According to this method, the boundary problem of electrodynamics is represented as internal and external problems. At the first stage the internal problem is solved. The field exciting in every macroscopic particle by an external source of electromagnetic energy is defined. At the second stage the external problem is solved, the complete electromagnetic field is defined which is a sum of an external field and scattering field. The diffraction of electromagnetic waves on linear structures in magnetoplasma is also considered on the basis of the received integral equations. The features of waves dispersion in different frequency ranges, the conditions of a resonance are determined. The dispersal equations are received which establish the accordance between parameters of linear structure and plasma at a resonance. The scattering electromagnetic fields are determined.

8:15

BT3 2 Anisotropic interaction forces between two vertical particles in the plasma sheath JAY KONG, LORIN MATTHEWS, TRUPELL HYDE, *CASPER - Baylor University* In a GEC reference cell, charged dust grains are levitated above the negative electrode, usually forming horizontal layers in the plasma sheath. Fast-moving ions in the sheath generate wake fields, creating vertical particle chains where the interaction forces between each particle in a pair are generally different due to the wake-field effect. This presentation will focus on an attenuated oscillation method designed to examine the resulting anisotropic interaction forces. This method is based on an experimental technique whereby dust particles are raised to a height Δh above their natural equilibrium employing an applied DC bias. Removal of this DC bias causes the dust particles to oscillate with attenuated amplitude, eventually returning to their original equilibrium position. The resulting oscillation spectrum displays features unique to the interaction between the particles. Recent experimental results will be presented.

8:30

BT3 3 Self consistent modeling of dusty plasma experiments within a GEC reference cell VICTOR LAND, ERICA SHEN,* LORIN MATTHEWS, TRUPELL HYDE, *Center for Astrophysics, Space Physics, and Engineering Research, Baylor University, Waco, TX, USA 76798-7316* CASPER conducts dusty plasma experiments in two GEC cells. Micrometer sized dust particles are introduced from the top. During their fall toward the lower electrode, they collect ions and electrons from the plasma and charge up. Due to the high electron mobility, this charge is negative and

the dust particles are trapped in the electric field above the bottom electrode. There, dust structures form, which might be crystalline. To describe these, knowledge of the local plasma parameters is needed. These could be obtained with probes, but these inevitably perturb the plasma and the dust, and probe contamination makes the collected data unreliable. Since the absorption of plasma on the dust changes the plasma, data obtained with probes in dust free plasma doesn't represent the parameters of dusty plasma. In this paper, the results of a self-consistent model that solves the plasma and the dust parameters simultaneously are presented, which aim to support data obtained from experiments, and to provide a better understanding of the forces acting on the dust, and of the changes in the plasma due to the presence of the dust.

*Participant in CASPER's Summer High School Scholars Program

8:45

BT3 4 Analytical model for the charge and temperature distributions of nanoparticles in a low pressure plasma accounting for ion-neutral collisions FEDERICO GALLI, UWE KORTSHAGEN, *University of Minnesota* An analytical model predicting the nanoparticle charge and temperature distributions in a low pressure plasma is developed. The model includes the effect of collisions between ions and neutrals in proximity of the particles. In agreement with experimental evidence for pressures of a few Torr a charge distribution that is less negative than the prediction from the collisionless orbital motion limited theory is obtained. Under similar plasma conditions an enhanced ion current to the particle is found. Ion-electron recombination at the particle surface, together with other particle heating and cooling mechanisms typical of silane-argon plasmas, is included in a particle heating model which predicts the nanoparticle temperature distribution. The effect of plasma parameters on the nanoparticle temperature distribution is discussed and the predictive power of the model is demonstrated against experimental evidence of temperature induced crystallization of silicon nanoparticles.

9:00

BT3 5 Spatial distributions of the size and the density of Cu particulates in high-pressure magnetron sputtering plasmas N. NAFARIZAL, *University Tun Hussein Onn Malaysia* N. TAKADA, K. SASAKI, *Nagoya University* It has been observed that magnetron sputtering plasmas are sometimes dusty, namely, they contain a large amount of particulates when they are operated at gas pressures higher than ~ 100 mTorr. In this work, we evaluated the spatial distributions of the size and the density of Cu particulates in the gas phase of a magnetron sputtering plasma source employing a Cu target. The evaluations of the size and the density were based on Rayleigh/Mie scattering of laser lights at two wavelengths of 457 and 672 nm. The size of particulates was estimated from the ratio of the scattered laser intensities, while the density was evaluated from the absolute intensity of the scattered laser light. A remarkable experimental result was that no Cu particulates were observed in the bright plasma region which was located near the target surface in all the discharge conditions. At an argon pressure of 400 mTorr and a discharge power of 4 W, we observed that the size of particulates in the outside of the bright plasma was relatively uniform, and more than 50% of particulates have diameters between 120 and 200 nm. On the other hand, the particulate density had a significant spatial distribution. The absolute particulate density ranged between 10^7 and 10^9 cm^{-3} , and it decreased monotonically with the axial distance from the bright plasma.

9:15

BT3 6 Complex Plasma with Two Distinct Particle Sizes BERNARD SMITH, LORIN MATTHEWS, TRUPELL HYDE, CASPER - *Baylor University* Dust particle clouds can be found in almost all plasma processing environments including both plasma etching devices and in plasma deposition processes. Dust particles suspended within such plasmas acquire an electric charge from collisions with free electrons in the plasma. If the ratio of interparticle potential energy to the average kinetic energy is sufficient, the particles will form either a "liquid" structure with short range ordering or a crystalline structure with long range ordering. Otherwise, the dust particle system will remain in a gaseous state. The preponderance of prior experiments used monodisperse spheres to form complex plasma systems. In order to determine the effects of a size distribution, multiple monodisperse particle sizes need to be examined to determine the manner in which phase transitions and other thermodynamic properties depend upon the overall dust grain size distribution. In this experiment, two-dimensional plasma crystals were formed from mixtures of $11.9 \mu\text{m}$ and $6.50 \mu\text{m}$ monodisperse particles in Argon plasma. With the use of various optical techniques, the pair correlation function was determined at different pressures and powers and then compared to measurements obtained for experiments employing a single size distribution of monodisperse spheres. Additionally, vibrational data was examined to determine other dust and plasma parameters.

SESSION CT1: MICROHOLLOW CATHODE DISCHARGES

Tuesday Morning, 14 October 2008

Salon E at 10:00

K. Nordheden, The University of Kansas, presiding

Contributed Papers

10:00

CT1 1 Absolute atomic oxygen density measurements in core and effluent of a micro scaled atmospheric pressure plasma jet* VOLKER SCHULZ-VON DER GATHEN, NIKOLAS KNAKE, STEPHAN REUTER, *Ruhr-Universitaet Bochum* KARI NIEMI, *Queen's University Belfast* The micro atmospheric pressure plasma jet (μAPPJ) is a capacitively coupled rf discharge (13.56 MHz, ~ 15 W transceiver power) developed, in particular, for optical diagnostics. The discharge is operated at a helium flow of about 1.4 slm with an admixture of oxygen (~ 0.5 vol.-%). In the effluent spatially resolved density distributions of the ground state oxygen atoms have been measured by two-photon absorption laser-induced fluorescence spectroscopy. After calibration by comparative measurements on xenon maximum densities of $2 \times 10^{14} \text{ cm}^{-3}$ have been measured. Variation of the admixture of molecular oxygen between 0 and 2 vol.-% reveals a maximum of the reactive oxygen species yield inside the effluent at 0.6 vol.-%. Varying the power a saturation of the oxygen density is observed beyond about 15 W. First spatially resolved investigations within the discharge core yielded dissociation degrees of more than 20%. While the admixture variation also results in an optimum atom production similar to the effluent, a power variation revealed significant deviations within the core region of the discharge.

*The project is supported by the DFG as project SCHU 2357-1.

10:15

CT1 2 Coupling of imaging and emission spectroscopy for microplasmas studies CLAUDIA LAZZARONI, *Ecole Polytechnique* NADER SADEGHI, *LSP, Grenoble, France* ANTOINE ROUSSEAU, *LPTP, Palaiseau, France* A microplasma is generated in the microhole of a metal-dielectric-metal sandwich at medium pressure in pure argon. The gas pressure ranges from 30 to 300 Torr; the hole diameter from 100 to 400 μm . The aim of our experiment is to study the radial dependence of the mechanism of atoms excitation and of the electronic density inside the microhollow cathode discharge. Imaging of the emission from the microplasma is performed with a spatial resolution of 2 μm . The electron density is estimated from the Stark broadening of the H_{β} -line. The radial distribution of the emission intensities of an Ar atomic line and an Ar^+ ionic line are used for the excitation study. Ar and Ar^+ lines are excited in the cathode sheath edge by beam electrons accelerated within the sheath. These two excitations show the decay of the energy of electrons in negative glow. The Ar line presents also production of excited atoms by recombination of argon ions with electrons at the center of the micro-hole. Work is in progress to evaluate the contribution of the static electric field on the Stark broadening.

10:30

CT1 3 Atmospheric pressure microdischarges utilizing nanoporous dielectric electrodes JIN HOON CHO, *Department of Electrical and Computer Engineering, Colorado State University, Fort Collins, Colorado 80523* WOONG MOO LEE, *Department of Chemistry and Division Energy Systems Research, Ajou University, Suwon 443-749, Korea* CAMERON MOORE, GEORGE COLLINS, *Department of Electrical and Computer Engineering, Colorado State University, Fort Collins, Colorado 80523* We report the generation of microplasmas that use electrodes with nanoporous dielectric surfaces. The electrodes used in the dielectric barrier discharge are made of aluminum rods or plates covered with nanoporous alumina films, $\sim 80 \mu\text{m}$ thick and mean pore diameters being $\sim 40 \text{ nm}$. The alumina nanoporous film was

grown onto Al rod via an electrochemical etching process. The microplasma was sustained using $\sim 10\text{W}$ of AC power at 10–30 kHz, with a gap of 100–500 μm between the rod, tube and plate shaped electrodes. The typical driving voltage and the electron density are $\sim 1200\text{V}$ and $10^{11} \sim 10^{12} \text{ cm}^{-3}$, respectively while the temperature at the discharge region is in the range of 310–350 K. This type of dielectric barrier discharge effectively generates low temperature uniform microplasmas that can be used for a variety of applications, including UV generation, surface treatment, biomedical treatment, and plasma chemical synthesis.

10:45

CT1 4 GEC Student Award for Excellence Finalist: Laser Diagnostics of High Pressure Microdischarge Plasmas* SERGEY BELOSTOTSKIY, VINCENT DONNELLY, DEMETRE ECONOMOU, *University of Houston* NADER SADEGHI, *Université J. Fourier de Grenoble* UNIVERSITY OF HOUSTON TEAM, UNIVERSITÉ J. FOURIER DE GRENOBLE COLLABORATION, Laser diagnostics were performed in the positive column of a high pressure (100s of Torr) parallel-plate DC microdischarge operating in argon or nitrogen. For 50 mA current and over the range of 300 – 700 Torr, Laser Thomson Scattering yielded $T_e = 0.9 \pm 0.3 \text{ eV}$ and $n_e = (6 \pm 3) \times 10^{13} \text{ cm}^{-3}$, in agreement with a mathematical model. Rotational Raman spectroscopy was performed for a set of N_2 pressures (400 – 600 Torr) to measure the gas temperature. T_g changed from $450 \pm 40 \text{ K}$ at 5 mA to $740 \pm 40 \text{ K}$ at 30 mA, and was nearly independent of pressure, within experimental error. Finally, spatially resolved diode laser absorption spectroscopy was used to measure the density of argon metastables. The metastable number density peaked at the plasma-sheath ($\sim 10^{14} \text{ cm}^{-3}$) interface in agreement with simulation. The gas temperature was also extracted from the Doppler width of the absorption profile.

*The authors thank the Department of Energy (Grant no. DE-FG02-03ER54713) for funding.

Invited Papers

11:00

CT1 5 Generation of microplasma ensemble and its functional interaction with electromagnetic waves.

OSAMU SAKAI, *Kyoto University*

Various patterns and structures of microplasma arrays were generated, and interactions between microplasmas and electromagnetic waves were investigated both for control of waves by microplasma ensembles and for production of microplasmas by waves. Using bipolar-voltage power supply with frequencies from several kHz to several MHz and insulated wires, several types of microplasmas were generated at atmospheric pressure with their electron density ranging from 10^{12} to 10^{13} cm^{-3} . They serve as equivalent dielectrics or metals according to their electron plasma frequency ranging from several GHz to several tens of GHz, with respect to the frequency of a propagating electromagnetic wave. When we installed such microplasmas forming a functional array in the propagation region of electromagnetic waves, microplasma arrays exhibited several types of performance; photonic crystals with band gaps, plasmonic waveguides, and metamaterials with extraordinary macroscopic permittivity and/or permeability. One of the significant advantages arising from use of microplasmas in a wave controller is their dynamic and tunable manner by changing external parameters such as generation power and working gas pressure. Especially rapid change of spatial generation patterns gives rise to transformation into another functional device. Another advantage is a role of complex functions arising from dispersion relations with frequency-dependent loss, which will lead to simultaneous and independent control of phase and attenuation of electromagnetic waves.

Contributed Papers

11:30

CT1 6 Modeling of Mode Transition Behavior in Argon Microhollow Cathode Discharges THOMAS DECONINCK, LAXMINARAYAN RAJA, *The University of Texas at Austin* Microhollow cathode discharges (MHCD) can be generated in a simple geometry comprising a cathode/dielectric/anode sandwich structure into which a blind or through hole is drilled. These microdischarges operate at a relatively high pressure of $\sim 10\text{s-}100\text{s}$ Torr with a hole dimension of $\sim 10\text{s-}100\text{s}$ μm . In this study, a fluid model with an argon chemistry is used to help clarify physical mechanisms occurring in a MHCD. The plasma is described using a self-consistent, multi-species, multi-temperature formulation. A variable secondary emission coefficient that depends on the local value of the electric field at the solid surface is used in our model. Computational results are compared to experiments performed in a similar set-up [1]. At low currents ($I < \sim 0.3$ mA), the discharge operates in the abnormal regime and is localized within the cylindrical hollow cathode. At higher current, the discharge expands over the outer surface of the cathode and operates in the normal regime. The differential resistivity of the discharge in this normal regime depends critically on the variable secondary electron emission model used in this study. [1] X. Aubert *et al.*, *Plasma Sources Sci. Technol.*, **16** (2007), 23-32.

11:45

CT1 7 Ignition of parallel Micro Hollow Cathode Discharges in He without ballasts THIERRY DUFOUR, *GREMI, University of Orleans* MONALI MANDRA, MATTHEW GOECKNER, *UTD, University of Texas at Dallas* PHILIPPE LEFAUCHEUX, PIERRE RANSON, *GREMI, University of Orleans* JEONG-BONG LEE, *UTD, University of Texas at Dallas* REMI DUS-SART, *GREMI, University of Orleans* LAWRENCE OVERZET, *UTD, University of Texas at Dallas* Microplasmas are of interest for many different applications including medical, micro TAS, plasma treatment . . . The purpose of our study is to switch on and control several microdischarges mounted in parallel on a single chip, without ballasting them individually. Microcavities used in our experiments are Ni:Al₂O₃:Ni sandwich structures. Holes are 80-180 μm diameter. DC microplasmas are created in He gas without flow with a pressure from 200 to 1000 Torr. A maximum power of 7 watts can be injected into one microdischarge. The area of the plasma spread on the cathode side is determined using an ICCD camera. A current density as high as around 10 mA/mm² could be evaluated. Abnormal glow regime can be obtained by limiting the cathode surface. By this way, it is possible to switch on all the microplasmas without using individual ballasts. We will also present results of microplasmas ignited in gas flow crossing the cavities and show the flow affects the microplasmas and their V-I curve.

SESSION CT2: ELECTRON/PHOTON INTERACTIONS WITH MOLECULES

Tuesday Morning, 14 October 2008; Salon A-D at 10:00

Chetan G. Limbachiya, P.S. Science and H.D. Patel Arts College, Kadi - Gujarat, India, presiding

Invited Papers

10:00

CT2 1 Electron- and Photon-Induced Fragmentation Dynamics in Simple Atoms and Molecules.*THOMAS RESCIGNO, *Lawrence Berkeley National Laboratory*

Advanced imaging techniques such as COLTRIMS, coupled with high-resolution electron- and new X-ray photon sources, have triggered a new class of kinematically complete experiments that probe the details of electron- and nuclear dynamics in simple atoms and small molecules. The interpretation of these experiments presents a formidable challenge for contemporary theory, often involving fully differential cross section and excited-state reaction dynamics calculations that require precise, non-perturbative quantum mechanical methodology. I will illustrate this topic with several examples in which state-of-the-art *ab initio* theory can shed light on experiments which probe electron and/or nuclear fragmentation dynamics in simple systems. The examples will include sequential and non-sequential two-photon double ionization of helium, diffraction effects in high-energy photo-double ionization of H₂, core-hole localization in molecular nitrogen, inner-valence shell fragmentation of carbon monoxide and electron-induced three-body breakup of water.

*Work performed under the auspices of the USDOE and supported by the OBES Division of Chemical Sciences.

10:30

CT2 2 Electron- Molecule Collisions: Recent results for "large" polyatomic molecules.*STEPHEN BUCKMAN, *Australian National University*

Electron interactions with molecular targets, particularly large polyatomic systems, pose a significant challenge for scattering theory and experiment alike. Many targets, such as those of relevance to radiation damage in the body, are difficult to model as they are generally large, polar systems, which are also highly polarisable. They can also be difficult to produce experimentally as they are either liquids or powders at room temperature. This talk will discuss some recent results for elastic scattering and vibrational excitation of molecules such as formic acid, tetrahydrofuran and 3-hydroxy tetrahydrofuran – all of which can be considered as useful analogues to studies of the larger molecular constituents of DNA. Work done in collaboration with Violaine Vizcaino, James Sullivan, Michael Brunger, Jason Roberts, Vincent McKoy and Carl Winstead.

*Supported by the Australian Research Council.

Contributed Papers

11:00

CT2 3 GEC Student Award for Excellence Finalist: Fluorescence Polarization of H₂, D₂, and N₂ Molecules Excited by Polarized Electron Impact* J.W. MASEBERG, T.J. GAY, *University of Nebraska* We report relative Stokes parameters for both molecular and dissociated atomic transitions in H₂, D₂, and N₂ excited by spin-polarized electrons. In the case of molecular transitions, we find that values of the normalized circular polarization fraction, P_3/P_e , for light emitted in the direction of electron spin polarization are non-zero for H₂ and D₂, but consistent with zero for N₂. Specifically, we have succeeded in rotationally isolating the H₂ $d^3\Pi_u \rightarrow a^3\Sigma_g^+ Q(1)$ 601.8 nm transition. It exhibits relatively large near-threshold values for P_3/P_e ($\sim 17\%$). This is in contrast to the null measurements for the N₂ $C^3\Pi_u \rightarrow B^3\Pi_g$ 380.5 nm and N₂⁺ $B^2\Sigma_u^+ \rightarrow X^2\Sigma_g^+$ 391.4 nm transitions. For the case of fluorescence from dissociated atomic fragments we observe non-zero circular polarization values for H, D, and N. The near-threshold P_3/P_e values observed for the Balmer-alpha H and D 656.3 nm transitions are nearly equivalent ($\sim 8\%$). For the N (³P)3p \rightarrow (³P)3s 824.2 nm transition we find P_3/P_e values of approximately -7%. This surprising negative sign indicates that the atomic fragment is spinning the "wrong way," i.e. in a direction opposite that of the incident electron responsible for the molecular dissociation.

*Support by NSF Grant PHY-0653379

11:15

CT2 4 Double Photoionization of H₂: Double Slit Interference?* DANIEL HORNER, *Los Alamos National Laboratory* SHUNGO MIYABE, *University of California, Davis* FELIPE MORALES, FERNANDO MARTIN, *Universidad Autonoma de Madrid, Spain* THOMAS RESCIGNO, *Lawrence Berkeley National Lab* C. WILLIAM MCCURDY, *Lawrence Berkeley National Lab and University of California, Davis* Using the method of exterior complex scaling and the finite element discrete variable representation, we are able to compute accurate time-independent wave functions for the double photoionization of H₂. Together with integral amplitude methods, these accurate wave function solutions allow us to calculate converged differential cross sections. We present the double differential cross section at photon energies between 130 eV and 240 eV. At these energies, recent experiments have observed angular distributions that were interpreted as double slit interference of the electrons ejected from near the two nuclei. With our theoretical methods, we are able to examine this question further and will offer an alternate interpretation based on the coherent mixture of parallel and perpendicular polarization in the circularly polarized light.

*Work performed under the auspices of the US DOE at LANL (Contract No. DE-AC52-06NA25396), LBNL (Contract No. DE-AC02-05CH11231), and DGI Project No. FIS2006-00298 (Spain)

11:30

CT2 5 Low Energy Elastic Scattering from Water* MUR-TADHA A. KHAKOO, JOHN MUSE, *Physics Department, Cal State University, Fullerton, USA* HELEN SILVA, MARIA CRISTINA A. LOPES, *Physics Department, Federal University of Juiz de Fora, Brazil* Differential electron scattering cross-sections have been measured for elastic scattering from water molecules. The method of relative flow, but with an aperture replacing traditional

gas collimating structures. In addition, the gas source was moved to determine the background scattering contribution. The measurements were taken at incident energies of 1eV to 100eV and scattering angles of 5° to 130°. Comparisons with theory and former experiments will be presented.

*Funded by the NSF (USA) and CAPES, CNPq (Brazil).

11:45

CT2 6 Ly- α and H- α Optical Excitation Functions Resulting From Photodissociation of H₂ and D₂* T.J. GAY, E. LITAKER, J.R. MACHACEK, *University of Nebraska* J.E. FURST, *University of Newcastle* A.L.D. KILCOYNE, LBL F. MARTIN, *Universidad Autonoma de Madrid* K.W. MCLAUGHLIN, *Loras College* J.L. SANZ-VICARIO, *Universidad de Antioquia, Columbia* The production of Ly- α and H- α radiation following photodissociation of H₂ plays a key role in astrophysical plasmas associated with planetary aurorae and new-star formation. However, these very basic cross sections are not well known at this time, due to the poor agreement between the extant experimental data and the best available theory [1]. We will present recent data we have taken at the Lawrence Berkeley Laboratory Advanced Light Source (ALS) for these excitation functions with H₂, HD, and D₂ targets with incident photon energies between 24 and 70 eV. We will discuss possible systematic errors in the available data sets, including those due to incident photon spectral impurity, target contamination, cascading, background gas quenching, and other target-pressure-dependent effects. [1] See J.D.Bozek *et al.*, *J. Phys. B* **39**, 4871 (2006), and references therein.

*Work supported by the NSF, DOE, and the University of Newcastle

SESSION CT3: MAGNETICALLY-ENHANCED AND RELATED PLASMAS

Tuesday Morning, 14 October 2008

Addison Room at 10:00

Pascal Chabert, CNRS-Ecole Polytechnique, France, presiding

Contributed Papers

10:00

CT3 1 Investigations of Magnetically Enhanced RIE Reactors with Rotating Magnetic Fields* NATALIA YU. BABAEVA, *University of Michigan* MARK J. KUSHNER, *Iowa State University* In Magnetically Enhanced Reactive Ion Etching (MERIE) reactors, a magnetic field parallel to the substrate enables higher plasma densities and control of ion energy distributions. Since it is difficult to make the B-field uniform across the wafer, the B-field is often azimuthally rotated at a few Hz to average out non-uniformities. The rotation is slow enough that the plasma is in quasi-equilibrium with the instantaneous B-field. For the pressures (10's mTorr or less) and B-fields (10's - 100's G) of interest, electrons are magnetized whereas ions are usually not. The orientation and intersection of the B-field with the wafer are important, as intersecting field lines provide a low resistance path for electron

current to the substrate. We report on a modeling study of plasma properties in MERIE reactors having rotating B-fields by investigating a series of quasi-steady states of B-field profiles. To resolve side-to-side variations, computations are performed in Cartesian coordinates. The model, *nonPDPSIM*, was improved with full tensor conductivities in the fluid portions of the code and $\mathbf{v} \times \mathbf{B}$ forces in the kinetic portions. Results are discussed while varying the orientation and strength of the B-field for electropositive (argon) and electronegative ($\text{Ar}/\text{C}_x\text{F}_y$, Ar/Cl_2) gas mixtures.

*Work supported by Applied Matl's and Semiconductor Res. Corp.

Invited Papers

10:30

CT3 3 On the Plasma Parameters in the High Power Impulse Magnetron Sputtering Discharge (HiPIMS).

JON T. GUDMUNDSSON, *University of Iceland*

The development of ionized physical vapor deposition (IPVD) was mainly driven by the formation of metal and nitride thin films into deep, narrow trenches and vias that are essential in modern microelectronics. More recently, the control of the ion energy and direction of the deposition species has proved to be an important physical tool in the growth process of new materials and new structures. Over the past few years, various ionized sputtering techniques have appeared that show a high degree of ionization of the sputtered atoms, in the range 50 – 90%¹. This is often achieved by the application of a secondary discharge to a magnetron sputtering discharge, either inductively coupled plasma source (ICP-MS) or a microwave amplified magnetron sputtering. High power impulse magnetron sputtering (HiPIMS) is a more recent sputtering technique that utilizes ionized physical vapor deposition (IPVD)². High density plasma is created by applying a high power pulses to a conventional planar magnetron sputtering discharge. The pulse power density is in the range 1 – 3 kW/cm², the pulse frequency 50 – 500 Hz and pulse length 50 – 500 μs . Measurements of the temporal and spatial behavior of the plasma parameters indicate peak electron density of the order of 10^{19} m^{-3} , that expands from the target with a fixed velocity that depends on the gas pressure³. The high electron density results in a high degree of ionization of the deposition material. Fractional ionization of the sputtered material has been measured to be over 90%⁴. This is important since ions are controllable with respect to energy and direction as they arrive to the growth surface. The spatial and temporal variation of the plasma parameters, electron density, plasma potential, and electron and ion energy, in a HiPIMS discharge are explored. The plasma physics of the HiPIMS will be discussed as well as some of the applications of the HiPIMS technique.

¹U. Helmersson, M. Latteman, J. Bohlmark, A. P. Ehasarian, and J. T. Gudmundsson, *Thin Solid Films* **513**(2006) 1-24

²U. Helmersson, M. Lattemann, J. Alami, J. Bohlmark, A.P. Ehasarian, and J.T. Gudmundsson, *Proceedings of the 48th Annual Technical Conference of the Society of Vacuum Coaters*, April 23-28, 2005, Denver, CO, USA, p.458

³J.T. Gudmundsson, J. Alami, and U. Helmersson, *Surf. Coat. Technol.* **161** (2002) 249 - 256

⁴J. Bohlmark, J. Alami, C. Christou, A. P. Ehasarian and U. Helmersson, *J. Vac. Sci. Technol.* **23** (2005), 18-22

Contributed Papers

11:00

CT3 4 The Use of Impulse Plasma in Surface Engineering

KRZYSZTOF ZDUNEK, *Faculty of Mater. Sci., Warsaw University of Technology, Poland* It is evident that impulse plasma ensures both the highest level of nonequilibrium and highest level of vapour ionisation. These conditions seemed to be especially suitable for synthesizing the phases with high energetic barrier of nucleation process. In our methods, called by us as the *Impulse Plasma Deposition (IPD)* the impulse plasma is generated and accelerated in a coaxial accelerator. The only source of electric energy in the plasma process is condenser battery charged to the

10:15

CT3 2 Effect of the gas injection profile on the gas composition in an ICP plasma source

VLADIMIR NAGORNY, *Mattson Technology, Inc.* VLADIMIR KOLOBOV, *CFD Research Corporation* It is shown that details of the gas injection in an ICP plasma source may affect not only the spatial distribution of neutral and ion fluxes on the surface of the wafer, but also the composition of the gases arriving to the wafer surface. The cause of this effect is the difference between the gas flow profile and spatial distribution of high energy electrons capable of dissociating and ionization the gas molecules. At gas pressures of 50-100mTorr, often used in plasma processing, this effect may be quite noticeable, since high energy electrons are localized close to the coils, and the overall particles balance strongly depends on the local balance in these regions, as shown in two simple examples.

voltage of order of kVs. During the discharge of condensers individual plasmoids are being accelerated in the coaxial generator by the Ampere force to the speed of the order of 10^4 ms^{-1} and directed to the non-heated substrate. The most characteristic feature of the is that the synthesis proceeds in the impulse plasma itself, with the participation of ions. The crystallization on ions (ionization degree of the impulse plasma is equal to 100%) makes individual plasmoids to be strongly enriched rather in clusters or particles agglomerates with dimensions of order of single nms than the atoms. Because of the very short life time of plasmoids (approx. 10^{-4} sec each) the surface coalescence of particles delivered to the substrate has a limited character. As a consequence the material of the layer has nanocrystalline, globular morphology.

11:15

CT3 5 Practical helicon sources using permanent magnets

FRANCIS F. CHEN, *UCLA* Helicon sources are known for efficient conversion of RF energy into plasma density, but the need for a large electromagnet has impeded commercial acceptance. A novel use of permanent magnets, in which the plasma is placed below, rather than inside, a ring magnet allow the plasma to be ejected toward the substrate. The dimensions of a single source and its magnet have been optimized by computation and tested experimentally. For large area coverage, a multiple-source array has been designed and tested. In this case, RF circuitry and coupling present problems that have been solved. Measurements show that an 8-tube module should produce $10^{12}/\text{cm}^3$ density 7" below a source only 6" in height with 2-3% uniformity. Stacked modules can cover arbitrarily large substrates with this new paradigm.

11:30

CT3 6 Time and space-resolved measurements of the neutral gas density in a helicon reactor by TALIF LAURENT LIARD,

ANE AANESLAND, JACQUES JOLLY, JEAN-LUC RAIMBAULT, PASCAL CHABERT, *LPTP - CNRS UMR 7648* Contemporary plasma reactors used for plasma processing or space plasma propulsion (Inductively Coupled or Helicon plasmas for instance) are characterized by a high electronic density. In these reactors, the electronic pressure can be as high as the neutral pressure, resulting in neutral depletion effects in the centre of the discharge. This phenomenon has been recently studied both theoretically (using fluid models¹ and experimentally^{2,3} In this presentation, we are interested in the dynamics of this phenomenon. By using a two photon laser induced fluorescence (TALIF) diagnostic in Xenon gas, radial measurements of the Xenon ground state density at different times are performed. We have studied both the ignition phase, and the afterglow relaxation. It appears, as expected, that the depletion in the centre occurs in a short time-scale, typically in the millisecond range. However, a longer timescale effect has also been observed, due to a change in the pumping speed.

¹J.-L. Raimbault *et al.*, *PoP*, 2007, 14, 013503

²A. Aanesland *et al.*, *Appl. Phys. Lett.*, 2007, 91, 121502

³D. O'Connell *et al.*, *J. Phys. D.*, 2008, 41, 035208

SESSION DT1: PLASMA-SURFACE INTERACTIONS

Tuesday Afternoon, 14 October 2008; Salon E at 13:30

CW Chung, Hanyang University, Korea, presiding

Invited Papers

13:30

DT1 1 Study of elementary processes of plasma-wall interaction in fusion devices by means of an inductively coupled hydrogen plasma in interaction with graphite surfaces.

GILLES CARTRY, *PIIM, CNRS - Universite de Provence*

In controlled fusion devices, the interaction of hydrogen plasma with graphite like walls leads to carbon erosion and hydrocarbon redeposition. When using tritium, which is a radioactive element, hydrocarbon redeposition in the reactor becomes a real safety issue. Therefore carbon erosion must be understood and limited. Our aim is to better understand fundamental mechanisms of hydrogen interaction with graphite. In this aim, we use an ultra-high vacuum set-up equipped with hydrogen guns (atomic and ionic species), with a versatile ICP source working as a plasma source or as an atomic source, and with two main surface diagnostics: High Resolution Electron Energy Loss Spectroscopy and Scanning Tunneling Microscopy. We will present a model for H adsorption process on graphite surface, and particularly will compare "hot" and "cold" H atom adsorption. We will deal with H(D) abstraction by D(H) atoms. Finally, we will examine ion interaction with graphite both in beams and in plasmas in order to better understand ion-neutral synergetic effects.

Contributed Papers

14:00

DT1 2 Manipulation of the bombarding ion energy distribution in fluorocarbon plasma etching AMY WENDT, FRANK BUZZI, YUK-HONG TING, *University of Wisconsin - Madison*

Ion bombardment is a key element of plasma etching for microelectronics fabrication and other materials processing applications. A sinusoidal voltage waveform typically produces a broad "bimodal" ion energy distribution (IED) at the substrate, with two ion flux maxima, at respective energies considerably above and below the average. In order to deconvolve the effect of ions of

multiple energies bombarding the substrate simultaneously, we have manipulated the waveform of the bias voltage to produce two ion flux maxima. By systematically tailoring the shape of the waveform, the energies and relative fluxes of the two IED peaks are varied independently over a 100 to 500 eV range in a fluorocarbon-based helicon plasma, while silicon dioxide and photoresist etch rates are monitored. Two experiments were conducted in which a 100 eV IED peak was combined with a higher energy peak, while the energy and relative flux of the high energy peak were respectively varied. In both cases, a relatively small contri-

bution of high energy ions leads to etch rate enhancement higher than predicted by a linear combination of single peak etch rates at the two energies. We speculate that high energy ion bombardment suppresses fluorocarbon deposition, enabling lower energy ions to more effectively contribute to etching reactions.

14:15

DT1 3 Atomic-scale cellular model and profile simulation of Si etching in chlorine- and bromine-containing plasmas: Effects of surface oxidation on evolution of feature profiles HIRO-TAKA TSUDA, SHOKI IRIE, MASAHI TO MORI, HIROAKI OHTA, KOJI ERIGUCHI, KOUICHI ONO, *Kyoto University* Profile simulation is indispensable for understanding the effects of complex surface reaction processes that occur during plasma etching, to achieve the nanometer-scale control of etched profiles and critical dimensions and their microscopic uniformity. This paper presents an atomic-scale model for feature profile evolution during Si etching in chlorine- and bromine-containing plasmas, with emphasis being placed on the effects of surface oxidation arising from impurity as well as added oxygen. The model incorporated an atomic-scale cellular model for surface reaction multilayers and the Monte Carlo calculation for the trajectory of ions and neutrals onto feature surfaces, taking into account chemical etching, ion-enhanced etching, deposition of etch products and by-products, and surface oxidation. The profile simulation was performed to reproduce experimental observations in Si etching at increased O_2 concentration in Cl_2/O_2 and HBr/O_2 plasmas; e.g., reduced profile anomalies near the feature bottom such as footing and microtrenching, increased thickness of passivation layers on feature sidewalls, increased sidewall tapering, enhanced inverse RIE lag, increased roughness of bottom surfaces, and residue or micropillar and etch stop that occur.

14:30

DT1 4 Mechanistic model of atomic recombination* J.D. GUHA, V.M. DONNELLY, *University of Houston* Recently we have started a new approach of studying atomic recombination at the reactor walls, by rapidly rotating a spinning substrate between the plasma and differentially pumped diagnostic chamber, thereby exposing the surface to the plasma, and then analyzing the reaction products few ms thereafter. We have investigated atom recombination in Cl_2 and O_2 plasmas with this technique. In a Cl_2 plasma, Cl_2 physisorbs and then desorbs over the time scale comparable to that for Cl recombination, thereby competing with Cl adsorption for active sites. With the plasma off, Cl_2 desorption flux increases nearly linearly with pressure. Cl recombination probabilities, γ_{Cl} , ranged from 0.01 to 0.1 and were found to increase with increasing n_{Cl}/n_{Cl_2} number density ratio (from 0.1 to 0.8) in Cl_2 plasmas. A multi-site adsorption model has been developed to explain the desorption kinetics of physisorbed Cl_2 . The total surface site density of $\sim 10^{15} \text{ cm}^{-2}$ was distributed with a Gaussian profile over binding energies (B.E) ranging from 7.8 to 19.8 Kcal/mol. For Cl_2 physisorption, the sites with B.E < 14Kcal/mol are mostly unsaturated, and give rise to the pressure scaling of Cl_2 desorption flux. For sites with B.E > 14Kcal/mol, the fractional surface coverage (θ_i) rises sharply with increasing B.E and pressure. The competitive adsorption of Cl_2 vs Cl at these high B.E sites is likely responsible for the observed dependence of γ_{Cl} on n_{Cl}/n_{Cl_2} .

*Lam Research Corporation, Fremont, CA

14:45

DT1 5 Surface loss rate of H and N radicals in H_2/N_2 plasma etching process CHANG SUNG MOON, KEIGO TAKEDA, TOSHIO HAYASHI, *Nagoya University* SEIGO TAKASHIMA, *Nagoya Urban Industries Promotion Corp.* MAKOTO SEKINE, *Nagoya Univ. and JST-CREST* YUICHI SETSUHARA, *Osaka Univ. and JST-CREST* MASAHARU SHIRATANI, *Kyushu Univ. and JST-CREST* MASARU HORI, *Nagoya Univ. and JST-CREST* As ULSI devices are down to nano-scale size, there have been many efforts to develop low dielectric constant (low-k) materials and establish the plasma etching technology. Especially, the interaction between the plasma and the surface has an enormous influence on characterizing the etching process. However, the reactions in contact with solid surface such as substrate and wall are very complicated and moreover, at present, there are many interactions unknown and they are not fully understood yet. In this study, surface loss probabilities of H, N radicals on stainless steel and organic low-k film surfaces are investigated by vacuum ultraviolet absorption spectroscopy (VUVAS) technique. The changes of H, N radical densities are quantitatively measured in H_2/N_2 plasma afterglow and the loss rates on each surface are evaluated. It is expected that the development of plasma etching process can be advanced by understanding the reaction of radicals with the surface during organic low-k etching process.

15:00

DT1 6 ABSTRACT WITHDRAWN

15:15

DT1 7 Effects of Remote Plasma Treatment on Surface Defects in ZnO Nanopowders JORGE PARAMO, RAUL PETERS, YURI STRZHEMECHNY, *Texas Christian University* The field of high-tech applications of ZnO nanostructures is rapidly growing. Because of the large surface/volume ratio in these systems, device performance in many cases is determined by surface and near-surface properties of the nanocrystals. The nature of the surface/subsurface defect states in nanosized ZnO is still ambiguous, and only in a small number of recent studies attempts were made to modify these states in a controllable fashion. In our work, we used remote plasma treatment of several commercially available ZnO nanopowders to manipulate their surface and subsurface defects. Temperature-dependent photoluminescence spectroscopy was employed to monitor the effects of nitrogen, hydrogen, and oxygen plasmas on the surface states. We demonstrated that those plasma species induce a variety of changes in the deep defect visible emission as well as in the bound-exciton luminescence, most likely associated with the surface/subsurface states. We also observed significant size-dependent effects of plasma treatment in our nanosystems.

SESSION DT2: BIOLOGICAL AND EMERGING APPLICATIONS OF PLASMA
 Tuesday Afternoon, 14 October 2008
 Salon A-D at 13:30
 E. Stoffels, Eindhoven University of Technology/Drexel University Philadelphia, presiding

Contributed Papers

13:30

DT2 1 GEC Student Award for Excellence Finalist: Atmospheric pressure generation of high fluxes of singlet oxygen for biological applications J. SANTOS SOUSA, *LPGP, CNRS-UPS, 91405 Orsay, France and IPFN, IST, 1049-001 Lisboa, Portugal* G. BAUVILLE, B. LACOUR, V. PUECH, *LPGP, CNRS-UPS, 91405 Orsay, France* M. TOUZEAU, *LTM, CNRS-UJF-INPG, 38054 Grenoble, France* J.L. RAVANAT, *CEA, Inac, SCIB/LAN CEA-UJF, 38054 Grenoble, France* The generation of singlet oxygen states, O₂(a¹D), by microplasmas has been studied experimentally. For binary He/O₂ mixtures, we previously reported that O₂(a¹D) densities of about 10¹⁵ cm⁻³ can be efficiently achieved at atmospheric pressure in a 3-electrode microcathode sustained discharge (MCSD) configuration[1]. One solution to increase the O₂(a¹D) number density is to add, in the He/O₂ mixture, an O-atom scavenger in order to reduce the quenching processes. Thus, we have studied the influence of adding small concentrations of NO molecules. We report experimental results showing that, in He/O₂/NO mixtures and at atmospheric pressure, O₂(a¹D) number densities higher than 10¹⁶ cm⁻³ were measured in the MCSD afterglow at total flow rates up to 30 l/min, resulting in O₂(a¹D) fluxes above 10 mmol/h. This opens opportunities for a large spectrum of new applications. Preliminary experiments were conducted showing that the developed system is particularly useful to study in details the reactivity of singlet oxygen with biological molecules such as DNA constituents. [1] G. Bauville et al., AIAA paper 2007-4025

Invited Papers

14:00

DT2 3 Interaction of Low Temperature Plasmas with Prokaryotic and Eukaryotic Cells.
 MOUNIR LAROUCSI, *Old Dominion University*

Due to promising possibilities for their use in medical applications such as wound healing, surface modification of biocompatible materials, and the sterilization of reusable heat-sensitive medical instruments, low temperature plasmas and plasma jets are making big strides as a technology that can potentially be used in medicine¹⁻². At this stage of research, fundamental questions about the effects of plasma on prokaryotic and eukaryotic cells are still not completely answered. An in-depth understanding of the pathway whereby cold plasma interact with biological cells is necessary before real applications can emerge. In this paper, first an overview of non-equilibrium plasma sources (both low and high pressures) will be presented. Secondly, the effects of plasma on bacterial cells will be discussed. Here, the roles of the various plasma agents in the inactivation process will be outlined. In particular, the effects of UV and that of various reactive species (O₃, O, OH . . .) are highlighted. Thirdly, preliminary findings on the effects of plasma on few types of eukaryotic cells will be presented. How plasma affects eukaryotic cells, such as mammalian cells, is very important in applications where the viability/preservation of the cells could be an issue (such as in wound treatment). Another interesting aspect is the triggering of apoptosis (programmed cell death). Some investigators have claimed that plasma is able to induce apoptosis in some types of cancer cells. If successfully replicated, this can open up a novel method of cancer treatment. In this talk however, I will briefly focus more on the wound healing potential of cold plasmas. ¹E. A. Blakely, K. A. Bjornstad, J. E. Galvin, O. R. Monteiro, and I. G. Brown, "Selective Neuron Growth on Ion Implanted and Plasma Deposited Surfaces," *In Proc. IEEE Int. Conf. Plasma Sci.*, (2002), p. 253. ²M. Laroussi, "Non-thermal Decontamination of Biological Media by Atmospheric Pressure Plasmas: Review, Analysis, and Prospects," *IEEE Trans. Plasma Sci.*, Vol. 30, No. 4, pp. 1409-1415, (2002).

13:45

DT2 2 Investigation of Cell Surfaces using Microplasma-Assisted Desorption/Ionization Mass Spectroscopy* JOSHUA SYMONDS, LAN SUN, *Georgia Institute of Technology School of Physics* FACUNDO FERNÁNDEZ, THOMAS ORLANDO, *Georgia Institute of Technology School of Chemistry and Biochemistry* THE CENTER FOR BIO IMAGING MASS SPECTROMETRY COLLABORATION,[†] Low-temperature, atmospheric pressure microplasmas have been developed for a wide array of uses. We have investigated one type of these devices, a Microhollow Cathode Discharge (MHCD) for desorbing and ionizing samples to be analyzed with standard mass spectroscopy techniques. Our work includes the development and use of MHCD's to analyze solid and liquid phase samples, with particular attention given to biologically-relevant substances. The goal of this line of research is to investigate, without causing undue fragmentation, the compounds present on and within cell membranes. By varying the properties of the plasma, including electron temperature, plasma density, and the plasma's interactions with the sample, we seek to investigate the role of different plasma components in the desorption/ionization events. Specifically, we seek to determine whether the process is dominated by emitted electrons, high energy (VUV) photons, metastable particles, or a combination thereof.

*The Center for Bio Imaging Mass Spectrometry, U.S. Department of Energy.

[†]<http://web.chemistry.gatech.edu/~bims/index.html>

Contributed Papers

14:30

DT2 4 GEC Student Award for Excellence Finalist: Interaction of Non-Thermal Dielectric Barrier Discharge Plasma with DNA inside Cells SAMEER KALGHATGI, CRYSTAL KELLY, GREGORY FRIDMAN, JANE CLIFFORD-AZIZKHAN, ALEXANDER FRIDMAN, GARY FRIEDMAN, *Drexel University* Direct non-thermal plasma is now being widely considered for various medical applications, viz; cancer treatment, coagulation, wound healing. However, the understanding of the interaction between non-thermal plasma and cells is lacking. Here we study the possibility that effects of the plasma treatment can penetrate through cellular membranes without destroying them. One of the most important of such effects to investigate would be DNA double strand breaks (DSB's) since these are some of the important events in a cell's life cycle. We measured DNA DSB's in mammalian cells using immunofluorescence and western blots. Hydrogen peroxide treatment was used as a positive control since it is known to induce massive DNA double strand breaks. The results indicate that short (5 seconds) direct plasma treatment at low power (0.2 W/cm^2) does produce DNA DSB's in mammalian cells. This means that somehow plasma penetrates inside the cells. Several questions arise about what is the mechanism of penetration and do the cells repair the DNA DSB's. We show that the cells do repair the DNA DSB's produced by short exposure of low power plasma. Although the detailed mechanisms are being investigated we confirmed that reactive oxygen species mediate interaction between plasma and DNA.

14:45

DT2 5 Characteristics of atmospheric pressure air micro slot plasma and application to bacterial inactivation IL GYO KOO, JIN HOON CHO, *Department of Electrical and Computer Engineering, Colorado State University, Fort Collins, Colorado 80523* WOONG MOO LEE, *Department of Chemistry and Division Energy Systems Research, Ajou University, Suwon 443-749, Korea* CAMERON MOORE, GEORGE COLLINS, *Department of Electrical and Computer Engineering, Colorado State University, Fort Collins, Colorado 80523* The E-coli was inactivated using an atmospheric pressure microplasma in air. The microplasma was generated between two parallel aluminum rods are 5 cm long, 3 mm in diameter, maintain $200 \mu\text{m}$ wide gaps between two electrodes, and covered with nanoporous alumina films^{1,2}. The 20 kHz AC driven discharge is generated between two parallel rods. The plasma gas temperature was measured by emission spectroscopy and FT-IR camera, which is so closed at room temperature. The E-coli sample placed between the two electrodes underwent chemical and physical treat on E-coli sample during the discharge. Experimental results demonstrated a colony forming unit reduction from 10^7 to 10^5 within 10 minutes treatment.

15:00

DT2 6 Finite element analysis of the plasma needle-biomaterial interaction at atmospheric pressure YUKINORI SAKIYAMA, DAVID GRAVES, *University of California at Berkeley* The atmospheric pressure RF-excited plasma needle is a non-thermal discharge sustained at the sharp tip of a needle in helium gas flow. The plasma needle has been applied to various biomedical applications. However, the mechanisms of the plasma-biomaterial interaction are only poorly understood. In this study, we focus on influences of humid air diffusing into the discharge domain on plasma chemistry. Our fluid model includes 49 species and over 700 elementary reactions in one-dimensional spherical coordinates. An expected concentration gradient of humid air is assumed to be present due to back diffusion of air against helium convective flow. Our simulation results indicate that O_2^+ and N_2^+ are dominant ions at the outer electrode corresponding to the biomaterial surface and that the most abundant neutrals near the outer electrode are O, O_2^* , and OH radicals. These results suggest that trace amounts of humid air can play a central role in plasma needle treatment.

15:15

DT2 7 Cold atmospheric air plasma jet for medical applications JUERGEN F. KOLB, ROBERT O. PRICE, MICHAEL STACEY, R. JAMES SWANSON, ANGELA BOWMAN, ROBERT L. CHIAVARINI, KARL H. SCHOENBACH, *Frank Reidy Research Center for Bioelectrics, Old Dominion University* By flowing ambient air through the discharge channel of a microhollow cathode geometry, we were able to sustain a stable 1.5-2 cm long afterglow plasma jet with dc voltages of only a few hundred volts. The temperature in this expelled afterglow plasma is close to room temperature. Emission spectra show atomic oxygen, hydroxyl ions and various nitrogen compounds. The low heavy-particle temperature allows us to use this exhaust stream on biological samples and tissues without thermal damage. The high levels of reactive species suggest an effective treatment for pathological skin conditions caused, in particular, by infectious agents. In first experiments, we have successfully tested the efficacy on *Candida kefyr* (a yeast), *E.coli*, and a matching *E.coli* strain-specific virus. All pathogens investigated responded well to the treatment. In the yeast case, complete eradication of the organism in the treated area could be achieved with an exposure of 90 seconds at a distance of 5 mm. A 10-fold increase of exposure, to 900 seconds caused no observable damage to murine integument.

SESSION ET1: DIELECTRIC BARRIER DISCHARGES AND DISPLAYS

Tuesday Afternoon, 14 October 2008

Salon E at 16:00

O. Sakai, Kyoto University, Japan, presiding

*Contributed Papers***16:00**

ET1 1 Homogeneous DBD in N₂: II. Simulation in 0D and 1D approaches SERGEY PANCHESHNYI, DZIMTRY TSYGANOV, PIERRE SEGUR, LAPLACE, *University of Toulouse, CNRS* In this paper we develop and validate a zero- and one-dimensional three-temperature plasmachemical model of a uniform DBD discharge in pure nitrogen at atmospheric pressure. The complete kinetic model includes 17 species (electrons, ions, neutrals) and 41 processes including excitation and ionization by electron impact, associative ionization, ion-electron recombination, and heavy species conversion. In the 0D model the electron density and the electric field are calculated using measured gap voltage and discharge current density that allows direct verification of the kinetic scheme. Using a comparison between the simulated and measured densities of N atoms, the importance of the surface dissociative electron-ion recombination process is shown. A simple analytical expression for the atom production, which provides a highly accurate description of the complete model, is presented. The role of surface processes for electric behavior of the discharge is analyzed using a self-consistent model. This 1D model is based on balance equations for charged species in the electric field which is described by Poisson's equation.

16:15

ET1 2 Nanosecond pulsed surface dielectric discharge development MARYIA NUDNOVA, *Moscow Institute of Physics and Technology* ANDREI STARIKOVSKII, *Drexel University* Subsequent images of surface nanosecond barrier discharge development were obtained with nanosecond time resolution. The velocities of discharge propagation were obtained, discharge uniformity and filling ratio of the gap by plasma has been investigated. SDBD modeling was performed in a hydrodynamic approximation for 3-dimensional geometry. To initialize the streamers formations near the edge of the high-voltage electrode the sinusoidal perturbation in the initial electron concentration was applied. The calculations of streamer propagation for such condition are discussed. The development of initial perturbation in X-Z plane is clearly seen. Developed streamers are not sensitive to initial pre-ionization. Also calculations with relatively small value of initial ionization $n_e(0) = 10^3 \text{ cm}^{-3}$ were carried out. Such initial concentration corresponds to single discharge propagation. The discharge propagation was calculated up to time $\tau = 2 \text{ ns}$. The mean velocity of the streamer was about 5 mm/ns, and typical size of single streamer was about 0.3 mm in good agreement with the experiment.

16:30

ET1 3 The gas conversion of methane with oxygen at atmospheric pressure using a cylindrical dielectric barrier discharge TOM MARTENS, DRAGANA PETROVIC, CHRISTOPHE DE BIE, ANNEMIE BOGAERTS, *Research Group PLASMANT, Department of Chemistry, University of Antwerp* WOUTER BROK, JAN VAN DIJK, *Department of Applied Physics, Eindhoven University of Technology* The conversion of methane to useful chemicals and liquid fuels currently requires steam reforming, which requires great amounts of energy input. We are currently investigating the possibilities of using a plasma activated system for this gas conversion. Due to the pulsed nature and the low operating temperature capabilities, we have chosen the atmospheric pressure dielectric barrier discharge as a setup to investigate whether it can be used as a more efficient gas conversion reactor. For this purpose we have developed a CH₄/O₂ chemical reaction set and used it in a 2D fluid model of a cylindrical dielectric barrier discharge, in which we also incorporate the influence of the gas flow. In this way we investigate whether we can optimize the production of methanol or formaldehyde. The parameters under study are the CH₄/O₂ ratio, the applied voltage characteristics, the gap width and the gas flow rate.

16:45

ET1 4 Pulsed plasma-enhanced chemical vapor deposition (P-PECVD) of silicon based materials with a low-frequency dielectric barrier discharge (DBD)* CHRISTOPHER J. OLDHAM, MATTHEW R. KING, C. RICHARD GUARNIERI, JEROME J. CUOMO, *Department of Materials Science and Engineering, NC State University* This work studied a P-PECVD process for the deposition of silicon based materials. In the process, the RF power is applied in specific "on" and "off" cycles. The process is operated in a DBD configuration at atmospheric pressure. In this pressure range, vapor phase growth typically dominates conventional processes, rather than the desired film growth. Our work has found by using the P-PECVD process, gas phase growth was eliminated and adhesion to the substrate was achieved. A growth process similar to atomic layer deposition (ALD) and conventional PECVD processing will be discussed.

*This work was funded by the Dean's office in the College of Engineering and the Department of Materials Science and Engineering

17:00

ET1 5 Development of a new plasma reactor for propene removal LINDA OUKACINE, JEAN-MICHEL TATIBOUET, *Université de Poitiers* The purpose of the study is to develop a new plasma reactor being applied to gas phase pollution abatement, involving a surface dielectric barrier discharge (SDBD) at atmospheric pressure. Propene was chosen as a model pollutant. The system can associate a SDBD with a volume dielectric barrier discharge (VDBD). A specific catalyst can be placed in post-plasma site in order to destroy the residual ozone after use it as a strong oxidant for total oxidation of propene and by-products formed by the plasma reactor. A comparative study has been established between the propene removal efficiency of these two plasma geometries. The results demonstrate that SDBD is a promising system for gas cleaning. The experiments show that ozone production depends on plasma system configuration and indicate the effectiveness of combining SDBD and VDBD. The NO_x formation remains very low, whereas ozone formation is the highest for the SDBD. The influence of some materials on the propene removal and the ozone production were studied.

17:15

ET1 6 Using Sensitivity Derivatives for Design and Computing Error Bounds in an Atmospheric Plasma Discharge Simulation* KYLE LANGE, W. KYLE ANDERSON, *Sim-Center: National Center for Computational Engineering - University of Tennessee at Chattanooga* The problem of applying sensitivity analysis to a one-dimensional atmospheric radio frequency plasma discharge simulation is considered. The derivations of forward mode direct differentiation and the reverse mode adjoint method are presented. Sensitivity derivatives computed from these methods are then shown to match derivatives computed using

finite differences. It is then demonstrated how sensitivity derivatives can be used within a design cycle to change experimentally variable quantities so as to increase or decrease a given cost function. It is also shown how sensitivity derivatives of rate and transport parameters can be used to compute error bounds for the computation of a given cost function. Finally, it is described how sensitivity analysis could be used in conjunction with experimental data to obtain better estimates for rate and transport parameters.

*Funding provided by Tennessee Higher Education Commission.

SESSION ET2: NEGATIVE ION PLASMAS

Tuesday Afternoon, 14 October 2008; Salon A-D at 16:00
Nicholas Braithwaite, The Open University, UK, presiding

Invited Papers

16:00

ET2 1 Discharges In Electronegative Gases.

R.N. FRANKLIN, *The Open University, Oxford Research Unit, UK*

This talk will come in three parts. First, the early work in electronegative plasmas, principally by Emeleus and co-workers in Iodine, and by Massey and co-workers in Oxygen. They were at opposite ends of the "spectrum" of electronegativity - the ratio of negative ion density to electron density. Secondly, we cover in more detail work in Oxygen, where in retrospect we know that too many parameters were included to reveal the underlying structure of electronegative plasmas. That is associated with Edgley and von Engel, and later with Ferreira and co-workers. From there until the present day we describe work coming from different directions, showing that by questioning prior assumptions, we have arrived at our present understanding. The basic elements are, that in general there is a negative ion core, surrounded by a conventional plasma, and that at low pressures the situation is significantly different from higher pressures. The talk will seek to avoid mathematical complexity and concentrate on the physics, explaining the reason for previous differences, and show the way forward for a more Complete understanding of the very complex problem of strongly electronegative plasmas and their structure when diluted by rare gases. All of this involves a multiplicity of ion species of both signs, and a variety of reaction rates.

16:30

ET2 2 Electronegative Plasma Discharge Equilibria.

ALLAN J. LICHTENBERG, *University of California, Berkeley - Electrical Engineering*

The equilibrium of electronegative discharges is studied in the plane-parallel approximation over a wide range of pressure and electron densities, encompassing a number of regimes that have previously been modeled analytically. The transitions between the various regimes (models) have been determined in the input parameter space. It is shown that for a given feedstock gas, these transitions can be found in terms of the two input parameters pl_p and $ne0lp$, where p is the pressure, $ne0$ the electron density, and lp the system half-length. Here $ne0$ is used as a convenient input related to the power, and the conversion from electron power to $ne0$ is given. The input parameter space is partitioned by whether ion flux to the wall or positive-negative ion recombination is the dominant positive ion loss mechanism. For each of the principal regimes, scaling laws are developed for the most important plasma parameters in terms of the input parameters. Extensions to 2D discharges and to plasmas with axial magnetic fields are briefly considered.

Contributed Papers

17:00

ET2 3 Global Models for Electronegative Discharges

DEREK D. MONAHAN, MILES M. TURNER, *Dublin City University, Ireland* The first step towards understanding a complex plasma is usually to develop a zero-dimensional or global model. This is difficult when the plasma is electronegative, because the literature contains many proposed models with different and sometimes contradictory detailed assumptions, and different domains of applicability. The appropriateness of such models in a given context

is often hard to assess. In this paper, we present a set of detailed kinetic simulations spanning a wide of range of parameters, especially with respect to electronegativity, collisionality, and type of negative ion destruction mechanism. We use these simulations as a benchmark to investigate the validity of a variety of proposed models for electronegative discharges. We reach two important conclusions: (i) that an accurate electron kinetics model is more important than any consideration relating to plasma transport in the presence of negative ions and (ii) that there exists a simple and

robust transport model that is in reasonable agreement with all of our benchmark simulations, when the electrons are treated properly. We therefore commend this approach as likely to offer reasonable accuracy for modelling any electronegative discharge where a global model is likely to be useful.

17:15

ET2 4 Negative Ion Extraction from a Pulsed NF₃ Plasma SVETLANA RADOVANOV, LUDOVIC GODET, RAJESH DORAI, VIKRAM SINGH, *Varian Semiconductor Equipment Associates* Negative ions that are ordinarily trapped inside a plasma can be extracted during the afterglow period immediately following the end of a pulse. During this time the ratio of negative ions to electrons dramatically increases because of the electrons higher mobility, enabling them to reach the walls more promptly than the ions. In the later phase of the afterglow an ion ion plasma is formed and negative ions become the dominant negative charge carriers. In this paper we report time resolved measurements of negative ion energy distributions during the on and off period of a pulsed radio frequency inductively coupled discharge at pressures from 20 to 150 mTorr of NF₃, peak powers of 1-3 kW at pulse repetition frequencies between 1 and 10 kHz and duty cycles of 20 to 70%. We show a large flux of negative ions immediately following plasma turnoff. We find that RF pulse repetition frequency, duty cycle and power, can be adjusted to produce efficient negative ion formation. These parameters also control the transition from electron-ion to ion ion plasma. We also show a comparison to a Hybrid Plasma Equipment Model of the steady state plasma properties during the on period and comment on the transient effects observed.

SESSION FTP1: POSTER SESSION I (19:00-21:30)

Tuesday Evening, 14 October 2008

Salon F-J at 19:00

I. Langmuir, presiding

FTP1 1 Inductively coupled plasmas This abstract not available.

FTP1 2 Probe measurements and optical emission spectroscopy in inductively coupled RF Ar/C₄F₈/O₂ discharges TAKASHI KIMURA, HATSUYUKI HANAKI, *Nagoya Institute of Technology* Measurements with a Langmuir probe and optical emission spectroscopy combined with actinometry are carried out in inductively coupled RF Ar/C₄F₈/O₂ discharges at the total pressure lower than 30mTorr for the Ar content ranging from 60% to 90%. Plasmas are produced in the cylindrical stainless steel chamber with 160 mm in inner diameter and 80 mm in length, where the power injected into the plasma is 140W. The structure of the measured electron energy probability functions can be changed from a Druyvesteyn distribution to a Maxwellian one as the Ar content decreases. The electron density measured at each fixed Ar content gradually decreases with increasing the O₂ content, whereas the measured effective electron temperature is not sensitive to the O₂ content. The atomic fluorine density measured at each fixed Ar content has the local maxima when the ratio of the O₂ content to C₄F₈ one is 0.3 and 0.7-0.8, whereas it has the local minimum when the ratio is about 0.6. The atomic oxygen density measured at each fixed Ar content decreases with the decrease in

the O₂ content, and then can not be deduced from the optical emission spectroscopy when the O₂ content is lower than C₄F₈ content. This work is partially supported by Grant-in-Aid from the Japan Society for the Promotion of Science.

FTP1 3 Effect of Oxygen on Ar metastables in inductively coupled plasma in O₂/Ar YUICHIRO HAYASHI, CHRISTIAN SCHARWITZ, TOSHIKI MAKABE, *Keio University* Oxygen plasma is widely used in material processing, and oxygen gas diluted by rare gases is employed for many practical reasons. In the present work we experimentally investigate the influence of the rare gas Ar in admixture of Oxygen and Ar by using optical emission and absorption spectroscopy. We have measured the density of Ar metastables (1s₅, 1s₃) in ICP at 13.56 MHz in O₂/Ar at 100 mTorr as functions of mixture ratio of O₂ (0-20 %) and dissipated power (50-150 W) by using laser absorption spectroscopy. The density of Ar metastables has a peak as a function of gas mixture at any power condition, and each of peak values has a similar magnitude of $1.8 \times 10^{11} \text{ cm}^{-3}$. At low percentage of Oxygen the density decreases with increasing the power, while at higher Oxygen content the density increases with increasing the power. The characteristics will imply that the collision and reaction processes for Ar metastable will differ at both of regions in the ICP.

FTP1 4 A reverse-blocking effect of antiparallel magnetic fields on electron transport in gas HIROTAKE SUGAWARA, *Hokkaido University* In order to analyze fundamental features of electron conduction in a magnetically neutral loop discharge (NLD) plasma, electron transport in CF₄ at 0.67 Pa along a magnetically neutral channel (NC) between gradient antiparallel **B** fields were simulated by a Monte Carlo method. The **B** field was set as $(B_x, B_y, B_z) = (0, 0, \hat{B}x)$ ($\hat{B} = \text{const} > 0$) to let the y-z plane be the NC as a simplified model of the electron path in the NLD plasma, and the **E** field was applied as $(E_x, E_y, E_z) = (0, E, 0)$ ($E = \text{const}$). Two modes of electron transport were observed. When $E < 0$, the electrons drifted in the $-E$ direction. They were confined near the NC and their spatial distribution $f(x)$ was a Gaussian with a standard deviation $\sigma_x \propto \hat{B}^{-1/2}$. The values of the mean electron energy $\bar{\epsilon}$, the effective ionization frequency ν_i , the average velocity W_y and the centroid drift velocity W_T were close to those in dc **E** fields without **B** field at the same E/N . The diffusion coefficients D_y and D_z were also close to the longitudinal and transverse diffusion coefficients D_L and D_T in the dc **E** field, respectively, but $D_x \approx 0$. In contrast, when $E > 0$, the electrons were led into the regions of stronger **B** field by the $\mathbf{E} \times \mathbf{B}$ drift away from the NC and they hardly drifted in the $-E$ direction because of the gyration. The parameters decreased slowly and their equilibrium values were not available in a trace up to 7.3 μs , but only D_x had its equilibrium value E/\hat{B} .

FTP1 5 Interaction Analysis of Multi-frequency RF powers in Dual Coil Inductively Coupled Plasma Etcher HEEYEOP CHAE, HAEGYOO CHANG, *Department of Chemical Engineering, Sungkyunkwan University, Suwon, 440-746, Korea* KUN JOO PARK, ROBERT KIM, *DMS Co., Ltd., Suwon, 445-810, Korea* In commercial plasma etching systems, more than one radio-frequency (RF) frequency powers are introduced to increase the controllability of the degree of dissociation, ion density, ion energy, uniformity and so on. In this work, the interaction within

multiple RF frequency was analyzed in a dual coil inductively coupled plasma system. 2MHz and 27MHz dual RF powers were introduced to the bottom electrode and 13.56MHz RF power was introduced to the dual coil on the top of the plasma chamber. Plasma density was determined by noninvasive plasma probe and ion energy was determined by measuring voltage waveform. The blanket silicon dioxide film was etched by Ar plasmas and photoresist film was etched by O₂ plasmas. Based on the physical and chemical analysis of blanket film analysis, the interaction of multi-frequency RF powers was analyzed in various process regimes.

FTP1 6 Spatio-temporal studies of argon metastables at the mode transition in an inductively coupled plasma* A.M. DALTRINI, S.A. MOSHKALEV, *Universidade Estadual de Campinas- Unicamp, Campinas, Brazil* T.J. MORGAN, *Department of Physics, Wesleyan University, Middletown, USA* R.B. PIEJAK, W.G. GRAHAM, *Centre for Plasma Physics, Queens University Belfast, Northern Ireland* Time and space resolved images of emission at 750.4 nm, 425.9 nm and 425 nm from an argon inductively coupled plasma in a GEC reference cell are reported. From line intensity ratio's information about the dynamic behaviour of the argon metastables atoms can be derived. Laser induced fluorescence has been used to determine the metastable atom densities. Maximum metastable densities are observed close to the coil and in the centre of the discharge and in the vicinity of transitions between low density (E, capacitively coupled) and high density (H, inductively coupled) modes. A rapid increase in the Ar metastable density with decreasing power was observed near the H to E mode transition. Electron temperature measurements based on line ratio measurements and Langmuir probe measurements, coupled to a model which incorporates metastable diffusion, are used to demonstrate how the spatio-temporal behaviour of the Ar metastable population influences the E-H mode transition.

*The authors acknowledge the financial support from the QUB IRCEP Distinguished Visiting Fellows Programme.

FTP1 7 Real-time measurement of electron temperatures and ion densities using self-bias effect in argon inductively coupled plasma KWANG-TAE HWANG, IK-JIN CHOI, CHIN-WOOK CHUNG, *Department of Electrical Engineering, Hanyang University, Republic of Korea* AC bias voltage was applied through a DC blocking capacitor between a probe and a signal generator. Self-bias potentials were changed with the amplitude of AC bias voltage, electron temperatures and ion densities. The electron temperature and ion density were measured from the variations of the self-bias potentials at various RF powers (100-500W) and pressures (5-50mTorr). The experimental results were in good agreement with those from Langmuir probes.

FTP1 8 Real time feedback control of plasma density by using a floating probe in inductively coupled plasmas SUNG-HO JANG, JIN-SUNG KIM, MIN-HYONG LEE, CHIN-WOOK CHUNG, *Electrical Engineering, Hanyang University, Republic of Korea* A real time feedback control of plasma density was carried out experimentally in inductively coupled plasma (ICP). The plasma density was measured by a floating probe (P&A Solutions, Wise probeTM) which can measure the plasma density in real time without plasma perturbation installed on a chamber wall,

and the measured information was fed back to actuator to influence the plasma density. This plasma control system allowed the plasma density to reach and keep the desired densities below 0.1% of the state error. To describe External disturbances, the pressure of the chamber was dropped from 10 mTorr to 5 mTorr by using a molecular flow controller. At the pressure disturbance, the density decreases, and recovers with 1.5% of the maximum error and 10 s of the settling time. In the comparison of active and inactive control with pressure disturbance, the maximum state errors were 1.5% and 40% respectively.

FTP1 9 Experimental investigation on Edge-to-Center density ratio in an inductively coupled plasma GUN-HO KIM, SUNG-HO JANG, CHIN-WOOK CHUNG, *Department of Electrical Engineering, Hanyang University, Republic of Korea* The plasma densities at the edge and center of a chamber in an inductively coupled plasma were measured by using a floating-type probe [1], which can measure ion density without changing sheath formation on the chamber edge. Measurements have been done in argon gas ranging in gas pressure between 5mTorr and 30mTorr. The ratios between edge and center density has been compared with theoretical ones. The Measured edge-to-center density ratios agree well with the tendency of theoretical values. It was found that the edge density has maximum values at 10mTorr, regardless of input powers. This can be understood by considering the dependence of the edge to center density ratio and center density on pressure. [1] M. H. Lee, S. H. Jang, C.W. Chung, *J. of Applied Physics*, 101, 033305 (2007)

FTP1 10 MATERIAL PROCESSING IN LOW PRESSURE PLASMAS: ETCHING, DEPOSITION, NEW MATERIALS

FTP1 11 Correlation between plasma OES and properties of B-doped polycrystalline diamond films* ALEXANDER PAL, MAXIM BELOUSOV, VIKTOR KRIVCHENKO, PAVEL MINAKOV, ALEXANDER RAKHIMOV, NIKOLAY SUETIN, VASILY SEN', Boron is effective ligand creating p-type conductivity in diamond. If diamond film has been created by MW-PECVD, the doping process can be realized by adding B-contained substance to the working mixture. At the same time morphology and doping level in many respects depend on processes occurring in MW plasma during film growth. These processes may be controlled by in-situ diagnostics of optical emission spectra (OES) of plasma. In this work we in-situ investigated OES of MW plasma in the region from 200 to 800 nm during B-doped polycrystalline diamond films (PDF) growth. Special attention was given to analysis of intensity of 249.7 nm line corresponding to 3s-2p transition of B atom. Relative intensity of this line allowed to measure amount of B in plasma. Hydrogen combined with ethanol and additives of trimethylborate was used as gas working mixture. All samples were grown on Si substrate (100) orientation. The morphology and B doping level of grown films were investigated by Raman spectroscopy using 532 nm laser radiation with power of 40 mW. Correlation dependences between OES features and Raman spectra along with temperature estimation of MW plasma were defined.

*The work was supported by ISTC, project 2968.

FTP1 12 Remote Plasma Assisted, Low-Temperature SiO₂ growth on SiC for MOS Device Applications J.M. WILLIAMSON, B.A. TOLSON, *Innovative Scientific Solutions, Inc., Dayton, OH 45440* S.F. ADAMS, J.D. SCOFIELD, *Air Force Research Laboratory, Wright-Patterson AFB, OH 45433* SiC is an attractive material for semiconductor device applications in environments too harsh for normal Si-based semiconductors. It has high thermal conductivity and breakdown electric field strength enabling high power and temperature operation. SiO₂ is readily grown on SiC by high-temperature (~ 1200 [r]C) thermal oxidation, but defect densities in the SiO₂/SiC interface limits device performance. Plasma-assisted oxidation of SiC is being investigated as a low-temperature alternative to thermal SiC oxidation to produce MOS devices with lower defect densities. SiC wafers were oxidized with a remote microwave plasma in an O₂ / Ar gas mixture at temperatures much lower than thermal oxidation. Recent results of the plasma assisted oxide growth process have shown significant improvement, with SiO₂ layers in excess of 600 Å at growth temperatures near 300[r]C. Results will be presented of the plasma assisted SiC oxidation including plasma optical diagnostics and oxide layer characterization.

FTP1 13 Modeling the direct injection of binary liquid droplets into low-pressure environments and plasmas IQBAL SARAF, DAISUKE OGAWA, MATTHEW GOECKNER, LAWRENCE OVERZET, *UT Dallas* We will present simulation results obtained from a model describing binary droplet evaporation in low pressure plasmas. The time required for a droplet to evaporate is a function of background pressure, initial T, droplet-vapor interactions, solute mole fraction and initial droplet size. A 25 μm radius droplet of hexane evaporates in less than 3 seconds at 100mTorr without plasma. The addition of plasma can decrease the evaporation time by more than an order of magnitude. We find that the evaporation time depends weakly on background pressure, gas temperature and electron temperature in presence of plasma; however, it strongly depends upon the plasma density. In addition, the model predicts that the temperature of the injected droplet first decreases by evaporative cooling (to ~ 200 K for hexane); however, once the solvent has fully evaporated, the plasma heats any remaining solute. As a result, the temperature can first fall to 200K then rise to nearly 700K in less than a second at a plasma density of 10^{11} cm⁻³.

FTP1 14 Inductively coupled plasma assisted RF magnetron sputtering synthesis of *n-p*-type ZnO QIJIN CHENG, *The University of Sydney* SHUYAN XU, SHIYONG HUANG, BISHUANG CHUA, JIDONG LONG, *Nanyang Technological University* EUGENE TAM, *The University of Sydney* KOSTYA OSTRIKOV, *CSIRO PLASMA SOURCES AND APPLICATION CENTER TEAM, PLASMA NANOSCIENCE TEAM*, Al- and N-doped ZnO thin films have been deposited on glass substrates using an inductively coupled plasma assisted RF magnetron sputtering deposition system. The electrical, optical and structural properties of the deposited films have been investigated using various characterization tools. At the optimum deposition conditions, room-temperature Hall effect measurements show that Al-doped ZnO is *n*-type with an electron concentration of 3.74×10^{18} cm⁻³ and mobility of 1.42 cm²V⁻¹s⁻¹, while the N-doped ZnO is *p*-type with a hole concentration of 3.32×10^{18} cm⁻³ and mobility of 1.31 cm²V⁻¹s⁻¹. XRD measurements show that both of Al-

and N-doped ZnO films are polycrystalline with the hexagonal structure, having a strong (002) preferential growth orientation. The two-layer structured ZnO *p-n* homojunctions have been fabricated on a glass substrate by depositing the Al-doped *n*-type ZnO film on the N-doped *p*-type ZnO film. The current-voltage measurements reveal a typical diode characteristic with a turn-on voltage at about 1.2 V under forward-biased voltage and a low leakage current under reverse-biased voltage.

FTP1 15 Mechanism of Niobium Etching in Ar/Cl₂ Microwave Discharge* J. UPADHYAY, M. RASKOVIC, S. POPOVIC, L. VUSKOVIC, *Department of Physics, Old Dominion University* L. PHILLIPS, A.-M. VALENTE-FELICIANO, *Thomas Jefferson National Accelerator Facility* Plasma based Nb surface treatment provides an excellent opportunity to eliminate surface imperfections [1] and increase cavity quality factor in important applications such as particle accelerators and cavity QED, as well as Josephson junctions [2]. We used a microwave glow discharge in Ar/Cl₂ mixture to remove impurities and mechanical damages from the surface of bulk niobium samples. The high etching rates, in the order of 1 μm/min were obtained using a less than 3%Vol concentration of Cl₂ gas. The etching rate dependence on discharge parameters such input power density, pressure and Cl₂ concentration was determined. Simultaneously, plasma emission actinometry was used to estimate the absolute densities of Cl, Cl⁺ and Cl₂ in the variable plasma conditions. This results, combined with results of discharge diagnostics, were used to determine the plasma etching mechanism. [1] M. Raskovic, et al., *Nuclear Instruments and Methods in Physics Research A* 569 663–670 (2006). [2] S. Gleyzes, et al., *Nature* 446, 297 (2007).

*Supported by DOE

FTP1 16 Novel Helmholtz-Inductively Coupled Plasma Source for Nano-scale MOSFETs KUN-JOO PARK, KEE-HYUN KIM, WON-MOOK LEE, *DMS Co., Ltd, #402, Sungshin Techno-Park Bldg. 509-7, Suwon, 443-803, Korea* HEEYEOP CHAE, *Dept. of Chemical Eng., SungKyunKwan Univ., Suwon, 440-746, Korea* IN-SHIK HAN, HI-DEOK LEE, *Dep. of Electronics Eng., Chungnam National Univ., Yuseong, Daejeon, 305-764, Korea* As the minimum feature size of MOSFET was continuously scaled down to the nano-scale regime, fine patterning using plasma etching process has become crucial in fabricating ULSI devices. Novel Helmholtz coil inductively coupled plasma (H-ICP) etcher is proposed and characterized for deep nano-scale CMOS technology. Various hardware split tests such as the distance between top and bottom coils, the distance between chamber ceiling and wafer, and the chamber height are applied for optimal design of the chamber or process condition. The uniformity is significantly improved using the optimum conditions. The plasma density obtained with H-ICP source was about 5×10^{11} /cm³, and electron temperature was about 2~3eV. The etching selectivity of polysilicon gate to ultrathin gate oxide is 482:1 with 10sccm of HeO₂. In this work, a novel H-ICP source was proposed for plasma etching with high uniformity and high selectivity suitable for nano-scale semiconductor devices. Various kinds of split were applied and the optimum condition was successfully applied for formation of nano-scale poly gates. The proposed H-ICP is successfully applied for formation of under 60 nm gate layers.

FTP1 17 Meter-Scale Microwave Plasma Production and its Application to Silicon Thin Film Deposition HIROTAKA TOYODA, YUDAI TAKANISHI, HIROTAKA ENDO, TATSUO ISHIJIMA, *Nagoya University* There has been a great need for meter-scale plasma sources for giant materials processing, such as thin film transistor manufacturing for meter-size liquid crystal display (LCD), deposition of silicon thin films for photovoltaic power generation and so on. Recently, we have developed a new technology for production of surface wave excitation [1]. In this paper, we demonstrate production of meter-scale large-area plasma with multiple waveguide lines. In the experiment, microwave power (< 30 kW) is coupled to the plasma through power divider, multiple waveguide lines and slot antennas. Optical and Langmuir probe measurements of Ar/H₂ plasma show production of very uniform plasma at a plasma density of $3.4 \times 10^{11} \text{ cm}^{-3}$ and a variance of 2% within an area of 0.9 m x 0.9 m. With use of carefully-designed gas manifold, microcrystalline silicon films are deposited on sample substrates. Deposition rate of ~ 0.3 nm/s with a variance of less than 10 % is obtained within an area of 0.6 m x 0.7 m. Uniformity of film quality such as film crystallinity is also confirmed. [1] H. Sugai, Y. Nojiri, T. Ishijima and H. Toyoda, 6th Int. Conf. on Reactive Plasmas and 23rd Symp. on Plasma Processing, (Matsushima, 2006), p.17.

FTP1 18 Effects of High Energy Ar Ions on Synthesis of Carbon Nanowalls SHINGO KONDO, OLIVERA STEPANOVIC, MAKOTO SEKINE, MASARU HORI, *Nagoya University* KOJI YAMAKAWA, SHOJI DEN, *Katagiri Engineering Co., Ltd.* MINEO HIRAMATSU, *Meijo University* Carbon nanowalls (CNWs) are composed of graphene sheets standing vertically on the substrate. In order to apply CNWs to various industrial fields, clarification of the growth mechanism is strongly required. In this study, the new apparatus of two radical sources with an ion source was constructed in order to understand the fundamental studies of growth of CNWs. In particular, we have focused on which radicals or ions contributed to the CNWs formation. The Si substrate heated at 580°C was exposed to fluorocarbon (CF_x) and H radicals, which were generated from C₂F₆, H₂ gases, in addition to Ar ions. In the case of Ar ion irradiation at an acceleration of 200 V with CF_x and H radicals at 2.5 Pa, CNWs of 30 nm in height were formed in 25 min. On the other hand, the CNW growth was not confirmed in the cases without Ar ion irradiation and with Ar irradiation at 100 V. From these results, it was found that the threshold of ion energy bombardment for synthesis of CNWs was 100 V. The effects of Ar ions on CNWs formation will be presented.

FTP1 19 Deposition of single and layered amorphous fluorocarbon films by C₈F₁₈ PECVD TATSUYA YAMAUCHI, KOUICHIRO MIZUNO, HIROTAKE SUGAWARA, *Hokkaido University* Amorphous fluorocarbon films were deposited by plasma-enhanced chemical vapor deposition (PECVD) using C₈F₁₈ in closed system at C₈F₁₈ pressures 0.1–0.3 Torr, deposition times 1–30 min and plasma powers 20–200 W@. The layered films were composed by repeated PECVD processes. We compared 'two-layered' and 'intermittently deposited' films, which were made by the PECVD, respectively, with and without renewal of the gas after the deposition of the first layer. The interlayer boundary was observed in the layered films, and that of the intermittently deposited films showed a tendency to be clearer when the deposition time until the interruption of the PECVD was shorter. The film thickness increased linearly in the beginning of

the PECVD and it turned down after 10–15 min, that was similar between the single and intermittently deposited films. It was considered that large precursors made at a low decomposition degree of C₈F₁₈ contributed to the film deposition in the early phase and that the downturn was due to the development of the C₈F₁₈ decomposition. This explanation on the deposition mechanism agrees qualitatively with our experimental data of pressure change and optical emission spectra during the deposition. This work is supported by Grant-in-Aid from Japan Society for the Promotion of Science.

FTP1 20 Modeling the chemistries of technical molecular plasmas JAMES J. MUNRO, JONATHAN TENNYSON, DANIEL B. BROWN, HEMAL N. VARAMBHIA, NATASHA DOSS, *University College London, Gower Street, WC1E 6BT, UK* Plasma chemistries, especially for molecular gases, are complicated. With a limited amount of molecular data available, it is hard to model these plasmas accurately; just a couple of feedstock gases can lead to a minimal model containing perhaps dozens of gas-phase species. The possible gas-phase and surface reactions that can occur could be in the tens of thousands; less than a hundred are typically used in chemistry models. Understanding the importance of various species and reactions to a chemical model is vital. Here we present the progress on constructing a package (Quantemol-P)[1] to simplify and automate the process of building and analyzing plasma chemistries e.g. SF₆/O₂, CF₄/O₂ and O₂/He. [1] J.J. Munro, J. Tennyson, *J. Vac. Sci. Tech. A*, accepted

FTP1 21 Surface Layers Modification of Tungsten-Cobalt Alloy by Low Pressure RF Plasmas* ILGIZAR SAGBIEV, ILDAR ABDULLIN, *Kazan State Technological University* VICTOR ZHELTOUKHIN, *Kazan State University* ROUSTEM SHARAFEEV, *Kazan State Technological University* A process of surface layer modification of tungsten-cobalt alloy by low pressure RF plasmas is investigated. Analysis of materials from 10 up to 700 nm by thickness was studied by both X-ray and auger electrons spectroscopy. There are three sublayers within the surface layer after plasma action. The outer sublayer is from 10 up to 500 nm by thickness. One consists of carbon of unordered or diamond like structure, contents of tungsten and cobalt is decreased monotonous up in surface. The transitional sublayer is from 150 up to 200 nm by thickness. Carbon state in this one correspondence to mix of C-C and C-W bonds, concentration of tungsten and cobalt is fluctuating. The modifying layer is raising to some limit at increasing the time of plasma action.

*Supported by RFBR, grant No. 07-01-00674a.

FTP1 22 Characterization of PET Samples Processed in an RF Oxygen Discharge RUSSELL L. RHOTON, MARY L. BRAKE, *Eastern Michigan University* A radio frequency plasma (13.56 MHz) was used to modify the surface of poly(ethylene terephthalate) (PET). Optical emission spectroscopy (OES) was used to characterize the plasma and the Sessile drop method was used to determine surface changes after processing. The OES changed depending upon the pressure of the plasma. Molecules of OH and atomic oxygen were observed at low pressures (~ 0.1 torr) whereas CO and atomic hydrogen were observed at higher pres-

tures (~ 1 torr). There was an observable change in the PET samples after processing; in particular, the surface was degraded. The Sessile drop method was used to determine the relative change in the wettability of the surface along a continuum from hydrophobic to hydrophilic.

FTP1 23 ARCS, JETS AND TORCHES

FTP1 24 Supersonic flow and electric potential of argon arc jet along open-field magnetic line HIROSHI AKATSUKA, YOH NAGAHARA, KAZUYUKI YOSHIDA, TOMOHIKO SHIBATA, HARUAKI MATSUURA, ATSUSHI NEZU, *Tokyo Tech.* We report plasma parameters of argon arc jet along open-field magnetic line. The argon arc plasma is generated under atmospheric pressure, and ejected through an anode-nozzle into a rarefied wind tunnel continuously with a uniform magnetic channel of 0.16 T. The anode-nozzle is sufficiently choked to flow the plasma at its acoustic velocity. The plasma is further accelerated into supersonic flow through the open-field line. We experimentally measure ion acoustic Mach number, 2-dimensional ion velocity, plasma space potential, electron temperature and density by a para-perp and a 4-tip Mach probes. We find electric potential drop, increase in ion Mach number up to about 3, and following velocity reduction to subsonic flow. We conducted numerical modeling, where we assume the divergence of the magnetic field was equivalent to the increase in the cross sectional area of flowing channel. We introduced the deceleration model with collisions between ions and neutral particles. The model simulates the deceleration of the plasma at downstream region much better than isentropic model.

FTP1 25 Study of the Anodic Region of Electric Arcs by a Two-Temperature Model MARGARITA BAEVA, SERGEY GORCHAKOV, DIRK UHRLANDT, *INP Greifswald, Felix-Hausdorff-Str. 2, D-17489 Greifswald, Germany* Electric arcs are widely used in such industrial applications as welding, cutting and waste treatment. In order to optimize the device parameters and operation conditions, amongst others understanding of the discharge physics in the boundary regions near the electrodes is necessary. The discharge properties in these regions are influenced by evaporating material and the plasma shows strong deviations from the local thermodynamic equilibrium. For the study of the arc-anode interaction a two-temperature, multi-component model for the anodic region has been developed and applied. The non-equilibrium mixture composition, corresponding transport coefficients and thermodynamic functions of the mixtures of gas and metal vapor were determined for the parameter range of interest. The energy balance of the anode has been derived by taking into account heat fluxes from the plasma, evaporation, as well as Ohmic heating of the anode. The properties of the non-equilibrium sheath near the anode are evaluated. Results for an argon arc in the presence of copper or iron vapor are presented and discussed.

FTP1 26 3D-simulation of an ICP torch and outside vapor deposition of SiO_2 MARGARITA BAEVA, DIRK UHRLANDT, *INP Greifswald, Felix-Hausdorff-Str. 2, 17489 Greifswald, Germany* A three dimensional model of an inductively coupled plasma torch and a moving target has been developed to describe the process of SiO_2 -deposition during the manufacturing of preforms for optical fibers. The model is based on the customized CFD-ACE+ commercial package. The steady state continu-

ity, momentum and enthalpy equations are solved assuming local thermal equilibrium and laminar flow, and optically thin plasma. The energy coupling to the plasma accomplished through the electromagnetic field of an induction coil and the radiation losses from the plasma are accounted for in the discretized fluid enthalpy equation as source terms. The surface reaction governing the deposition process is included to serve as a boundary condition for the species mass fractions in the fluid. The equation of heat transfer in the substrate has been completed to account for the real motion (both translation and rotation) of the substrate. The model developed supplies information about the flow, temperature, electromagnetic field, and the deposition rate on the target surface and torch walls for real geometries. It can be applied to study the influence of various operating parameters on the deposition rate as well as optimization of equipment and productivity.

FTP1 27 Comparative simulation studies of a magnetically rotating arc MARGARITA BAEVA, DIRK UHRLANDT, *INP Greifswald, Felix-Hausdorff-Str. 2, 17489 Greifswald, Germany* Magnetically rotating arcs have been increasingly adopted in DC arc plasma devices for diagnostics and material processing, modern circuit breakers, etc. The need to study arc behavior has motivated modeling activities based on computational fluid dynamics coupled with electromagnetics. A three-dimensional model of a DC plasma torch at atmospheric pressure has been developed based on the customized CFD-ACE+ commercial package. It is applied to study the behavior of a magnetically rotating arc in argon. The simulation studies are performed comparatively in terms of 1) two-temperature description (different electron T_e and heavy particle (T) temperatures) and 2) local thermal equilibrium (LTE) ($T_e = T$). Temperature discrepancies between electron and heavy particles are found in the arc fringes and near the gas inlet. In the presence of axial magnetic field, the gas temperature gets lower in the arc core. The electron temperature profile is wider than the gas temperature one. Apart from the differences between 2-T and LTE model results, both models yield the same qualitative arc behavior. With increasing external axial magnetic field, the high temperature plasma region constrains in axial direction and expands in radial direction.

FTP1 28 Modeling of low current vacuum arc deflection under transverse magnetic field LIJUN WANG, SHENLI JIA, WEI YUAN, ZONGQIAN SHI, *State Key Laboratory of Electrical Insulation and Power Equipment, Xi'an Jiaotong University, Xi'an, 710049, China* Transverse magnetic field (TMF) electrode has been used extensively in vacuum interrupter. But, the internal physical mechanism of vacuum arc under TMF is not very clear. For vacuum arc research, it is not enough only through experiments. Currently, modeling and simulation has been regarded as a kind of promising tool to understand vacuum arc. In this paper, based on two-fluid model and Maxwell equations, magneto-hydrodynamic (MHD) model of vacuum arc under TMF is obtained. In this model, mass conservation, momentum conservation, ion energy conservation, electron energy conservation, and magnetic transport equation are included, the self-generated magnetic field of vacuum arc is also considered. The partial differential equations in the model are solved by FLUENT software. Based on this model, the deflection effect of vacuum arc under transverse magnetic field (TMF) is simulated and analyzed. As the preliminary research, deflection effect of low current vacuum arc (LCVA) under different TMF strengths is simulated in this paper. Simulation results show that the deflection effect will be increased with

the increase of external TMF. In this paper, only two-dimensional steady MHD model is used. But, some physical mechanism of TMF vacuum arc also can be disclosed through the two-dimensional model. The more complete model of TMF vacuum arc (such as transient model, three-dimensional model, and higher current vacuum arc model) should be considered in the future.

FTP1 29 Ferromagnetic Material Effects on Air Arc Behavior XINGWEN LI, RUI LI, DEGUI CHEN, RUICHENG DAI, *Xi'an Jiaotong University* The paper is devoted to study the influence of ferromagnetic material effects on arc behavior in low voltage electric apparatus. With the self-programmed interface, one 2-D magneto-hydrodynamics (MHD) arc model can be developed based on the commercial software FLUENT and ANSYS, to study the vapor of ferromagnetic material effects on air arc behavior. Then the corresponding interruption experiments are performed to verify the simulation qualitatively. It demonstrates that the vapor of ferromagnetic material is disadvantageous to arc interruption characteristics. In addition, the influence of the size of the ferromagnetic splitter plate on arc motion is simulated. It shows that the bigger splitter plate may accelerate the arc motion.

FTP1 30 Modeling the Transport Phenomena in the Solution Precursor Plasma Spraying* YANGUANG SHAN, *University of Shanghai for Science and Technology* Solution precursor plasma spraying has been used to produce finely structured ceramic coatings with nano- and sub-micrometric features. This process involves the injection of a solution spray of ceramic salts into a DC plasma jet under atmospheric condition. During the process, the solvent vaporizes as the droplet travel downstream. Solid particles are finally formed due to the precipitation of the solute, and the particle are heated up and accelerated to the substrate to generate the coating. This work describes a 3D model to simulate the transport phenomena and the trajectory and heating of the solution spray in the process. The jet-spray two-way interactions are considered. A simplified model is employed to simulate the evolution process and the formation of the solid particle from the solution droplet in the plasma jet. O'Rourke's droplet collision model is used to take into account of the influence of droplet collision. The influence of droplet breakup is also considered by implementing TAB droplet breakup models into the plasma jet model. The temperature and velocity fields of the jet are obtained and validated. The particle size, velocity, temperature and position distribution on the substrate are predicted.

*This work is supported by the National Natural Science Foundation of China (Project No. 50706027), and the Shanghai Leading Academic Discipline Project (No. J50501).

FTP1 31 Effects of Geometry and Excitation Frequency on Plasma Torch Temperature DOUGLAS SCOTT, IL GYO KOO, KAZUNARI SATO, CAMERON MOORE, GEORGE COLLINS, *Department of Electrical and Computer Engineering, Colorado State University, Fort Collins, Colorado 80523*. Temperatures of atmospheric pressure plasma jet effluent were measured spectroscopically in argon with 2% hydrogen under conditions of constant delivered power. Different inner diameters of the mm-size plasma tube, excitation frequencies from several MHz to > 100 MHz, and gas velocities resulted in measurements that indicate each of these parameters strongly affect temperature of the effluent plume. The data suggest that energy either flows in the plume or two the tube wall: plume and tube temperature are

complementary. We present a heat flow model and analysis that agrees with experimental data, and from these data we estimate the diameter of the plasma in the upstream tube. We also present spatially resolved measurements along the plasma axis.

FTP1 32 MAGNETICALLY ENHANCED PLASMAS This abstract not available.

FTP1 33 Studies on spatial structures of plasma localization under various external magnetic field and geometry parameters in capacitively coupled neutral loop discharges MURAT VURAL, FATIH SIRIN, RALF PETER BRINKMANN, *Theoretical Electrical Engineering, Ruhr-Universität-Bochum, D-44780 Bochum, Germany* The neutral loop discharge (NLD) is an RF driven low pressure discharge with three magnetic coils placed coaxially outside the vacuum chamber, generating an axisymmetric magnetic field that vanishes at the so-called magnetic neutral loop (NL). In a capacitively coupled neutral loop discharge (CCP-NLD), the accelerating electrical field is generated by applying an RF potential to external electrodes; the corresponding electric field lines are co-planar to the magnetic field lines but perpendicular to the NL. The reactor chamber has the form of a regular cylinder of different radii and constant height. This paper studies the impact on the electron density and electron energy of variations in the reactor dimensions and external magnetic field parameters in a CCP-NLD by means of spatially resolved particle-in-cell/Monte Carlo simulations. The influence of the reactor geometry and neutral gas pressures between 0.5 Pa and 10 Pa on the homogeneity and heating mechanism are also shown.

FTP1 34 The spatial and temporal variation of potentials in the HIPIMS discharge PALL SIGURJONSSON, *University of Iceland* PÉTTUR LARSSON, DANIEL LUNDIN, ULF HELMERSSON, *Linköping University* JON TOMAS GUDMUNDSSON, *University of Iceland* We describe measurements of the plasma parameters in a high power impulse magnetron sputtering (HIPIMS) discharge. A Langmuir probe is used to determine the plasma parameters, such as the electron temperature T_{eff} , the electron density n_e , the floating potential V_f and the plasma potential V_{pl} , as well as the electron energy distribution function (EEDF). The spatial and temporal variation of the plasma parameters and electron energy distribution function are recorded in the pressure range 3 – 20 mTorr. The electron density peaks at $5 \times 10^{18} \text{ m}^{-3}$ for 40 – 80 mm distance from the target surface for all pressures investigated. The electron temperature reaches its peak value of 1.5 – 3 V roughly 80 μs after pulse initiation, in the pressure range 5 – 20 mTorr. The plasma potential and the floating potential peak at the end of the pulse. We will in particular describe the spatial variation of the plasma and floating potentials at various times during the discharge.

FTP1 35 The 2nd Harmonic ECR Microplasma for Low Pressure Condition HIROSHI FUJIYAMA, AKIHIRO YUKISHIGE,*KE YAN, MASANORI SHINOHARA, *Nagasaki University* TATSUYUKI NAKATANI, *Toyo Advanced Technology* Plasma generation in narrow closed space has been succeeded for the pressure of 0.01 Torr and gap length of 500 μm in xenon gas for the 2nd harmonic Electron Cyclotron Resonance (2nd harmonic ECR). Resonant confinement of electrons at the 2nd harmonic ECR leads to interesting micro plasma characteristics: the higher electron density, the lower plasma potential, the lower elec-

tron temperature and the effective power absorption against with the well-known ECR plasma. PIC-MC simulation of low pressure micro plasma supported such interesting plasma characteristics obtained by the experiments. It was also investigated on the plasma density and temperature for various ratio of Surface Dimensions/Volume of plasma. In the experiments, it was found that the typical micro plasma characteristics: the higher electron density, the lower plasma potential, the lower electron temperature became remarkable. The ionization degree for the 2nd harmonic ECR plasma in the present research, showed about 10^{-3} by 2 order higher than that of PDP micro plasma.

*d707240k@cc.nagasaki-u.ac.jp

FTP1 36 LASERS: BREAKDOWN AND SPARKS

FTP1 37 ABSTRACT WITHDRAWN

FTP1 38 Breakdown Behavior in Air and n-Butane Mixtures Leading to Combustor Ignition Modeled using Effective Ionization Coefficients S.F. ADAMS, *Air Force Research Laboratory* A.A. KUDRYAVTSEV, S.M. POPUGAEV, *St. Petersburg State University* V.I. DEMIDOV, *West Virginia University* C.Q. JIAO, *ISSI Inc.* The process of electron attachment in electronegative air-hydrocarbon gas mixtures can be an impediment to the arc ignition process in a combustion engine. The optimized conditions to produce ignition include a gas mixture with a minimal ionization coefficient. Data on ionization rates and ion reactions in various air-hydrocarbon mixtures is necessary, though, for a proper theoretical analysis of the ignition process. The known set of cross-sections and rate constants for simple methane (CH₄) is often used and results extrapolated to heavier hydrocarbons. Recently, experimental data on cross-sections, ionization rates and ion reactions in n-butane (n-C₄H₁₀) were reported which allow for reliable models of ignition in more complex fuel mixtures. This paper presents an analysis of breakdown and ignition using air and n-butane mixtures.

FTP1 39 Frequency Effect on RF Gas Breakdown VALERIY LISOVSKIY, *Kharkov National University, 4 Svobody sq., Kharkov, 61077, Ukraine* VLADIMIR YEGORENKOV, *Kharkov National University* JACQUES JOLLY, *Laboratoire de Physique et Technologie des Plasmas, Ecole Polytechnique, Palaiseau 91128, France* JEAN-PAUL BOOTH, *Laboratoire de Physique et Technologie des Plasmas, Ecole Polytechnique* We registered rf breakdown curves of the parallel-plate capacitive discharge in the range of frequency values from 13.56 MHz to 105 MHz with the inter-electrode gap of 3 cm and in the hydrogen pressure range of values from 0.001 to 1 Torr. Rf breakdown curves for the frequencies up to 40 MHz possess the diffusion-drift branch with a multi-valued section, then with lowering the pressure the Paschen and multipactor branches are observed. For higher frequency values the diffusion drift branch assumes a U-shaped form, it does not possess a multi-valued section and transforms directly to the multipactor branch. On increasing the frequency the rf breakdown voltage of the multipactor branch grows linearly, and the minimum of the diffusion-drift branch is shifted to the range of higher gas pressure and rf voltage values.

FTP1 40 The effect of the ion-enhanced field emission on the CF₄ discharges in microgaps* MARIJA RADMILOVIC-RADJENOVIC, BRANISLAV RADJENOVIC, *Institute of Physics, Belgrade-Serbia* Recently, much attention has been paid to studies on CF₄ due to its practical utility as a feed gas for plasma etching in the semiconductor industry. In order to reduced feature sizes on microelectronic devices, it is necessary to determine the breakdown voltage in microgaps. In this paper, semi-empirical expression for the breakdown voltage based on the numerical solutions of the equation that describes the DC breakdown criteria in CF₄ microdischarges has been suggested.

*The present work has been carried out under MNZZS 141025 project.

FTP1 41 Two-dimensional Effects in High Power Microwave Breakdown SANG KI NAM, CHUL-HYUN LIM, JOHN VERBONCOEUR, *University of California Berkeley* A major limiting factor in transmission of high power microwave radiation is dielectric window breakdown. A one-dimensional particle-in-cell/Monte Carlo collision (PIC/MCC) model was used to study dielectric window breakdown from vacuum multipactor to collisional microwave discharge for noble gases [1]. It showed that multipactor on the dielectric window drives breakdown at low pressure, and volumetric collisional ionization is the main mechanism for breakdown at high pressure. A Monte Carlo (MC) model was also used to investigate dielectric window breakdown in two-dimensionals, including spatial variation of the microwave electric field in transverse direction [2]. The breakdown times were consistent with their experiment data and also showed the interesting feature of electron clusters above the window. MC, however, is not self-consistent and neglects the space charge effect resulting from the charge build-up. In this work, two-dimensional PIC/MCC was employed to investigate the breakdown in oxygen including the space charge effect. [1] H.C. Kim, and J.P. Verboncoeur, *Phys. Plasmas*, 13, 123506(2006). [2] J.T. Krile, A.A. Neuber, and H. G. Krompholz, *Appl. Phys. Lett.*, 89, 201501(2006).

FTP1 42 Simulation of a streamer breakdown in air SERGEY PANCHESHNYI, AICHA FLITTI,* *LAPLACE, University of Toulouse, CNRS, France* GEORGE NAIDIS, *Joint Institute for High Temperatures RAS, Russia* A numerical code that uses an adaptive grid refinement strategy for the computation of filamentary discharges within the diffusion-drift approximation in 2D and 3D geometry was applied for streamer simulation. The numerical discretization are based on finite volume methods and have 2nd order accuracy in space and time. The main stages of streamer discharge development in air are presented up to the moment of spark formation. In the case of fast breakdown, the plasma conductivity increases thanks to the accumulation of active particles that changes the balance between the rates of generation and loss of electrons due to the acceleration of processes such as detachment, stepwise, and associative ionization, etc. The evolution of plasma composition after the channel bridges the gap has been simulated using ZDPlasKin library in 0D approach; the kinetic model includes 14 components and 48 reactions. This approach exhibits a good agreement with measurements and can be easily applied for other gases and conditions.

*Permanent address: University of Science and Technology of Oran, Algeria

FTP1 43 Branching Patterns in Multi-Atmospheric Pressure Corona Discharges With Positive and Negative Bubbles NATALIA YU. BABAEVA, *University of Michigan* MARK J. KUSHNER, *Iowa State University* The branching of streamers occurs in most high pressure gases and liquids. One mechanism for streamer branching may be inhomogeneities in the path of the streamer – a solid particle, aerosol or a region of different density, one extreme being a bubble in a liquid. To lend insights into how positive (an included volume of higher density) or negative (volume of lower density) bubbles might produce branching in high pressure gases, we computationally investigated the role of randomly distributed bubbles on the propagation of a streamer in atmospheric (and greater) pressure humid air. The plasma hydrodynamics model, *nonPDPSIM*, uses an unstructured mesh to simultaneously resolve reactor scales and bubbles. Radiation transport, and photoionization in bubbles are included by implementing a Green's function propagator. Positive streamers encountering a single slightly negative bubble in its path tends to converge into the bubble that has a higher rate of ionization. Streamers encountering slightly positive bubbles tend to branch around the regions of lower ionization. Photoionization producing electrons in remote highly negative bubbles which have a proportionally larger E/N can lead to remote sources of plasma that launch their own streamers. If the bubbles are within a few photon absorption lengths of the streamer (or other bubbles), these streamers may link together.

FTP1 44 Kinetic Model of a Nanosecond Afterglow in Air SARA ABBATE, DENIS PACKAN, ALAIN BROCC, *ONERA* CHRISTOPHE LAUX, *Ecole Centrale Paris* In recent decades an active interest has been shown for applications of non equilibrium plasmas to combustion. Many laboratories in Europe, US and the former Soviet Union have achieved combustion improvements by using plasma technologies, in particular nanosecond discharges due to their energy-efficient excitation of mixtures. Major effects have been noticed in the reduction of the delay time of combustible mixtures, along with auto ignition and stabilisation of flame in lean mixtures. Different mechanisms have been proposed in the literature to explain the observed effects and to build on the experiments, but a complete understanding of the principles is still lacking. The aim of our work is to develop a tool for the numerical simulation of the discharge and after-glow phenomena in a pulsed discharge scheme, with an emphasis on kinetics and plasma phenomena, in order to understand the role of plasmas in the combustion processes. Since recent experiments have demonstrated the fundamental role played by electronically and vibrationally excited air species to enhance combustion [1], we develop a complete vibrationally-specific kinetic scheme in air environment. The kinetic model is validated by mean of experimental measurements. [1] G. Pilla, C. Laux PhD Thesis 21/01/08

FTP1 45 GLOWS: DC, PULSED, RF, MICROWAVE, INDUCTIVE, OTHERS

FTP1 46 Experiment and global model of inductively coupled RF Ar/N₂ discharges TAKASHI KIMURA, HIROKI KASUGAI, *Nagoya Institute of Technology* Plasmas containing N₂ have been attracted as a source of active species such as the active atomic nitrogen and the excited nitrogen molecules in the field of material science. In this study, measurements with a Langmuir probe and optical emission spectroscopy are carried out in inductively coupled RF (13.56 MHz) Ar/N₂ discharges in the total pres-

sure range from 20mTorr to 100mTorr, changing the N₂ content from 5% to 50%. Plasmas are produced in the cylindrical stainless steel chamber with 160 mm in inner diameter and 40 mm in length, where the power injected into the plasma is 200W. The structure of the measured electron energy probability function (EEPF) can be approximated as a Druyvesteyn-like distribution at any N₂ content. The electron density, which is on the order of 10^{16} - 10^{17} (m⁻³), increases with increasing the Ar content, whereas the effective electron temperature slightly decreases. The vibrational and rotational temperatures can be estimated from the optical emission spectroscopy of N₂ second positive system. The vibrational temperature is higher than 10000K at any experimental condition, and the rotational temperature monotonically increases from 500K to 1000K with the increase in the Ar content. Moreover, the N₂ dissociation rate, which corresponds to the density ratio of N to N₂, can be estimated by actinometry. The dissociation rate reaches the maximum when the Ar content is about 85%.

FTP1 47 Fluid modelling and analysis of the constriction of the dc positive column in argon MYKHAYLO GNYBIDA, DETLEF LOFFHAGEN, DIRK UHRLANDT, *INP Greifswald, Felix-Hausdorff-Str. 2, 17489 Greifswald, Germany* A self-consistent fluid model describing the positive column of a DC argon discharge was developed. This model consists of the coupled solution of balance equations for the charge carriers, excited species, mean electron energy, and gas temperature in the plasma, Poisson's equation for the radial potential, and a current balance determining the axial electric field. Different assumptions concerning the electron energy distribution function (EEDF) were adapted to calculate electron transport and rate coefficients as a function of the electron mean energy. Simulations were carried out for currents from 1 to 100 mA and pressures from 100 to 500 Torr. The predicted voltage-current characteristics and electron density profiles are used to identify the transition from glow to constricted mode of the argon discharge. The results are compared with data from experiments. The impact of the various assumptions for the EEDF (Maxwellian, Druyvesteyn, solution of 0D Boltzmann equation with and without inclusion of electron-electron collisions) is discussed. The influence of cumulative ionization, electron-electron collisions, and gas heating in forming the EEDF as well as electron-ion recombination are found to be main reasons for the constriction of the glow discharge.

FTP1 48 Normal Mode of DC Glow Discharge VALERIY LISOVSKIY, *Kharkov National University, 4 Svobody sq., Kharkov, 61077, Ukraine* NADIYA KHARCHENKO, VLADIMIR YEGORENKOV, *Kharkov National University* We registered the normal current density j of the dc glow discharge in the nitrogen pressure range $p = 0.3 - 10$ Torr and determined the quantity j/p^2 . Experiments were carried out in a T-shaped tube, the cathode was located at one end of the horizontal part of T, whereas another electrode (anode at the bottom of T) was grounded. Photos were taken through a window at the opposite end of the horizontal part of T exposing the cathode and the images were digitized. According to a generally accepted opinion this quantity j/p^2 had to remain constant on varying the current I in the normal mode. This proved to be valid only for $p < 1$ Torr. At higher pressure values the current growth was accompanied with a decrease of the quantity j/p^2 . In a plasma column of small cross section the current density is larger to compensate for the increased loss of charged particles from the discharge volume.

FTP1 49 VI characteristics and spatial emission profiles of hollow cathode discharge N. ŠKORO, D. MARIC, G. MAL-
 OVIĆ, Z. LJ. PETROVIC, *Institute of Physics, Belgrade, Serbia*
 V. MIHAILOV, R. DJULGEROVA, *Institute of Solid State Phys-
 ics of Bulgarian Academy of Sciences, Sofia, Bulgaria* Our aim is
 to relate electrical properties of the hollow cathode devices to the
 spatial structure of the discharge, including discharge formation
 period. Special attention was given to the development of the
 hollow cathode effect. Commercial hollow cathode lamp sealed at
 3.5 Torr (Ne) with cylindrical Mn cathode with bottom and a ring
 shaped anode was used. We measured VI characteristic and using
 emission profile images established current dependence of the
 peak emission intensity of the discharge. According to our data,
 hollow cathode discharge can be represented as a combination of
 discharges between parallel plates and inside the cavity. As the
 hollow cathode effect develops, the discharge moves from the
 cathode edge into the cavity, while the current density and emis-
 sion intensity increase significantly. At the same time, the dis-
 charge voltage decreases. We were able to trace in time the dis-
 charge formation in several distinctive regimes of operation. Thus,
 we could connect certain points in transient phase with discharge
 spatial structure, revealing the discharge behavior.

**FTP1 50 Temperature Effects on Propagating Shock Waves in
 Glow Discharge Plasmas*** NIRMOL PODDER, AARON LO-
 CASCIO, *Troy University, Troy, AL* The time-history of the shock
 wave propagation in glow discharge plasma starting from the
 plasma switch-on or switch-off is produced. After a few tens of ms
 of the plasma switch-on, the photo acoustic deflection (PAD) pro-
 files of the laser beams produced by the shock-front gas density
 gradients show increased signs of broadening, and both the shock
 wave propagation velocity and the laser deflection width start to
 increase nonlinearly as the temperature of the discharge is ex-
 pected to rise from its room temperature value, and quickly reach
 their relatively fixed steady-state values at about 120 ms after the
 switch-on of the glow discharge at fixed discharge current 35 mA
 and gas pressure 15 Torr. At the plasma switch-off, the trend in the
 propagation velocity is reversed linearly, and that in the deflection
 width non-linearly as the afterglow plasma cools rapidly to its
 room temperature.

*This work is supported by the DOE.

**FTP1 51 Characteristics of a Propagating Shock Wave in Gas
 Discharges*** AARON LOCASCIO, NIRMOL PODDER, *Troy
 University, Troy, AL* LANE ROQUEMORE, *Princeton Plasma
 Physics Lab* Acoustic shock waves are launched in both neutral
 and ionized gases and their properties are measured with pressure
 sensors, laser beams, and a high-speed camera. The pressure sen-
 sors yield information on the total gas pressure, the deflection of
 the laser beams gives an indication of the gas density, and the
 high-speed camera captures the dynamics of the propagating
 shock wave. Shock wave propagation velocities (\sim Mach 2) are
 determined from all three methods and compared well with one
 another. The emission characteristic and structure of the shock-
 front are obtained from the laser beam deflection signals and the
 camera images.

*This work is supported by the DOE.

**FTP1 52 Kinetic dispersion relation for electrostatic electron
 waves in a low-pressure collisional plasma** J. OBERRATH, R.P.
 BRINKMANN, *Ruhr-University Bochum, Germany* For the ki-
 netic description of plasma waves a number of approaches are
 common: 1) the Vlasov equation is discussed, if collisions be-
 tween particles can be neglected, 2) the BGK collision term is
 used in a weakly ionized plasma to take collisions into account,
 and 3) the Fokker-Planck approach is applied to describe waves in
 Coulomb collision dominated plasmas. We investigate electro-
 static electron waves in a weakly ionized low-pressure plasma
 dominated by electron-neutral collisions. We assume an isotropic
 collision term with a constant collision frequency instead of the
 BGK term because of the huge mass difference between electrons
 and neutrals. This allows the derivation of the dispersion relation
 from the linearized Boltzmann-Poisson system for homogeneous
 longitudinal waves. In contrast to established dispersion relations
 our relation is able to describe the influence of collisions on the
 electrostatic wave propagation of electrons. The dispersion rela-
 tion including the dispersion function for a Maxwell distribution is
 a special case of our result. A similar description is given in [1],
 where the distribution function is expanded to spherical harmonics in
 velocity space and terms of higher orders are neglected. We do not
 resort to such an expansion but treat the electron distribution func-
 tion in full. [1] S.B. Biragov et al, *Radiophys. Quantum Electron.*
 28 (1985) 743-748

**FTP1 53 Non-local effects in spatial distribution of excitation
 rates in positive column of glow discharge plasma of molecular
 gases*** ANATOLY KUDRYAVTSEV, EUGENE BOGDANOV,
 LEV TSENDIN, *St. Petersburg State University* At simulations of
 gas-discharge plasmas the electron distribution function (EDF) is
 usually calculated using a local approximation (LA) which is ap-
 plicable only when electron energy relaxation length $le < R$ –
 plasma size. For atomic gases $le > 100l$ (l – electron free-path-
 length), so the LA for EDF is not valid up to high pressures. By
 contrast, in molecular gases due to strong vibrational excitation
 with low energy threshold, the length le is small $le \sim l$. And so it is
 assumed everywhere that the LA for EDF calculation in molecular
 gases is valid in any cases when diffusive approximation $R > l$ is
 applicable. In this report it is shown that in molecular gases local
 approximation is inapplicable on the discharge periphery, where
 ambipolar field exceeds longitudinal field. A heating of fast elec-
 trons in ambipolar field gives rise to excitation constants from
 centre to periphery of discharge.

*The work was supported by the RFBR grant # 06-02-17317.

**FTP1 54 The Monte-Carlo get finished in hollow cathode
 theory – a source equation is incoming!** VLADIMIR GORIN,
Kyiv National Taras Shevchenko University The hollow cathode
 effect (HCE) in glow discharge occurred rather hard bean for theo-
 reticians. Classical local Engel and Shtenbek cathode dark space
 theory does not work under conditions of HCE because it is not
 possible to neglect inertia of electron here. The electron distribu-
 tion function has many features and it is far from Maxwellian one.
 The absence of non-local source model from Paschen invention of
 a hollow cathode in 1916 till today forced to use Monte-Carlo
 methods. It meant an absence of any equation for a source of
 ionization in a hollow cathode! Time to find this equation is com-
 ing. It is an integral equation, which is derived from kinetic equa-
 tion and determines a non-local dependence of ionization source
 on electric field through phase trajectories of electron motion.

When simplification of local dependence is possible, the equation can be transformed into ordinary differential equation and then it is coincident with a continuity equation of classical Engel-Shtenbek model. In joining with field equations the source equation enables to calculate current voltage characteristics of simple glow and hollow cathode discharge and see the HCE in mathematical simulation.

FTP1 55 PLASMA CHEMISTRY

FTP1 56 ABSTRACT WITHDRAWN

FTP1 57 A Simulation of Gas Temperature Distribution in a Microcell Plasma in Ar by Considering Ion Impact on and Radiation Heat Transfer from a Chamber Wall HISAHITO MITSUHASHI, *Keio University* TAKASHI YAGISAWA, TOSHIKI MAKABE, Microcell plasma has been attracting our attention to an emission device, conductive device and reactive plasma source for processes etc. Microcell plasma has intrinsic characteristics, i.e., wall controlled high density plasma. Then, it will be important for us to investigate the flow of the external electrical energy to the neutral gas molecule and surface of the microcell for the purpose of the control of the efficiency for plasma production, ion acceleration, and wall heating etc. In the present work, we simulate the spatial temperature distribution of neutral Ar in capacitively coupled microcell plasma sustained at 13.56 MHz by the consideration of the energy conservation equation of gas molecules under the heat transfer on and radiation from the electrode and wall. We mainly discuss the heating of the chamber wall by the impact of energetic ions and the heating of feed gases in the chamber. The dependence of the gas density on the gas heating will be also discussed.

FTP1 58 Plasma-enhanced catalysis at atmospheric pressure, using a dielectric barrier discharge. J.A. REES, D.T. LUNDIE, D.L. SEYMOUR, T.D. WHITMORE, *Hidden Analytical* The combination of plasmas and catalysis under moderate temperatures is an emerging area. The techniques are commonly combined in one of two ways. In the first of these the catalyst is introduced into the plasma while in the second, the catalyst is placed down-stream of the discharge. The introduction of a plasma to a catalysis system may produce a change in the distribution or type of reactive species available for reaction or a change of catalyst properties, such as an increase in dispersion or a change in catalyst structure. In the present work, a micro-reactor that allows the study of catalysis using temperature-programmed techniques. The reactor also allows a dielectric barrier discharge (DBD) to be generated over the whole length of the catalyst region or to precede it. The DBD produces a cool plasma at atmospheric pressure and generates surface modifications of the catalyst and is a source of ions and radicals for reaction processes. Test reactions have been studied to show differences in reaction product distributions and activation temperatures when compared with the catalyst alone. Reaction product distributions were measured using a Hiden, capillary-inlet, mass spectrometer. A molecular beam inlet, mass/energy spectrometer was also used to study the constituents of the DBD plasma.

FTP1 59 Low temperature conversion of molecular species via a hybrid plasma discharge – catalytic process ED BARNAT, *Sandia Laboratories, NM* Various avenues are being pursued towards developing more sustainable energy sources to meet current and future energy requirements. Central to these energy surety related concerns is the efficiency of a given processes (chemical reaction) employed for synthesis of these fuels or energy sources. We present results from our preliminary studies on using low-temperature non-equilibrium discharges, coupled to active surfaces as a means of efficiently dissociating key molecular species that may be used towards fuel synthesis. Specifically, we focus on dissociating carbon dioxide to form carbon monoxide which is used in conjunction with hydrogen to generate syngas and higher hydrocarbons. While studies have been performed using various plasma sources, we primarily use a ‘hybrid’ plasmas with tuned E/N that has been demonstrated to efficiently dissociate carbon dioxide[1]. [1] S. N. Andreev et. al, *Spectrochimica Acta A* **60**, 3361 (2004).

FTP1 60 Molecules production/losses on surfaces under plasma exposure O. GUAITELLA, D. MARINOV, A. ROUSSEAU, *LPTP, CNRS, France* The production/losses of molecules on surfaces such as walls plasma reactors is interesting for numerous applications but especially for plasma/catalyst coupling used in air treatment devices. The processes like adsorption, desorption, surface production or destruction of molecules on different surfaces are crucial to understand the kinetics of molecule oxidation by air plasma. These mechanisms are studied for C₂H₂, NO and NO₂ molecules in a low pressure discharge (1mbar) in a 50 cm long tube with IR tunable diodes to perform time resolved in situ measurements during the plasma ‘on’ phase as well as after switching off the plasma. Surfaces are treated by different plasmas (capacitive or DC discharge) in Ar, O₂, N₂ or air, for several pretreatment durations, injected powers, with pulsed or continuous plasma. These parameters are used to separate cleaning of adsorption sites from adsorption of reacting species which could both induce losses of molecules considered on surface. After these different pre-treatment procedures, two kinds of experiments are made: i) the study of molecule losses on pre-treated surfaces by introducing a controlled amount of molecules in the closed tube reactor; this gives information about the adsorption of the introduced molecule on vacant sites or its reactivity with species already adsorbed during the pre-treatment ii) the production of molecules by a N₂ or O₂ plasma reacting with species adsorbed on wall during pretreatment.

FTP1 61 Comparison Study of Methane Conversion in Low Temperature DC Plasma Reactor with Catalytic High Temperature Fixed Bed Reactor* HAMID REZA BOZORGZADEH, NASER SEYED-MATIN, *Research Institute of Petroleum Industry (R.I.P.I.), Iran* AMIN AZIZNIA, MORTÉZA BAGHALHA, *Department of Chemical Engineering, Sharif University of Technology, Iran* This work reports the results of oxidative coupling of methane in the presence of a Na₂WO₄/Mn/SiO₂ catalyst within the temperature range of 1023–1123 K and a low temperature, atmospheric co-axial cylinder DC corona discharge reactor. Catalytic high temperature reactions were conducted in a quartz tube reactor with Na₂WO₄/Mn/SiO₂ catalyst. A methane/oxygen feed ratio of 4:1 with argon as a diluent gas with total flow of 100, 130, 170 & 200 ml/min has been studied in this investigation for both methods. The plasma reactor was a 15 cm stainless steel

co-axial cylinder which cylinder is grounded. Acetylene and hydrogen were the major products of co-axial cylinder DC corona reactor. In the catalytic reactor, ethylene has the highest selectivity and no trace of acetylene was found. The comparison between two methods is also discussed.

*This work is supported by National Iranian Oil Company (N.I.O.C.).

FTP1 62 Interconnected Microcavity Plasma Arrays: New Opportunity For Microplasma Chemical Reactors SUNG-JIN PARK, TYLER ANDERSON, JEFFREY MA, JIE ZHENG, CHERK LAM, J. GARY EDEN, *University of Illinois at Urbana-Champaign* Various microchemical reactors consisting of parallel, linear arrays of interconnected cylindrical microcavity plasma devices have been fabricated by replica molding in ultraviolet-curable polymer. Tests of 10×10 arrays of $400 \mu\text{m}$ dia. devices with $125 \mu\text{m}$ wide gas flow channels have been conducted in rare gas and Ar/CS₂ flows and excitation of the array with a sinusoidal voltage. Visible chemiluminescence ($\lambda \sim 505 \text{ nm}$) resulting from the $A \rightarrow X$ transition of CS₂⁺ and the deposition of a (C - S)_n microstructured polymer have been observed in the Ar/CS₂ flow experiments. Microplasma properties in a restricted gas flow and the potential of these arrays for microchemical applications will be discussed.

FTP1 63 PLASMA DIAGNOSTICS

FTP1 64 Controllable optical emission spectroscopy plasma diagnostic system* P.L. STEPHAN THAMBAN, *University of Texas at Dallas* JIMMY HOSCH, *Verity Instruments* DANIEL SELF, MATTHEW GOECKNER, *University of Texas at Dallas* Optical emission spectroscopy (OES) does not always produce signals useful for plasma diagnostics, including endpoint detection. Fluctuations in plasma power or deposition on walls, cause the OES signal to drift. To overcome such shortcomings, we have developed a method and tool that allows independent control of both electron energy (E_e) and density (n_e). A description of the method and resulting tool will be presented. We will show how we can alter the operation of the system to change just E_e but not n_e . Thus, we can preferentially probe specific transitions of a given species, or across multiple species. Such ability allows one to probe specific species for use in endpoint detection. We will also show that we can correlate electrical measurements to OES data. Here, the OES signal can be directly correlated to the anode current, a measure of n_e . Finally, we will show how this system can be adapted for use on numerous plasma systems as either an endpoint tool or an advanced diagnostic, allowing the collection of data that has not been possible to date.

*This work was supported by Verity Instruments.

FTP1 65 Self-trapping of fast electrons and spectral measurements in short constricted discharge with cold cathode* J.C. BLESSINGTON, WVU S.F. ADAMS, *Air Force Research Laboratory* V.I. DEMIDOV, *UES, Inc.* B.A. TOLSON, *ISSI, Inc.* M.E. KOEPKE, *WVU* It is known that the effect of self-trapping of the fast electrons in a plasma [1] can be used to regulate plasma properties and be useful for technological applications. It has been demonstrated experimentally that this effect is well pronounced in

the cathode region of discharges. The measured wall potential in this discharge region is much higher than a few kT_e , where T_e is the electron temperature (average energy). The measurements have been conducted in short constricted discharges with a cold cathode in argon. Application of additional voltage to the discharge walls causes a redistribution of fast electron fluxes to the boundaries and changes in the intensities of argon spectral lines. Measurements of the relative intensities of spectral lines with wavelengths of 419.8 nm and 420.1 nm give a simple estimation of metastable argon atom distribution [2], which depends on the discharge configuration. 1. C. A. DeJoseph, V. Demidov, J. Blessington, and M. Koepke, *Euro Phys. News*, 38, #6, 21 (2007). 2. C. A. DeJoseph, *J. Phys. B: At. Mol. Opt. Phys.*, 38, 3805 (2005).

*This work is supported by AFOSR.

FTP1 66 The use of a hairpin resonator probe and emission spectroscopy to determine instabilities during silicon etching DAVID KAVANAGH, MOHAMMED MORSHED, STEPHEN DANIELS, *Dublin City University* The hairpin resonator probe is a diagnostic method which determines electron density. The probe was placed in a capacitively coupled plasma SF₆ plasma during the etching of silicon and the steady state electron density determined. Due to the absence of substrate cooling, the temperature increase in the chamber as the etch process progressed begins to heat and damage the photoresist. As a result the photoresist begins to desorb and outgas, releasing organic polymers into the discharge. These effluents react with the bulk plasma chemistry and have the effect of reducing the electron density measured by the probe. Optical emission spectroscopy was also used to monitor emissions from the plasma. Emissions from non process gasses were also observed as a result of the photoresist heating. These results allow for the consideration of the hairpin resonator probe as a diagnostic for plasma process monitoring

FTP1 67 Characterization of the Basic Operational Properties of the Capillary Plasma Electrode (CPE) Discharge JOSE LOPEZ, WEIDONG ZHU, *St Peters College* MARGARET FIGUS, *Merck & Co. Inc.* KURT BECKER, *Polytechnic University* Various approaches have been pursued to create stable atmospheric pressure discharges by extending the lifetime of the diffuse phase of the discharge to hundreds of microseconds. Previous research showed that the stability of the diffuse mode is dependent on the frequency (in the kHz range), gas type, power, mode of the excitation, and geometrical confinement. The Capillary Plasma Electrode (CPE) discharge is able to produce stable atmospheric pressure nonequilibrium plasmas. The CPE is similar in design to a barrier-electrode discharge, but has perforated dielectrics. This configuration, aside from exhibiting a diffuse mode of operation, also exhibits the so-called "capillary jet" mode, in which the capillaries "turn on" and a bright plasma jet emerges from the capillaries. The capillary jets from adjacent capillaries overlap so that the discharge appears uniform when the electrode contains an array of holes. There appears to be a threshold frequency for the capillary jet formation, which is strongly dependent on the L/D ratio of the capillaries, where D is the diameter of a capillary and L its length. This current work explores these modes of operation of the CPE by characterizing the electrical and optical emission properties of this discharge.

FTP1 68 Effect of multiphoton ionization of metastable and ground-state molecules in laser Thomson scattering diagnostics A. KONO, K. FUKUYAMA, M. ARAMAKI, *Nagoya University* In laser Thomson scattering diagnostics of low temperature plasmas, the probe laser beam is focused to obtain a sufficient signal to noise ratio, and the laser energy density in the focal region is very high. Therefore, one must be certain that possible electron production due to multiphoton ionization is negligible in comparison with the unperturbed plasma electron density. We are carrying out a systematic study of determining multiphoton ionization efficiency in the focal region of frequency-double Nd:YAG laser (532 nm). The laser beam is focused between the electrodes of a small dc-biased parallel-plate probe, whose current due to the collected charge arising from multiphoton ionization is detected by a digital oscilloscope. Preliminary results indicate the following. For 200-mJ laser pulse focused with a $f=400$ mm lens, metastable Ar atoms are ionized with a high probability, while no significant ionization occurs for ground-state Ar atoms. Ground-state O_2 molecules give rather large multiphoton ionization signal and Thomson scattering measurements for medium pressure ($1 > \text{Torr}$) O_2 plasma would require careful control of laser energy density in the focal region. Measurements for other gases are in progress.

FTP1 69 Phase resolved measurement of anisotropic electron velocity distribution functions in a radio frequency discharge DIRK LUGGENHOELSCHER, DRAGOS CRINTEA, VIKTOR KADETOV, CHRISTOPHER ISENBERG, UWE CZARNETZKI, *Ruhr University Bochum* In inductively coupled radio frequency discharges the electron velocity distribution function is harmonically modulated in time and this is equivalent to the oscillating current density generated in the plasma by the induced electric field of the antenna. This oscillation is measured temporally resolved by Thomson scattering with a frequency doubled Nd:YAG laser with a pulse length of 8 ns which determines the temporal resolution. From the measured electron velocity distribution the electron temperature and the density can be derived. The displacement of the distribution shows the drift of the electron ensemble along the direction of the induced field. Further, we will introduce a novel phase resolved emission spectroscopic technique that allows absolute measurement of the same quantity by analyzing the modulation of the atomic excitation by electron collisions. The experiment is carried out in an ICP ($f = 13,56$ MHz) with a planar antenna of 10 cm radius in argon at low pressures in the Pa regime.

FTP1 70 Optical diagnostics of Ar plasmas using $3p^55p \rightarrow 3p^54s$ emissions with consideration of excitation out of metastable levels* R.O. JUNG, JOHN B. BOFFARD, CHUN C. LIN, A.E. WENDT, *University of Wisconsin-Madison* For argon plasmas, optical emissions corresponding to $3p^54p \rightarrow 3p^54s$ (668-1150 nm) are often exploited for diagnostic purposes. Metastable atoms, having large electron-impact excitation cross sections and potentially high densities in a plasma can contribute significantly to these emissions. At high densities however, $3p^54p \rightarrow 3p^54s$ emissions can be strongly reabsorbed by metastable atoms, misleading results. In a 600 W, 1 mTorr ICP, our white light absorption measurements give a metastable density of $\sim 2 \times 10^{10} \text{ cm}^{-3}$. Here the observed $2p_6 \rightarrow 1s_5$ branching fraction is 0.24 in contrast to the expected value of 0.71 in the absence of radiation trapping. This discrepancy is resolved by accounting for radiation trapping. Emissions from $3p^55p$

$\rightarrow 3p^54s$ (395-470 nm) however, are less affected by radiation trapping, making them favorable candidates for optical diagnostics. We have combined our $3p^55p \rightarrow 3p^54s$ optical emission, metastable density, and Langmuir probe measurements for a series of ICP conditions (1-25 mTorr, 10-800 W) with previously measured cross sections in order to develop a self-consistent model.

*Supported by the National Science Foundation.

FTP1 71 Laser Thomson Scattering Diagnostics in the Low-Temperature Plasmas HYUN-JONG WOO, KYU-SUN CHUNG, *Hanyang University* Laser Thomson Scattering (LTS) is the non-invasive method for measuring the electron temperature and its density, which can be used for the calibrations of electric probes within collisional and magnetized plasmas. For LTS diagnostics in the low-temperature plasmas, one need to special optics for detection of the scattered light with restricting the Rayleigh and Stray lights. For this, one uses the Triple Grating Spectrometer (TGS), which is composed of Rayleigh block (notch filter for Rayleigh light) and double grating filter (DGF). All focusing lenses are used with achromatic doublet configuration for reducing the non-linear optical effects such as spherical aberration, coma, etc. The specifications of the grating and achromatic doublet lens are 1800 gr/mm with the dimensions of 84 mm \times 84 mm and 400 mm of focal length with the diameter of 100 mm, respectively. In this configurations, the linear dispersion is given as 1.006 nm/mm. Considering the dimension of Charged Coupled Device (CCD) with the linear dispersion, the LTS system can be measure the electron temperatures of less than 10 eV (in most laboratory plasmas). The initial measurement of LTS measurement and comparative study with single probe are done in Divertor Plasma Simulator (DiPS) with the following plasma parameters; plasma density of $10^{11} - 10^{13} \text{ cm}^{-3}$, electron temperature of 1-4 eV, and the magnetic field of 0.2-1 kG, respectively.

FTP1 72 Electron energy distribution function in low-pressure argon plasmas sustained by surface waves L. STAFFORD, D. LAPIERRE, N. EDDINE, *Universite de Montreal* R. KHARE, V. DONNELLY, *University of Houston* Surface wave (SW) plasmas have attracted considerable attention because of their interest in materials processing. In such plasmas, the spatially averaged plasma frequency ω_p is larger than the wave frequency ω and this ensures the condition for SW propagation. However, due to a spatial plasma density inhomogeneity, local plasma resonances at which $\omega_p = \omega$ can occur over the density profile close to the discharge walls. This can result in large and sharp peaks of the SW electrical field. Through kinetic modeling, it was found that this effect can result in fast electron generation. However, this was never observed experimentally. We used trace-rare-gas-optical-emission-spectroscopy to measure the electron temperature (T_e) and electron energy distribution function (EEDF) in a 50 mTorr Ar plasma operating at 2.45 GHz and sustained in a 8 mm quartz tube. By selecting Ne, Ar, Kr, and Xe lines excited from the ground state which are characteristic of the high energy portion of the EEDF, we found that T_e increased from 5 to 10 eV as the observation point was moved away from the launcher. On the other hand, a constant value of $T_e = 3.1 \pm 0.6$ eV was obtained using Ar, Kr and Xe lines excited to a significant extent through impact with lower energy electrons. Such high-energy tail was not observed in 600 MHz plasmas sustained in a 26 mm tube.

FTP1 73 Measurement of pulse mode ICP plasma using multi-frequency floating probe* MYUNG-SUN CHOI, SEOK-HWAN LEE, GON-HO KIM, *Division of Energy Systems Engineering, Seoul National University, Seoul, 151-744 Korea* Recently in plasma process, pulse mode operation of plasma source is getting popular for various processing products and it interests more in the in-situ property of pulse mode plasma. Newly a floating probe method which uses harmonic distortion of current has been introduced for in-situ plasma monitoring with a minimum perturbation and it may suit to pulse mode plasma measuring. Harmonic distortion of probe current due to sheath nonlinearity which is a strong function of electron temperature is analyzed in the frequency domain by Fast Fourier Transform(FFT), and the plasma density is obtained from the Bohm current model. To eliminate the sheath displacement current and stray current, multi-frequency correction is used which draws out the sheath conduction current by extrapolation of current-frequency relation. This multi-frequency floating probe method is evaluated with the Langmuir probe data in CW and pulse mode ICP argon plasma. The work on pulse mode plasma characteristic such as an EEDF and the transitions of plasma density and electron temperature and its effect to the floating probe measurement will be discussed.

*Work supported by Ministry of Commerce, Industry and Energy (MOCIE: Grant No. 10014462).

FTP1 74 New method to measure the electron temperature in Ar/He mixture capacitive discharge HYO-CHANG LEE, MIN-HYONG LEE, CHIN-WOOK CHUNG, *Electrical Engineering, Hanyang University, Republic of Korea* The electron temperatures were obtained in Ar or Ar/He capacitive discharge by using the new method to measure the electron temperature from a floating potential and a substrate potential [1]. In Ar discharge, as the gas pressures decrease the electron temperatures decrease from 4.0 eV to 1.2 eV, and as the input RF powers increase the electron temperatures slightly decrease from 3.5 eV to 2.8 eV. In the Ar/He discharge, the electron temperatures do not change linearly with the mixing ratio. However the electron temperatures increase abruptly near $P_{He}/P_{Ar+He} = 1$. These results agree well with electron temperatures measured by a floating type probe [2]. [1] Min-Hyong Lee, Ik-Jin Choe, and Chin-Wook Chung, *J. Korean Phys Soc.* 51, 1307 (2007). [2] Min-Hyong Lee, Sung-Ho Jang, and Chin-Wook Chung, *J. Appl. Phys.* 101, 033305 (2007).

FTP1 75 Experimental measurements of the total energy loss in low pressure inductively coupled argon plasma YOUNG-KWANG LEE, MIN-HYONG LEE, CHIN-WOOK CHUNG, *Hanyang University* Total energy lost per electron-ion pair lost (ϵ_T) was measured experimentally in a low pressure inductively coupled argon plasma. ϵ_T represents not only the elastic and inelastic collision energy loss of electron-neutral but also the kinetic energy loss when the electron and ion escape to the wall. In order to determine ϵ_T , the modified power balance of a global model (spatially-averaged) is properly derived using some assumptions. A floating-type probe working at very low bias voltage (~ 1.0 V) was applied to obtain the electron temperature and plasma density at the plasma-sheath boundary. At 10 mTorr, the measurement shows that the measured $\epsilon_T \sim 100$ V gradually decreased with absorbed power and began to saturate. These ϵ_T are consistent with the theoretical results by Lee *et al.* [1]. [1] Min-Hyong Lee, Sung-Ho Jang and Chin-Wook Chung, *Phys. Plasmas*, 13, 053502 (2006)

FTP1 76 Dielectric thickness monitoring method by using dual frequency in processing plasmas SUNG-HO JANG, GUN-HO KIM, CHIN-WOOK CHUNG, *Electrical Engineering, Hanyang University, Republic of Korea* The wall condition of a chamber lead to change in plasma state, and therefore it can be very important factor in processing plasmas. Real time measurement method of dielectric film thickness on the wall was developed. This method used the impedance difference of the coated dielectric material because the impedance is a function of the frequency of applying voltage. The experiment was conducted at various pressures and rf powers. The experimental result showed that the thickness of aluminum oxide (Al_2O_3) film could be obtained well. And the changes in the thickness of the deposited dielectric film on the wall in processing plasmas were observed in real time.

FTP1 77 Thermal, Electrical, and Optical Measurements of Electrical Discharges in Saline CAMERON MOORE, *Colorado State University* ARLEN WARD, *Department of Mechanical Engineering, Colorado State University, Fort Collins, Colorado 80523* KAZUNARI SATO, GEORGE COLLINS, *Department of Electrical and Computer Engineering, Colorado State University, Fort Collins, Colorado 80523* We report measurements of electrical discharges in saline that are electrically excited at 100 kHz from a commercial electrosurgical system. Using a one-dimensional thermocouple array, we estimate that these discharges in saline, in contrast to prior work, induce local temperatures > 100 C. Simultaneous measurement of voltage, current, and optical emission of Na^* at 589 nm show that these discharges have frequent arcs, and that these arcs dominate energy flow into the saline. Finally we present measurements of Stark splitting of the sodium D1 and D2 resonant emission lines and from these data estimate the thickness of sheath-like region where most of the applied voltage is dropped.

FTP1 78 Mode transitions in radio-frequency plasmas* DEBORAH O'CONNELL, KARI NIEMI, TIMO GANS, BILL GRAHAM, *Queens University Belfast* Inductively coupled radio-frequency plasmas can be operated in two distinct modes. At low power and comparatively low plasma densities the plasma is sustained in capacitive or so-called E-mode. As the plasma density increases a transition to inductive H-mode is observed. This transition region is of particular interest and governed by non-linear dynamics and under certain conditions can result in structure formation with strong spatial gradients in the light emission. The two modes show pronounced differences in various measurable quantities e.g. electron densities, electron energy distribution functions, ion energy distribution functions, dynamics of optical light emission. Thus, the synergy of employing various diagnostics simultaneously yields improved understanding of the non-linear dynamics during the mode transition. The electron and ion energy distribution functions exhibit different characteristic shapes in each mode. The two distinct operation modes can be identified through the higher harmonic components of both the current and optical light emission.

*Supported by: EU (FP7), EPSRC and Impedans Ltd.

FTP1 79 A simple analysis method for the I-V curve of Single Langmuir Probes IKJIN CHOI, CHIN-WOOK CHUNG, *Department of Electrical Engineering, Hanyang University, Republic of Korea* In single Langmuir probes, the derivation of the electron temperatures from I-V characteristics is not easy and simple because of the difficulties in obtaining ion currents. The electron temperatures are usually found from a logarithm slope of the electron current that the ion current was subtracted from the probe current. In this paper, a simple method regardless of ion currents will be introduced and demonstrated. If electrons are in a Maxwellian distribution, the electron temperature is simply given by $I_p / (dI_p/dV)$ at a plasma potential where I_p and V are the probe current and the bias voltage. In this case, ion current theories were not needed because the ion current becomes zero at the plasma potential. The electron temperatures from this method are used to derive plasma densities from electron saturation currents. This simple analysis was a good agreement with that from the electron energy distribution measurement when the electron distribution was a Maxwellian. This analysis was applied in Bi-Maxwellian electron distributions and some discussion will be presented.

FTP1 80 Mass and energy spectroscopy of fluorocarbon plasmas. J.A. REES, *Hidden Analytical* It is helpful for many processing plasmas which are operated using fluorocarbon and similar gases to have available information on the nature of the ions generated in the plasma and on the energies with which they impact on surfaces exposed to the plasma. To illustrate the range of data which may be obtained using a Hidden mass/energy spectrometer attached to a plasma reactor, measurements for RF plasmas in CF_4 , CF_3I , CCl_2F_2 , and $CHClF_2$ in a parallel-plate reactor are outlined. Of particular interest, are the data obtained for the production of negative ions. For the experiments carried out with a 10 Watt plasma in $CHClF_2$, the dominant negative ions were H^- , Cl^- and F^- . For each of these species, the relative rates of production from the parent gas and the mixture of neutral fragments produced by dissociation in the plasma were determined for electron energies of between 0.5 and 30eV. In the presence of a plasma, the contributions to the negative ion population of electron attachment to the dissociation fragments are also clearly seen. In the absence of a plasma, the electron attachment rates measured for the production of CF_3^- ions from the parent CF_4 , show clearly the contributions of two formation path ways via the ground and excited states of the temporary CF_4^- ions first formed in the electron/molecule collisions. The ability of the mass/energy analyser to observe the energies of the attachment products is helpful.

FTP1 81 Improvement of copper vapor laser characteristics by zinc additive YURIJ SHPENIK, VOLODYMYR KELMAN, YURIJ ZHMENYAK, *Institute of Electron Physics NAS Ukraine* The influence of Zn atom additive on "pure" copper vapor laser output characteristics was studied. Two-section discharge tube (DT) with an external heated Zn reservoir placed at the center between ceramic sections with Cu pieces was elaborated. The pulsed periodical longitudinal discharge was excited in the DT with Cu-Zn-Ne admixture by a traditional circuit using thyatron generator with resonant overcharge of a storage capacitor. Experimental investigations established that the width, energy and power of laser pulses increased when Zn atoms at appropriate temperature $\sim 500^\circ C$ of zinc containing reservoir diffuse into discharge. The registered increasing of pulse energy was up to 50% comparatively with the energy without additive with peak energy at $\sim 600^\circ C$. Additional absorption experiments and modeling the ab-

sorption of Zn atom resonant line in the DT (taking into account Doppler and dispersion line broadening) consistent with the conclusion that not only optical resonant pumping by 213.9 nm Zn atom line, but other processes also might be taken into account to explain the influence effects (second kind collisions between resonance state zinc and metastable copper state atoms).

FTP1 82 Extraction of electron energy distribution functions from Langmuir probes using integrated step function response and regularized least squares solver AHMED ELSAGHIR, STEVE SHANNON, *NC State University, Department of Nuclear Engineering* Electron energy distribution function (EEDF) extraction from Langmuir probe data is an ill-posed problem due to the integral relationship between electron current and EEDF with respect to probe voltage. Curve fitting solutions to extract this EEDF assume a specific type of distribution. Point by point extraction of the second derivative relationship uses a small fraction of the integrated data to extract the EEDF. Recently EEDF extraction techniques have been evaluated using regularized solutions to the integral problem.¹ These techniques do not assume any mathematical representation of the EEDF and solve the integral problem for any function that best represents the EEDF. In this paper the electron current for arbitrary functions is derived assuming that the electron density is a sum of step functions representing such a function. This technique for EEDF extraction is validated by adding noise to numerically generated data and using a regularized least squares method to calculate the original function by solving for the individual step function contribution to the total electron current. The methodology, reconstruction, and comparison to current best-known methods will be presented.

¹Gutiérrez-Tapia and Flores-Llamas, *Phys. Plasmas* **11** 5102 (2004)

FTP1 83 Analysis of spectral line shapes in HID plasmas* HARTMUT SCHNEIDENBACH, STEFFEN FRANKE, MARTIN WENDT, MARGARITA BAEVA, *INP Greifswald, Felix-Hausdorff-Str. 2, D-17489 Greifswald, Germany* The optical emission spectroscopy is widely used for the temperature determination in high-intensity discharge plasmas. The spectral lines are in general strongly reabsorbed around the line centre at high pressures. The plasma parameters can be determined by fitting the measured spectral radiances with radiation transport calculations where the knowledge of the line profile and broadening mechanisms is required. For sufficiently strong reabsorption spectral lines become self-reversed. Bartels and Karabourniotis developed methods which make use of the special features of the spectral radiance at the reversal maxima. The plasma layer properties are approximately represented by an inhomogeneity parameter. The application of these approximations for fitting measured spectral radiances is proposed. High-pressure mercury discharges without and with metal halide additives have been analyzed. The different methods for the temperature determination have been compared and their applicability has been discussed for different spectral lines.

*This work was partly supported by the German Federal Ministry for Education and Research (BMBF, FKZ 13N8604).

FTP1 84 Optical emission spectroscopy diagnostic of pure vapor Ni plasma CORNEL POROSNICU, ANA MIHAELA LUNGU, CATALIN TICOS, CRISTIAN P. LUNGU, *National Institute for Laser, Plasma and Radiation Physics, Romania* The method studied extensively in our group for materials processing is based on the thermionic vacuum arc (TVA) principle. In TVA, the high-density plasma is localized above the anode, whereas the substrates are placed away from the core of the plasma. This enables thin films deposition to be carried out at low substrate temperatures even for the highest melting point materials. Also, although it is arc plasma, the TVA can be used to prepare particle free films of pure materials. The TVA plasma parameters were evaluated using the analysis of the optical emission radiation of the plasma running in pure vapors. The plasma parameters obtained are anode (Ni pool) temperature, vapor pressure, evaporation rate and electron temperature (evaluated by using the ratio of the atomic emission lines) as function of the dissipated power between electrodes. It was found that plasma parameters are increasing with the power and during arc plasma have relatively constant values.

FTP1 85 Langmuir probe measurements in a VHF dielectric plasma etcher LEONID DORF, KARTIK RAMASWAMY, KEN COLLINS, WALTER MERRY, *Applied Materials* Langmuir probe (LP) measurements in a realistic VHF CCP discharge are complicated by a number of factors, such as absence of a well-defined DC ground reference and unpredictable behavior of standard electronic components at VHF. The VHF source can produce plasma very efficiently; therefore, to reach the same plasma density, VHF discharges require lower power than HF discharges. Nevertheless, even at low source power ($\sim 100\text{--}200\text{W}$ with $N_e \leq 10^{10}\text{ cm}^{-3}$), RF potential in a VHF CCP discharge can be large, especially compared to that in an ICP discharge with similar parameters. Uncompensated RF potential distorts both electron and ion parts of the measured V-I characteristic, resulting in unrealistic plasma parameters. Here, we present preliminary results of our work to develop a LP system suitable for measurements in a 162 MHz dielectric plasma etcher. The probe design employs many previously developed RF compensation techniques. Furthermore, all electronic components of the probe and the measuring circuit were characterized using a network analyzer to select adequate values. The probe was used to study the effects of magnetic field, input power, pressure, and other operating conditions on electron and ion density profiles. Electron temperature was found to be in the range of 1.8 – 3.5 eV, and the shape of ion saturation curve was found to be in agreement with OML theory.

FTP1 86 INTERACTION OF PHOTONS WITH ATOMS AND MOLECULES

FTP1 87 Controlling and stopping vibrational wave packets in D_2^+ with fs laser pulses* UWE THUMM, *Kansas State University* THOMAS NIEDERHAUSEN, *University of Madrid* Ionization of neutral D_2 molecules by a short pump laser pulse may create a vibrational wave packet on the lowest ($1s\sigma_g^+$) adiabatic potential curve of the D_2^+ molecular ion. We investigated the possibility of manipulating the bound motion, dissociation, and vibrational-state composition of D_2^+ nuclear wave packets with a sequence of ultra-short, intense, near infrared control laser pulses. Our numerical results show that a single control pulse with an appropriate time delay can quench the vibrational state distribution

of the nuclear wave packet by increasing the contribution of a selected stationary vibrational state of D_2^+ to more than 50%. We also demonstrate that a second control pulse with a carefully adjusted delay can further squeeze the vibrational-state distribution, suggesting a multi-pulse control protocol for preparing stationary excited nuclear wave functions. With the subsequent fragmentation of the molecular ion with a probe pulse, we suggest a scheme for experimentally assessing the degree at which the nuclear motion in small molecules can be controlled, cf., Phys. Rev. 77, 013407 (2008).

*Supported by NSF and the U.S. DoE.

FTP1 88 Time-series analysis of vibrational nuclear wave packet dynamics* UWE THUMM, *Kansas State University* THOMAS NIEDERHAUSEN, *Kansas State University (now University of Madrid)* BERNOLD FEUERSTEIN, *Max-Planck Institut fuer Kernphysik, Heidelberg* We discuss the extent to which measured time-dependent fragment kinetic energy release (KER) spectra and calculated nuclear probability densities can reveal 1) the transition frequencies between stationary vibrational states, 2) the nodal structure of stationary vibrational states, 3) the ground-state adiabatic electronic potential curve of the molecular ion, and 4) the progression of decoherence induced by random interactions with the environment. We illustrate our discussion with numerical simulations for the time-dependent nuclear motion of vibrational wave packets in the D_2^+ molecular ion caused by the ionization of its neutral D_2 parent molecule with an intense pump laser pulse. Based on a harmonic time-series analysis, we suggest a general scheme for the full reconstruction, up to an overall phase factor, of the initial wave packets based on measured KER spectra, cf., Phys. Rev. A 77, 063401 (2008).

*Supported by the NSF and the U.S. DoE.

FTP1 89 A Fully Relativistic B-Spline R-Matrix Method for Electron and Photon Collisions with Atoms and Ions* OLEG ZATSARINNY, KLAUS BARTSCHAT, *Drake University* We have extended our B-spline R-matrix (close-coupling) method [1] to fully account for relativistic effects in a Dirac-Coulomb formulation. Our numerical implementation of the close-coupling method enables us to construct term-dependent, non-orthogonal sets of one-electron orbitals for the bound and continuum electrons. This is a critical aspect for complex targets, where individually optimized one-electron orbitals can significantly reduce the size of the multi-configuration expansions needed for an accurate target description. Core-valence correlation effects are treated fully *ab initio*, rather than through semi-empirical model potentials. The method is described in detail and will be illustrated by comparing our theoretical predictions for e-Cs collisions [2] with benchmark experiments for angle-integrated and angle-differential cross sections [3], various spin-dependent scattering asymmetries [4], and Stokes parameters measured in superelastic collisions with laser-excited atoms [5]. [1] O. Zatsarinny, Comp. Phys. Commun. 174, 273 (2006). [2] O. Zatsarinny and K. Bartschat, Phys. Rev. A 77, 062701 (2008). [3] W. Gehenn and E. Reichert, J. Phys. B 10, 3105 (1977). [4] G. Baum *et al.*, Phys. Rev. A 66, 022705 (2002) and 70, 012707 (2004). [5] D.S. Slaughter *et al.*, Phys. Rev. A 75, 062717 (2007).

*Supported by the NSF under PHY-0555226 and PHY-0757755.

FTP1 90 Differential Cross Sections of Two-Photon Double Ionization of He From Time-Independent and Time-Dependent Calculations* DANIEL HORNER, *Los Alamos National Laboratory* ALICIA PALACIOS, THOMAS RESCIGNO, *Lawrence Berkeley National Laboratory* C. WILLIAM McCURDY, *Lawrence Berkeley National Laboratory and University of California, Davis* The method of exterior complex scaling allows us to compute numerically converged time-independent and time-dependent wave functions describing two unbound electrons on a large, but finite volume. With these wave functions, using formally exact integral methods, we are able to extract the observable cross sections. We present total, single differential, and fully differential cross sections for two-photon double ionization of helium above and below the threshold for sequential ionization (54.4 eV). The sequential, two step, double ionization mechanism produces characteristic features seen in the total and differential cross sections. Furthermore, the fully differential cross section shows that even below the sequential ionization threshold two-photon double ionization is largely a process where each electron absorbs a single photon and then correlation between the electrons leads to double ionization.

*Work performed under the auspices of the US DOE at LANL (Contract No. DE-AC52-06NA25396), LBNL (Contract No. DE-AC02-05CH11231)

FTP1 91 Quantum-beat Spectroscopy of Molecular Dynamics in Ultrashort Laser Fields UWE THUMM, *Kansas State University* THOMAS NIEDERHAUSEN, *Kansas State University (now University of Madrid)* BERNOLD FEUERSTEIN, THORSTEN ERGLER, ARTEM RUDENKO, ROBERT MOSHAMMER, JOACHIM ULLRICH, *Max-Planck Inst. fuer Kernphysik, Heidelberg* Reaction Microscope-based, complete, and time-resolved Coulomb explosion imaging of vibrating and dissociating D_2^+ molecules with femtosecond time-resolution allowed us to perform an internuclear distance (R -)dependent Fourier analysis of the corresponding wave packets. Our wave packet propagation calculations demonstrate that the obtained two-dimensional R -dependent frequency spectra enable the complete characterization of the wave packet dynamics and directly visualize the field-modified molecular potential curves in intense, ultrashort laser pulses, cf., *Phys. Rev. Lett.* **99** 153002 (2007) and *Phys. Rev. A* **77**, 063401 (2008).

FTP1 92 POSITRON ATOM/MOLECULE COLLISIONS

FTP1 93 Elastic electron and positron scattering from argon ALLAN STAUFFER, *York University* ROBERT MCEACHRAN, *Australian National University* In order to obtain accurate elastic differential cross sections for electron and positron scattering from the noble gases at intermediate energies, the effect of the open inelastic channels must be taken into account. We have developed a complex optical potential which does this [1] and have applied this to scattering from argon. Detailed results will be shown. [1] S. Chen, R.P. McEachran and A.D. Stauffer, *J. Phys. B* **41**, 025201 (2008).

FTP1 94 High Resolution Studies of Low Energy Positron Collisions with Helium STEPHEN BUCKMAN, JAMES SULLIVAN, PETER CARADONNA, ADRIC JONES, CASTEN MAKOCHEKANWA, DANIEL SLAUGHTER, *Australian National University* MARK STEVENSON, BIRGIT LOHMANN, *University of Adelaide* CENTRE FOR ANTIMATTER-MATTER STUDIES COLLABORATION, A high resolution, trap-based beam of positrons has been used to study total scattering, positronium formation and direct ionization of He atoms. The energy resolution of the positron beam is typically 65 meV, and measurements have been carried out at incident positron energies between 1 and 60 eV. The experimental arrangement consists of a pulsed beam of positrons from a Surko trap combined with a gas cell containing the helium target gas and a retarding potential analyzer (RPA). The beam is confined radially using a 500 gauss magnetic field and the RPA allows absolute cross sections to be obtained by measuring the scattering rate for each process. Normalisation depends only on a measurement of the target gas pressure (in the milli-Torr range) and the length of the scattering cell. Results will be compared with previous measurements and contemporary theory.

FTP1 95 Role of multimode excitations and inelastic escape channels in positron-molecule attachment* C.M. SURKO, *Univ. of California, San Diego* J.A. YOUNG, *Jet Propulsion Lab* Experiments have shown that positrons, like electrons, can attach a variety of molecules via vibrational Feshbach resonances (VFR). Because of the positron's unique annihilation channel, one can probe particularly short-lived resonances by examining features in the positron energy-resolved annihilation spectra. We discuss here energy-resolved annihilation spectra for a variety of molecules and relate these results to theory [1]. In particular, we examine the role of multi-mode excitations, which are found to produce VFR in a number of small molecules [2] and may participate in the enhancement of single-mode resonances in large molecules [3]. Also discussed is how fluorine substitution in a large hydrocarbons produces a strong inelastic escape channel. This, in turn, limits resonance lifetimes and decreases the magnitudes of the annihilation resonances above the inelastic threshold [3]. [1] G. F. Gribakin & C. M. R. Lee, *Phys. Rev. Lett.*, **97**, 193201 (2006). [2] J. A. Young, C. M. Surko, G. F. Gribakin, and C. M. R. Lee, *Phys. Rev. A*, in press (2008). [3] J. A. Young & C. M. Surko, *Phys. Rev. A*, **77**, 052704 (2008).

*This work is supported by NSF, grant PHY 02-44653.

FTP1 96 Positron-molecule binding energies measured via resonances in annihilation* J.A. YOUNG, *Jet Propulsion Lab* C.M. SURKO, *Univ. of California, San Diego* Measurements of positron-molecule annihilation using a monoenergetic positron beam have revealed distinct features due to vibrational Feshbach resonances (VFR). The presence of these features implies the existence of positron-molecule bound states. The shifts in the energies of the resonant peaks from those of the vibrational modes provides a measure of the binding energies. In this paper, we present positron-molecule affinity data for thirty molecular species, which range from < 1 meV for small molecules such as ethane and ethylene to more than 300 meV for hexadecane and naphthalene. We relate these positron affinities to various physical parameters such as polarizability, ionization potential and dipole moment [1]. We also describe recent results of a quantitative theoretical model for VFR-mediated positron attachment to small

molecules [2, 3]. [1] J. A. Young & C. M. Surko, *Phys. Rev. A*, **77**, 052704 (2008). [2] G. F. Gribakin & C. M. R. Lee, *Phys. Rev. Lett.*, **97**, 193201 (2006). [3] J. A. Young, C. M. Surko, G. F. Gribakin, & C. M. R. Lee, *Phys. Rev. A*, in press (2008).

*This work is supported by NSF, grant PHY 02-44653.

FTP1 97 ELECTRON MOLECULE COLLISIONS

FTP1 98 Thermalization of High Energy Electrons in Nitrogen VLADIMIR STOJANOVIC, ZELJKA NIKITOVIC, ZORAN PETROVIC, *Institute of Physics* Electron thermalization in pure nitrogen and in air (N₂/O₂) is studied by Monte Carlo technique for electron energies from 20 eV up to 10 keV. Spatially resolved emission is accounted for by counting number of specific emissions at pressures 1 Torr and 760 Torr. Relaxation of electron energy is followed by using a set of data for nitrogen and oxygen including elastic and inelastic collisions and realistic energy partitioning in ionizing collisions. The secondary electrons born in ionization events are found to affect significantly emission of the 2⁺ band. The energy dependences of the effective collision (and emission) probabilities for 391.4 nm and 337.1 nm emission lines and ionization are calculated. These data are used in attempts to use atmospheric fluorescence due to cosmic rays to detect very high energy elementary particles.

FTP1 99 Electron Impact Single Ionization of Atoms and Molecules: Three-Dimensional Images for the Electron Emission XUEGUANG REN, THOMAS PFLUEGER, ARNE SENFTLEBEN, ALEXANDER DORN, JOACHIM ULLRICH, *Max-Planck-Institute for Nuclear Physics, Heidelberg, Germany* While electron impact ionization for the simplest atomic species hydrogen and helium can be handled well by theory, more heavy atoms and molecules pose severe challenges. Presently we are performing systematic (e,2e) experiments in the impact energy range below 200 eV for various atomic targets as Ne and Ar, and for molecular species as H₂, Ar₂, N₂, O₂ and CO₂. The goal is to provide benchmark cross sections covering the full solid angle and a large range of ejected electron energies and momentum transfers by applying an experimental multi-particle imaging technique (Reaction Microscope).

FTP1 100 Fragmentation studies of CF⁺ and HF⁺ ions in collisions with cold electrons OLDRICH NOVOTNY, S. ALTEVOGT, M.H. BERG, D. BING, H. BUHR, H. FADIL, M. FROESE, J. HOFFMANN, B. JORDON-THADEN, C. KRANTZ, M. LANGE, M. LESTINSKY, M. MENDES, S. NOVOTNY, D.A. ORLOV, A. PETRIGNANI, A. SHORNIKOV, T. SORG, J. STUETZEL, A. WOLF, *Max-Planck-Institut für Kernphysik, Saupfercheckweg 1, D-69117 Heidelberg, Germany* A.S. JAROSHEVICH, *Institute of Semiconductor Physics, 630090 Novosibirsk, Russia* The fundamental molecules composed of atoms from the second row of the periodic table (C,N,O,F) have a rich structure of excited potential curves that can be probed at high energy resolution by observing fragmentation processes following collisions with quasi-monochromatic electrons. Experiments of this type are performed in merged electron and ion beams at the ion storage ring TSR in Heidelberg, Germany. Using a cold, photocathode-produced electron beam, experiments on the system CF⁺ yield rich structure in the collision energy dependence of both dissociative recombination (DR) and excitation (DE). The

fragment-imaging technique shows a strong collision energy dependence of final ground and excited states of DR products. Moreover, an angular anisotropy of DR is observed for elevated collision energies. DR of HF⁺ displays extremely low kinetic energy release of neutral fragments yielding resolution on initial rotational states of the ions. This predestines HF⁺ to be used as "molecular thermometer."

FTP1 101 Dissociative Electron Attachment of Water Molecules HIDEHITO ADANIYA, TIMUR OSIPOV, BENEDIKT RUDEK, THORSTEN WEBER, SUN LEE, MARCUS HERTLEIN, ALI BELKACEM, *Lawrence Berkeley National Lab* A COLTRIMS method is developed to measure the kinetic energy and angular distribution of fragment negative ions arising from dissociative electron attachment of molecules. A low energy pulsed electron gun is used in combination with pulsing the extraction plate of the COLTRIMS spectrometer. This technique is applied to study the negative oxygen anion channel for the three resonances, ²B₁, ²A₁, ²B₂ and resonances of water. The measured kinetic energy of the O- fragment gives a good measure of the two-body channel versus three-body channel for each resonance. The angular distribution of the O- fragments with respect to the electron beam direction is found to reflect well the symmetry of the resonance states. The experimental results are compared to the theoretical prediction.

FTP1 102 On the reaction rates in the low pressure nitrogen discharge JON TOMAS GUDMUNDSSON, EYTHOR GISLI THORSTEINSSON, *University of Iceland* We use a global (volume averaged) model to study the dissociation of the nitrogen molecule and the role of metastable species in a low pressure (1 - 100 mTorr) high density nitrogen discharge. The collisional energy loss per electron ion pair created is evaluated for the nitrogen atom and the nitrogen molecule. We explore and compare the reaction rates for the creation and destruction of the positive ions N⁺ and N₂⁺, the atomic nitrogen in the ground state N(⁴S), the metastable atom N(²D) and the metastable molecule N(A³Σ_u⁺). Furthermore, the dissociation mechanism in the nitrogen discharge is investigated as a function of power and pressure. The discharge is dominated by atomic nitrogen at low pressure and by molecular nitrogen at the higher pressures.

FTP1 103 ION SWARMS

FTP1 104 Arrival Time Spectra of Heavy Particles in Hydrogen Discharge VLADIMIR STOJANOVIC, ZELJKA NIKITOVIC, ZORAN PETROVIC, *Institute of Physics* LABORATORY FOR GASEOUS ELECTRONICS TEAM, Arrival time spectrum of electrons and heavy particles in Townsend discharge at very high E/N is determined by using Monte Carlo technique. Three dimensional Monte Carlo codes are used for simulation of coupled kinetics of electrons, ions and fast neutrals. The electron collisions are represented by the anisotropic cross section set with available data for energy partitioning. Heavy particle collisions are represented by latest cross section set compiled by Phelps. Trajectories of H⁺, H₂⁺ and H₃⁺ ions, fast H and fast H₂ are followed up to the electrodes where arrival time is recorded. Energy relaxation of the neutral particles is followed down to the energy limit of 5

eV. These results are used to obtain the integrated particle flux data that can be compared either to experimental emission integrated data or to data obtained by current integration. The results of simulation allow us separation of different contributions and tests of models of interactions.

FTP1 105 Models of H α Doppler emission profiles from cathode fall discharges in hydrogen A.V. PHELPS, *JILA, University of Colorado and NIST* Doppler profiles are calculated for the H α line excited in collisions of fast atoms, ions, molecules, and electrons with H₂ in the cathode fall of low-pressure, moderate-current hydrogen discharges. We use a multi-beam model of the particle fluxes and energy distributions, assumed angular distributions of particles approaching and reflected by the cathode, and a simplified cathode fall model. Spectral profiles are compared with measurements parallel and perpendicular to the tube axis for the conditions reported by Cvetanović et al.¹ Excitation is principally by fast H atom collisions with H₂ as they approach and leave the cathode and by the electrons leaving the cathode. The calculated relative magnitudes of the wings and core of the parallel and perpendicular H α line profiles and the sensitivity of the emission produced by reflected atoms to cathode material are in agreement with experiment.

¹N. Cvetanović, M. M. Kuraica, and N. Konjević, *J. Appl. Phys.* **97**, 033302 (2005).

FTP1 106 Ion flux energy distributions in a hydrogen-filled drift tube at high E/N ARTHUR PHELPS, *JILA, University of Colorado and NIST* Ion flux energy distributions are calculated for H⁺, H₂⁺, and H₃⁺ ions in H₂ for low-current, uniform-electric-field drift tubes at 1 kTd < E/N < 10 kTd and 5 × 10²⁰ ≲ Nd ≲ 3 × 10²¹ m², where E is the electric field, N is the gas density, and d is the electrode separation. We use updated cross sections in a multi-beam model of the spatial and energy dependent particle fluxes. Calculated distributions at the cathode are compared with experiments by Rao et al.¹ and detailed theory by Bretagne et al.² Hypothetical large increases in the total momentum transfer cross sections for H⁺ and H₃⁺ at 100 to 1000 eV yield approximate fits to the relative experimental distributions at high energies at moderate E/N. However, these fitted distributions are much too small at low ion energies. Similar discrepancies occur for analytic solutions of the Boltzmann equations using simplified reaction cross sections and the almost free-fall conditions for H⁺ at 10 kTd.

¹M. V. V. S. Rao, R. J. Van Brunt, and J. K. Olthoff, *ESCAMPIG '96*.

²J. Bretagne, G. Gousset, T. Šimko, M.V.V.S. Rao, R. J. Van Brunt, Y. Wang, J. K. Olthoff, B. L. Peko and R. L. Champion, *ESCAMPIG '96*.

FTP1 107 HEAVY PARTICLE COLLISIONS

FTP1 108 Alignment relaxation of Ne*(2p_i [J=1]) atoms due to collisions with He(1s²) atoms VAIBHAV KHADILKAR,* *Lamar University* HIRAKU MATSUKUMA, MASAHIRO HASUO, *Kyoto University* CRISTIAN BAHRIM, *Lamar University* Alignment relaxation of atoms induced by collisions offers accurate information regarding the anisotropic atom-atom potentials and has many applications in atomic and plasma physics. Here we

report the energy-averaged cross sections for destruction of alignment $\sigma^{(2)}$ and the rate coefficients for disalignment K_{DA} of Ne*(2p⁵ 3p; 2p_i [J=1]) atoms due to He atom collisions using a many-channels close-coupling method based on a modified model potential for the HeNe*(2p⁵ 3p) system [1]. Comparison with measurements using laser-induced fluorescence spectroscopy (LIFS) [2] and Hanle signals [3] is reported. The LIFS method measures K_{DA} due to intra-multiplet transitions, while the analysis of Hanle signals gives $\sigma^{(2)}$, which incorporates both the intra- and inter-multiplet transitions. Good agreement between theory and experiments was found for the 2p₂, 2p₅, and 2p₇ states at 77 K < T < 350 K when a static polarizability for each Ne*(2p_i) state is added to the long-range potentials of the HeNe*(2p⁵ 3p) system given in Ref.[4]. [1] Bahrim C and Khadilkar V 2008 *J. Phys. B* **41** 035203 [2] Seo M, Shimamura T, Furatani T, Hasuo M, Bahrim C and Fujimoto T 2003 *J. Phys. B* **36** 1885 [3] Carrington C G and Corney A 1971 *J. Phys. B* **4** 869 [4] Bahrim C, Kucal H and Masnou-Seeuws F 1997 *Phys. Rev. A* **56** 1305

*(presently at UT Dallas)

FTP1 109 Ionization of Atomic Hydrogen by 75keV Proton Impact* AARON LAFORGE, MICHAEL SCHULZ, JADON ALEXANDER, *Missouri University of Science & Technology Physics Dept.* The dynamics and interactions of the few-body problem is one of the most fundamental problems in physics due to the fact that the Schrödinger equation is not solvable in closed form for more than two mutually interacting particles. A proton colliding with atomic Hydrogen is a particularly important system to study the few-body problem for its simplicity (only three particles involved), and the underlying force, electromagnetism, being completely known. We performed a kinematically complete experiment to study ionization in this collision system. The fully momentum analyzed recoil ions and scattered projectiles were measured in coincidence so that the ejected electron momentum can be deduced from momentum conservation. As a result, it is possible to extract the maximum information about the collision dynamics for this benchmark system. Multiple differential cross sections will be compared to data obtained recently for p + He collisions, for which serious discrepancies to theory were found [1]. [1] N.V. Maydanyuk et al., *Phys. Rev. Lett.* **94**, 243201 (2005)

*Funded by the National Science Foundation.

FTP1 110 He Single Ionization in Collisions with "Fixed-in-Space" MeV H₂⁺ Ions SHAOFENG ZHANG, JAN SUSKE, DANIEL FISCHER, KAI-UWE KUEHNEL, SIEGBERT HAGMANN, MICHAEL SCHULZ, ALEXANDER VOITKIV, BENNACEUR NAJJARI, ANDREAS KRAUSS, XINWEN MA, ROBERT MOSHAMMER, JOACHIM ULLRICH, *Max-Planck-Institut für Kernphysik* Two center effects in collisions of fast ions with H₂ molecules have been studied intensively. We investigated in a kinematical complete experiment the ionization of He in collisions with H₂⁺-molecular ions at 0.5 and 1.0 MeV at the Max Planck Institute for Nuclear Physics at Heidelberg. The momenta of the recoiling He ions and the electrons produced in the collisions were measured using a "Reaction Microscope." The fragments of the H₂⁺ were separated by a dipole magnet after the

interaction region and detected by two position sensitive MCP detectors. From this information the orientation and the internuclear distance of the molecular ion at the instance of the collision could be determined. Pronounced structures are found both in the experimental data and theoretical calculations, indicating that the emitted He electron shows a slight preferential emission parallel to the molecular axis. According to our theoretical calculations the effects are due to two-center interference, which turned out to be strongly dependent on the type of approximated molecular wave function used in the calculations.

FTP1 111 Single Electron Capture by C^{4+} from Atomic and Molecular hydrogen at low energies* DWAYNE JOSEPH, *Department of Physics, Florida A&M University* BIDHAN SAHA, *Department of Physics, Florida A&M University* Electron Capture is well known to be an important collision process in nearly all types of plasma environments from terrestrial laboratories [1] to solar system atmospheres [2] to astrophysical sources. Ion-molecule collisions have received less attention both theoretically and experimentally than its atomic counterpart due to extra degree of freedom. We report here our calculation using ab initio structure calculations. We compare our findings with other available theoretical and experimental results. [1] R. K. Janev, in "Atomic and Molecular Processes in Fusion Edge Plasmas" (Plenum Press, NY, 1995), p1. [2] T. E. Cravens, *Science* 296, 1042 (2002).

*Supported by NSF-CREST.

SESSION GW1: PLASMA AERODYNAMICS AND PROPULSION II

Wednesday Morning, 15 October 2008; Salon E at 8:00

W. Lempert, The Ohio State University, presiding

Invited Papers

8:00

GW1 1 Electron and Ion Transport in Hall Effect Thrusters.*JEAN-PIERRE BOEUF, *LAPLACE, CNRS and Univ. of Toulouse*

Hall Effect Thrusters (HETs) are gridless ion sources that can provide thrust on the order of 80 mN per kW of electrical power, with propellant velocity in the 20-30 km/s range. HETs are well suited for tasks such as satellite station keeping and are also considered for interplanetary missions. For these missions, where a small thrust is needed over a long period of time, their large propellant velocity makes them much more efficient than chemical thrusters and allows important cost reduction. The plasma in HETs is generated in the channel between two concentric dielectric cylinders. The anode is located at one end of the channel and the cathode is outside the channel. Gas (xenon) is injected through the anode and is ionized by electrons flowing to the anode. Xenon ions are accelerated by the electric field resulting from a drop of electron conductivity induced by the presence of a magnetic field barrier perpendicular to the electron path from cathode to anode. After a general introduction on space propulsion, the lecture will focus on basic physics questions related to electron and ion transport in a HET. Since most of the neutral flow is ionized, the neutral gas density in the exhaust region of a HET is not large enough to allow collisional electron transport across the magnetic field and to explain experimental measurements. We will describe recent efforts¹ aimed at understanding the observed anomalous transport, and present a synthesis of results from Particle-In-Cell (PIC) models, Hybrid Models, Laser Induced Fluorescence measurements and Collective Scattering (CS) experiments. PIC simulations predict and CS experiments seem to confirm that electron transport perpendicular to the magnetic field is due to the development of an azimuthal drift instability.

*Support: ANR, contract N ANR-06-BLAN-0171, TELIOPEH project ("Transport ELEctronique et IOnique dans les Propulseurs à Effet Hall")

Contributed Papers

8:30

GW1 2 Plasma-assisted ignition at high temperatures ILYA

KOSAREV, NICKOLAY ALEKSANDROV, SVETLANA KIN-DUSHEVA, SVETLANA STARIKOVSKAYA, *Moscow Institute of Physics and Technology* ANDREI STARIKOVSKII, *Drexel University* Non-equilibrium plasma of a pulsed nanosecond discharge can be used as an initiator of combustion process in gaseous mixtures. It was shown that, at the temperatures close to the ignition threshold, the time between the start of the experiment and a sharp increase in gas temperature and radical concentrations in combustible mixture (the autoignition delay time) decreases significantly when a short pulsed high-voltage discharge is applied to the system in the beginning of the experiment. Based on a detailed description of the gas discharge and combustion kinetics the kinetic mechanism of the plasma effect on ignition delay has been proposed. The production of electrons, ions, atoms, radicals and excited particles in the discharge and its near afterglow was calculated using the experimental data on $E/N(t)$ and $I(t)$ in the discharge. The analysis showed that by the beginning of the ignition process all active particles have been transported into atoms and radicals. The combustion kinetics was calculated using the standard mechanisms with additions of these species. A good correlation has been obtained between the experiments and calculations for the decrease in the ignition delay time.

8:45

GW1 3 PEGASES - plasma propulsion with electronegative

gases* ANE AANESLAND, PASCAL CHABERT, GARY LERAY, ALBERT MEIGE, JEAN-LUC RAIMBAULT, *LPTP, Ecole Polytechnique* A new concept of plasma propulsion is proposed, where the thrust is provided by both positive and negative ions resulting in a globally neutral beam downstream (in space). The basic idea is to create an ion-ion plasma (electron free region) at the periphery of a highly ionised plasma core such that positive and negative ions can be extracted either simultaneously or alternately by dc biased extractor grids. As the extracted beam is globally neutral there is no need for a neutralizer downstream. The recombination of positive and negative ions is very efficient compared to ion electron recombination. Hence, a fast recombination downstream of the thruster is expected, suppressing the common problems of a downstream plasma behind the thrusters. The ion-ion plasma region is formed in the periphery of a moderately magnetized plasma where the electrons are confined along the magnetic field lines while the ions are not: The applied magnetic field therefore acts as an electron filterer resulting in a stratified plasma with an electro-positive core (electrons and ions) and an ion-ion plasma (electron free) at the periphery. The propellant has to be a strongly electronegative gas in order to effectively create negative ions. The best candidate seems to be iodine, I₂, which has a high electron affinity, has a low ionisation threshold, is inexpensive, and does not require heavy and large gas tanks since it is in solid state with a high vapour pressure at room temperature.

*This research was supported by a Marie Curie Intra-European Fellowship within the 6th European Community Framework Programme.

9:00

GW1 4 Multiprocessor Modeling of Dielectric Barrier Discharge Plasma Actuator ALEXANDRE LIKHANSKII, VLADIMIR SEMAK, *Penn State University* DMITRY OPAITS, MIKHAIL SHNEIDER, *Princeton University* SERGEY MACHERET, *Lockheed Martin* The dielectric barrier discharge (DBD) plasma actuators have been studied both experimentally and numerically for the last decade. The single processor numerical simulations were able to qualitatively describe physics of DBD using some simplifications, such as modeling smaller time and geometrical scales [1] or neglecting some physical processes. For the quantitative description of DBD all physical phenomena of plasma generation, dynamics and decay should be comprehensively described at the experimental conditions. The present work describes the successful development of the multiprocessor numerical model and characterizes the physics of the DBD. The applicability of the currently used approaches for the further optimization of the model, such as modeling small scale DBDs or omitting physical processes, will also be discussed. I. A.V. Likhanskii, M.N. Shneider, S.O. Macheret and R.B. Miles, *J. Appl. Phys.* **103**, 053305 (2008).

9:15

GW1 5 Experimental Study of the Microdischarge Plasma Thruster (MDPT)* UTSAV KC, PHILIP VARGHESE, LAXMINARAYAN RAJA, *Department of Aerospace Engineering and Engineering Mechanics, The University of Texas at Austin, Austin, TX 78735* Small satellite propulsion requirements dictate the need for a scaled down propulsion device capable of providing low thrust with small impulse bits. We have designed and studied a simple miniaturized thruster called Microdischarge Plasma Thruster (MDPT). It comprises a tri-layer sandwich structure with a dielectric layer sandwiched between two electrode layers, and a contoured through hollow drilled into the structure. Each layer is 100's microns in thickness and the hole diameter of the same order. Argon is used as the propellant gas with flow rates of ~ 1 SCCM. The pressure is adequate to produce a stable microdischarge between the electrodes even with modest voltages (~ 1000 V). The microdischarge adds heat to the supersonic portion of the flowing gas which is shown to produce additional thrust over the baseline cold gas flow. The studies have also demonstrated that the MDPT exhaust plume is composed of ions albeit at low concentrations, suggesting possibility of MDPT to be operated in a mixed electrothermal/electrostatic mode. We present discussion of multiple discharge operating modes and electrical characteristics of the MDPT. Spectral measurements of the plume are used to determine its composition and calculate its temperature. The momentum thrust of the MDPT is measured with a torsion balance.

*This work was supported by AFOSR under grant FA9550-06-1-0176.

SESSION GW2: CHARGED PARTICLE SURFACE INTERACTIONS

Wednesday Morning, 15 October 2008; Salon A-D at 8:00
Steve Shannon, North Carolina State University, presiding

Invited Papers

8:00

GW2 1 Organising Atoms, Clusters and Proteins on Surfaces.

RICHARD E. PALMER, *Nanoscale Physics Research Laboratory, The University of Birmingham, Birmingham B15 2TT, UK*

This talk will discuss new developments in the creation of nanoscale surface features and their applications in biomedicine. Electron-surface interactions and plasma methods play a crucial role in both the production and analysis of these "atomic architectures." At the extreme limit, electron injection from the tip of a scanning tunnelling microscope (STM) enables bond-selective manipulation of individual polyatomic molecules [1]. On a more practical level, the controlled deposition of size-selected clusters [2], generated by magnetron sputtering and gas condensation followed by mass selection, represents a surprisingly efficient route to the fabrication of surface features of size 1-10 nm, the size scale of biological molecules such as proteins. STM and AFM measurements show the clusters can act as binding sites for individual protein molecules. For example, the pinning of size-selected AuN clusters ($N = 1-2000$) to the (hydrophobic) graphite surface presents binding site for sulphur atoms and thus for the cysteine residues in protein molecules. Systematic studies of different proteins [3] provide "ground rules" for residue-specific protein immobilisation by clusters and have led to the development of a novel biochip for protein screening by a spin-off company. The 3D atomic structure of the clusters is highly relevant to such applications. We show that measurement of the scattered electron beam intensity - specifically, the high angle annular dark field (HAADF) signal - in the scanning transmission electron microscope (STEM) allows us (a) to count the number of atoms in a cluster on the surface and (b) to determine a 3D atom-density map of the cluster when an aberration-corrected STEM is used [4]. 1. P.A. Sloan and R.E. Palmer, *Nature* **434** 367 (2005). 2. S. Pratontep, P. Preece, C. Xirouchaki, R.E. Palmer, C.F. Sanz-Navarro, S.D. Kenny and R. Smith, *Phys. Rev. Lett.* **90** 055503 (2003). 3. R.E. Palmer, S. Pratontep and H.-G. Boyen, *Nature Materials* **2** 443 (2003); R.E. Palmer and C. Leung, *Trends in Biotechnology* **25** 48 (2007). 4. Z.Y. Li, N.P. Young, M. Di Vece, R.E. Palmer, A.L. Bleloch, B.C. Curley, R.L. Johnston, J. Jiang, J. Yuan, *Nature* **451** 46 (2008).

8:30

GW2 2 Neutralization dynamics of hydrogen anions near flat and vicinal surfaces.^{†*}UWE THUMM, *Kansas State University*

I will scrutinize the role of intermediate electronic surface and image states on the charge-transfer dynamics during collisions of H^- anions with atomically flat Pd, Cu, and Ag surfaces of (100) and (111) symmetries using a wave-packet propagation approach [1]. For these surfaces I will show how differently located band gaps, surface -, and image states lead to easily visualized differences in the evolution of the active electron's probability density: i) Long-lived surface states of the (111) surfaces tend to localize electronic density near the surface and facilitate recapture by the projectile, while H^- is more efficiently neutralized near (100) surfaces whose surface state appears as a broad resonance embedded in the bulk valence band. ii) Image states that are degenerate with the metal conduction band favor, while image states that are degenerate with the band gap hinder recapture. In the second part of my talk I will discuss negative-ion interactions with stepped nano-structured surfaces based on effective potentials for the active electron's interaction with the surface that we derived within a Thomas-Fermi von Weizsaecker model [2]. For 50eV projectiles, we find an enhancement of electron loss near the steps due to the Smoluchowski effect. In consequence, negative-ion survival is more likely for projectiles that approach steps from above than from below [3]. [†] In collaboration with Himadri Chakraborty (Northwest Missouri State Univ.) and Boyan Obreshkov (Kansas State Univ.) [1] H. Chakraborty, T. Niederhausen, and U. Thumm, *Nucl. Instrum. Meth. B* **241**, 43 (2005); *Phys. Rev. A* **70**, 052903 (2004). [2] B. Obreshkov and U. Thumm, *Phys. Rev. A* **74**, 012901 (2006); [3] B. Obreshkov and U. Thumm, *Surf. Sci.* **601**, 622 (2007).

*Supported by the NSF and U.S. DoE.

Contributed Papers

9:00

GW2 3 Revibrational Spectra of Molecules Sputtered of Carbon Surfaces* PREDRAG KRSTIC, *Oak Ridge National Laboratory*

Irradiation of the carbon surfaces by hydrogen isotopes results in processes of crucial importance for the carbon based divertor tiles of a fusion reactor. Thus the sputtering and implantation, result in erosion, plasma pollution, and tritium retention, as well as carbon deposition all over the reactor first wall. The molecules chemically sputtered upon impact of deuterium of deuterated carbon surface are various hydrocarbons as well as We study the translational and rovibrational energy and angular spectra of sputtered molecules. The energy distributions of ejected molecules confirm the partial thermalization of the impact cascade. Sputtered hydrocarbon molecules have rovibrational energies in the range 1.5-2 eV, with relatively cold translational and rotational motion, close to 0.5 eV. In contrast, translational and rovibrational energies of sputtered deuterium molecules are close to 1 eV, with approximate equipartition between rotational and vibrational modes.

*Research supported by DOE, through Oak Ridge National Laboratory, managed by UT-Battelle, LLC under contract DE-AC05-00OR22725 and through SciDac program.

9:15

GW2 4 Study of oxygen ion beam decomposition and energy profiles after scattering from metal surface OLEKSIY VOZNIY, GEUN YOUNG YEOM, *Sungkyunkwan University* Ion beam, extracted from inductively coupled oxygen plasma, was neutralized during scattering from a set of parallel metal plates. Energy distribution and the neutralization probability of the reflected O^+ and O_2^+ ions was measured during the scattering. It was found that the beam of monatomic ions has broader energy distribution which was often accompanied by multiple peaks of the distribution function. The ratio of monatomic and diatomic ions of the beam shows exponential increase against the acceleration potential showing considerable input of the elastic scattering into the ion decomposition. Neutralization efficiency of the both beams was compared for the different regimes of ion beam scattering.

SESSION GW3: LASERS, BREAKDOWNS AND SPARKS

Wednesday Morning, 15 October 2008

Addison Room at 8:00

Z.Lj. Petrovic, *Institute of Physics Belgrade*, presiding

8:00

GW3 1 Applicability of Generalized Peek's Law to Scaling of Corona Onset Voltages in Electropositive Gases YAN-MING LI, *Osram Sylvania*

We have developed the steady state positive corona model with the ionization zone physics in the point-plane configuration. The geometry is axisymmetric, consisting of a pointed anode of small tip radius and a planar cathode. The model solves the Poisson equation, drift dominated electron and the positive ion transport equations with the nonlinear Townsend ionization source terms, to give the complete electric field, electron and positive ion density distributions. The corona plasma properties can be determined as function of discharge current, ranging from the pico-ampere up to a milli-ampere. The calculated voltage-current characteristics obeyed the Townsend equation, agreeing with the general experimental observations. The model is applied to different electropositive gases, argon, xenon, nitrogen and mercury. Corona onset potentials are determined based on the discharge voltages at very low currents. Extensive parametric study for argon positive corona with varying anode tip radius, gap distance and gas pressure has been completed. All the simulated corona onset voltages are very well described by the generalized Peek's Law [1]. At sufficiently high current in the range of 0.1 mA, discharge filament is formed near the anode tip. [1] Peek F. W., *Dielectric Phenomena in High Voltage Engineering*, McGraw Hill, New York (1929).

8:15

GW3 2 Modeling of the propagation of streamers in methane-air mixtures using the 3-group SP_3 photoionization model*

N.Y. LIU, V.P. PASKO, A. BOURDON, S. CELESTIN, P. SE-GUR, E. MARODE, *Florida Tech* Non-thermal plasma assisted ignition and combustion receives increasing attention recently [e.g., Starikovskaia, *J. Phys. D*, 39, R265, 2006]. Experimental and numerical work has shown that the application of transient plasma discharges (including the stages of streamer propagation and streamer-to-spark transition) in the ignition of propane-air or methane-air mixtures significantly reduces the ignition delay time [e.g., Pancheshnyi et al., *IEEE Trans. Plasma Sci.*, 34, 2478, 2006; Naidis, *J. Phys. D*, 40, 4525, 2007]. In this work, we study the propagation of streamers in methane-air mixtures. We have recently developed a photoionization model based on radiative transfer theory, called 3-group SP_3 model, for the simulation of streamer discharges in air [Bourdon et al., *Plasma Sources Sci. Technol.* 16, 656, 2007; Liu et al., *Appl. Phys. Lett.*, 91, 211501, 2007]. In this talk, we show it is straightforward to apply the 3-group SP_3 model to the simulation of streamers in methane-air mixtures. We report the modeling results on the propagation of streamers in methane-air mixtures and the associated heating of the gas mixtures. We also discuss the effects of addition of methane to air on the dynamics of the streamer.

*This research was supported by the PSS Department of Florida Tech and by NSF ATM 0725360 grant to Penn State University.

8:30

GW3 3 Optical Breakdown Based on Resonant Enhanced Multi-Photon Ionization and Electron Avalanche Ionization in Gas Mixtures MIKHAIL SHNEIDER, ZHILI ZHANG, RICHARD MILES, *Princeton University* We present the results of the experimental and theoretical study of a new kind of optical breakdown in gases with ionization amplification by the combination of Resonant Enhanced Multi-Photon Ionization (REMPI) and subsequent avalanche ionization. As an example, the Ar:Xe mixture was studied. Coherent microwave Rayleigh scattering (radar REMPI) was used to measure REMPI and avalanche ionization. It was shown that REMPI ionization of a relatively small density component (Ar) can catalyze the avalanche ionization process in a buffer gas (Xe) by the use of a laser beam at very low intensity. Theoretical plasma dynamic model verifies the finding. Based on the presented results, several important applications are possible. First, it can improve the detection sensitivity of Radar REMPI. Second, it suggests that plasma generation can be achieved at reduced gas densities or laser beam intensities. Here we can suggest the following two methods: 1. Long laser pulse: The pulse front generates REMPI and subsequent pulse initiates avalanche ionization and Joule heating. 2. Two subsequent laser pulses: A short laser pulse tuned on a REMPI of mixture component generates weakly ionized REMPI plasma and a long off-resonant laser pulse for the avalanche ionization and Joule heating.

8:45

GW3 4 Scaling of an Electric Discharge Excited Oxygen-Iodine Laser* JOHN BRUZZESE, MUNETAKE NISHIHARA, WALTER LEMPERT, J. WILLIAM RICH, IGOR ADAMOVICH, *The Ohio State University* Electric discharge excited oxygen-iodine laser apparatus has been scaled to increase the electric discharge volume and power, the laser mixture flow rate, and the gain path in the $M=3$ laser cavity. Specifically, singlet delta oxygen

(SDO) generator discharge power has been increased at least up to 3.5 kW, laser mixture flow rate up to 0.5 mole/sec, and gain path up to 10 cm. Steady-state run time of the new scaled-up laser apparatus at these conditions is up to 10 sec. Two different discharge configurations have been used to generate singlet delta oxygen, crossed nanosecond pulser / transverse DC sustainer discharge and capacitively coupled transverse RF discharge. Flow temperature downstream of the discharge, singlet delta oxygen yield, and laser gain have been measured in a wide range of discharge powers, nitric oxide mole fraction in the main oxygen-helium flow, and oxygen percentage in the mixture, at discharge pressures ranging from 60 to 90 torr. The results demonstrate that SDO yield increases with the discharge power for both discharge configurations, although highest yields achieved so far remain low, 3.6-3.7%, due to fairly low energy loading per oxygen molecule in the discharge. Small signal gain measured in the $M=3$ cavity of the new laser apparatus is up to 0.116%/cm (2.3% gain per single pass), at the flow temperature of $T=125$ K.

*Support of Joint Technology Office is gratefully acknowledged.

9:00

GW3 5 Laser emission at $\lambda = 337.1$ and $\lambda = 357.7$ nm of N_2 molecules in inductively coupled plasma ALEXANDER RAZHEV, DMITRY CHURKIN, *Institute of Laser Physics SD RAS* Pulsed inductively coupled plasma for inversion population formation on electronic transitions of neutral atoms and molecules of gases was used. UV inductive N_2 laser at $\lambda = 337.1$ nm and $\lambda = 357.7$ nm has been created. The system for formation of the pulsed inductive discharge of the cylindrical form in gases was described. Results of an experimental investigations of spectral, temporal and energy parameters of spontaneous and laser radiation of the inductive N_2 laser operated in pure nitrogen and gas mixtures of N_2 with NF_3 and SF_6 are presented. The generation only at $\lambda = 337.1$ nm, corresponding to the (0 - 0) band of the second positive system of $C^3\Pi_u \rightarrow B^3\Pi_g$ transition of nitrogen molecules was obtained in pure nitrogen pumped by inductive discharge. The generation at $\lambda = 337.1$ nm and $\lambda = 357.7$ nm was obtained in gas mixtures of N_2 with NF_3 and SF_6 . Under optimal conditions the behavior of $\lambda = 337.1$ nm to $\lambda = 357.7$ nm intensities was approximately as 10:1. Total mixture pressure was varied in a range 0.1 - 3 Torr. The maximal generation energy of 4.5 mJ at pulse duration (FWHM) 15 ± 1 ns was achieved. Laser beam had a ring shape with external diameter about 42 mm and the thickness of 1.0 - 1.5 mm. Inductive N_2 laser could operate with pulse repetition rate up to 50 Hz. The present work has been supported by RFBR, Grant # 06-02-16149-a.

9:15

GW3 6 Influence of nitrogen oxides on singlet delta oxygen production in pulsed discharge for electric discharge oxygen-iodine laser ANDREY IONIN, YURII KLIMACHEV, ANDREY KOZLOV, ANDREY KOTKOV, *Lebedev Physical Institute of Russian Academy of Sciences* IGOR KOCHETOV, ANATOLY NAPARTOVICH, (TRINITY) OLEG RULEV, LEONID SELEZNEV, DMITRY SINITSYN, NIKOLAY VAGIN, NIKOLAY YURUSHEV, *Lebedev Physical Institute of Russian Academy of Sciences* LEBEDEV PHYSICAL INSTITUTE OF RUSSIAN ACADEMY OF SCIENCES TEAM, TRINITY TEAM, Influence of nitrogen oxides NO and NO₂ on specific input energy (SIE) and time behavior of singlet delta oxygen (SDO)

luminescence excited by pulsed e-beam sustained discharge in oxygen was experimentally and theoretically studied. NO and NO₂ addition into oxygen results in a small increase and a decrease of SIE, respectively. Addition of 0.1-0.3 percent of nitrogen oxides was experimentally and theoretically demonstrated to result in notable enhancement of SDO lifetime, which is related to a decrease of atomic oxygen concentration in afterglow. For getting

high SDO concentration at gas pressure 30-60 Torr for the time interval less than 0.5 s one needs to add not less than 0.2 percent of nitrogen oxides into oxygen. Temperature dependence of relaxation constant for SDO quenching by unexcited oxygen was estimated by using experimental data on time behavior of SDO luminescence.

SESSION HW: ALLIS PRIZE LECTURE

Wednesday Morning, 15 October 2008; Salon A-E at 10:00
Peter Ventzek, Ventzek Consulting Engineering, presiding

10:00

HW 1 Ionization dynamics of atoms by strong, ultra-short laser pulses.

KENNETH KULANDER, *Lawrence Livermore National Laboratory*

The multiphoton double ionization of He is observed to be far more efficient than would be expected based on the second electron leaving some time after the first, at a significantly higher intensity, in an uncorrelated sequence. Therefore some sort of correlated two-electron process, called non-sequential ionization (NSI), is required. NSI has been modeled theoretically using everything from 'exact' full spatial 3D (and model 1D) quantum calculations to completely classical trajectory representation. A commonly studied quasi-classical, rescattering scheme reproduces the general characteristics of the observations, but it fails at the threshold. Its predicted intensity for the onset of NSI is at least a factor of two too high. A new resonance process that addresses this problem has been developed and tested on a 1D model for which exact solutions are easily obtained. This model's NSI threshold behavior leads to the prediction of a path to double ejection that involves a new laser-induced doubly excited (autoionizing) state. The analysis of the results, particularly in relation to NSI in real He measurements, will be presented.

SESSION LW1: PLASMA DIAGNOSTICS I

Wednesday Afternoon, 15 October 2008
Salon E at 13:30

Noah Hershkowitz, University of Wisconsin-Madison, presiding

13:30

LW1 1 Formation and Propagation of the Plasma Bullets

Emitted by a Pulsed Plasma Jet ASMA BEGUM, ERDINC KARAKAS, MOUNIR LAROUSI,* *Old Dominion University*

Recently non-thermal atmospheric pressure plasma jets have been playing an important role in plasma processing including biomedical applications. This is due to the ability of providing plasmas not confined by electrodes. In this paper we report experimental investigations on the characteristics of the plasma jet emitted by a pulsed plasma generator, the "Plasma Pencil." Two ring electrodes attached to the surface of alumina disk are inserted in a dielectric tube and separated by a small gap. One of the two electrodes is connected to a high voltage pulse generator. Using ICCD we show that the plume is a series of plasma packets/bullets traveling at high velocities. Correlation between the discharge current and ICCD images reveals when and how the bullets are emitted from the device. Using optical emission spectroscopy, we will present spatially resolved emission spectra which give indications of the evolution of the various chemical species contained in the plasma bullets. In addition, we will show the effects of an external electric field and gas flow on the evolution and chemistry of the plasma bullets.

*Director, Laser and Plasma Engineering Institute

13:45

LW1 2 Stark broadening for determination of electron density and electron temperature in an atmospheric pressure arc*

JENNA R. PUCKETT, MATTHEW R. KING, CHRISTOPHER J. OLDHAM, JEROME J. CUOMO, *Department of Materials Science and Engineering, NC State University*

Determining basic plasma parameters for low frequency, atmospheric pressure discharges is often difficult. However, insight into these parameters is imperative for understanding fundamental processes in all plasma applications. Because Stark broadening of lines in the hydrogen Balmer series depend on electron temperature (T_e) and electron density (N_e), lineshape analysis can be used to determine these parameters. This technique has been developed in the literature and we find it can be applied to a low frequency, atmospheric pressure arc. The effects of power and frequency on N_e and T_e were examined in a gas mixture of argon and 0.5% hydrogen using an Ocean Optics HR2000 spectrometer (groove density of 2400mm⁻¹). Nitrogen was added to study the effect of other gases on plasma parameters with the Stark broadening technique.

*This work was funded by the Dean's Office in the College of Engineering and the Department of Materials Science and Engineering.

14:00

LW1 3 Measurement of Plasma density in High Intensity Discharge Lamps by THz Interferometry

ALEX KIECKHAFFER, JOHN CURRY, *NIST*

A THz interferometer has been constructed with the goal of directly measuring plasma electron densities in High Intensity Discharge (HID) lamp plasmas. The use of THz frequencies has several advantages. Primary of these is the ability to measure high densities. The 0.6 THz system constructed is capable of measuring densities up to 4×10^{15} cm⁻³. Additionally,

the short wavelength of 0.6 THz radiation will allow focal spot sizes smaller than a millimeter in diameter, thus enabling high spatial resolution measurements. The system also differs from traditional microwave interferometry in that heterodyning has been eliminated. In inductively driven lamps the plasma recombines twice per AC cycle, when the voltage drops below a critical value. This time-dependent phase shift of the THz beam will allow calculation of density as a function of time. Zero-points can be acquired during the measurement itself due to the twice-per-cycle recombination of the plasma. Detection using electro-optical or nonlinear optical methods can easily achieve the time resolution required for these measurements, while maintaining sufficient signal-to-noise levels for detection without the assistance of lock-in amplification.

14:15

LW1 4 Microwave In-Phase and Quadrature Detection of E-Beam Generated Air Plasma* ROBERT VIDMAR, CHRIS RAMSAYER, *University of Nevada, Reno* KENNETH STALDER, *Stalder Technologies and Research* Microwave In-phase and Quadrature (I/Q) measurements at 10 GHz are discussed in the context of determining plasma parameters. Plasma generated in laboratory air with a pressure from 1 mTorr to 636 Torr is modeled as collisional plasma. The electron temperature is close to the bulk gas temperature at high pressure or up to a few eV at low pressure. Plasma generation is produced with 10-ms pulses of electrons from a 100-keV 5-mA electron gun, which then propagate through a 12.7- μm aluminum transmission window into a 400-liter test cell. A differential measurement approach is described that extends the dynamic range of the I/Q magnitude measurement from tens of dB to a small fraction of a dB. Amplification of the phase measurement is used to increase sensitivity. Ultimate sensitivity and filtering of both measurements are discussed in the context of mixer shot noise, Johnson noise, and pulse duration. Representative measurements and the procedure to convert raw data into estimates of electron number density and electron momentum transfer collision rate are discussed.

*This material is based on research sponsored by the Air Force Research Laboratory, under agreement numbers FA9550-05-1-0087 and FA9550-07-1-0021.

14:30

LW1 5 Laser Deflection (Schlieren) Measurements of Hg Density in an Ultra High Pressure Arc Lamp* J. KANE, M. KATO, [†]J.E. LAWLER, *University of Wisconsin* The very high gas densities and excellent quality arc tubes of Ultra High Pressure (UHP) Hg arc lamps create opportunities for unusual diagnostics. An experimentally derived density map of a 213 bar UHP lamp is reported. The deflection of a laser beam by temperature induced density/index gradients is reconstructed through an Abel inversion. This deflection technique is most sensitive in the mantle unlike emission techniques which are sensitive in the arc core. The resulting map is compared to previous measurements of the temperature in the arc core as well as theoretical models of the temperature in the arc mantle.

*Supported by NSF CTS 0613277.

[†]also USHIO INC.

14:45

LW1 6 $\text{N}_2(A^3\Sigma_u^+)$ density in ICP N_2 plasmas measured by diode laser cavity-ringdown absorption spectroscopy Y. HORIKAWA, *Nagoya University* K. KURIHARA, *Toshiba Corp.* K. SASAKI, *Nagoya University* There are two candidates for the precursor for nitriding silicon surfaces by nitrogen plasmas: atomic nitrogen and molecular nitrogen at the metastable $A^3\Sigma_u^+$ state. The goal of our work is to identify the nitriding precursor by comparing the precursor densities with the nitriding performance. In this work, we measured the $\text{N}_2(A^3\Sigma_u^+)$ density in ICP nitrogen plasmas by cavity-ringdown absorption spectroscopy (CRDS) at the first positive band. By employing a diode laser as the light source, a sensitive detection limit of 10^{-6} for absorption was obtained in our CRDS system. We observed that the increase in the $\text{N}_2(A^3\Sigma_u^+)$ density with the rf power was gentle and was saturated at a high rf power. The $\text{N}_2(A^3\Sigma_u^+)$ density decreased with the nitrogen gas pressure significantly, and the $\text{N}_2(A^3\Sigma_u^+)$ density at 100 mTorr was approximately 1/10 of that at 20 mTorr. We also measured the N atom density at the ground state by vacuum ultraviolet absorption spectroscopy at the $4S^o - 4P$ transition. As a result, it was observed that the increase in the N atom density with the rf power was steeper than that in the $\text{N}_2(A^3\Sigma_u^+)$ density. In addition, the N atom density increased with the nitrogen gas pressure. At the conference, we will discuss the kinetics of $\text{N}_2(A^3\Sigma_u^+)$ and N by comparing their densities.

15:00

LW1 7 Estimating and controlling the atomic oxygen content in an argon-oxygen plasma BERNARD KEVILLE, *Dublin City University, Ireland* DEREK D. MONAHAN, MILES M. TURNER, Oxygen rich plasmas have been applied in many plasma processing applications for decades. In most such applications, process yield could be improved significantly by applying closed loop control of atomic oxygen radical concentration. The design of effective, real time, closed loop control algorithms is facilitated by simple dynamical models of the relationship between inputs, or actuators in control terminology, and the process quantities to be controlled. In the case of an oxygen rich plasma process, one requires the relationship between the inputs - flow-rate set points, forward power from the RF supply and residence time, for example - and the oxygen radical density. With the aid of an argon-oxygen plasma simulation, this presentation describes how, with the aid of simplified dynamical models of the process, one would design model-based control algorithms for the real-time, closed loop control of oxygen radical density. A sine qua non of real time, closed loop control is an accurate estimate of the process quantities to be controlled. Although actinometry provides a non-invasive method for estimating species densities, atomic oxygen actinometry is complicated by the fact that photon emission can occur through dissociative as well as direct excitation, leading to potential ambiguity between the emission intensity and the actual radical concentration in the plasma. Optimal estimation of process states given indirect measurements corrupted by process and measurement noise is a classical topic in control theory and has yielded some spectacular results, notably the ubiquitous Kalman filter.

15:15

LW1 8 Integrated Plasma-Surface Kinetics Model to Predict Deposition Rates in an HDP-CVD Reactor ANANTH BHOJ, PRASHANTH KOTHNUR, RON KINDER, *Novellus Systems, Inc.* A comprehensive model for HDP-CVD reactors used in semiconductor processing, such as the Novellus SPEED, remains challenging due to the complex coupling of plasma transport, gas-phase and surface chemical reaction pathways in the chamber. The Hybrid Plasma Equipment Model (HPEM) is employed here to predict deposition rates at the wafer. The HPEM has a Surface Kinetics Module (SKM) that accepts species fluxes from the plasma, computes deposition/etch rates and coverage of various

surface resident species and modifies sticking coefficients of plasma species based on their surface reactivity. Discharges in Ar/O₂/SiH₄ generated at a few mTorr and 2 – 6 kW power deposition in a dome-shaped 200-mm chamber are considered. The gas-phase and surface reaction mechanisms build on those used by Meeks *et al.* [1] for their well-mixed reactor model. The effect of varying power, pressure and wafer temperature on plasma characteristics and the ensuing effects on deposition rates and surface coverage of species at the wafer will be discussed. [1] E. Meeks, R. S. Larson, P. Ho, C. Apblett, S. M. Han, E. Edelberg, E. S. Aydil, *J. Vac. Sci. Technol. A*, **16**(2), 544 (1998).

SESSION LW2: ELECTRON/POSITRON ATOM COLLISIONS

Wednesday Afternoon, 15 October 2008; Salon A-D at 13:30

M.A. Khakoo, California State University at Fullerton, presiding

Invited Papers

13:30

LW2 1 Calculation of Atomic Data for Plasma Applications.*

OLEG ZATSARINNY,[†] *Drake University*

Accurate and complete datasets for atomic structure and collision parameters are important for many applications in plasma physics, in particular the modeling and diagnostic of discharges. In recent years, we have developed a general computer code [1], based on the close-coupling expansion, that allows for the calculations of such data both for the target structure (energy levels and oscillator strengths) and electron collisions with atoms and ions. The general idea behind such calculations will be discussed, as well as the expected accuracy of the results, current limitations of theory, recent developments including a fully relativistic version [2], and planned extensions for the future. The method will be illustrated with oscillator strengths and electron collision cross sections for the noble gases He-Xe, alkali metals such as a Na and Cs, ions such as FeII, and very heavy targets such as Au and Hg. [1] O. Zatsarinny, *Comp. Phys. Commun.* **174** (2006) 273. [2] O. Zatsarinny and K. Bartschat, *Phys. Rev. A* **77** (2008) 062701.

*Work supported by the NSF under PHY-0555226 and PHY-0757755.

[†]This work was performed in collaboration with Klaus Bartschat.

Contributed Papers

14:00

LW2 2 Positron Scattering from Neon* AL STAUFFER, *York University, Canada* ROBERT MCEACHRAN, JAMES SULLIVAN, CASTEN MAKOCHEKANWA, PETER CARADONNA, ADRIC JONES, DANIEL SLAUGHTER, STEPHEN BUCKMAN, *CAMS, Australian National University* A joint experimental and theoretical investigation of low-energy positron-neon scattering has been carried out. The experimental studies have used a high-resolution, trap-based beam and scattering cell to obtain absolute cross sections for total scattering, total elastic scattering and positronium formation. The experimental and theoretical total elastic cross section are compared from near threshold up to the positronium formation threshold at ~ 15 eV. Theoretically, the elastic differential cross section has also been calculated up to 50 eV including, where appropriate, absorption effects via an *ab initio* absorption potential.

*Supported by the Canadian and Australian Governments.

14:15

LW2 3 Low-Energy Electron Collisions with Copper and Gold Atoms*

KLAUS BARTSCHAT, OLEG ZATSARINNY, *Drake University* We have extended the *B*-spline *R*-matrix (close-coupling) method [1] to fully account for relativistic effects in a Dirac-Coulomb formulation [2]. The computer code was applied to electron-impact excitation of the $(3d^{10}4s)^2S_{1/2} \rightarrow (3d^{10}4p)^2P_{1/2,3/2}$ and $(3d^{10}4s)^2S_{1/2} \rightarrow (3d^94s^2)^2D_{5/2,3/2}$ transitions in Cu and the corresponding transitions $(5d^{10}6s)^2S_{1/2} \rightarrow (5d^{10}6p)^2P_{1/2,3/2}$ and $(5d^{10}6s)^2S_{1/2} \rightarrow (5d^96s^2)^2D_{5/2,3/2}$ in Au. Our numerical implementation of the close-coupling method enables us to construct term-dependent, non-orthogonal sets of one-electron orbitals for the bound and continuum electrons. This is a critical aspect in the present problems, especially for the outermost d and s orbitals. Furthermore, core-polarization effects are accounted for *ab initio* rather than through a model potential. Our results will be compared with recent experimental data [3] and predictions from other

theoretical approaches [4]. [1] O. Zatsarinny, *Comp. Phys. Commun.* **174**, 273 (2006). [2] O. Zatsarinny and K. Bartschat, *Phys. Rev. A* **77**, 062701 (2008). [3] M. Maslov, P.J.O. Teubner, and M.J. Brunger, *Phys. Rev. A* **77**, in press (2008). [4] D.V. Fursa, I. Bray, and R.P. McEachran, private communication (2008).

*Work supported by the NSF under PHY-0555226 and PHY-0757755.

14:30

LW2 4 Electron-photon coincidence experiment in full scattering angle range LUKASZ KLOSOWSKI, MARIUSZ PIWINSKI, DARIUSZ DZICZEK, KATARZYNA PLESKACZ, STANISLAW CHWIROT, *Nicolaus Copernicus University, Institute of Physics, Grudziadzka 5/7, 87-100 Torun, Poland* Electron impact coherence parameters (EICP) have been measured with coincidence technique for various collisional systems since 1970s. Large discrepancies occurring in various theoretical predictions could not be resolved because of lack of experimental data for large scattering angles. Experiments that provide data for the largest scattering angles have not been carried out for seemingly simple reason – finite dimensions of electron beam sources and energy analyzers. Such measurements are possible if electron trajectories are suitably modified by magnetic field (*Rev. Sci. Instrum.* **67** (1996) 2372). It has been also shown recently that the magnetic angle changer (MAC) could be used in EICP measurements (*Meas. Sci. Technol.* **18** (2007) 3801, *J. Phys. B: At. Mol. Opt. Phys.* **41** (2008) 055202). The principles of MAC operation and the design of the device used in coincidence experiment are presented together with new experimental data on EICPs for 100 eV e-He 2^1P_1 impact excitation for full scattering angle range.

14:45

LW2 5 Electron scattering from atomic gallium: data for plasma physics modeling* D.V. FURSA, I. BRAY, *CAMS Curtin University* Accurate electron-atom collision data is of primary importance for plasma physics modeling. Often the number of required transitions is very large and realistically can only be provided by theoretical calculations of electron-atom collisions. With development of sophisticated scattering methods, such as Convergent Close Coupling (CCC) method and R-matrix (RM) method, accurate collision data can be obtained for large number of scattering systems. Recent developments in CCC and RM methods allow for accurate calculations of target atoms which are strongly affected by relativistic effects. Gallium is one such target, with the ground state being a P-state that is strongly affected by spin-orbit interaction resulting in fine-structure splitting of 0.1 eV. We have performed fully-relativistic CCC calculations of electron scattering from gallium and compared with the available experimental and theoretical data. We find large discrepancies with the collision data used for the modeling of gallium-iodine positive column discharge plasma, which recently attracted substantial attention as a possible candidate for designing nontoxic (mercury-free) light sources.

*Support from the Australian Research Council is gratefully acknowledged.

15:00

LW2 6 Absolute angle-differential cross sections for near-threshold electron-impact excitation of neon* MICHAEL ALLAN, *University of Fribourg* KAI FRANZ, HARTMUT HOTOP, *University of Kaiserslautern* OLEG ZATSARINNY, KLAUS BARTSCHAT, *Drake University* Absolute angle-differential cross sections for excitation of neon atoms to the four ($2p^53s$) and selected ($2p^53p$) and ($2p^53d$) levels have been determined as a function of electron energy up to 3.5 eV above threshold at scattering angles of 0° , 45° , 90° , 135° and 180° . Some cross sections were also recorded as function of scattering angle from 0° to 180° , which was possible through the use of a “magnetic angle changer.” Comparison of the experimental data with theoretical predictions based on Breit-Pauli *B*-splineR-matrix calculations shows overall good agreement regarding both the absolute values and the details of numerous resonant features. Some discrepancies remain, however, whose possible origin will be discussed at the conference.

*Work supported by the Swiss, German, and United States National Science Foundations.

15:15

LW2 7 Electronic Excitation of low-lying Excited States of Argon and N2 by Electron Impact* SUBHENDU MONDAL, JULIAN LOWER, STEPHEN BUCKMAN, *CAMS, Australian National University* GUSTAVO GARCIA, *CSIC, Madrid* We have used a low energy, time-of-flight (ToF) electron spectrometer to measure absolute cross sections for the near-threshold excitation of low-lying levels of N2 and for the 4s and 4p manifolds of states in argon. The measurements cover an energy range from 12.5 – 15 eV and an angular range from 50-125[r]. The absolute values of the cross sections are obtained by reference to the absolute elastic scattering cross section. The ToF technique has the advantage that the transmission of the energy analyser is independent of energy and it thus removes one of the major uncertainties involved in such measurements with conventional electrostatic spectrometers.

*Supported by the Australian and Spanish Governments.

SESSION MWPI: POSTER SESSION II
Wednesday Afternoon, 15 October 2008
Salon F-J at 16:00
I. Langmuir, presiding

MWPI 1 ELECTRON ATOM/MOLECULE COLLISIONS

MWPI 2 The Coulomb Four-Body Problem: Electron Impact Double Ionization of Helium in the Threshold Regime XUEGUANG REN, ALEXANDER DORN, JOACHIM ULLRICH, *Max-Planck-Institute for Nuclear Physics, Heidelberg, Germany* Double ionization of helium by electron impact represents one of the most fundamental four-body problems. While various experiments exist for fast collisions the threshold region where theories predict a strongly correlated and fully symmetric emission with 120° relative angles of the three electrons is unexplored concern-

ing differential measurements. We present kinematical complete experiments for impact energies 27 eV and 5 eV above the threshold. At the lower energy clear signatures for the threshold region being reached and the symmetric electron emission are observed.

MWP1 3 Electron Impact K-shell Ionization Cross Sections*

M.A.R. PATOARY, M. ALFAZ UDDIN, A.K.F. HAQUE, M. SHAHJAHAN, A.K. BASAK, M.R. TALUKDER, *Department of Physics, University of Rajshahi, Rajshahi, Bangladesh* BIDHAN SAHA, *Department of Physics, Florida A&M University* A new semi-empirical model comprising few important features of the DM [1] model and Bell [2] model is used to evaluate the electron impact K-shell ionization cross sections of 30 atomic targets ranging from H to U ($Z=1-92$). Details results will be presented at the conference [1] H. Deutsh, K. Becker, T. D. Mark, *Int. J. Mass Spect.* 177, 47 (1998). [2] K. L. Bell, H. B. Gilbody, J. G. Hughes, A. E. Kingston and F. J. J. Smith, *Phys. Chem. Ref. Data* 12, 891 (1983).

*BCS thanks NSF-CREST for support.

MWP1 4 Total and Total ionization Cross sections for Germanium hydrides GeH_x ($x=1-4$) on electron impact from 0.1 eV to 5 keV*

MINAXI VINODKUMAR, *V.P. Science College, V V Nagar* CHETAN LIMBACHIYA, *P.S. Science College, Kadi - 382715* KIRTI KOROT, *V.P. Science College, V V Nagar* K.N. JOSHIPURA, *Dept. of Physics, S.P. University, V V Nagar* NIGEL MASON, *Dept. of Physics and Astronomy, Open University, MK76AA, UK* Germanium hydrides, in particular germane, GeH_4 , are widely used as feed gases in plasma deposition and doping processes in the semiconductor industries. In this paper we report electron impact total cross sections from 0.1 eV to 5 keV for GeH_x ($x=1-4$). We employed R-matrix method using Quantemol N[1] till 15 eV and spherical complex optical potential formalism (SCOP) [2-3] beyond 15 eV. We also report total ionization cross sections using our Complex Scattering Potential - ionization contribution (CSP-ic) [2,3] for these targets. [1] J.Tennyson, D.B. Brown, J.Munro I.Rozum, H.Varambhia, *N.Vinci Journal of Physics: Conference Series* 86 (2007) 012001 [2] M. Vinodkumar, C. Limbachiya, K.N. Joshipura, K. Korot, *Eur. J. Phys. D.* (2008) DOI: 10.1140/epjd/e2008-00106-3 [3] M. Vinodkumar, C. Limbachiya, K.N.Joshi-pura, K. Korot, Nigel Mason *Int. J. Mass Spectrom* 273 (2008) 145.

*MVK and CGL thank UGC for Major & Minor Projects.

MWP1 5 Low Energy Elastic Scattering from n-Propanol and n-Butanol*

M.A. KHAKOO, J. MUSE, *Cal. State U. Fullerton, CA, USA* H. SILVA, M.C.A. LOPES, *Federal U. of Juiz de Fora, MG, Brazil* C. WINSTEAD, V. MCKOY, *CalTech, Pasadena, CA, USA* R.F. DA COSTA, E.M. DE OLIVEIRA, M.A.P. LIMA, *State U. of Campinas, SP, Brazil* M.H.F. BETTEGA, *Federal U. of Parana, Curitiba, Brazil* L.G. FERREIRA, *U. of Sao Paulo, SP, Brazil* M.T. DO N. VARELLA, *Federal U. of ABC, Santo Andre, SP, Brazil* Measured and calculated elastic electron scattering differential cross sections are reported at incident energies of 1, 2, 5, 10, 15, 20, 30, 50, and 100 eV. The measurements employed the

relative flow method with He as the standard gas and an aperture collimating gas source. The calculated results are obtained from two different implementations of the Schwinger multichannel method: one that takes all electrons into account and is adapted for parallel computers and another that uses pseudopotentials and considers only the valence electrons. Both sets of calculations include polarization effects. Comparison between the measured and calculated cross sections is found to be quite satisfactory.

*Funded by NSF, DOE (USA) and CAPES, CNPq, FAPEMIG, FAPESP, Finep (Brazil)

MWP1 6 Atomic Data of Electron Collisional and Radiative Processes and Modeling of non-LTE Krypton Plasmas*

ARATI DASGUPTA, *NRL* ROBERT W. CLARK, *Berkeley Scholars Inc.* JOHN L. GIULIANI, JACK DAVIS, *NRL* We have developed a detailed multilevel atomic model for K-, L- and M-shell krypton, and investigated its impact on the radiation hydrodynamics on a krypton gas puff driven by the redesigned Sandia National Laboratory ZR accelerator. The atomic model employs an extensive atomic level structure to accurately model the dynamics and the spectroscopic details of the emitted radiation. The atomic data was obtained using the state-of-the-art Flexible Atomic Code, and all relevant collisional and radiative atomic processes such as electron-impact excitation, ionization, radiative and dielectronic recombination were included in generating the model. The enormous number of fine-structure levels were judiciously lumped to create a database that is detailed but manageable. We have analyzed the behavior in the krypton K- through M-shell ionization stages using temperature and density conditions that have been predicted in hydrodynamics calculations of implodes.

*Work supported by DOE/NNSA.

MWP1 7 Differential Cross sections for Electron-Impact Ionization of Atomic Helium and Molecular Hydrogen for both Coplanar and Perpendicular Plane Scattering*

OLA ALHAGAN, DON MADISON, *Missouri University of Science and Technology* XUEGUANG REN, ARNE SENFTLEBEN, ALEXANDER DORN, JOACHIM ULLRICH, *Max-Planck-Institut für Kernphysik* DMITRY FURSA, IGOR BRAY, *Curtin University, Perth, Australia* The effect of electronic and nuclear charge distributions can be studied by comparing atomic and molecular ionizing collisions for homoelectronic and homonuclear atoms and molecules. Experimental and theoretical differential cross sections will be presented for electron-impact ionization of atomic helium and molecular hydrogen for both coplanar and perpendicular plane scattering. Since the effects of electronic charge distributions and nuclear charge distributions on the fully differential cross sections are most pronounced for low energy electrons, results will be presented for one electron having an energy of 4 eV and the other one having 12 eV in the final state. Electronic and nuclear effects will be analyzed individually.

*Work Supported by NSF.

MWPI 8 HEAVY PARTICLE COLLISIONS II

MWPI 9 Electron-electron correlations assessed analyzing doubly differential angular distributions in double ionization of helium by proton impact MARCELO CIAPPINA, *Max-Planck-Institut für Physik komplexer Systeme* MICHAEL SCHULZ, *Physics Department and LAMOR, University of Missouri-Rolla* TOM KIRCHNER, *Institut für Theoretische Physik, TU Clausthal* DANIEL FISCHER, ROBERT MOSHAMMER, JOACHIM ULLRICH, *Max-Planck-Institut für Kernphysik* Double ionization (DI) of helium by ion impact presents a singular scenario to study electron-electron correlation in atomic physics. Recent experimental data have revealed signatures of this feature in the doubly differential cross sections in terms of the angles of the two emitted electrons [1]. We present an exhaustive theoretical and experimental study of these cross sections, by disentangling the contribution of the different mechanisms that contribute to DI [2]. To this end, first order and higher order distorted wave theories are implemented jointly with the Monte Carlo Event Generator method (MCEG) [3]. This latter tool allows us to incorporate efficiently all the experimental conditions in the theoretical models. [1] M. Schulz et al, *J. Phys. B* **38**, 1363-1370 (2005). [2] M. F. Ciappina et al, *PRA* (in preparation) (2008). [3] M. Dürr et al, *Phys. Rev. A* **75**, 062708 (2007).

MWPI 10 Theoretical Fully Differential Cross Sections for Heavy Particle Transfer-Excitation Collisions A.L. HARRIS, D.H. MADISON, J.L. PEACHER, M. SCHULZ, *Missouri University of Science and Technology* Recent experimental measurements of four body collision processes present a stringent test of theory. To date, experimental results have been presented for ionization plus excitation, charge transfer plus excitation, and charge transfer plus ionization. Most of the experimental and theoretical effort so far has concentrated on ionization plus excitation. However, the transfer-excitation process provides a unique opportunity to study initial state electron correlation effects. In the transfer-excitation process for proton-helium scattering, an incident proton captures one electron from a helium atom, and the remaining electron is left in an excited bound state of the helium ion. We will present theoretical results using a full four-body approach, taking each particle into account. This allows for complete flexibility for treating each particle, which provides the opportunity to examine the effects of different types of interactions. Theoretical fully differential cross sections (FDCS) compared with experimental results will be presented.

MWPI 11 Theoretical Fully Differential Cross Sections for Transfer-Ionization A.L. HARRIS, D.H. MADISON, J.L. PEACHER, *Missouri University of Science and Technology* Recent experimental measurements of four body collision processes present a stringent test of theory. To date, experimental results have been presented for ionization plus excitation, charge transfer plus excitation, and charge transfer plus ionization. Most of the experimental and theoretical effort so far has concentrated on ionization plus excitation. Theoretical fully differential cross sections (FDCS) will be compared with experimental results for the transfer-ionization process for proton-helium collisions. In the experiment, the incident proton captures one electron from a helium atom, and the remaining electron is ejected into the continuum as

a free particle. The theoretical approach we use is a fully quantum-mechanical four-body approach, taking each particle into account. This approach has complete flexibility in the choice of wavefunctions, allowing for the role different interactions to be explored.

MWPI 12 PLASMA DIAGNOSTICS II

MWPI 13 Separation of binary gas mixtures flowing through sampling orifices RAINER JOHNSEN, *University of Pittsburgh* BARUN CHATTERJEE, *Bose Institute, Calcutta* Sampling of ions from a reaction vessel through a small orifice into a differentially pumped ion mass spectrometer is a standard plasma-diagnostic method. In this context one faces the question if and to what extent the composition of a gas mixture, e.g. a carrier gas with an admixture of a reagent, is altered by the outflow of gases through the orifice, which is often in the transition regime between molecular and viscous flow. Our experience has shown that gas separation must be taken into account in drift tube measurements of ion-molecule reaction. However, the effect is poorly understood, somewhat counter-intuitive, and no rigorous theoretical treatment is available. We report here a series of drift-tube measurements, in which we used ion-molecule reactions to determine actual reagent concentrations as a function of carrier gas flow. We show that a simple semi-empirical model, in which the coupling of gas flows is modeled using the Langevin equation, reproduces observations reasonably well. The formula can be expressed in terms of easily available parameters and thus may be useful to investigators who need to assess gas separation effects in their applications.

MWPI 14 Fundamental Study of Interfacial Heat Transfer by Low-Pressure Non-Equilibrium Discharge Plasmas YUSUKE KITAKA, ATSUSHI NEZU, HARUAKI MATSUURA, HIROSHI AKATSUKA, *Tokyo Institute of Technology* We examine influence of plasma parameters of molecular discharges in a state of non-equilibrium on the substrate temperature during the plasma irradiation. We treat oxygen microwave discharge with its discharge pressure 0.5 – 2 Torr. The vibrational and the rotational temperatures of an excited states of OH radicals are measured by optical emission spectroscopy (OES), and the substrate temperature by thermocouple. As a result, it was confirmed that lowering of the vibrational and the substrate temperatures were almost similar, while the absolute value of the substrate temperature was a little lower. To understand the heat transfer phenomenon by non-equilibrium plasma, we simulate movement of the particle by molecular dynamic (MD) method under the assumption of a Lennard-Jones potential. We confirmed reasonable variation in the surface temperature of the heat sink and the change in surface temperature according to the projectile conditions.

MWPI 15 Mass spectrometry of radicals created in plasma needle discharge SASA LAZOVIC, NEVENA PUAC, GORDANA MALOVIC, *Institute of Physics, Pregrevice 118, 11080 Belgrade, Serbia* ANTONIJE DJORDJEVIC, *Faculty of Electrical Engineering, Bulevar Kralja Aleksandra 73, 11080 Belgrade, Serbia* ZORAN LJ. PETROVIC, *Institute of Physics, Pregrevice 118, 11080 Belgrade, Serbia* We present diagnostics of the properties of a plasma needle operating at atmospheric pressure. Our configuration has additional grounded copper ring placed near the tip of the needle. Generated plasma has a larger volume and lower ignition powers with the ring. This configuration is convenient

both for treatment of samples and for mass spectroscopy. Our measurements were performed on a standard size plasma needle that we originally used for the treatment of plant cells. Similar work of Stoffels et al. has been done on the 'robust' version of the plasma needle that generates an elongated jet of 4 mm length and consumes higher powers. After some efforts we were able to make plasma needle to operate for conditions similar to those used during the treatments of biological samples. Hiden HPR60 mass analyzer was used to obtain the mass spectra. Plasma mode transition was observed for higher values of power transmitted to plasma. Concentrations of N, O, NO, NO₂ and O₃ were measured. We have also measured spatial profiles of emission and voltage and current waveforms by derivative probes placed close to the tip of the needle.

MWP1 16 Electron-Beam Generated Air Plasma: Microwave I/Q Detection of Plasma Properties and Optical Measurements of Nitrogen and Ozone to Quantify Plasma Spatial Distribution* ROBERT VIDMAR, CHRIS RAMSAYER, *University of Nevada, Reno* KENNETH STALDER, *Stalder Technologies and Research* Microwave and optical measurements are used to quantify the electron number density, the electron momentum transfer collision rate, nitrogen emissions, and ozone production. The plasma is produced by an electron beam source that generates 10-ms pulses of approximately 5 mA at 100 keV into a 400 liter test cell through a 12.7 μm aluminum transmission window. The target gas is laboratory air with measurements at pressures from 1 mTorr to 636 Torr. Details relating to the 10 GHz microwave In-phase and Quadrature detector are presented as well as representative measurements and the procedure to convert raw data to values of electron number density and electron momentum transfer collision rate. Detection of nitrogen emissions at 337.1 nm and ozone absorption at 254 nm are used to estimate the spatial volumetric ionization rate on the optical plane of observation and the spatial distribution across the optical plane.

*This material is based on research sponsored by the Air Force Research Laboratory, under agreement numbers FA9550-05-1-0087 and FA9550-07-1-0021.

MWP1 17 Generation and Diagnostics of Microwave Discharge Expanding Nitrogen Plasma TOMOHIKO SHIBATA, KAZUYUKI YOSHIDA, ATSUSHI NEZU, HARUAKI MATSUURA, HIROSHI AKATSUKA, *Tokyo Institute of Technology* We examine a microwave discharge expanding nitrogen plasma on its vibrational and rotational temperatures (T_v , T_r) by using optical emission spectroscopy (OES), and on its electron density and temperature by using a double probe. In the present study, we generated microwave discharge plasma in a cylindrical quartz tube (26 mm i.d.) and the plasma flowed and expanded rapidly into a rarefied gas wind tunnel with its pressure 2.6×10^{-3} torr. The microwave output power was set at 300 W. The gas flow rate was set at 300 ml/min. In OES measurement, we measured the band spectra of 1stPS and 2ndPS. We compare the experimentally measured spectrum with the calculate one to determine T_v and T_r of the generated plasma. Electron temperature did not reduce monotonically, which is due to complicated energy relaxation process contributed by metastables or vibrational levels. Intensity of 2ndPS decreased more rapidly than that of 1stPS, which is considered to be mainly due to the lowering of T_e . We found different way of variation in T_v of 1stPS and that of 2ndPS.

MWP1 18 Electric field measurements in high-pressure hydrogen environments with a few nanosecond time resolutions KAZUNOBU KOBAYASHI, TSUYOHITO ITO, *Osaka University* UWE CZARNETZKI, *Ruhr-University Bochum* SATOSHI HAMAGUCHI, *Osaka University* Coherent Raman scattering (CRS) measurement is a promising technique for measuring electric field in high-pressure environments. In this study, we demonstrate electric field measurements with a few nanosecond time resolutions in high-pressure hydrogen environments. The measurements are performed within the gap between two electrodes driven by pulsed nanosecond voltages. Two pulsed ns laser beams (532 nm and 683 nm) are employed for the measurements. In hydrogen molecules those two laser beams together with the electric field induce a coherent IR signal at a wavelength of 2.4 μm . Without discharge, the square root of the IR strength is proportional to the applied voltage, which is measured with a voltage probe and an oscilloscope at the powered electrode; suggesting that the measurements are successfully performed with a few ns time resolutions. Measurements with dielectric barrier discharges show reductions of the electric field probably due to charges near/on the dielectric barrier.

MWP1 19 The affects of micro-droplet injection on low pressure plasmas* DAISUKE OGAWA, IQBAL SARAF, M. GOECKNER, L. OVERZET, *The University of Texas at Dallas* Directly injecting liquid micro-droplets into low pressure plasmas opens a variety of possibilities including the ability to use new precursors for film deposition. Understanding how the injection of these droplets affects the plasma is important to an overall optimization. Toward that end, results of microwave interferometry and optical emission spectroscopy will be presented in conjunction with film microscopy and analysis. Our initial results show that the time dependent electron density as well as optical emission intensity in capacitively coupled plasmas can change substantially when injecting liquid micro-droplets. For example: There is a fast decrease in the electron density as the droplets enter the plasma (msec time-scale). This decrease in the electron density appears to be much faster than the pressure rise caused by the evaporation of the micro-droplets (~ 40 msec). In addition, there is a very slow rise back to the original state (~ 5 sec time scale) which is liquid dependent. Neither result is unexpected. Both will be discussed in the presentation.

*Supported in part through SPRING/AFOSR grant FA9550-05-1-0393.

MWP1 20 Visible emission from exploding wire in water* MILAN SIMEK, VACLAV PRUKNER, JIRI SCHMIDT, KAREL KOLACEK, JAROSLAV STRAUS, OLEKSANDR FROLOV, *Institute of Plasma Physics AS CR, v.v.i.* DEPARTMENT OF PULSE PLASMA SYSTEMS TEAM, Exploding wire in water generates non-ideal strongly coupled plasma, which can model some phenomena appearing in interior of stars, in inertial confinement fusion, in plasma physical-chemistry, in rocket engines, etc. This complicated 2-phase transitions process can be hardly modeled numerically because of missing material data at extremely high pressures. Therefore, the basic question relevant for radial energy transport estimates – when between wire and water a water-vapor-layer is created (if any) – has to be answered experimentally. For this purpose the waveforms of the driving current and the H-alpha line emission were measured simulta-

neously. First spectrometric results obtained by means of photon-counting technique will be discussed. Other spectroscopic data in visible range can yield valuable information about plasma periphery and about layer between plasma and surrounding liquid water.

*Work supported by GA CR (contract 202/06/1324), GA AS CR (contracts KAN 300100702, and 100430702), and MEYS CR (contract LA08024).

MWPI 21 Direct Ion Energy Measurements at the RF Biased Electrode in Noble and Hydrocarbon Gas Discharges

A. BABY, C.M.O. MAHONY, P.D. MAGUIRE, *Nanotechnology and Integrated Bio Engineering Centre, University of Ulster* We report direct measurements of ion energy distributions at the biased substrate electrode in a RF ICP discharge using a mass-energy analyser thus allowing exploration of greater bias voltage and frequency ranges. IEDs for pure Ar, He and He:Ar or Ar:C₂H₂ mixtures for pressures up to 90mTorr, mean bias voltages up to 150V and bias frequencies up to 27MHz, are compared with existing single and multi-species [1] IED models. With associated Langmuir probe, ion flux probe and sheath width measurements we observe that lighter ion IEDs deviate from the model and this also affects interpretation of the multiple-species IED model. At high biases we also note deviation from models, probably due to additional capacitively-coupled power input at the substrate electrode. We have mapped the IED spread and peak intensity variation across frequency and pressure ranges, respectively, in order to exploit IED tailoring for technological applications, particularly for the deposition of high integrity carbon based films. In Ar:C₂H₂ narrow spread IEDs were achieved, required for new diamond-like carbon deposition and growth modeling. Mean energies up to 100eV were obtained with 15% - 20% spread, depending on gas ratio, pulsed bias and frequency. [1] Sobolewski M A et. al. J. Appl. Phys. **91** (2002) 6303.

MWPI 22 Comparison of measured metastable ion density with laser induced fluorescence, to electron number density determined with a Langmuir probe, in Ar plasmas as a function of pressure

YOUNG-CHUL GHIM(KIM), *Dept. Engineering Physics, UW-Madison, Madison, Wisconsin 53706* NOAH HERSHKOWITZ,* *Dept. Engineering Physics, UW-Madison, Madison, Wisconsin 53706* The laser induced fluorescence (LIF) signal intensity measured with a diode laser in Ar plasmas is compared to Langmuir probe determined electron number density (n_e). Plasmas with $n_e \sim 10^9 \text{ cm}^{-3}$ and $T_e \sim 1 \text{ eV}$ are generated for pressures varying from 0.05 - 5.00 mTorr in a dc multidipole hot filament discharge The Ar II excitation transition at 668.614 nm is adopted to create Ar ion metastable fluorescence, and the metastable Ar ion velocity distribution functions (ivdfs) in bulk plasmas are measured. The area under the ivdf curve increases as the pressure is raised, with a maximum signal area at 0.6 mTorr. Then the area decreases with further increases in pressure, whereas the electron number density increases monotonically. The LIF signal has not yet been found at neutral pressure greater than 5 mTorr: In addition, the profile of the area normalized to the electron number density shows that the ratio is fairly constant over the presheath regime and increases as the diagnosed volume gets closer to the sheath.

*Work funded by DOE grant No. DE-FG02-97ER54437

MWPI 23 Spatiotemporally Resolved E-H transition in an Inductively Coupled Plasma in Ar by using ICCD Camera SA-TOSHI MORISHITA, YUICHIRO HAYASHI, TOSHIKI MAKABE, *Keio University* Inductively coupled plasma (ICP) has been widely used as a high density plasma source in various applications. It is well-known that ICP has two operating modes, E and H modes, and the transition between both modes shows a strong hysteresis in electrical and optical characteristics. We have been investigating the characteristics of the ICP through a series of measurements. In our recent study, we exhibited 2D-plasma images from the net excitation rate of Ar(2p1) caused by high energy electrons with energy greater than 13.6 eV during the E-H transition in Ar at 300 mTorr in the ICP driven by a single-turn current coil on the sidewall of a quartz tube. The time-resolved 2D-space image is a result of the integrated signal along the axial direction perpendicular to the coil plane by ICCD camera. In the present work, we discuss the mode transition from the change of the active region in the 2D-t image of the net excitation rate of Ar(2p1) by sweeping the external coil current in Ar for 100, 300, and 500 mTorr.

MWPI 24 Estimation of Electron Temperature and Frequency Components in a Dual Frequency Capacitively-Coupled Plasma Processing Reactor

TORU ITO, YUN MO, HORIZOME MASAHIRO, *Tokyo Electron Ltd.* The measurement of electron temperature in RF plasma sources with Langmuir probes is difficult because of the influence of rf noise. We attempted to estimate the electron temperature in a capacitively-coupled plasma processing reactor with a Surface Wave Probe [1] which employs microwaves. We also estimated the frequency spectrum with the sensitive PAP [1, 2]. We measured the harmonics which appeared in the bulk plasma for various experimental conditions in the dual-frequency [60 MHz and 2MHz] capacitively-coupled plasma processing reactor. We estimated RF power spectra for several experimental conditions like RF power [500-2000W], gas pressure [3-20Pa], and gas species [Ar, CF₄]. The measurement results suggest the existence of energy transport among several frequency spectrum. [1] K. Nakamura, M. Ohata, and H. Sugai: J. Vac. Sci. Technol. A **21**, 325 (2003). [Opt] [2] T. Shirakawa and H. Sugai: Jpn. J. Appl. Phys. **32**, 5129 (1993).

MWPI 25 Effect of wafers on measurement of gas temperature in RF plasma

VLADIMIR MILOSAVLJEVIC, *NCPST & School of Physics, Dublin City University, Dublin, Ireland* DAVID KAVANAGH, STEPHEN DANIELS, *NCPST, Dublin City University, Dublin, Ireland* Analyzing the optical emission spectrum of atomic fluorine and fluorine base molecules, a gas temperature is measured in an Oxford Instruments® RF plasma discharge. The experiments are conducted with silicon or photoresist wafers, as well without any wafer. The gas composition is pure SF₆ as well a mixture of SF₆ and O₂, the working pressure is 13 Pa and the flow for all gases is constant at 100 sccm. The RF power is changed from 75W to 300W. The dependence of gas temperature on the chemical structure of surface/wafer, RF power and gas composition ratio between SF₆ and O₂ is investigated. The gas temperatures were determined by recording molecular bands of SiF (436.82 nm) and CF₂ (248.7 nm), and the spectral line of F (703.75 nm). Since a rotational temperature has been used widely as a neutral gas temperature measurement in different types of plasmas, in this work we present a correlation between gas temperature determinate by molecular bands and atomic spectral lines. We have only direct control of SF₆ and O₂ gases, therefore the

contribution of carbon and silicon in the plasma discharge is indirectly controlled only by the RF power. The results show that for some specific ratios of SiF_6 and O_2 the neutral gas temperature via molecule bands is difficult to determine.

MWP1 26 Experimental investigation of electron density in pulse plasma source by microwave resonance probe ALBERT R. ELLINGBOE, VLADIMIR MILOSAVLJEVIC,* *NCPST & School of Physics, Dublin City University, Dublin, Ireland* The time-dependent spatial electron density distribution in a constricted, pulsed plasma source is measured using a floating hairpin resonance probe and an extrapolation method is described for determining the peak in electron density from the experimental data. Using these techniques a detailed characterization of the spatio-temporal evolution of the electron density, outside the constricted region above the anode of the pulsed plasma source is presented. The electron density increases sharply during the creation phase and the rate of increase is found to decrease with distance from the axis of the constricted channel. By modeling the plasma creation characteristics versus position, the electron density along the axis of the constricted pulsed plasma sources can be determined.

*Faculty of Physics, University of Belgrade, Serbia

MWP1 27 Plasma diagnostic through the five prominent oxygen triplets VLADIMIR MILOSAVLJEVIC, *NCPST, Dublin City University, Ireland* EMANUELE RAGNOLI, *Department of Electronic Engineering, National University of Ireland, Ireland* STEPHEN DANIELS, NIAL MACGEARAILT, *NCPST, Dublin City University, Ireland* SHANE McLOONE, JOHN RINGWOOD, *Department of Electronic Engineering, National University of Ireland, Ireland* Oxygen is one of most frequently used gas in plasma discharge. Therefore, determination of plasma parameters through analysis of oxygen emission would be a powerful tool. Fifteen most prominent oxygen spectral lines have been measured at different experimental plasma condition. Those oxygen lines belong to five oxygen triplets: 777, 844, 645, 725 and 615 nm. These fifteen O I spectral lines belong to the different transitions/multiplets and have the different upper energy level. The difference of upper energy levels among these oxygen spectral lines is greater than 2 eV. Also, the spectral lines from triplets 645 nm, 725 nm and 615 nm of O I have an upper energy level very close to dissociation of molecular oxygen (12.06 eV). Data is collected for a range of operator contribution in an Ar-O₂-Cl/HBr/C₂F₆ gas mixture discharge, by Jobin Yvon spectrometers. The emission strengths and profile shapes are found to be dependent on plasma tool settings (power, gas mixture and pressure). Correlation of plasma internal state will be presented.

MWP1 28 Measurement of Ar Excited Atoms Temperature in D.C planar Discharge by Diode laser technique MONA MEHRANFAR, *Tehran North Branch, Azad University, Tehran, Iran* MAJID ESHGHABADI, KIOUMARS YASSERIAN, MAHMOOD GHORANNEVISS, *Plasma Physics Research Center, Science and Research Campus, Azad University, Tehran, Iran* A diode laser has been used to measure the temperature of Ar atoms. A D.C discharge is employed to make the Ar excited atoms between two planar stainless steel electrodes in a Pyrex glass tub.

The laser beam passes through the plasma. This laser is calibrated on 772.3nm corresponding to the high intensity wavelength of light which emitted by Ar atoms. The diode laser input power is modulated as saw tooth mode by a signal generator. The temperature of the Ar atoms is calculated by full-width-half-maximum (FWHM) of Doppler absorption curve. Details of results will be discussed in full paper.

MWP1 29 Langmuir probe RF plasma compensation using simulation method AASIM YOUSIF AZOOZ, The problem of RF compensation in plasma Langmuir probe data is analyzed by simulation procedure. It is pointed out that this type of compensation can be accounted for through proper mathematical transformation applied to the RF contaminated Langmuir probe data to reproduced the actual probe I-V data which are not affected by the RF. Matlab based computer software is presented. The software automatically deduces the value of the probe voltage shift induced by the RF, apply the proper transformation to the I-V data and calculates the actual plasma parameters. These parameters include the plasma potential, plasma electron temperature, plasma electron density and the electron energy distribution function EEDF.

MWP1 30 PLASMA SURFACE INTERACTIONS

MWP1 31 Simulation of surface roughness by 3D level set method* BRANISLAV RADJENOVIC, MARIJA RADMILOVIC-RADJENOVIC, ZORAN PETROVIC, *Institute of Physics, Belgrade-Serbia* Reactive Ion Etching is a major process in the fabrication of semiconductors devices for transferring patterns from masks to semiconductors substrates. One of the limiting factors in applications of plasma etching in new generations of plasma technologies will be the control of plasma induced roughness or perhaps control of the surface roughness by plasma etching. In this paper we consider both large scale roughness, sidewall roughness and roughness in general by using a 3D level set method. Predictions of surface roughness are based on statistical variations of the properties of the material and ion flux. In addition, we study how stochastic properties of material on different scales and of the beam affect the resulting roughness.

*The present work has been carried out under MNZZS 141025 project.

MWP1 32 Simulation of Interaction Between RF Plasmas and Roughly Surface ILGIZAR SAGBIEV, *Kazan State Technological University* OLGA PANKRATOVA, VICTOR ZHELTOUKHIN, *Kazan State University* An interaction between RF plasmas and roughly surface at pressure 13.3-133 Pa was investigated theoretically. A sheath near the specimen treated in RF plasmas consists of two zones. The first one is the Debye layer about 10 μm by thickness and the second one is oscillatory zone from 0.5 up to 2 mm by thickness. In the last electrons move synchronous to electric field change. The main role of oscillatory zone is acceleration of ions up to 100 eV. Ion stream is focused on surface asperities due to bending of electric intensity lines in the Debye layer.

MWP1 33 Start-up behavior of argon discharge near a flat dielectric* ANA SOBOTA, *Eindhoven University of Technology* ALEXANDRE LEBOUVIER, *Ecole polytechnique de l'universite d'Orleans* NICOLAAS J. KRAMER, WINFRED W. STOFFELS, EDDIE M. VAN VELDHUIZEN, *Eindhoven University of Technology* The topic of surface discharges on a dielectric is well known among electrical engineers, because streamer development on isolation material results in breakdown and short circuits. Discharge ignition in presence of a dielectric is interesting for the lighting industry as well, where the dielectric wall of a lamp plays a potentially important role in the lamp ignition. Fast measurements on the initial appearance and velocity of a discharge in presence of a dielectric were done in argon (100 mbar to 1 bar) using an ICCD camera. We found that the discharge velocity along dielectric surfaces has a tendency to increase as the discharge approaches the grounded electrode. The average discharge velocity decreases with increasing pressure, with increasing rise time of the high voltage ignition pulse and with increasing repetition rate of the high voltage pulses. Measured velocities are in range from 2×10^5 to 2×10^6 m/s.

*Work was supported by Philips Lighting, Eindhoven.

MWP1 34 Analysis of dust particles produced due to interaction between graphite and deuterium helicon plasmas SHINYA IWASHITA, KAZUNORI KOGA, MASAHARU SHIRATANI, *Kyushu University* Formation mechanisms of dust particles due to interaction between carbon walls and plasmas in fusion devices have attracted considerable attention, because they pose two potential problems: they can contain a large amount of tritium and their existence in fusion devices may lead to deterioration of plasma confinement. To obtain information on formation mechanisms of dust particles of nm in size in fusion devices, we have generated deuterium helicon discharge plasmas which simulate divertor plasmas in fusion devices and then we have collected and analyzed dust particles produced due to interaction between graphite and the plasmas. Dust particles are made of carbon and can be classified into three kinds: small dust particles below $1 \mu\text{m}$ in size, large flakes above $1 \mu\text{m}$ in size, and agglomerates which consist of primary particles of 10 nm. These three kinds suggest three formation mechanisms, that is, CVD growth, carbon films peeled from walls, and agglomeration [1]. There exist a large number of small dust particles below $1 \mu\text{m}$ in size. All of these features are quite close to those of dust particles collected during the main discharges of LHD. [1] Y. Watanabe, et al. *J. Vac. Sci. Technol.*, A14, 540 (1996).

MWP1 35 Surface Control as a Function of Processing Conditions in an FC Plasma Environment CALEB NELSON, SANKET SANT, LAWRENCE OVERZET, MATTHEW GOECKER, *University of Texas at Dallas* Many factors are known to affect surface conditions in a plasma environment, including radical and ion fluxes, ion energy, surface temperatures, and surface materials. However, the complex nature of highly polymerizing plasmas often prohibits the isolation of individual control and variable processing conditions. A novel approach using a combination of the flexible modified GEC reference cell and a simplified surface model founded on the assumption that most surface processes occur at open bond sites yields sticking and etch coefficients of radicals and ions. The modified GEC reference cell allows the option of changing chamber dimension, wall material, and wall temperature. Such control is required to develop an understanding

of plasma-wall and subsequent wall-to-wall interactions. Of particular importance is the variable electrode gap and the combination of various feed gas mixtures. This allows radical densities to be controlled almost independently of ions and etching radical densities. The isolation of these parameters permits the partial deconvolution of the film growth rate model and the quantification of sticking and etch yield coefficients.

MWP1 36 Polymer processing by electron beam generated plasmas in argon, oxygen, nitrogen environments and their mixtures* EVGENIYA LOCK, SCOTT WALTON, RICHARD FERNSLER, *Naval Research Laboratory* Polymers have unique physio-chemical properties that make them attractive for organic electronics applications. However, their inherent low surface energy can be problematic. Wet chemical processing, flames and plasma treatments have been successfully applied to alter the polymer surface properties but plasma treatments are often favored because they change only the surface without altering the bulk properties. Plasmas can also cause roughening or even surface damage. Electron beam generated plasmas have several unique features that distinguish them from the conventional discharges - intrinsically low electron temperature (< 1 eV), resulting in smaller plasma potentials and in lower incident ion energies (1-5 eV). These energies are comparable with the bond strengths found in most polymers, so they are sufficient to invoke chemical surface modification with limited morphology changes. In this study, polymer modifications resulting from electron beam plasma generation in argon, oxygen and nitrogen environments and their mixtures are investigated. The polymers of interest include polystyrene, polymethylmetacrylate and ultra-high molecular weight polyethylene. The effects of the plasma process parameters including treatment time and duty factor, as well as mixture composition on surface energy, chemistry and morphology are presented.

*This work was sponsored by ONR.

†NRL/NRC Postdoctoral Research Associate

MWP1 37 HIGH PRESSURE GLOW DISCHARGES

MWP1 38 Experimental and theoretical investigations of singlet oxygen production by high-pressure microdischarges J. SANTOS SOUSA, *LPGP, CNRS-UPS, 91405 Orsay, France and IPFN, IST, 1049-001 Lisboa, Portugal* B. EISMANN, S. PANCHESHNYI, L.C. PITCHFORD, *LAPLACE, CNRS-INPT-UPS, 31062 Toulouse, France* V. PUECH, *LPGP, CNRS-UPS, 91405 Orsay, France* LPGP TEAM, LAPLACE TEAM, The so-called Micro-Cathode Sustained Discharge (MCSD), which is a three-electrode configuration using a Micro-Hollow Cathode Discharge (MHCD) as a plasma cathode, can be operated as a non-self-sustained discharge with low values of the reduced electric field and of the gas temperature. As a result, these MCSDs can efficiently generate large amounts of singlet delta oxygen, $\text{O}_2(1\text{D})$. The remarkable stability of the MCSD has allowed us to operate glow discharges, free from the glow-to-arc transition, in rare-gas/oxygen mixtures at pressures up to atmospheric ($P=100\text{--}1000\text{mbar}$). High concentrations of $\text{O}_2(1\text{D})$, from 10^{15} up to 10^{16}cm^{-3} , were measured in the MCSD afterglow for rare gas flow in the range $100\text{--}30000\text{sccm}$, varying oxygen partial pressure ($p(\text{O}_2)=1\text{--}20\text{mbar}$) and different discharge currents ($I=1\text{--}12\text{mA}$). The 0D plasma kinetics code ZDPlasKin [1] was used to calculate the generation of $\text{O}_2(1\text{D})$ in the MCSD for different

discharge and flow conditions and to estimate its density as a function of distance in the afterglow. Similar trends are observed in model and experiment, and detailed comparisons will be shown. [1] S.Pancheshnyi et al., these proceedings

MWP1 39 Characterization of a streamer-initiated atmospheric pressure plasma jet for spatially guided pulsed plasma generation BRIAN SANDS, *UES, Inc.* BISWA GANGULY, *Air Force Research Laboratory* We examine the characteristics of a streamer-initiated atmospheric pressure plasma jet (APPJ) terminated by a cathode ground plane in air. The plasma jet is generated using a 12 kV submicrosecond voltage pulse exciting a single positively biased electrode wrapped around a 3 mm diameter glass capillary with a 2 slm, 5% Ar/He mixture, gas flow. This APPJ device is distinguished from flow-driven APPJs by its ability to generate excited species *in situ* over its length. The presence of the cathode downstream provides ionization gain that is not characteristic of flow-driven APPJs in similar configurations but rather is characteristic of a single dielectric barrier microdischarge filament that is confined to the capillary axis. With a conducting cathode, this discharge filament can carry several Amps of current in a ~ 30 ns pulse. In this experiment, we study this atmospheric pressure plasma source with cathode materials of varying resistivity including conducting metals, semiconducting silicon, and insulating dielectrics at distances up to 3 cm from the capillary tip. We monitored spatiotemporally resolved emission intensities from the Ar/He/air discharge to track the relative gain of electron impact excitation across the gap. This will be correlated with current and voltage measurements to estimate energy deposition in the gap.

MWP1 40 Repetitive nanosecond-pulsed discharge in high-pressure hydrogen environments TSUYOHITO ITO, KAZUNOBU KOBAYASHI, *Osaka University* UWE CZARNETZKI, *Ruhr-University Bochum* SATOSHI HAMAGUCHI, *Osaka University* High pressure discharges have attracted much attention recently, and employment of a repetitive nanosecond-pulsed power is one of the promising methods for generating non-thermal discharges in high pressure environments. Electric field is one of the most important parameters in discharge dynamics, which, we believe, should be understood to improve their applications. In this paper, we study the dynamics of a repetitive (10 kHz) nanosecond-pulsed discharges, generated in high pressure (near atmospheric pressure) hydrogen environments, with measurements of the time-dependent electric field distributions. The measurements are performed by coherent Raman scattering (CRS) analysis of hydrogen molecules, induced by two nanosecond laser beams and the electric field. The experimental results show temporal effects of charges in the space (and/or on the dielectric barrier, when we employ a dielectric barrier discharge). More details revealed by optical emission studies and particle simulations will be presented.

MWP1 41 Fluid modeling of a microwave micro-plasma at atmospheric pressure J. GREGORIO, *IPFN IST Lisboa / LPGP UPS Orsay* R. ALVAREZ, *IPFN IST Lisboa* C. BOISSE-LAPORTE, *LPGP UPS Orsay* L.L. ALVES, *IPFN IST Lisboa* In this paper we study a microwave (2.45 GHz) reactor that can produce high-density (10^{14} - 10^{15} cm $^{-3}$), low power (~ 10 W) plasmas in ambient air or in controlled environments at atmospheric pressure, within the end-gap of a microstrip line, by using a continuous wave excitation. The gap corresponds to a 50-200

μm slit, between two metal blades with 6-14 mm width. Here we present a numerical model describing the micro-plasma sustained with this device, in view of complementing its experimental characterization [1,2]. The simulation tool is a one-dimensional (between metal blades), stationary fluid-type code that solves the charged particle and the electron mean energy transport equations (for argon), together with Poisson's equation for the space-charge electrostatic field and Maxwell's equation for the electromagnetic excitation field. Results yield coupled powers of less than 10 W, for a slit with 100 μm and a maximum electron density of 10^{14} cm $^{-3}$. [1] J.Gregorio, L.L.Alves, P.Leprince, O.Leroy, L.Teule-Gay and C.Boisse-Laporte, 2007 Bull. Am. Phys. Soc. 52, 22 [2] J.Gregorio, L.L.Alves, P.Leprince, O.Leroy and C.Boisse-Laporte, 2008 19th ESCAMPIG, Granada, Spain

MWP1 42 Study of a microwave micro-plasma reactor at atmospheric pressure J. GREGÓRIO, *LPGP UPS Orsay / IPFN IST Lisboa* P. LEPRINCE, O. LEROY, *LPGP UPS Orsay* L.L. ALVES, *IPFN IST Lisboa* C. BOISSE-LAPORTE, *LPGP UPS Orsay* In this paper we study a 2.45 GHz microwave micro-plasma source, working in air and in argon at atmospheric pressure. The discharge is sustained within a slit (50 μm -200 μm wide and 6mm width), delimited by two metallic blades placed at the end of a microstrip line [1]. The reactor has two impedance matching units that allow tuning the resonance frequency and the quality factor of the circuit. Optical emission spectroscopy diagnostics allow to deduce the plasma rotational temperature (T_{rot}). In air discharges, the N_2 transition $\text{C}^3\Pi_u\text{-B}^3\Pi_u$ yielded T_{rot} between 900 and 1400 K, for 30-45 W input powers and 50-100 μm slits. In argon discharges, the OH transition $\text{A}^2\Sigma^+-\text{X}^2\Pi$ was used, and T_{rot} was found between 500 and 600K, for 8-15W input powers and 50-150 μm slits. For these discharges, the argon electron excitation temperature was found between 0.3 and 0.6 eV. Measurements of the H_β Stark broadening suggest an electron density of the order of 10^{14} cm $^{-3}$. [1] J. Gregorio, L.L. Alves, P. Leprince, O. Leroy and C.Boisse-Laporte, 2008 19th ESCAMPIG, Granada, Spain

MWP1 43 Modeling of high-frequency driven discharges at medium and high pressure PHILIPP MERTMANN, STEFAN BIENHOLZ, PETER AWAKOWICZ, *Ruhr-University Bochum*, AEPT THOMAS MUSSENBRÖCK, RALF PETER BRINKMANN, *Ruhr-University Bochum*, TET INSTITUTE FOR PLASMA TECHNOLOGY TEAM, INSTITUTE FOR THEORETICAL ELECTRICAL ENGINEERING TEAM, Since the end of the 1980s the interest in non-thermal plasmas at medium and high pressure is rapidly growing. Particularly diffuse homogeneous glow discharges are of great interest not only in the scientific context. Due to their enormous potential for technological applications these non-equilibrium discharges have drawn considerable attention. However, the number of contributions to systematic modeling and simulation of high-pressure glow discharges is small. To study the dynamics of such discharges we propose a model of a capacitive discharge for the medium-pressure and the high-pressure regime. The model consists of a set of simplified fluid equations for each charged species coupled self-consistently to Poisson's equation using the method of matched asymptotic expansion. First simulation results for the dynamics of the plasma sheath will be discussed.

MWP1 44 Numerical Simulations of an atmospheric pressure discharge using a two dimensional fluid model MUHAMMAD M. IQBAL, MILES M. TURNER, *Dublin City University, Ireland*
We present numerical simulations of a parallel-plate dielectric barrier discharge using a two-dimensional fluid model with symmetric boundary conditions in pure helium and He-N₂ gases at atmospheric pressure. The periodic stationary pattern of electrons and molecular helium ions density is shown at different times during one breakdown pulse for the pure helium gas. The temporal behavior of the helium metastables and excimers species density is examined and their influences on the discharge characteristics are exhibited for an APD. The atmospheric pressure discharge modes (APGD and APTD) are affected with small N₂ impurities and the discharge mode structures are described under different operating conditions. The uniform and filamentary behavior of the discharge is controlled with the variable relative permittivity of the dielectric barrier material. The influence of nitrogen impurities plays a major role for the production of the filaments in the after glow phase of He-N₂ discharge and the filaments are clearly observed with the increased recombination coefficient of nitrogen ions. The creation and annihilation mechanism of filaments is described with the production and destruction of nitrogen ions at different applied voltages and driving frequencies for a complete cycle. The results of the fluid model are validated by comparison with the experimental atmospheric pressure discharge results in He-N₂ plasma discharge.

MWP1 45 RF Micro Atmospheric Pressure Plasma Jet: Numerical Simulation and Laser Diagnostics KARI NIEMI, JOCHEN WASKOENIG, TIMO GANS, *Centre for Plasma Physics, Queen's University Belfast, Northern Ireland, UK*
Micro atmospheric pressure plasma jets (μ -APPJs) can provide high concentrations of radicals at a low gas temperature, particularly for modification of sensitive surfaces, e.g. in biomedicine. The diagnostics of microplasmas is extremely challenging, therefore numerical simulations offer a further insight. The presented 1D-model is a numerical fluid-model across the discharge gap. Dual frequency excitation promises enhanced radical production. Numerical simulations are restricted due to the lack of available data for surface processes which are crucial in case of the extraordinary high surface to volume ratio. These data can be derived using measurable quantities as fixed input parameters of the model. The μ -APPJ provides an excellent optical diagnostic access to the discharge volume. Absolute atomic radical densities can be measured by two-photon laser-induced fluorescence spectroscopy. Absolute measurements require knowledge of collision-induced de-excitation processes or time resolved measurement of the fluorescence decay, e.g. with a tuneable UV Fourier-limited Pico-second laser system.

MWP1 46 ArI and H β Line Broadening in Microplasma Jet and DC Microhollow Cathode Plasmas at Atmospheric Pressure BOGOS SISMANOGLU, JORGE CORRÉA, CARLOS OLIVEIRA, MARCELO GOMES, JAYR AMORIM, *Departamento de Física, Instituto Tecnológico de Aeronáutica*
Direct current microplasma jet and microhollow cathode discharges are studied in argon at atmospheric pressure. The microplasma jet consists of tungsten-carbide needle and a metallic plate. Various needle diameters (150 to 1000 μ m) were used. The needles are operated as the cathode or anode. Microhollow cathode is a sandwich of metal-dielectric-metal with a micro hole (200 to 1000 μ m diameter). Charged plasma particles induce broadening of lines due to

Stark effect. The electric microfield also induces broadening of ArI 603.213nm and 565.070nm lines. These two lines are sensitive to Van der Waals and Stark broadening. The broadening of these two lines enables us to evaluate gas temperature, electron temperature and density. These parameters are dependent on discharge operating mode: abnormal (low and high current) and normal. Calculations take into account the characteristic of two-temperature plasma and the ion dynamic effect in lines broadening. The results for microjets are well similar to those obtained also with Balmer H β and H α lines in Ar-2% H₂ mixture gases: n_e from 4.0×10^{14} to $2.0 \times 10^{15} \text{ cm}^{-3}$ and $T_e \cong 0.6 \text{ eV}$. As anode, the needle generates microjets with T_g from 400 to 900K, at high current (from 20 to 130mA).

MWP1 47 Electrical and optical characteristics of a low-frequency atmospheric plasma discharge* CHRISTOPHER J. OLDHAM, MATTHEW R. KING, C. RICHARD GUARNIERI, JEROME J. CUOMO, *Department of Materials Science and Engineering, NC State University*
The electrical and optical characteristics of a capacitive discharge operated at atmospheric pressure were studied. The discharge was operated with and without dielectric barriers to investigate how the discharge behaved using a low frequency power source. Plasma formation was found at three main harmonics; 30 kHz, 80 kHz, and 150 kHz. In addition, other higher frequency components approaching the MHz regime were found to contribute to plasma generation. The presence of the dielectric barriers significantly effected discharge properties. With the electrodes covered by dielectric barriers, the alpha-gamma transition occurs with increasing power. Without dielectric barriers, the discharge was constricted and operated only in the abnormal mode of operation. Spatial results from the He I (706 nm) emission profile along with gas temperature measurements from the N₂⁺ rotational band will be presented.

*This work was funded by the Dean's office in the College of Engineering and the Department of Materials Science and Engineering

MWP1 48 Traces of Accumulated Charges on Dielectric Electrode in Self-Organization in Barrier Discharge Generated by Piezoelectric Transformer HARUO ITOH, *Chiba Institute of Technology*, KENJI TERANISHI, *The University of Tokushima*, KAZUTO KOBAYASHI *Chiba Institute of Technology*, NAOYUKI SHIMOMURA, *The University of Tokushima*, SUSUMU SUZUKI, *Chiba Institute of Technology*
Discharge plasmas excited by nano-meter longitudinal vibration of piezoelectric transformers (PTs) has been investigated to construct compact plasma reactors for practical applications. In the experiments aimed to develop a PT-based excimer lamp, self-organization phenomenon in the DBD [1] was observed as regularly hexagonal patterns of microdischarges in He and Ar with a small amount of air impurities [2]. Time-resolved observation of the self-organized patterns is performed by ICCD camera to clarify the phenomenon. In the images, we found dark spots arrayed hexagonally in a weak emission on the PT surface whose arrangement well coincides with that of bright hexagonal filaments. The dark spots are considered as the traces of the accumulated charges on the dielectric electrode, which interrupt the hexagonally-filamentary discharges. [1] L. Stollenwerk et al., Phys. Rev. Lett., 98, 255001 (2007). [2] H. Itoh, et al., IEEE Trans. Plasma Sci., 36, 1348 (2008).

MWP1 49 DIELECTRIC BARRIER DISCHARGES, DISPLAYS

MWP1 50 Homogeneous DBD in N₂: I. LIF, TALIF and electrical measurements NICOLAS GHERARDI, ET-TOUHAMI ES-SEBBAR, CHRISTIAN SARRA-BOURNET, NICOLAS NAUDE, FRANCOISE MASSINES, *LAPLACE - Universite de Toulouse - CNRS/UPS/INP* In this paper we compare two different discharges that can be obtained in a DBD configuration, that is to say the filamentary discharge (usual regime in atmospheric DBD) with the Atmospheric Pressure Townsend Discharge (APTD), which is a homogeneous regime obtained in nitrogen atmosphere. The aim is to help in the understanding of the processes which control the transition from one regime to the other. To do so, the discharge is characterized through electrical measurements, coupled with optical diagnostics among which Laser Induced Fluorescence (LIF) for radical density measurements. The influence of the addition of small quantities of additives on the stability of the N₂ APTD is followed: the absolute density of N, O and NO are reported in N₂/O₂ and N₂/N₂O mixtures. One interesting result is that while the electron density is much lower in the APTD than in the filamentary discharge, the Townsend discharge is really efficient for the creation of N atoms: densities as high as $3 \times 10^{14} \text{ cm}^{-3}$ has been measured. These measurements are used to validate numerical models presented in paper "Homogeneous DBD in N₂: II. Simulation in 0D and 1D approaches" by S. Pancheshnyi et al.

MWP1 51 Cold Atmospheric-Pressure Plasmas Applied to Active Packaging of Fruits and Vegetables* PATRICK PEDROW,[†]SULMER FERNANDEZ,[‡]MARVIN PITTS,[§] *Washington State University* Active packaging of fruits and vegetables uses films that absorb molecules from or contribute molecules to the produce. Applying uniform film to specific parts of a plant will enhance safe and economic adoption of expensive biofilms and biochemicals which would damage the plant or surrounding environment if misapplied. The pilot application will be to apply wax film to apples, replacing hot wax which is expensive and lowers the textural quality of the apple. The plasma zone will be obtained by increasing the voltage on an electrode structure until the electric field in the feed material (Argon + monomer) is sufficiently high to yield electron avalanches. The "corona onset criterion" is used to design the cold plasma reactor. The apple will be placed in a treatment chamber downstream from the activation zone. Key physical properties of the film will be measured. The deposition rate will be optimized in terms of economics and fruit surface quality for the purpose of determining if the technique is competitive in food processing plants.

*Avista Corp. provided equipment for this research.

[†]School of EECS

[‡]School of EECS

[§]Biological Systems Engineering.

MWP1 52 Efficiency of pulse-mode dielectric barrier discharge excimer lamp in constant duty cycle HARUAKI AKASHI, *Dept. Appl. Phys., National Defense Academy, Japan* AKINORI ODA, *NIT YOSUKE SAKAI, Hokkaido Univ.* Efficiency of pulse-mode dielectric barrier discharge (DBD) excimer lamp under constant duty cycle with increasing applied voltage

has been simulated using two dimensional fluid model[1]. Xe gas with 300Torr pressure is assumed. And the simulated region considered in this model is 1cm(gap length)x3cm(radial length). Periodical boundary conditions are assumed for the radial direction boundaries. The both electrodes are covered with dielectrics and their thickness is 0.2cm. 5~ 8kV trapezoid shape voltage is applied with the same voltage rising ratio and 50% duty ratio waveform with 200×10^3 pps repetition rate. The discharge occurs at the rising edge and tailing edge of applied voltage. 172nm VUV intensity obtained from first discharge is higher than second one in lower applied voltage (< 6kV) case. And in higher voltage case, the intensity from second discharge becomes higher. This is explained by shortening of interval time between the discharges. The short interval time makes higher initial electron density for second discharge. As a results, the input and 172nm VUV output power increases with increasing applied voltage, but the efficiency decreases. Because of inefficient surface discharge [1]H. Akashi et al, *IEEE Trans. Plasma Science*, Vol.33,No.2(2005,4)pp.308-309.

MWP1 53 The influence of impurities on the electrical behaviour of high pressure noble gas plasmas TOM MARTENS, AN-NEMIE BOGAERTS, *Research Group PLASMANT, Department of Chemistry, University of Antwerp* WOUTER BROK, JAN VAN DIJK, *Department of Applied Physics, Eindhoven University of Technology* Since reactor designs are rarely completely the same, gases of different quality grades are being used and since in simulations the impurity levels are sometimes used to fit the simulated breakdown voltages to the experimental values, we focus our current research on the influence of different levels of gas impurity on the electrical characteristics of dielectric barrier discharges in atmospheric helium. For matters of simplicity and to be able to make comparison with results published in literature, we focus on nitrogen impurities and use a fluid model to describe the discharge. Our results show that when the nitrogen content rises, the amount of current pulses in each half period increases, a phenomenon that has been investigated experimentally by Radu et al. [*IEEE Trans. Plasma Sci.*, Vol. 31(6), 1363-1378]. Interestingly, our results show that the power consumption shows a steep drop and becomes minimal at about 3800 ppm and quickly rises again for higher impurity levels. This drop coincides with the transition from 2 to 3 current pulses and appears to originate from the decrease of the peakwidth with rising nitrogen content. This drop is followed by a quick increase in power consumption due to an extra current pulse at 4000 ppm.

MWP1 54 Experimental study of a novel micro-wire dielectric barrier discharge JORIS CREEMERS, ALEC DE KUYPER, PETER BRUGGEMAN, CHRISTOPHE LEYS, *Ghent University* Many types of dielectric barrier discharge (DBD) configurations have been studied in the past as a way to produce non-thermal plasma at atmospheric pressure. Most are based on parallel plane or coaxial electrodes. The electrode configuration studied in this paper has a coaxial geometry, where the inner electrode is a novel glass-coated micro-wire coil. We investigate the effects of the very small diameter of the wire (~ 30 μm) on the characteristics of the discharge. The influence of the excitation frequency (50 Hz - 50 kHz) on the current waveform is analyzed. In view of applications, the ozone production efficiency is compared with standard DBDs.

MWP1 55 Self synchronization of surface discharges KATIA ALLEGRAUD, ANTOINE ROUSSEAU, *LPTP* Surface dielectric barrier discharges (SDBD) are mainly investigated for airflow control. In this paper, they are used to study surface processes in dielectric barrier discharges. A previous study has shown the self triggered behavior of a SDBD: the plasma initiates through several simultaneous and adjacent filaments around the electrode [1]. This phenomenon has been investigated under the name of collective effects, where the light of a first filament can trigger the ignitions its neighbors [1, 2]. It allows initiating several tens of streamers during a current peak of ~ 50 ns. In the present study, we propose to investigate the self synchronization of the discharge in a two electrodes system: the setup consists of two high voltage electrodes on the same glass plate. A third electrode, under the plate, is grounded. ICCD measurements show that the discharge appears simultaneously on both electrodes on a 50 ns time scale. Nano-second resolved measurements of the streamers propagation reveal that the ignitions on one electrode can be delayed by few nanoseconds in respect to the other one. This means that the discharge from a first electrode can trigger the second one. Finally, iCCD measurements allow calculating the streamers propagation velocity, varying from 3.4×10^7 cm/s at the beginning of the propagation to 0.7×10^7 cm/s at the end of the propagation [3]. [1] K. Allegraud, O. Guaitella, A. Rousseau, *J. Phys. D.: Appl. Phys.* 40 7698–7706 (2007) [2] O. Guaitella, F. Thevenet, C. Guillard, A. Rousseau, *J. Phys. D.: Appl. Phys.* 39 2964–72 (2006) [3] K. Allegraud, A. Rousseau, submitted to *IEEE Transactions on Dielectrics and Electrical Insulation*

MWP1 56 Optical and electrical characteristics of N_2 micro-discharges produced in coplanar surface DBD geometry* MILAN SIMEK, VACLAV PRUKNER, JIRI SCHMIDT, *Institute of Plasma Physics AS CR, v.v.i. DEPARTMENT OF PULSE PLASMA SYSTEMS TEAM*, Basic optical and electrical characteristics of nitrogen micro-discharges generated in an AC surface DBD reactor with coplanar electrode arrangement were studied at atmospheric pressure by means of the ICCD microscopy and spectrometry complemented with the multi-channel photon-counting. Temporal evolutions of N_2 -2.PG (second positive), N_2 -HIR (Hermann infrared), NO-gamma and N_2^+ -1.NG (first negative) bands induced by an individual H-shaped micro-discharge generated during positive/negative AC half-cycle were acquired and analyzed. Typical emission waveforms were inspected as function of both frequency and amplitude of the modulated AC driving high-voltage, in the case of a) a single micro-discharge produced during an AC half-cycle and b) multiple, equally spaced micro-discharges produced during an AC half-cycle. Observed waveforms and obtained characteristic time constants will be discussed in the frame of electron impact excitation/ionization, $N_2(A)+N_2(A)$ energy pooling and $N_2(A)+NO$ resonant energy transfer processes.

*Work supported by the GA CR (contract no. 202/08/1106).

MWP1 57 COMPUTATIONAL METHODS FOR PLASMAS

MWP1 58 A stabilized finite element method for gas discharge modelling MARKUS BECKER, DETLEF LOFFHAGEN, FLORIAN SIGENEGER, *INP Greifswald* WERNER SCHMIDT, *Department of Mathematics and Computer Science, University of Greifswald* Fluid models consisting of Poisson's equation for the electric potential, continuity equations for the relevant plasma species and the electron energy balance are widely used for the theoretical description and analysis of glow discharges. The discretization of the corresponding partial differential equations by means of standard finite difference and element methods leads to serious restrictions for the spatial mesh spacing Δx resulting from the condition $|P_e| \leq 1$ for the local Péclet number P_e whose fulfillment prevents spurious oscillations. To avoid this problem, a stabilized finite element method was developed by choosing upwind test functions instead of the same basis for the test and trial spaces. Using the example of a one-dimensional low-pressure glow discharge in argon with an electrode gap of 1 cm it is shown that this improved method yields stable and non-oscillatory results, even if the condition $|P_e| \leq 1$ is not fulfilled. As an advantage of the new technique it is demonstrated that the numerical results do not exhibit the excessive diffusive behavior as the often used stabilizing Scharfetter-Gummel scheme and upwind finite difference methods.

MWP1 59 Particle-in-Cell Simulations of an Overdense Plasma Sustained by Microwaves* RONALD BRAVENEC,[†] *Fourth State Research* CHRISTINE ROARK, *Tech-X Corporation* MERRITT FUNK, LEE CHEN, *Tokyo Electron America* DAVID SMITHE, PETER STOLTZ, ED KASE, *Tech-X Corporation* Sustainment of plasmas by microwaves in an overdense state ($\omega < \omega_{pe}$), where the waves should be cut off, is not completely understood. Using the VORPAL particle-in-cell code,¹ we study in 2-D the interaction of electromagnetic waves propagating through an insulating dielectric at arbitrary angle into an unmagnetized plasma. Of particular interest is the predicted resonance of the waves at the location in the sheath where $\omega = \omega_{pe}$.² This resonance can magnify the electric fields and accelerate electrons to high energies. The simulations include ionization using a Monte-Carlo type model with energy-dependant cross section, which allows us to study the buildup of plasma. We are also studying the effects of secondary emission from the dielectric surface, where copious secondary emission is seen to reduce or even momentarily reverse the sign of the sheath electric field. Our secondary emission model allows for energy and incident angle dependant yield, and produces a specific energy spectrum of outgoing particles. Simulations for various plasma densities and gas pressures will be presented.

*supported by Tokyo Electron America

[†]under contract to Tokyo Electron America

¹C. Nieter and J. R. Cary, *J. Comp. Phys.*, **196**, 448 (2004).

²Yu. M. Aliev, *et al.*, *Plasma Sources Sci. Tech.* **1**, 126 (1992).

MWP1 60 ZDPlasKin: a new tool for plasmachemical simulations SERGEY PANCHESHNYI, BENJAMIN EISMANN, GERJAN HAGELAAR, LEANNE PITCHFORD, LAPLACE, *University of Toulouse, CNRS* We present ZDPlasKin (Zero-Dimensional Plasma Kinetics) freeware utility which was developed for a wide range of complex plasmachemical simulations in various gas mixtures. Our approach is based on a local approximation of the evolution of species densities obtained by solving the conservation equations. In a first step a pre-processor is used to translate a list of species, reactions and corresponding rate constants in a simple user-friendly text format into a FORTRAN 90 module. This automatically generated module contains the definition of the problem, an interface to the DVODE_F90 ODE solver and a set of supplementary routines. It includes as well an automated link to BOLSIG+, a Boltzmann equation solver based on the two-term approximation, which provides the electron transport rates and the rates of electron-neutral collisions. In a second step, execution of the code yields the time evolution of the species densities and the reaction rates. A simple acquisition algorithm allows tracing of time-averaged species densities and corresponding source terms and reaction rates for sensitivity analyses. Examples will be presented to demonstrate the simple interface and efficiency of the utility. The utility will be soon available for downloading from the LAPLACE web site <http://www.laplace.univ-tlse.fr>.

MWP1 61 Electric dipole moments in conducting particle Coulomb crystals KE QIAO, LORIN MATTHEWS, TRUELL HYDE, *CASPER - Baylor University* Coulomb crystals have been studied extensively, but in general assuming the constituent dust particles are comprised of some form of insulating material. Crystals formed from particles composed of conducting materials should exhibit differences in behavior due to the free electrons on the particle surface, which create a completely different surface charge distribution and electric dipole moments than those seen in insulating particles. A molecular dynamics (Box_Tree) simulation is employed to investigate the structure and dynamics of conducting particle systems, including electric dipole effects. The results are compared to experimental data from ordered dusty plasmas systems comprised of gold-coated particles.

MWP1 62 LIGHTING PLASMAS: GLOWS, ARCS, FLAT PANELS, NOVEL SOURCES, OTHERS

MWP1 63 Emission characteristics on light source array using micro hollow cathode plasma TAKAYUKI OHTA, NAOKI TAKOTA, YOSHIHIRO TACHIBANA, MASAFUMI ITO, *Wakayama University* YASUHIRO HIGASHIJIMA, *NU System Co., Ltd.* HIROYUKI KANO, *NU EcoEngineering Co., Ltd.* SHOJI DEN, *Katagiri Engineering Co., Ltd.* MASARU HORI, *Nagoya University* We have developed a light source array for an absorption spectroscopy using micro hollow cathode plasma. The light source is capable of emitting multi-lines of metallic atoms for measuring absolute densities of metallic atoms simultaneously in sputtering, MBE, CVD processes, and so on. In this study, the emission characteristics of the light source were investigated. Emission intensities of metallic atoms and the rotational temperatures of the N₂ second positive system were measured as functions of cathode length or cathode diameter. The emission intensity of Cu atom increased with a decrease in the cathode length from 20mm to 3mm. The applied voltage was 400 V, the pressure was 0.01 MPa, and the current was 40 mA. The current density which

was applied to the Cu pipe cathode becomes larger in the shorter pipe length, so that the emission intensity became larger. The N₂ rotational temperature was used for evaluating the neutral gas temperature and was evaluated to be from 510 to 750 K.

MWP1 64 UV Discharge Lamp on Water Vapor YURIJ SHPENIK, VOLODYMYR KELMAN, YURIJ ZHMENYAK, ANDRIJ HENERAL, *Institute of Electron Physics NAS Ukraine* The development of non-coherent sources of UV radiation based on safe and nontoxic gaseous mixtures have good aspect for different applications. Present paper for the first time reports about experimental investigations of high voltage pulse-periodic discharge in water vapor. The observed time integrated emission spectra in the range 250-325 nm at the estimated water vapor pressure 0.1 mm Hg shown three different parts: part I (250-275 nm) is attributed to B-A electronic transition of hydroxyl OH molecule; part II (275-300 nm) and part III (300-325 nm) – to the A-X electronic transition of OH molecule. The most intensive were the bands, connecting with vibration transitions (1-0) 283 nm and (1-1) 309 nm. No other radiating species were detected. Time-dependent measurement clearly indicated that the emission pulse coincides with current pulse and the electron impact processes defines the properties of the discharge emission. The average output power of the lamp was estimated 1.5 W at 0.2 % efficacy. The use of hard water D₂O instead of H₂O results the increasing of output power approximately to twice.

MWP1 65 The influence of double ionization on the arc attachment in high intensity discharge lamps* FRANK SCHARF, ANDRE BERGNER, JUERGEN MENTEL, *Ruhr-Universitaet Bochum, Germany* So far, only single ionization has been considered for the simulation of arc attachments in high intensity discharge lamps.^{1,2} However, it was found (and supported by experiments³) that the electrons reach temperatures where double ionization is not negligibly small anymore for certain conditions. To investigate the effect this has on the arc attachment, we qualitatively include double ionization in the calculation of the so-called transfer functions (namely the heat flux q_p and current density j). These transfer functions are necessary to simulate the arc attachment numerically. In the new transfer functions, ion densities for ions with single and double charge are calculated from an analytical solution of the Saha equations. These densities are used to calculate a reduction of the ion energy caused by the additional energy drain the double ionization process represents. It is however assumed that the ion current is still driven by the singly charged ions. This simplification allows only qualitative results. [1] L. Darbringhausen *et al.* *J. Phys. D: Appl. Phys.* **38** (2005) 3128 [2] N. A. Almeida *et al.*, *J. Phys. D: Appl. Phys.* **37** (2004) 3107 [3] G. Kuhn and M. Kock, *Phys. Rev. E* **75** 1 (2007) 016406 *Supported by the DFG within Graduiertenkolleg 1051

MWP1 66 Breakdown characteristics of high intensity discharge lamps filled with xenon* MARTIN WENDT, SILKE PETERS, MANFRED KETTLITZ, FLORIAN SIGENEGGER, *INP Greifswald, Felix-Hausdorff-Str. 2, 17489 Greifswald, Germany* A comparison between measured and modelled breakdown voltages of HID lamps filled with xenon at pressures of 0.1–5 bar is presented. Measurements of current and voltage characteristics and high speed photography were done on specially prepared lamps at voltage rise times of 1 MV/s to 2×10^5 MV/s. The model consists of the Poisson equation and continuity equations

for electrons and ions using the drift-diffusion approximation for the particle fluxes. Transport parameters for the electrons as functions of E/N have been determined by solving the 0-D Boltzmann equation. Appropriate boundary conditions couple the plasma to the outer circuit. The model is solved on a 1-D, inhomogeneous grid using an adaptive time step. Following the cubic interpolated propagation scheme each time step is divided into advective and non-advective parts. The latter is solved by applying the Crank-Nicholson scheme. The model gives a cathode-directed ionization front which turns into a cathode sheath. The model breakdown voltages increase with filling pressure and voltage rise time and are in good agreement with experiments.

*This work was supported by the German Federal Ministry for Education and Research (BMBF, FKZ 13N8604).

MWP1 67 Laser Induced Fluorescence on Molecular Discharges HJALMAR MULDER, ARIJ RIJKE, VINCENT GI-RAULT, WINFRED STOFFELS, *Eindhoven University of Technology* In the last half century, mercury has been used widely as the radiating species in many low pressure fluorescent lamps. Mercury primarily radiates at 254 nm and 185 nm. These photons excite a phosphor that fluoresces back to the ground state producing visible photons. This process reduces the efficiency because much of the energy of the UV photons has to be discarded. Using a species that emits light closer to or even in the visible range reduces these losses. Ideally the species (or a mixture of several species) should build up the whole visible spectrum, much like in HID lamps. InBr seems to be a good candidate for such a lamp, because it is an efficient radiator that emits most of its light around 370 nm; much closer to the visible part of the spectrum. In order to get insight in the energy transfer processes going on in these molecules we have conducted a laser induced fluorescence (LIF) experiment on InBr vapour and on a plasma. We have measured the decay times of different rovibrational levels of the InBr-molecule as well as the spectral distribution of the fluorescence from these levels. From the former we calculated the rotational temperature of the plasma and from the latter we calculated the Franck-Condon factors for the A-state as well as the vibrational temperature.

MWP1 68 Determination of Ba-emitter densities along electrodes in high pressure sodium lamps by optical absorption spectroscopy MICHAEL WESTERMEIER, JENS REINELT, PETER AWAKOWICZ, JUERGEN MENTEL, *Ruhr-University of Bochum, Germany* Nowadays, high pressure sodium lamps gain more importance in various fields of lighting e.g. for horticulture lighting. To achieve a long lifetime, a detailed understanding of the density of the barium emitter around the lamp electrodes and its interaction with them is needed. The lamp under investigation has a special research design. It is downscaled to a 140 W lamp and equipped with a sapphire discharge tube to allow optical observations. Ba is stored in a tungsten coil around the rod shaped tungsten electrodes and transported to the tip during operation. By measuring the absorption of the 553 nm Ba resonance line the spatially resolved Ba density around the electrodes during lamp operation is determined. As backlight a filtered UHP-lamp is installed. The measuring results show a decrease of Ba along the electrode axis representing a diffusion process. Further results will be shown for different lamp operating parameters (e.g. current, frequency) and combined with the measured electrode temperature profiles.

MWP1 69 Iodine pressure in high intensity discharge lamps ALEXANDER DUNAEVSKY, JUN-MING TU, *Philips Lighting North America* The dynamics of the partial pressure of iodine influence the emission properties of metal halide lamps. In addition, various processes in the discharge affect the iodine pressure. Monitoring the partial pressure of iodine by high-resolution spectroscopy (HRS) can be a very powerful, non-destructive diagnostic tool for metal halide lamp development, if the mechanisms responsible for the pressure changes are understood. Thermodynamic modeling can help to interpret some effects observed experimentally. In this study, the iodine pressure in quartz sodium-scandium metal halide lamps with various chemical additive ratios is measured using the HRS technique. The correlations between partial pressures predicted by modeling and observed experimentally are analyzed.

MWP1 70 NEGATIVE IONS, SHEATHS AND DUSTY PLASMAS

MWP1 71 Ion-ion plasmas by electron magnetic filtering: 2D fluid simulation and applications to space propulsion ALBERT MEIGE, *LPTP, Ecole Polytechnique* GERJAN HAGELAAR, *Laplace, Universite Paul Sabatier* PASCAL CHABERT, *LPTP, Ecole Polytechnique* A two-dimensional magnetized plasma fluid simulation is developed to investigate the electron magnetic filtering in an electronegative plasma. The model uses the first three moments of the Boltzmann equation, namely the continuity equation, the conservation of momentum and an energy equation for the electrons. An oxygen plasma in a grounded cylinder is simulated. The magnetic field is uniform and parallel to the system revolution axis. When the magnetic field strength is sufficient, electrons are confined in the center of the discharge, resulting in an ion-ion plasma (electron-free plasma) at the periphery of the discharge. Applications to space propulsion are presented.

MWP1 72 A study of negative ion production on surface in H₂ and D₂ plasma GILLES CARRY, LOÏC SCHIESKO, JOUNAYD BENTOUNES, MARCEL CARRERE, JEAN-MARC LAYET, *PIIM, CNRS - Universite de Provence* PLASMA-SURFACE TEAM, We present a study of negative ion (NI) generation on surface in H₂ and D₂ plasmas. A mass spectrometer (EQP300) is placed in the diffusion chamber of a helicon plasma reactor and faces a one square centimetre sample (graphite, copper...). The sample is negatively biased with respect to the plasma. Positive ions strike the sample in normal incidence and NI formed (H⁻ and D⁻) upon bombardment are repelled from the surface toward the plasma and collected by the mass spectrometer. Through the measurement of negative Ion Distribution Function (IDF) we investigate basic mechanisms governing NI production on surfaces in interaction with H₂ plasma. Particularly, we have shown that two electrons capture by incoming positive ions explains IDF tail but is not the main mechanism explaining NI production. On the contrary, we demonstrated sputtering of adsorbed hydrogen atom as NI accounts for most of negative ions created. We also demonstrated NI production on graphite surface is proportional to ion flux and has bell shape dependence with positive ion energy.

MWPI 73 The collisional capacitive RF sheath and the assumption of a sharp electron edge* RALF PETER BRINKMANN, *Ruhr University Bochum, Theoretical Electrical Engineering* The transition from quasi-neutrality to charge depletion is one of the characteristic features of the plasma boundary sheath. It is often described in terms of the so-called step model which assumes a transition point (electron step) where the electron density drops from a value equal to the ion density (in the bulk) to a value of zero (in the sheath). Inserted into Poisson's equation, the step model yields an expression for the field which is realistic deep in the sheath but fails to merge correctly into the ambipolar field of the bulk. This work studies the consequences of that approximation for the example of the collision-dominated, capacitive RF sheath by Lieberman [1]. First, the model is solved exactly, using a relaxation scheme. Then, the step approximation is applied which recovers Lieberman's semi-analytical solution. It is demonstrated that the step approximation induces a spurious divergence of the ion density at the sheath edge and prevents a matching of the sheath model to a bulk model. Integral sheath quantities, on the other hand, like the capacitance or the overall voltage drop, are faithfully reproduced. [1] M. A. Lieberman, *IEEE Trans. Plasma Sci.* 16, pp. 638-644 (1988).

*Support from the Deutsche Forschungsgemeinschaft is gratefully acknowledged.

MWPI 74 Study of an electron-attracting sheath: the effect of secondary electron emission GILLES CARTRY, LOIC SCHIESKO, MARCEL CARRERE, JEAN-MARC LAYET, *PIIM, CNRS - Université de Provence* PLASMA-SURFACE TEAM, A copper sample facing a mass spectrometer (EQP300) is biased positively beyond plasma potential in low pressure argon plasma. Some Ar^+ and Ar^{2+} ions are created in the sheath by electrons extracted from plasma and are accelerated toward the mass spectrometer where they are detected according to their energy. Ion energy is related to the local sheath potential at which the ion has been created. Providing careful energy calibration of the mass spectrometer, Ion Distribution Function (IDF) allows probing in a non perturbative way electron attracting sheath potential. We observe a strong decrease of the ion signal some few volts before sample bias. We attribute this effect to the presence of secondary electrons shielding the sample potential. Potential profile and IDFs are computed using a model including secondary emission. Fit of Ar^+ and Ar^{2+} IDFs provides an estimation of secondary emission yield and secondary electron temperature.

MWPI 75 Interaction of dust particles in a plasma with an external source of gas ionization* ANDREY STAROSTIN, ANATOLY FILIPPOV, ALEXANDER PAL, ANATOLY ZAGORODNY, The interaction of two dust particles in no equilibrium plasma at elevated pressures has been studied. An asymptotic theory of screening, which leads to a two-exponential dependence of the dust particle potential on distance with different shielding lengths, is used to determine the electrostatic energy of the system of charges associated with the two dust particles. The dependence of the electrostatic energy on interparticle distance has been found to have a minimum, as in equilibrium plasma. The interaction force between the dust particles has been determined. It turned out to be asymmetric - for different charges the forces acting on the first and second dust particles are not equal. The force equality takes place only for the sinks of plasma particles proportional to the dust particle charge. This is the result of an asymmetric charge separation near dust particles with different

charges and indicates that the interaction force in no equilibrium plasma is no potential in the common case. The potential energy of the interaction between the dust particles has been determined for the case of equal forces. Attraction between likely charged particles with different (in magnitude) charges has been found to be possible only when they come very close to each other. Relations for modified coupling parameter of an interaction potential that consists of two exponential terms with different shielding lengths were derived.

*The work was supported by RFBR, grant 08-02-01324-a.

MWPI 76 New insights into the anion formation mechanisms in dusty acetylene discharges MING MAO, *PLASMANT Research Group, Dept. of Chemistry, Univ. of Antwerp* JAN BENEDIKT, ANGELO CONSOLI, *Arbeitsgruppe Reaktive Plasmen, Fakultät für Physik und Astronomie, Ruhr-Universität Bochum* ANNEMIE BOGAERTS, *PLASMANT Research Group, Dept. of Chemistry, Univ. of Antwerp* Dust (or nanoparticle) formation is a well-known phenomenon occurring in reactive gas plasmas, such as silane or acetylene. Under some conditions, the dust formation is considered to be harmful, whereas for other applications, it turns out to be beneficial. In this presentation, the initial mechanisms of nanoparticle formation and growth in radiofrequency (RF) acetylene (C_2H_2) plasmas are investigated by means of a comprehensive self-consistent one-dimensional (1D) fluid model. Based on the comparison of our calculation results with available experimental data for acetylene plasmas in the literature, some new mechanisms for negative ion formation and growth are proposed. Possible routes are considered for the formation of larger (linear and branched) hydrocarbons C_{2n}H_2 ($n=3-5$), which contribute to the generation of C_{2n}H^- anions ($n=3-5$) due to dissociative electron attachment. Moreover, beside the C_{2n}H^- ions, also the vinylidene anion (H_2CC^-) and higher $\text{C}_{2n}\text{H}_2^-$ anions ($n=2-4$) are found to be important plasma species. This project was supported financially by the Fund for Scientific Research (FWO) Flanders (Project G. 0068.07), the Interuniversity Attraction Poles Programme of the Belgian State (Belgian Science Policy; Project P6/42) and the CALCUA computing facilities of the University of Antwerp.

MWPI 77 Peculiarity of Positron Annihilation on Atoms and Particles of Dust Space Plasma of Galactic Center VIKTOR I. GRAFUTIN, TAT'YANE L. RAZINKOVA, *Federal State Unitary Enterprise* EUGENE P. PROKOP'EV, *Federal State Unitary Enterprise and Moscow Institute of Electronic Technology* A.I. ALIKHANOV, *Institute for Theoretical and Experimental Physics* Research of properties of positron states has great importance in a modern science and technology. Therefore last years intensive development of positronics of various substances and their states is observed. The special role is represented with researches in the field of space positronics. It is process positron annihilation in the dust space plasma on the basis of our calculations and data analysed. It is shown that formation of positronium atom in dust space plasma with the large concentration of the charged particles of a dust can occur as by means of processes of interaction of positrons to atoms H and free electrons and processes of interaction of positrons with the charged particles of dust space plasma. In such space plasma the output of positronium atom about what speak experimental data of space laboratory Integral is possible practically 100 %. Proceeding from sizes of diffusion coefficient the

sizes of particles of a dust particles in space plasma exceeds size of the order 100 of nanometer. The size of particles is comparable to length of diffusion of positrons, i.e. $0.1 \div 1$ microns. These received sizes of particles well coincide with data of optical observations.

MWP1 78 CAPACITIVELY COUPLED PLASMAS

MWP1 79 Properties of capacitive He/SF₆/O₂ and He/CF₄/O₂ discharges at atmospheric pressure TAKASHI KIMURA, HIROKI TANAHASHI, *Nagoya Institute of Technology* Electrical and optical measurements of atmospheric pressure capacitive radio frequency (13.56 MHz) He/SF₆/O₂ and He/CF₄/O₂ discharges are carried out at the mixture compositions of fluorine compound gas and oxygen of 0.5%. Those discharges are produced between two planar electrodes of 40mm- ϕ at the gap length of 1.0 mm in the dissipated power range from 40W to 180W. The total flow rate of helium and reactive gases is kept at 7(l/min), and the small amount of Ar (= 10 sccm) is also fed in order to estimate the atomic fluorine density by actinometry. From the measured waveforms of the applied voltage and the RF current, the atmospheric pressure He/CF₄/O₂ discharges are capacitive, whereas the He/SF₆/O₂ discharges are greatly resistive at most of our experimental conditions. The atomic fluorine density in those discharges should be estimated by actinometry, where the intensities at 704 nm emitted from the excited atomic fluorine and 750nm emitted from the excited Ar are used. The atomic fluorine density increases markedly with increasing oxygen content, and then reaches each maximum when the ratio of the oxygen content to the sum of the oxygen and fluoride compound gas contents is around 0.2-0.5. The atomic fluorine density in those discharges is on the order of 10^{14} cm⁻³. This work was supported in part by Research Foundation for the Electrotechnology of Chubu.

MWP1 80 Plasma activation caused by local rf power supply*

F. SIGENEGER, R. BASNER, D. LOFFHAGEN, *INP Greifswald, Germany* H. KERSTEN, *IEAP, Christian-Albrechts-Universität, Kiel* The response of a capacitively coupled rf discharge in argon at 13.56 MHz to a local supply of additional rf power at the passive electrode was investigated experimentally and theoretically. The study has been performed at the reactor PULVA-INP which possesses a segmented passive electrode. Its central pixel was driven by an additional rf voltage with the same frequency and phase as the main power supply. The large enhancement of the local power density becomes obvious from the intensive light emission in front of this pixel. Furthermore, the pronounced change of the potential was demonstrated by the sensitive response of microparticles in the sheath. An axisymmetric fluid model of the plasma has been implemented to study the observed phenomenon theoretically. The model comprises particle balance equations of electrons and ions, Poisson's equation and the electron energy balance equation. The results of the model calculations demonstrate the structural change of the potential and the local increase of the electron density and power density in front of the central pixel. The strongly increased excitation rate corresponds to the observed enlargement of the light emission.

*This work has been supported by the Deutsche Forschungsgemeinschaft under SFB-TR 24.

MWP1 81 Diagnostics of ballistic electrons in a DC/RF hybrid capacitively coupled plasma reactor LIN XU, *University of Houston* LEE CHEN, *Tokyo Electron America* ALOK RANJAN, *University of Houston* MERRITT FUNK, RON BRAVENEC, *Tokyo Electron America* DEMETRE ECONOMOU, VINCENT DONNELLY, *University of Houston* RADHA SUNDARARAJAN, *Tokyo Electron America* UNIVERSITY OF HOUSTON TEAM, TOKYO ELECTRON AMERICA TEAM, The DC/RF hybrid is a capacitively coupled plasma etcher with RF voltage on the bottom electrode and negative DC bias on the upper electrode. This configuration can significantly alleviate the electron shading effect and preserve photoresist integrity during plasma etching. It is thought that a group of ballistic electrons is responsible for these results. These high-energy electrons start as secondaries emitted from the negatively-biased DC electrode and accelerate across the DC sheath. They acquire high enough energy in the sheath such that they can cross the bulk plasma without gas-phase collisions. The ballistic electrons either strike the RF electrode or are trapped in the plasma bulk depending on the RF phase. Two gridded energy analyzers mounted on the back of the RF electrode were used to determine the energy distribution of ballistic electrons. The dependence of the ballistic electron energy distribution on DC voltage, pressure and RF power will be presented and compared with simulation results.

MWP1 82 Secondary electrons in dual-frequency capacitive discharges

MILES M. TURNER, *Dublin City University, Ireland* Phase resolved optical emission spectroscopy has offered deep insight into the behaviour of electrons in plasma discharges, nowhere more so than in the case of dual-frequency discharges, where the presence of the two frequencies leads to complicated electron dynamics. An open question in the physics of these discharges is the importance of secondary electrons, emitted from electrodes by such processes as ion impact and photo-emission. Because the electrode surface state is poorly known, it is difficult to say anything a priori about the significance of these processes. In this paper we will present particle-in-cell simulations of dual-frequency discharges under conditions approximating those of the experiments, and we will attempt to draw conclusions concerning the importance of secondary electron effects, based both on the observed spatio-temporal pattern of optical emission, and on measurements of the plasma density carried out using hair-pin probes. The conclusion of this investigation is that secondary electron phenomena cannot be neglected under these conditions.

MWP1 83 Modelling and Simulation of multi-frequency capacitive discharges

STEFAN BIENHOLZ, PHILIPP MERTMANN, PETER AWAKOWICZ, *Ruhr University Bochum, AEPT* THOMAS MUSSENBRÖCK, RALF PETER BRINKMANN, *Ruhr University Bochum, TET* In material processing applications the energy distribution function and the angular distribution function of energetic ions which are accelerated by the electric field in the plasma boundary sheath play a crucial role. The calculation of such distribution functions requires either large computational cost within the frame of numerical simulation of a plasma reactor as a whole or the electric field is assumed to be given by simple expressions. However, an appropriate discharge (or sheath) model is needed. In this contribution we propose a locally one-dimensional model of a capacitive discharge based on a ion fluid description

self-consistently coupled to Poisson's equation. The model allows for self-consistent calculation of the electric field for (arbitrary) multi-frequency discharge excitation and thus for calculation of ion distribution functions by means of an efficient Monte-Carlo code.

MWP1 84 Skin effect in an asymmetrical, capacitive discharge

MICHAEL KLICK, *Plasmetrex GmbH, D12489 Berlin, Germany* TORBEN HEMKE, THOMAS MUSSEN BROCK, RALF PETER BRINKMANN, *Ruhr University Bochum, D44780 Bochum, Germany* The electrostatic approximation reduces the set of Maxwell's equations to the much simpler Poisson equation and is often employed for modeling and simulation of radio frequency driven capacitive low pressure discharges. It is now widely acknowledged that the neglect of induction phenomena breaks down for large-area and high-density plasmas. But there is still a lack of analytical models which allow an easy handling and understanding of the skin effect in asymmetrical systems. We present an electrodynamic 2d model for a cylindrical, asymmetrical CCP. We use a simplified boundary condition for the RF current density to achieve a considerable simplification of the mathematical approach. Thus the sheath at the driven electrode can be included readily. Advantages and restrictions of the analytical solution are discussed in comparison to numerical simulation results.

MWP1 85 On the possibility of making a geometrically symmetric RF-CCP discharge electrically asymmetric*

UWE CZARNETZKI, BRIAN G. HEIL, *Ruhr-University Bochum, Inst. for Plasma and Atomic Physics, 44780 Bochum, Germany* RALF PETER BRINKMANN, THOMAS MUSSEN BROCK, *Ruhr-University Bochum, Lehrstuhl f. Theoretische Elektrotechnik, 44801 Bochum, Germany* A simple solution to the demand of controlling independently ion flux and ion energy in capacitive discharges is presented. When a temporally symmetric, multi-frequency voltage wave form containing one or more even harmonics is applied to a discharge, even a geometrically symmetric one, the two sheaths are necessarily asymmetric and a DC self bias develops. Optimally, this is achieved by simultaneously applying an RF voltage composed of the phase locked fundamental and its second harmonic. The resulting DC self bias and hence the ion energy is a nearly linear function of the phase angle between the two applied RF voltages. In geometrically symmetric discharges the roles of the two electrodes can be reversed by just using the phase. The phase angle control of the ion energy leaves the applied RF voltage and frequency and thereby the plasma density, electron temperature, and ion flux effectively unchanged. An analytical model and a hybrid fluid dynamic-Monte Carlo simulation analysis are presented.

*Work was supported by the DFG in the frame of SFB591 and GK1051.

MWP1 86 Electric Field Reversals in the sheath region of capacitively coupled RF discharges at different pressures*

JULIAN SCHULZE, *Ruhr University Bochum* ZOLTAN DONKO, *Hungarian Academy for Science* BRIAN HEIL, DIRK LUGGENHOELSCHER, THOMAS MUSSEN BROCK, RALF PETER BRINKMANN, UWE CZARNETZKI, *Ruhr University Bochum* Electric field reversals in single and dual-frequency capacitively coupled RF discharges are investigated at different pressures. Phase resolved optical emission spectroscopy is used to measure the excitation of the neutral background gas caused by the field reversal during sheath collapse. The resulting spatio-temporal

excitation profiles are compared to results of a fluid sheath model in the single frequency case and a Particle in Cell simulation in the dual-frequency case. The results show that field reversals occur in both cases, in different gases and at different pressures. An analytical model gives insight into the mechanisms causing the reversal of the electric field. In the dual-frequency case a comparison between PIC simulation and analytical model is performed. It shows that the field reversal is caused by a combination of electron inertia and collisions of electrons with the neutral background gas. The model also shows that at low pressures electron inertia is the cause of the observed field reversal.

*Funded by the DFG through SFB591 and GRK1051 and the Hungarian Scientific Research Fund.

MWP1 87 Multiband carbon monoxide laser (2.5 – 4.0 and 5.0 – 6.5 micron) pumped by capacitive slab RF discharge

ANDREY IONIN, ANDREY KOZLOV, LEONID SELEZNEV, DMITRY SINITSYN, *Lebedev Physical Institute of Russian Academy of Sciences* LEBEDEV PHYSICAL INSTITUTE OF RUSSIAN ACADEMY OF SCIENCES TEAM, Overtone lasing and fundamental band tuning was for the first time obtained in a carbon monoxide laser excited by repetitively pulsed capacitive slab RF discharge (81.36 MHz). RF discharge pulse repetition rate was 100–500 Hz. The active volume was 3x30x250 cubic mm. Laser electrodes were cooled down to 120 K. Gas mixture CO:air:He at gas pressure 15 Torr was used. The optical scheme "frequency selective master oscillator - laser amplifier" was applied for getting fundamental band tuning. Single line lasing with average power up to several tens of mW was observed on about 100 rotational-vibrational transitions of CO molecule within the spectral range 5.0–6.5 micron. Multiline overtone lasing was observed on about 80 spectral lines within the spectral range 2.5–4.0 micron, with maximum single line average output power 12 mW. The total output power of the slab overtone CO laser came up to 0.35 W, with laser efficiency 0.5 percent. The results of parametric studies of capacitive slab RF discharge in carbon monoxide mixtures, and overtone and fundamental band CO laser characteristics are discussed.

MWP1 88 PLASMA APPLICATIONS

MWP1 89 Growth and characterization of CNT Forests using Bimetallic Nanoparticles as Catalyst*

KYUNG-HWAN LEE, *The University of Texas at Dallas* A. SRA, *University of Texas Southwestern Medical Center at Dallas* H. JANG, *The University of Texas at Dallas* B. CHOI, *Korea Institute of Industrial Technology* L. OVERZET, G. LEE, D. YANG, *The University of Texas at Dallas* We study the growth of Multiwall carbon nanotubes (MWCNT) using bimetallic nanoparticles (NP) as catalyst rather than zerovalent metal ions such as Fe, Ni, Co. One advantage of using bimetallic NP is that both the size and shape and composition (atomic ordering) can be controlled. We will describe a simple method of producing bimetallic Fe-Pt, Fe-Co alloy nanoparticles and compare MWCNT growth using them to Fe catalyst growth. The synthesis of Fe, Fe-Pt, Fe-Co NP was carried out using a bottom-up polyol process. Subsequent growth of MWCNT forests was accomplished by PECVD using acetylene as precursor. TEM and SEM analysis of the sample cross-section grown at substrate temperature of 680 °C indicates that the diameters of the CNTs are ~ 10-20 nm while height of the forest varies from 30

μm for Fe to $5 \mu\text{m}$ for Fe-Pt and $80\text{-}100 \mu\text{m}$ for Fe-Co. The number of walls in the CNTs and the graphitization content could be manipulated by varying the temperature (increasing to 760°C) or by pre-treatment of the nanoparticles with oxygen plasma.

*Work supported in part by: Korea Institute of Industrial Technology.

MWP1 90 Modeling of Electron Field Emission Properties of Carbon Nanotubes* MARIJA RADMILOVIC-RADJENOVIC, BRANISLAV RADJENOVIC, *Institute of Physics, Belgrade-Serbia* The strength and flexibility of carbon nanotubes (CNTs) make them of potential use in controlling other nanoscale structures, which suggests they will have an important role in nanotechnology engineering. One of the most promising future applications is employing carbon nanotubes in electron field emission devices. Studies, however, have been mostly focused on using CNTs both as conductors and semiconductors. Nevertheless, the effect of the field emission in CNTs can be considered from the aspect of electrical breakdown. In this paper we are studying the case for CNTs as nanoelectrodes for electric discharges, operating at high E/N and with high field enhancement factors. It was shown that the electric field is dramatically enhanced near the cap of a nanotube with large variation of local field distribution.

*The present work has been performed under MNZZS 141025

MWP1 91 Audio frequency modulated RF discharge at atmospheric pressure* NICHOLAS BRAITHWAITE, YVONNE SUTTON, DAVID SHARP, *The Open University* JON MOORE, *B and W Group Ltd* An atmospheric pressure RF arc discharge, generated using a low voltage chopper and a Tesla coil resonant at about 300 kHz, forms a stable, silent, flame-like luminous region some 3 mm in diameter and 40 mm long, rooted to the electrodes by visible hot spots. It is known and we have confirmed that audio frequency modulation of the drive voltage makes the discharge act as an audio loudspeaker (tweeter) with its monopole radiation pattern constrained only by the electrodes. Time resolved 'total' optical emission reveals an intensity variation that is synchronous with the audio frequency. Electrical characterisation of the high frequency discharge has been carried out. In the steady state, the high frequency arc burns without generating significant quantities of ozone, as determined by a commercial ozone detector. This is consistent with the high gas temperature within the arc, as measured by optical emission spectroscopy of molecular nitrogen. Phase-locked emission measurements illustrate the acoustic coupling.

*Project supported by B & W Group Ltd.

MWP1 92 Reacting Flow Imaging Using Point to Plane Pulsed Air/Hydrocarbon Discharge DAVID WISMAN, *UES Inc* BISWA GANGULY, *Air Force Research Laboratory* We report the use of a positive polarity point-to-plane pulsed corona discharge to obtain a time-resolved visualization of the reaction zone in a premixed propane-air flame. In the initial phases of the discharge the higher gas temperature along the flame reaction zone provides a higher E/n path that preferentially guides the streamer discharge to the cathode. Following the initial streamer phase, an increased plasma conductivity of the fully developed discharge, caused in part by lowering the attachment rate of electrons to O_2 , allows the plasma conduction current to preferentially distribute along the high temperature flame reaction zone. The resulting N_2

C-B emission from the localized discharge provides a visualization of the flame front. The short ICCD gate time (100 ns) allows for capture of the N_2 C-B emission without the need for spectral filtering, and thus permitting imaging up to 1 kHz repetition rate. Imaging the plasma emission after the discharge has been fully developed allows for the monitoring of small scale instabilities in the reaction zone, which can be an important tool for understanding the combustion dynamics. We will also report the effect of flame equivalence ratio on the plasma emission intensity and its impact on the usefulness of high speed imaging.

MWP1 93 Characterization of Ar/H₂/Air Supersonic Flowing Microwave Discharges* D.J. DRAKE, S. POPOVIC, L. VUSKOVIC, *Old Dominion University* We performed a detailed characterization of a microwave cavity discharge in the supersonic flow of Ar/H₂/Air mixtures. The supersonic flow was generated using a convergent-divergent nozzle upstream of the discharge region. Gases were premixed in the stagnation chamber at room temperature by adding up to 10% hydrogen and up to 45% air to pure argon. A cylindrical cavity was used to sustain a discharge in the mixtures in the pressure range of 100-600 Pa. Optical emission spectroscopy was used to observe the effects of hydrogen and air admixtures to plasma parameters and populations of excited species.

*Supported by NASA Marshall Space Flight Center.

MWP1 94 Parametric Studies on Thrust Produced by Pulsed DBD Plasma Actuators DMITRY OPAITS, *Princeton University* ALEXANDRE LIKHANSKII, *The Pennsylvania State University* SOHAIL ZAIDI, MIKHAIL SHNEIDER, *Princeton University* SERGEY MACHERET, *Lockheed Martin Aeronautics Company* RICHARD MILES, *Princeton University* A number of works have demonstrated the utility of dielectric barrier discharge (DBD) plasma actuators for aerodynamic control. Recent experiments and computations showed that a novel voltage waveform consisting of high-voltage nanosecond repetitive pulses superimposed on a low-frequency sinusoidal voltage can produce significantly enhanced wall jets compared with those generated with conventional sinusoidal voltage. We proposed and used what is essentially a non-self-sustained discharge: the plasma is generated by repetitive short pulses, and the pushing of the gas occurs primarily due to the low frequency (bias) voltage. The advantage of this non-self-sustained discharge is that the parameters of ionizing pulses and the driving bias voltage can be varied independently, which adds flexibility to control and optimization of the actuator performance. This work will present results of parametric studies of the plasma produced thrust at different parameters of the voltage waveform, such as frequency and shape of the bias voltage and duration and repetition rate of the pulses.

MWP1 95 Improved Nonambipolar Electron Source operation with permanent magnets JESSE GUDMUNDSON, *Dept. Engineering Physics, UW-Madison, Madison, Wisconsin 53706* NOAH HERSHKOWITZ, ** Dept. Engineering Physics, UW-Madison, Madison, Wisconsin 53706* The Nonambipolar Electron Source (NES), is a Radio Frequency (rf) plasma-based electron source that does not rely on electron emission at a cathode surface. All electrons are extracted at an electron sheath through a biased ring and all ions are lost radially to a biased Faraday shield. The electromagnetic B field in the original NES has been replaced by a NdFeB permanent magnet array. The magnet array consists of a

ring of radially aligned magnets followed by a ring of axially aligned magnets producing a peak field of approximately 850 Gauss. Measurement of the magnetic field was in good agreement with field predicted by the FEMM code. Optimization of the single turn antenna and biased ring will be discussed. Operating with argon, at least 15 A of electron current was extracted using a flow rate of 15 sccm Ar at approximately 10 mTorr and 600 W of RF power at 13.56 MHz. For comparison, the original NES required 1200 W of power to achieve 15 A of extracted current. Compared to the previous coil design, the NdFeB magnets are lighter weight, require no power, and provide a greater peak magnetic field.

*Work funded by DOE grant No. DE-FG02-97ER54437

MWPI 96 Flow separation control by plasma actuator with nanosecond pulse discharge ANDREI STARIKOVSKII, *Drexel University* DMIRTY ROUPASSOV, *Moscow Institute of Physics and Technology* ANDREI NIKIPELOV, *NEQLab Research* MARYIA NUDNOVA, *Moscow Institute of Physics and Technology* Boundary layer separation control by plasma actuator with high-voltage pulsed periodic nanosecond excitation is presented. Actuator-induced gas velocities show near-zero values for nanosecond pulses. The measurements performed have shown overheating of discharge region at fast ($\tau \approx 1 \mu\text{s}$) thermalization of the plasma imputed energy. The mean values of such heating for the plasma layer can reach 70, 200 and even 400 K for 7, 12 and 50 ns pulse duration, respectively. The emerging shock wave together with the secondary vortex flows disturbs the main flow. The resulting pulsed-periodic disturbance causes an efficient transversal momentum transfer into the boundary layer and further flow attachment to the airfoil surface. Thus for pulsed nanosecond periodic DBD the main mechanism of impact is the energy transfer and heating the near-surface gas layer. The following pulse-periodic vortex movement stimulates redistribution of the main flow momentum. The experiments have shown high efficiency of the given mechanism to control boundary layer separation, lift and drag force coefficients, and acoustic noise reduction in the Mach number range of 0.05 to 0.85.

MWPI 97 Streamer Discharges in Water and their Application JUERGEN F. KOLB, SHU XIAO, NOAH SCULLY, RAVINDRA P. JOSHI, KARL H. SCHOENBACH, *Frank Reidy Research Center for Bioelectrics, Old Dominion University* Electrical discharges in liquids have been widely investigated for transient high voltage insulation and switching applications. Despite extensive efforts, the mechanism of breakdown initiation and formation of streamers are not completely understood, in particular for the application of short, sub-microsecond pulses. Regardless, streamers in water generated under these conditions are an attractive means of water treatment for a variety of applications, such as remediation of chemical and biological pathogens in waste-water, purification of drinking water, the cleaning of algae from freshwater ponds. Radicals, ultraviolet light, high electric fields and shockwaves are all considered as possible mediators of the effects, and all of which are generated in the streamer propagation process. We will present experimental results on the initiation and propagation of streamers in water and discuss the mechanisms. Further selected applications will be presented.

MWPI 98 Decomposition of electrostatic-precipitated diesel particulate materials with nitric oxides using dielectric barrier discharge* YUKIHIKO YAMAGATA, YOSUKE FUJII, *Interdisciplinary Graduate School of Engineering Sciences, Kyushu Univ., Japan* KATSUNORI MURAOKA, *Faculty of Engineering, Chubu Univ., Japan* A newly developed decomposition technique for diesel particulate materials (DPM) and nitric oxides was demonstrated. This is based on the combination of dielectric barrier discharge (DBD) with condensation/localization technique. Using an electrostatic precipitation (EP) operated under a negative corona discharge, DPM were collected in a reactor that is able to generate DBD. More than 95% of DPM emitted from a real diesel engine were continuously collected for 60 min at DC -5 kV. Subsequently, the EP-collected DPM were decomposed in a model gas including NO molecule by DBD operated at AC 60 Hz. In the presence of DPM, a large amount of NO was decomposed in comparison with that in the absence of DPM. It was shown that DPM and NO acting as the oxidant and reductant, respectively, were decomposed simultaneously and effectively by DBD. It is also suggested that water vapor in the exhaust gas improves the NOx decomposition rate.

*This work has been partially supported by Grant-in-Aid for Scientific Research from the Ministry of Education, Science, Sports, Culture and Technology of Japan.

MWPI 99 Pulsed-plasma destruction of phenol in an aqueous solution KOHKI SATOH, HIDEYUKI ITABASHI, *Muroran Institute of Technology* YASUSHI MIYAZAKI, *Nippon Steel Corporation* HIDENORI ITOH, *Muroran Institute of Technology* An aqueous solution of phenol is exposed to pulsed-discharge plasma, and the decomposition characteristics of phenol are investigated for the different composition of a background gas. It is likely that OH radicals, produced by the collision between water vapour and energetic electrons in the pulsed plasma creeping on a water surface, are responsible for the decomposition of phenol in the solution for all kind of background gases. It is probably that OH radicals, produced by N_2 molecules excited in metastable state ($\text{N}_2(A^3\Sigma_u^+)$), and O_3 assist the phenol decomposition in pure N_2 and in pure O_2 , respectively. In $\text{N}_2\text{-O}_2$ mixture, the decomposition rates of phenol stay at lower values, since NO_x reduces O_3 concentration and inhibits the O_3 production. In Ar-O_2 mixture, the decomposition rate of phenol increases with an increase of Ar mixture-ratio; therefore, Ar atoms excited in metastable states ($\text{Ar}(4^3P_2)$, $\text{Ar}(4^3P_0)$) are responsible for the decomposition of phenol at higher mixture ratio of Ar.

MWPI 100 Interaction of DC Microhollow Cathode Discharge Plasma Micro Jet with Liquid Media WEIDONG ZHU, JOSE LOPEZ, *St Peters College* KURT BECKER, *Polytechnic University* There have been different approaches in studying the interaction between plasma and liquid, such as sustained plasmas in contact with liquids and pulsed electric discharge in liquids. Recently, we have discovered that stable plasma can be sustained within a gas cavity maintained inside liquid media. A prototype device with key dimensions in sub-millimeter range were operated successfully in de-ionized water and turbo molecular pump oil with ambient air, pure nitrogen or pure oxygen used as the operating gas. Hydrogen Peroxide production in de-ionized water with ambient air as the working gas is estimated to be about 80 mg/L after 15 minutes plasma jet-water interaction while energy consumption

is only about 8-10 W. With the radicals readily generated and directly introduced into the liquid media, it could lead to applications such as in-liquid bio-waste treatment, bio-rich liquid modification, in-situ monitoring/sensing, and filtration of by-products from VOC treatment by plasma.

MWPI 101 Properties of plasma-liquid system with transversal discharge VOLODYMYR SHAPOVAL, Description of different plasma-liquid systems and their comparative analysis are presented in this work. There are various types of self-sustained electrical discharges with electrodes submerged into liquid, and discharges with one "liquid" electrode as well as secondary discharges with "liquid" electrodes, which can be applied for water treatment. This dynamic plasma-liquid systems have well-developed plasma-liquid interface and large surface-to-volume ratio. Plasma-liquid system based on the discharge in the gas channel formed by the gas flow immersed into the liquid was studied in this work. Phenol solutions were used as working liquids. It was shown that investigated plasma-liquid system is very effective for the phenol destruction in water due to the formation of chemically active oxidants in sufficient amount. The efficiency of phenol destruction increases with increasing of the time of plasma-chemical processing in the reactor. It was shown that regime with negative polarity of "liquid" electrode is more effective for plasma-chemical processing than with positive polarity.

MWPI 102 Growth of carbon nanofibers in plasma-enhanced chemical vapor deposition IGOR DENYSENKO, *V. N. Karazin Kharkiv National University* KOSTYA OSTRIKOV, *CSIRO* EUGENE TAM, *The University of Sydney* PLASMA NANOSCIENCE TEAM, A theoretical model describing the plasma-assisted growth of carbon nanofibers with metal catalyst particles on top is proposed. Using the model, the plasma-related effects on the nanofiber growth parameters such as the surface diffusion growth rate, the effective carbon flux to the catalyst surface, the characteristic residence time and diffusion length of carbon on the catalyst surface, and the surface coverages, have been studied. It has been found how these parameters depend on the catalyst surface temperature and ion and etching gas fluxes to the catalyst surface. The optimum conditions under which a low-temperature plasma environment can benefit the carbon nanofiber growth are formulated. It has been also found how the plasma environment affects the temperature distribution over the length of the carbon nanofibers. Conditions when the temperature of the catalyst nanoparticles is higher than the temperature of the substrate holder are determined. The results here are in a good agreement with the available experimental data on the carbon nanofiber growth and can be used for optimizing synthesis of nanoassemblies in low-temperature plasma-assisted nanofabrication.

MWPI 103 Nanostructures under extreme non equilibrium plasma conditions of dense plasma focus device MAHESH SRIVASTAVA, *University of Delhi* KOSTYA OSTRIKOV, *CSIRO* PLASMA NANOSCIENCE TEAM, In this poster, we will present the formation of nanostructures due to highly energetic, high fluence ions of different material produced due to high density, high temperature (1-2 KeV), extremely non-equilibrium pulsed plasma produced in a Dense Plasma Focus (DPF) device. Glow discharge and the magnetron sputtering discharge has weakly ionized, low temperature and low density plasma which produces ions in the discharge for the formation of nanostructures.

In the present case we are using a 3.3 KJ Mather type DPF device which is powered by 30 microfarad 15 KV fast discharging energy storage capacitor. The material whose nanostructures is to be formed is fitted on the top of the anode in the form of a disc. The hot and dense argon plasma formed during discharge causes the ionization of the material. The material ions along with argon ions move upwards in a fountain like structures and the nanostructures are formed on different substrates which are mounted on the substrate holder and is inserted from the top of the plasma chamber. Kinetic Monte Carlo simulation is being used to explain the formation of such nanostructures.

MWPI 104 III-V Semiconductor Quantum Dots – Plasma-related controls AMANDA RIDER, *The University of Sydney* KOSTYA OSTRIKOV, *CSIRO* IGOR LEVCHENKO, EUGENE TAM, *The University of Sydney* PLASMA NANOSCIENCE TEAM, Binary and ternary III-V semiconductor materials are of great interest for a range of applications. The ability to precisely tailor optoelectronic properties is required for widespread technological implementation of III-V quantum dots (QDs) – this may be achieved through a deterministic level of control over QD size, composition and internal structure during the initial stages of growth. The aim of this paper is to achieve a stoichiometric QD composition at the earliest possible time and to elucidate the benefits of conducting QD growth in a plasma environment. To that end, binary and ternary III-V QD growth is simulated in both neutral- and ionized- gas environments. The impact of using plasma/ion-related effects (via ionizing a portion of the influx and the presence of an Ar background plasma) is taken into account by including substrate heating and a reduction in surface diffusion activation energy. Incorporating plasma-related tools at the beginning of growth affords many advantages – in this work, however, we are predominantly interested in the smaller stoichiometrization times and thus more homogeneous QDs.

MWPI 105 Plasma grown surface bound single wall nanotubes EUGENE TAM, KOSTYA OSTRIKOV, *The University of Sydney* PLASMA NANOSCIENCE TEAM, Many researchers believe that Vertically Aligned Single Wall Carbon Nanotubes (VASWCNTs) are the answer to many foreseen issues with today's semiconducting industry involving miniaturization. However dense arrays of surface bound VASWCNTs can only ascertain a maximum length after which growth seems to halt, something of which is commonly attributed with catalyst poisoning. Nucleation of VASWCNTs also seems to require extremely high temperatures, unsuitable for direct growth of VASWCNTs onto nanoelectronic devices, however there has been some recent experimental evidence that sub 500[r]C growth of VASWCNTs is possible. In this poster, Monte-Carlo simulations have been used to elucidate the effects of plasmas on the substrate and lateral surfaces of the nanotubes, increasing mobility, adsorption and desorption. In addition to surface interactions, plasmas also allow for the control of precursor trajectories allowing adatoms to land closer to the base of the VASWCNT. We show that the precursor distribution along the lateral surface of the nanotubes is the primary cause for the VASWCNTs to slow down and, using appropriate plasma conditions, longer VASWCNTs and growth rates up to an order of magnitude higher than their neutral counter parts can be achieved in plasma environments.

MWP1 106 Plasma deposition of metal catalyst nanoparticles and carbon nanotubes: a KMC study IGOR LEVCHENKO, *The University of Sydney* KOSTYA OSTRIKOV, PLASMA NANOSCIENCE TEAM, In this work, the formation of metal catalyst nanoparticles and growth of carbon nanotubes from a low-temperature plasma environment is studied by kinetic Monte Carlo numerical technique. The numerical simulations were used to model the main surface processes including the carbon diffusion on substrate and nanotube surfaces, metal catalyst saturation with carbon, and formation of the nanotubes on saturated catalyst. We demonstrate that control of the Ni and carbon influxes from plasma provides a very effective control of the surface processes, and eventually results in the formation of arrays of densely-packed metal catalyst nanodots and effective growth of single-wall nanotubes. The use of plasma of higher degree of ionization provides more uniform saturation of metal catalyst nanoparticles with carbon, and thus results in the formation of uniform array of the carbon nanotubes. We also demonstrate that the nano-structured electric fields near the substrate surface covered with growing nanotubes play a very important role in the growth, thus providing an additional effective tool for the growth control.

MWP1 107 Optimizing order in PECVD quantum dot arrays with applications in quantum information MICHAEL DELANTY, *The University of Sydney* KOSTYA OSTRIKOV, CSIRO IGOR LEVCHENKO, *The University of Sydney* STOJAN REBIC, *Macquarie University* PLASMA NANOSCIENCE TEAM, Quantum Dot Arrays (QDAs) are of increasing interest in nano-sized technologies due to their highly tunable optical and electronic properties. Spatially ordered, self organized QDAs are highly sought after in many applications such as lasers, solar cells and photo-detectors. However, current self organized fabrication approaches cannot produce high density spatially ordered QDAs, which has resulted in unwanted line broadening in the QDA spectra. Here we show that it is possible to create dense QDAs that are highly ordered using a plasma based technique. The local ordering parameters introduced take into account the highly confined wavefunctions of quantum dots and have wide application in characterizing experimental QDAs. The Plasma Enhanced Chemical Vapor Deposition (PECVD) model used is a multiscale, hybrid numerical simulation that improves upon previous work by including more realistic surface diffusion processes. The most ordered arrays are then used as the basis of a new type of optical quantum CNOT gate. The performance of this gate is assessed and its dependence on spatial order is demonstrated. This work represents a significant step forward in using PECVD for solid state quantum computing.

MWP1 108 Generation of dynamic metamaterial by using spoof surface plasmon on patterned silicon substrate assisted with microplasma array DAE-SUNG LEE, OSAMU SAKAI, KUNIHIDE TACHIBANA, *Department of Electronic Science and Engineering, Kyoto University, Kyoto-daigaku Katsura, Nishikyo-ku, Kyoto, 615-8510, Japan* KYOTO UNIVERSITY TEAM, Recently, there has been a growing interest in metamaterials which are designed as composite materials and show extraordinary macroscopic properties. Dynamic metamaterials composed of an integrated assembly of microplasma with a 2D periodic structure, whose electron density is 10^{13} - 10^{16} cm⁻³ and spatial

distribution is macroscopically homogeneous and microscopically has a functional structure, have a potential to design the electromagnetic and optical properties of materials for a variety of applications. An array of microplasma cells was fabricated on a silicon substrate, which can not only be partially transparent in the terahertz spectral range but serve as a discharge electrode, and characteristics of a 2D dynamic metamaterial were investigated by terahertz wave time-domain spectroscopy. Such a periodic structure gives rise to an effective impedance or permittivity for surface modes which enables abnormal transmittance arising partly from spoof surface plasmons. In addition, since it is possible to control the generation of microplasmas by external parameters, permittivity of a metamaterial in bulk can be adjusted dynamically.

MWP1 109 Effect of ozone on sterilization of *Penicillium digitatum* using non-equilibrium atmospheric pressure plasma TAKAYUKI OHTA, SACHIKO ISEKI, MASAFUMI ITO, *Wakayama University* HIROYUKI KANO, *NU EcoEngineering Co., Ltd.* YASUHIRO HIGASHIJIMA, *NU System Co., Ltd.* MASARU HORI, *Nagoya University* Methyl bromide has been sprayed to the crops for protecting from insects and virus, but has high ozone depletion potential. Thus, the development of substitute-technology has been strongly required. We have investigated a plasma sterilization for spores of *Penicillium digitatum*, which causes green mold disease of the crops, using non-equilibrium atmospheric pressure plasma. The sterilization was caused by UV light, ozone, O and OH radicals. In this study, ozone density was measured and the effect to sterilization was discussed. The plasma was generated at an alternative current of 6kV and Ar gas flow rate of 3L/min. In order to investigate the sterilization mechanism of ozone, the absolute density of ozone was measured using ultraviolet absorption spectroscopy and was from 2 to 8 ppm. The sterilization by this plasma was larger than that by the ozonizer (O₃:600ppm). It is confirmed that the effect of ozone to the sterilization of *Penicillium digitatum* would be small.

MWP1 110 An Atmospheric Pressure Cold Plasma Plume for Biomedical Applications* XINPEI LU, *College of EEE, Hua-Zhong University of Science & Technology* The roles of various plasma agents in the inactivation of bacteria have recently been investigated. However, up to now, the effect of the charge particles on the inactivation of bacteria is not well understood. In this paper, an atmospheric pressure plasma jet device, which generates a cold plasma plume carrying a peak current of 300 mA, is used to investigate the role of the charge particles in the inactivation process. It is found that the charge particles play a minor role in the inactivation process when He/N₂(3%) is used as working gas. On the other hand, when He/O₂(3%) is used, the charge particles is expected to play an important role in the inactivation of bacteria. Further analysis shows that the negative ions O₂⁻ might be the charge particles that are playing the role. Besides, it is found that the active species including O, O₃, and metastable state O₂^{*}, can play a crucial role in the inactivation of the bacteria. But the excited He*, N₂C³Π_u, and N₂⁺B²Σ_u⁺ have no significant direct effect on the inactivation of bacteria. It is also concluded that heat and UV play no or minor role in the inactivation process.

*Work supported by the Chang Jiang Scholars Program, Ministry of Education, People's Republic of China.

SESSION PR1: FLUOROCARBON PLASMAS I
 Thursday Morning, 16 October 2008; Salon E at 8:00
 Truell Hyde, Baylor University, presiding

Invited Papers

8:00

PR1 1 Study of the ion induced etching for Si and SiO₂ with F⁺ and CF_x(X=1,2,3)⁺ ions.

KAZUHIRO KARAHASHI, *Osaka University*

Dry etching with reactive plasma has been widely used in the fabrication of semiconductors. For the development of integrated semiconductor devices, more precise control of the etching process is required for further progress. It is known that reactive ion species and reactive neutral species, which are produced in plasma, play a great role in etching reactions. However, the mechanism for the etching reaction has not yet been quantitatively described because the individual reactive species cannot be controlled independently in the conventional etching apparatus. It is necessary to clarify the roles of individual reactive ion bombardments and neutral species. A beam experimental method is a very useful tool for investigating the interactions of individual species with surfaces. Thus, we developed a mass-analyzed low-energy ion beam system for investigating the interaction of reactive ion with surfaces. It irradiates analyzed single-species ions onto sample surfaces. The irradiation chamber was maintained in the ultrahigh vacuum condition throughout our experiments. The system has neutral beam sources that independently irradiate a neutral species onto the sample surface. The system can simulate an etching reaction in a plasma environment. To investigate surface reactions for etching processes, we have determined the etching yields by incident ion, detected the scattering species and desorbed products with a differentially pumped rotatable quadrupole mass spectrometer (QMS), and measured surface modification during ion irradiation by X-ray photoelectron spectroscopy. The QMS provided time-resolved measurements and could be synchronized with pulsed ion beam. In the present work, we have investigated etching yields and time of flight distribution and angular distribution of desorption products for Si or SiO₂ by F⁺ and CF⁺ (x = 1-3) ion bombardments which are considered to be the main ion species in fluorocarbon plasmas. These results clearly show that the etching reaction on SiO₂ differs from that on Si surface.

Contributed Papers

8:30

PR1 2 Initial Formation of Carbon Nanowalls Synthesized by Ar Ions and CF_x/H Radicals

SHINGO KONDO, OLIVERA STEPANOVIC, MAKOTO SEKINE, MASARU HORI, *Nagoya University* KOJI YAMAKAWA, SHOJI DEN, *Katagiri Engineering Co., Ltd.* MINEO HIRAMATSU, *Meijo University* Carbon nanowalls (CNWs) consist of graphene sheets standing vertically on the substrate. Due to their unique structures, they have attracted much attentions for various applications. In order to clarify the growth mechanism, in-situ observation of the initial growth stage of CNWs is extremely important. In this study, the new apparatus of CF_x and H radical sources with C₂F₆ and H₂ gases and an Ar ion source was constructed, and in-situ observation on the substrate surface was performed employing a spectroscopic ellipsometer. When a gas flow ratio of H₂ to C₂F₆ was 1:2 with Ar ions accelerated at 200 V at 2.5 Pa, CNWs started to grow in 7 min. The refractive index and the extinction coefficient of the material were approximately 1.3 and 0.2, respectively, and it included voids of more than 80 %. Hence, it was estimated that CNWs had with metallic graphite, which was also confirmed by Raman spectroscopy and SEM. On the basis of these results, the growth mechanism of CNWs is discussed.

8:45

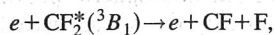
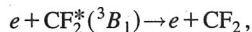
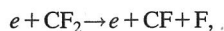
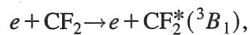
PR1 3 Critical roles of CF₄ and SiCl₄ plasma treatments on AlGaIn/GaN transistor performance

ANIRBAN BASU, IL-ESANMI ADESIDA, *University of Illinois* Advancements of AlGaIn/GaN transistors for high speed and high power applications are tied to realization of high quality gate/ohmic contacts.

Plasma processing of semiconductor surfaces plays a crucial role in the contact formation process. Our findings indicate that plasma treatments of gate and source/drain regions by CF₄ and SiCl₄ plasmas, respectively, affect AlGaIn/GaN transistor performance significantly. The CF₄ plasma incorporates fluorine ions in the AlGaIn epilayer that critically affects the contact barrier height and electron transport in the electron gas at the AlGaIn/GaN interface. Therefore, important metrics such as leakage current, mobility and sheet concentration can be controlled using plasma conditions. The implications of such plasma treatment in affecting the ultimate device performance will be discussed. Results related to plasma induced effects such as creation of defects and diffusion of fluorine will be presented in the context of AlGaIn/GaN transistor performance. The SiCl₄ plasma treatment on AlGaIn/GaN surface is a complex process that triggers multiple competing phenomena such as introduction of defects, creation of vacancies and implantation of ions. Our observation of enhanced mobility and sheet concentration in SiCl₄ plasma treated samples indicate soft ion implantation of silicon. Its implications on ohmic contact formation and other device performances will be discussed.

9:00

PR1 4 On the effect of additional CF₂ scattering data on a CF₄/O₂ plasma etch simulation JAMES J. MUNRO, NATASHA DOSS, JONATHAN TENNYSON, *University College London, Gower Street, WC1E 6BT, UK* SONG-YUN KANG, MASATO KAWAKAMI, SUMIE SEGAWA, *Tokyo Electron Limited, Technology Development Center, 650 Mitsuzawa, Hosaka-cho, Nirasaki-Shi, Yamanashi, Japan 407-0194* An analysis of the effect of adding a number of new CF₂ processes to a CF₄ and a CF₄/O₂ plasma chemistry model is presented. A CF₄ and a CF₄/O₂ capacitively coupled plasma (CCP) etch process is simulated using a zero-dimensional global plasma model. The reaction data is then extended using a new set of electron impact reaction rates for CF₂. Namely,



the addition of which leads to a significant change in the concentration of CF₂. These electron-impact reaction rates are derived from cross-section calculations using Quantemol-N[1]. Measured etch-rates from an equivalent CCP tool are used to validate the model. [1] J. Tennyson et al, *J. Phys.: Conf. Ser.*, 86, 012001 (2007).

9:15

PR1 5 Li⁺ attachment mass spectrometric investigation of high-mass neutral species in the downstream region of Ar/CF₄, Ar/CF₄/O₂ and Ar/CF₄/H₂ plasmas KENJI FURUYA, *Kyushu University* HIROSHI OKUMURA, YUJI TAMAI, AKIHIRO IDE, AKIRA HARATA, KYUSHU UNIV. TEAM, Recently gaseous high-mass species have received significant attentions as important contributors to the nucleation of films and particulates in fluorocarbon plasmas. We have unambiguously identified the gaseous high-mass neutral species in the downstream region of the Ar/CF₄ plasma [1], using the Li⁺ attachment ionization technique that is a fragment-free ionization method. In this report, we show the results of mass analysis of high-mass neutral species in the Ar/CF₄/O₂ and Ar/CF₄/H₂ plasmas as well as Ar/CF₄. In the Ar/CF₄ plasma, we observed C_nF_{2n+2} (n = 2-7) and C_nF_{2n} (n = 4-8) as neutral species. Adding O₂ to the Ar/CF₄ plasma resulted in the intensity decrease of C_nF_{2n+2} and C_nF_{2n}, especially of those with relatively small n values. C_nF_{2n}O (n = 1-7) were newly observed in the Ar/CF₄/O₂ plasma. In contrast, adding H₂ to the Ar/CF₄ plasma resulted in the production of various new compounds, such as C_nF_{2n-2} (n=3-8), C_nF_{2n-4} (n=3-9), C_nF_{2n+1}H (n=1-7), C_nF_{2n-1}H (n=2-8), C_nF_{2n-3}H (n=4-9) and C_nF_{2n-5}H (n=5-9). These species are produced through the abstraction of F from various C_nF_m species by the H radical and the addition of H to them. [1] K. Furuya, S. Yukita, H. Okumura, A. Harata, *Chem. Lett.* 34, 224 (2005).

SESSION PR2: ION ATOM COLLISIONS I

Thursday Morning, 16 October 2008; Salon A-D at 8:00

M. Schulz, Missouri University of Science and Technology, presiding

Invited Papers

8:00

PR2 1 Contemporary theoretical methods to treat atomic processes in gaseous and plasma environments: Heavy particle collisions studied using supercomputers.

DAVID SCHULTZ, *Oak Ridge National Laboratory*

Interactions among photons, electrons, ions, atoms, molecules, and surfaces are ubiquitous within gaseous and plasma environments and their detailed description is fundamental to understanding and controlling these scientifically and technologically important states of matter. Reaching a more accurate and comprehensive knowledge of such atomic processes has been greatly aided by use of contemporary computational resources and through a close interplay with advancing experimental techniques. Following an introduction to atomic processes in gaseous and plasma environments and of methods used to solve the heavy particle collision problem, recent studies will be described which have been enabled by massively parallel computer solutions.

8:30

PR2 2 Electronic Correlation in Ion-Atom Collisions.

JAMES COLGAN, *Los Alamos National Laboratory*

LEWIS FOSTER, *CNA*

In this talk, I will examine the correlated electronic dynamics that occur during single and double ionization of helium by ion impact. A non-perturbative time-dependent close-coupling method (TDCC) is applied to fully describe the interaction between the outgoing ionized electrons. Also, the projectile-atom interaction is constructed as a multipole

expansion that includes monopole, dipole, quadrupole, and octopole terms. Excellent agreement is obtained between our TDCC calculations and experimental measurements for single and double ionization cross sections for antiproton impact of helium. At an impact energy of 1 MeV we find that the double-to-single ionization ratio is twice as large for antiproton impact as for proton impact, confirming a long-standing unexpected experimental measurement. I will also report on our progress towards fully differential cross sections for 6 MeV proton impact double ionization of helium.

Contributed Papers

9:00

PR2 3 Theoretical study on one- and two-electron processes involving capture in ion-Helium collisions TOM KIRCHNER, MYROSLAV ZAPUKHLYAK, *Institut fuer Theoretische Physik der TU Clausthal* Motivated by recent efforts to disentangle the effects of heavy-particle-electron couplings and electron-electron interactions on differential cross sections in ion-atom collisions [1,2] we have carried out a rather comprehensive theoretical study on various one- and two-electron processes that include capture over a broad range of impact energies. The calculations are based on the independent electron model, the two-center basis generator method for orbital propagation, and the eikonal approximation to extract angular-differential cross sections from impact-parameter-dependent transition amplitudes. Selected results for proton, He²⁺, and Ar¹⁵⁺...¹⁸⁺ impact on helium atoms will be presented and compared with experimental and previous theoretical data where available. In general, good agreement with measurements is found, even for shell-specific capture in highly-charged argon impact collisions, for which close-coupling calculations are very demanding. The status of theory will be assessed and future directions will be pointed out. [1] A. Hasan et al., *Phys. Rev. A* **74**, 032703 (2006) [2] M. Zapukhlyak, et al., *Phys. Rev. A* **77**, 012720 (2007)

9:15

PR2 4 Isotope Effects in Ion-Atom Collisions* CHARLES HAVENER, *Oak Ridge National Laboratory* The ion-atom merged-beams apparatus at Oak Ridge National Laboratory is used to measure charge transfer for low energy collisions of multi-charged ions with H and D. The apparatus has been relocated and upgraded to accept high velocity beams from the 250 kV High Voltage Platform at the Multi-Charged Ion Research Facility. Isotope effects for charge transfer processes have recently received increased attention. (Stolterfoht et al, *PRL* **99**, 103201 (2007)). The higher velocity beams allow, for the first time, measurements with both H and D from keV/u down to meV/u collision energies. When charge transfer occurs at relatively large distances (via radial couplings) the ion-induced dipole attraction leads to trajectory effects (Havener et al., *ICPEAC XVII Proceedings*, Brisbane, 1991) causing differences in the charge transfer cross section for H and D. Such a strong isotope effect has now been directly observed for Si⁴⁺ + H(D), but not for N²⁺ + H(D). Strong effects have been predicted in the charge transfer cross section for the fundamental system He²⁺ + H(D, T) (Stolterfoht et al.) at collision energies where charge transfer occurs primarily through united-atom rotational coupling. Currently we are exploring systems where isotope effects in rotational coupling can be measured.

*Work supported by the Division of Chemical Sciences, Office of Basic Energy Sciences, and the Division of Applied Plasma Physics, Office of Fusion Energy Sciences, U. S. DoE under Contract No. DE-AC05-00OR22725 with UT-Batelle, LLC.

SESSION PR3: HIGH PRESSURE DISCHARGES AND LIQUIDS

Thursday Morning, 16 October 2008

Addison Room at 8:00

L. Vuskovic, Old Dominion University, presiding

8:00

PR3 1 Diagnostics of nonequilibrium atmospheric pressure plasma with ultra high electron density for surface cleaning processes HIROTOSHI INUI, YUTO MATSUDAIRA, MASARU HORI, *Nagoya University* NAOFUMI YOSHIDA, *Fuji Machine Mfg. Co., Ltd.* HIROYUKI KANO, *NU Eco-Engineering Co., Ltd.* Surface cleaning process using a nonequilibrium atmospheric pressure plasma has advantage of high throughput, expandability to large-area and nonuse of vacuum system. In this study, the surface modification on a glass substrate by using a nonequilibrium atmospheric pressure plasma was investigated. To characterize the plasma, the gas temperature and electron density were measured using optical emission spectroscopy (OES), and the ground-state atomic oxygen radicals O(³P) were measured by vacuum ultraviolet absorption spectroscopy (VUVAS). Cleaning efficiency was estimated by the contact angle of water droplet on the glass surface after plasma treatment. The cleaning efficiency was increasing with the increasing mixing ratio O₂/(O₂+Ar) to 1%, and then saturated. The cleaning mechanism will be discussed based on the relationship with O(³P) density and gas temperature.

8:15

PR3 2 Diagnostics of Microwave Bubble Plasma in Liquid HIROTAKA TOYODA, HIROYASU SUGIURA, RYOTA SAITO, TATSUO ISHIJIMA, *Nagoya University* Plasma production in the liquid phase has attracted much attention due to its potential applications such as biomedical or environmental processes. As a new technique, we have developed bubble plasma production in liquid with use of pulsed microwave from a slot antenna, and have succeeded in decomposing harmful chemicals such as trichloroethylene (TCE). In this work, optical emission and absorption spectroscopies were adopted to diagnose the microwave bubble plasma. OES result indicated strong OH emission from the plasma, suggesting production of reactive OH radical in the bubble plasma from water vapor. Furthermore, plasma density of the bubble plasma was investigated by time-resolved Stark broadening spectroscopy. To give insight into the reactive species in the liquid phase, plasma-treated water was investigated with UV/VIS optical absorption spectroscopy and a chemical reagent that is sensitive to hydrogen peroxide. From these measurements, existence of hydrogen peroxide in the liquid phase was confirmed.

8:30

PR3 3 Propagation of pulsed discharges in water PAUL CECATO, OLIVIER GUAITELLA, ANTOINE ROUSSEAU, *LPTP, CNRS, Ecole Polytechnique, France* The present discharge is a corona-like filamentary plasma at atmospheric pressure in water. Initiation and discharge propagation have been studied. Pulsed high voltage is applied in a point to plane electrode configuration for submicrosecond duration. In order to monitor the propagation of the discharge two ICCD camera are used with an adjustable delay. The discharge initiates at the positive electrode. A bright spot is formed at the point and can be interpreted as a gas bubble nucleation. Then several plasma filaments propagate radially and simultaneously from the electrode at a constant velocity of 3.5e6 cm/s. No streamer head can be seen even with gate as short as 1ns. After hundreds of nanoseconds branching occurs and the previous filaments become brighter as they supply more current. The propagation velocity does not depend on the applied voltage, the gap and the conductivity of the water. This propagation velocity remains constant during the propagation. The discharge stops when the applied voltage falls below a threshold voltage. The measured propagation velocity is one order of magnitude lower than gas phase streamers.

8:45

PR3 4 GEC Student Award for Excellence Finalist: Creation of Stable Plasma-Liquid Interfaced Reactive Field using Ionic Liquids KAZUHIKO BABA, TOSHIRO KANEKO, RIKIZO HATAKEYAMA, *Department of Electronic Engineering, Tohoku University* The gas-liquid interfacial region which is the boundary between plasmas and liquids, activating physical and chemical reactions, has attracted much attention as novel reactive field in nano-bio material creation. Due to the unique properties of ionic liquids such as their extremely low vapor pressure and high heat capacity, we succeeded in creating the reactive gas (plasmas)-liquid (ionic liquids) interfacial field under a low gas pressure condition, where the plasma ion behavior can be controlled. The effects of plasma ion irradiation on the liquid medium are for the first time quantitatively revealed. In connection with the plasma ion irradiation, the potential structure and optical emission properties of the gas-liquid interfacial plasma are investigated by changing a polarity of the ionic liquid electrode in order to evaluate the ionic liquid-plasma interactions. These results would contribute to systematizing the field of gas-liquid interfacial plasma physics for its applications.

9:00

PR3 5 Properties of plasma-liquid system based on the discharge in gas channel with liquid wall at the ultrasonic cavitation VALERIY CHERNYAK, SERGEY OLSHEWSKII, IRYNA PRYSIAZHNEVYCH, OLENA SOLOMENKO, The influence of the ultrasonic cavitation on the properties of the plasma-liquid system was studied. Discharge in the gas channel formed by airflow immersed into the liquid with microdefects was investigated. Different regimes of the discharge (with and without air) were explored. Optical emission spectroscopy was made of its plasma. Absorption spectra of distilled water after plasma treatment in such system were measured. It was found that presence of ultrasound in the plasma-liquid system during the discharge burning leads to the considerable enhancement of the intensity of main spectral components (hydroxyl band, copper and hydrogen lines). Revealed broadening of H_{α} line in the emission spectra of plasma of the investigated discharge can be connected with presence of cavitation effect in working liquid caused by applied ultrasound. It was shown that all liquids treated at the presence of ultrasound absorb more than those in case without ultrasound. Treated liquids are unstable in a time.

9:15

PR3 6 Diagnostics of plasma reaction fields in supercritical fluid by using micro-Raman spectroscopy TAKA AKI TOMAI, HIROKAZU KIKUCHI, KOYA SAITO, *The University of Tokyo* HIROHARU YUI, *Science University of Tokyo* KAZUO TERASHIMA, *The University of Tokyo* Supercritical fluid (SCF) is a promising medium, which has superior transport properties, such as liquid-like high density and gas-like high diffusivity. Recently, discharge plasma generated in SCF has attracted much attention as extremely high reaction field. In previous study, it was found that carbon nanostructured materials, such as carbon nanotubes, can be synthesized effectively from supercritical CO_2 near the critical point. In this study, to verify the existence of characteristic microstructures of SCF, we diagnose the molecular clustering and density fluctuation in barrier discharge plasma reaction fields by micro-Raman spectroscopy. It was found that the decrease in the density of CO_2 during plasma generation is less than 0.02 g/cm^3 (the critical density of CO_2 : 0.467 g/cm^3), as compared with that in the case of the neat CO_2 , for wide pressure ranges from gaseous to supercritical conditions. Moreover, it was experimentally verified that the density fluctuation observed near the critical point persists in the plasma reaction field. We will present the further detail with the results of other supercritical medium, CHF_3 , in addition to CO_2 , at 61st Gaseous Electronics Conference (GEC).

SESSION QR1: FLUOROCARBON PLASMAS II

Thursday Morning, 16 October 2008; Salon E at 10:00

J-P Booth, LPTP Ecole Polytechnique, France, and MJ Brunger, Flinders University, SA, Australia, presiding

10:00

QR1 1 Control of Fluorocarbon Plasmas for Next-Generation ULSI Devices.

TETSUYA TATSUMI, *Sony Corporation*

Fluorocarbon (C-F) plasma is widely used in the etching of dielectric materials (SiO_2 , Si_3N_4 , and $SiOCH$). Models for controlling C-F plasma [1] and controlling the surface reaction during etching [2] have been proposed. Using these models, good etching results can be obtained after optimizing the absolute densities of reactive species as well as the ion energies. However, next-generation ULSI devices will have smaller pattern sizes, so we need to reduce the pattern-width variation and the degradation thickness of each stacked film to within several nanometers. Even small plasma fluctuations

can severely degrade device properties. Furthermore, the densities of reactive species (CF_x , O, H, etc.) are sensitive to the surface condition of the chamber wall. The etching properties, therefore, can be shifted by changes in chamber parts, dry cleaning, and/or polymer or metal deposition on chamber walls. To suppress fluctuations in etching performance, we need to understand and completely control the plasma-wall reactions. Using an equipment engineering system (EES) is one way to predict plasma conditions in real time. (An EES is a tool for statistical calculation of etching properties that uses all signals from an etching system, such as flow rate, power, capacitance of matching network, etc.) We analyzed results of plasma-wall reactions and improved the prediction method of etch rate fluctuation using an EES. The simultaneous use of a physical model (supported by in-situ signal monitoring of plasma parameters) and a statistical model is promising for suppressing plasma fluctuation in mass production. [1] T. Tatsumi et al, *Jpn. J. Appl. Phys., Part 1* 37 (1998) 2394. [2] T. Tatsumi, *Applied Surface Science*, 253 (2007) 6716.

10:30

QR1 2 New insights into fundamental ion-surface interactions.

MICHAEL GORDON, *University of California - Santa Barbara*

Collisions of ions with surfaces at low energy (< 1 keV) are important in reactive ion etching of semiconductors, dielectrics, and metals. For example, ion bombardment strongly influences etch rates, anisotropy, and selectivity through physical sputtering, momentum-assisted product removal, and modification of reaction rates. Fundamental understanding of these issues requires detailed information about scattering dynamics. We report results from beam scattering experiments involving mass-filtered ions (F^+ and CF_x^+) with tunable energy (50-1000 eV) and high flux off several surfaces (Si, Al, Ag). Topics to be discussed include: (1) electronic excitations in hard collision events (inelastic losses and F^{++} formation); (2) pre-collision fragmentation of CF_x^+ ions which result in fast exit products such as C^+ , F^- , and CF^- ; (3) high yields of fast F^- ; and (4) F_2^- formation via an Eley-Rideal mechanism. For instance, energy losses for single-scatter events of F^+ off Si and Al show that F^{++} can be formed through double electron promotion which "turns-on" above a critical collision energy. Velocity analysis of daughter fragments from CF_3^+ impact on Si and Ag point to projectile fragmentation before the hard collision step. Finally, energy spectra of F^+ , F^- , and F_2^- leaving Si and Ag show three distinct scattering channels: single-scatter binary-like elastic events, another at low energy that cannot be explained as simple sputtering, and still another where fast F_2^- is formed via abstraction. These results illustrate that product species can suffer significant inelastic losses as well as show faster-than-SIMS behavior which may have dramatic effects on profile evolution in plasma etching.

11:00

QR1 3 Electron Scattering from Fluorocarbons and Their Radicals.*

TODD MADDERN, *Flinders University*

In spite of their importance to industry, experimental studies of electron interactions with highly-reactive CF_x radicals are seldom reported in the literature. A crossed electron-molecular beam experiment, featuring a skimmed nozzle beam with pyrolytic radical production, has been used to measure absolute cross sections for electron scattering from the CF_2 molecule. A new technique for placing measured cross sections on an absolute scale is applied for molecular beams formed as skimmed supersonic jets. Absolute differential cross sections for CF_2 are reported for incident electron energies of 3-50 eV and over an angular range of 15-135 degrees. Integral cross sections are subsequently derived from those data. The present data are compared to theoretical predictions for the differential and integral scattering cross sections.

*In conjunction with L. R. Hargreaves, J. Francis-Staite, M. J. Brunger, ARC Centre of Excellence, School of Chemistry, Physics and Earth Sciences, Flinders University, and S. J. Buckman, ARC Centre of Excellence, Australian National University, Australia.

11:30

QR1 4 Molecular dynamics simulations of blanket and small feature etching in fluorocarbon- and fluorine-containing plasmas.

JOSEPH VEGH, *University of California, Berkeley, Dept. of Chem. Eng.*

As device scale-down continues, fundamental understanding of etch mechanisms at very small dimensions (< 10 nm) is becoming increasingly important for the development and control of future plasma processing steps. We utilize molecular dynamics (MD) simulations to examine the interactions of representative plasma species from typical fluorocarbon (FC) and F containing etch systems on Si substrates. Our current MD work examines the etching of very small (< 5 nm) features. By using an amorphous C masking layer (or confined beams of the desired dimension with no masking layer), ions (Ar^+ , CF_x^+) and radicals (CF_x and F) were used to fabricate trenches and holes in Si substrates. The nature and formation of the feature sidewalls are examined in detail, and the limitations of hole size are explored, including the collapse of the masking layer at very small dimensions (~ 2 nm) and the transport of etchants and products into and out of the feature. For the maskless confined beam experiments, etch limitations are primarily transport related as depth increases. In order to maintain pattern transfer fidelity and limit mask collapse, 'pulsed' etching was simulated by alternating bombardment of the surface with CF_x radicals and Ar^+ or Ar^+/F . The chemistries for this scheme were chosen to optimize selectivity between the C mask and the Si substrate. We compare the small feature simulations to our

previous MD studies of blanket etching of Si with various FC/F/Ar⁺ ratios. These simulations established a clear relationship between FC layer thickness and the Si etch yield at steady-state and showed semi-quantitative agreement with plasma experiments in the literature. We discuss how these effects translate to the Si yields in small feature etching, in relation to the surface compositions along the sidewalls and bottoms of the features.

SESSION QR2: ELECTRON IMPACT IONIZATION OF ATOMS AND MOLECULES

Thursday Morning, 16 October 2008; Salon A-D at 10:00

Klaus Bartschat, Drake University, presiding

Invited Papers

10:00

QR2 1 Out of plane (*e,2e*) experiments on helium autoionizing levels.*

N.L.S. MARTIN, *University of Kentucky*

Out-of-plane (*e,2e*) measurements and calculations are reported for the helium autoionizing levels $(2s^2)^1S$, $(2p^2)^1D$, $(2s2p)^1P$, and for direct ionization.¹ We present the data as both angular distributions and energy spectra over the resonances. While the recoil peak almost vanishes in the angular distribution for direct ionization, it remains significant for the autoionizing levels and exhibits a characteristic shape for each orbital angular momentum $L = 0,1,2$. These findings can qualitatively be explained by an L -dependent addition to the ionization amplitude. A first order distorted-wave calculation underestimates the recoil peaks, but a second-order model in the projectile – target interaction can quantitatively reproduce their observed magnitudes. As for the angular distributions a second order theory is necessary to reproduce the experimental energy spectra.

*This work was supported by the United States National Science Foundation under Grant Nos. PHY-0555541.

¹B. A. deHarak, K. Bartschat and N. L. S. Martin, Phys. Rev. Lett. 100, 063201 (2008)

10:30

QR2 2 Recent progress in (*e,2e*) and (*e,3e*) ionisation of small atoms and molecules.

AZZEDINE BENNANI, *LCAM, Bat 351, Université Paris-Sud XI, F-91405 Orsay*

The (*e,2e*) collisions are electron impact ionising processes where the two emerging electrons are fully analysed in energy and momentum and detected in coincidence. The corresponding triple differential cross section (TDCS) has been experimentally and theoretically studied for a wide variety of kinematics and geometries, symmetric or asymmetric, coplanar or non coplanar. See, for example, [1-3] for some reviews. A large body of the published works concerns the ionisation of helium. This has resulted in an increasing and encouraging agreement between theoretical predictions and experimental data for simple targets such as H and He, and has allowed for the exploration of the interaction dynamics in more and more detail. However, the situation does not look as satisfactory for more complex, many-electron atomic targets (not to mention molecular targets) for which the agreement between experiment and theory deteriorates significantly. We will describe new coplanar (*e,2e*) results for ionisation of several noble gases (He, Ne, Ar) [4,5] as well as small molecules (H₂, N₂, CH₄, ...) [6,7], under kinematics which have remained rather unexplored to date and characterised by large energy transfer and close to minimum momentum transfer from the projectile to the target. The experimental results are used as a sensitive test of a number of state-of-the-art available theoretical models for multi-electron atoms or for molecules. In the case of H₂, based on a *direct* comparison between experimental results for He and H₂, we observe [6] an oscillatory pattern which is attributed to the destructive or constructive interference effects due to the scattering from the two H-nuclei. *Keywords:* (*e,2e*); TDCS; Electron impact ionisation; Interference effects [1] Ehrhardt H, Jung K, Knoth G and Schlemmer P 1986 Z. Phys. D: Atoms, Molecules and Clusters 1 3-32 [2] Lahmam-Bennani A 1991 J. Phys. B: At. Mol. Opt. Phys. 24 2401 [3] Weigold E and McCarthy I E 1999 in Electron Momentum Spectroscopy, Kluwer Academic/ Plenum Publishers, New York [4] Catoire F, Staicu Casagrande E M, Nekkab M, Dal Cappello C, Bartschat K and Lahmam-Bennani A 2006 J. Phys. B: At. Mol. Opt. Phys. 39 2827-2838 [5] Naja A, Staicu Casagrande E M, Lahmam-Bennani A, Stevenson M, Lohmann B, Dal Cappello C, Bartschat K, Kheifets A, Bray I and Fursa D V 2008 J. Phys. B: At. Mol. Opt. Phys. 41 in press [6] Staicu Casagrande E M, Naja A, Mezdari F, Lahmam-Bennani A, Bolognesi P, Joulakian B, Chuluunbaatar O, Al-Hagan O, Madison D H, Fursa D V and Bray I 2008 J. Phys. B: At. Mol. Opt. Phys. 41 025204 [7] Naja A, Staicu Casagrande E M, Lahmam-Bennani A, Nekkab M, Mezdari F, Joulakian B, Chuluunbaatar O and Madison D H J 2007 J. Phys. B: At. Mol. Opt. Phys. 40, 3775-3783.

Contributed Papers

11:00

QR2 3 GEC Student Award for Excellence Finalist: Atomic and Molecular Signatures for charged particle ionization*

OLA AL-HAGAN, DON MADISON, *Missouri University of Science and Technology, Rolla, Missouri, USA* CHRISTIAN KAISER, ANDREW MURRAY, *University of Manchester, Manchester, UK* Charged particle ionization of atoms and molecules has been studied over several years and two prominent features are observed for both atoms and molecules – one where the bound electron is ejected in a direction which conserves momentum for a classical projectile-electron collision (the binary peak) and a smaller feature where this electron is ejected in the opposite direction (recoil peak). These conventional studies are all performed in the projectile scattering plane. Here we report results for a plane perpendicular to the conventional plane, and we find two new features – one the same for both atoms and molecules and one completely opposite. Quantum calculations are used to ascribe simple classical descriptions to these features.

*Work Supported by NSF

11:15

QR2 4 Electron impact ionization of the rare gases: neon, argon and xenon*

B. LOHMANN, M.A. STEVENSON, L.R. HARGREAVES, *CAMS, University of Adelaide* K. BARTSCHAT, *Drake University* I. BRAY, D.V. FURSA, *CAMS, Curtin University* A. KHEIFETS, *Australian National University* Detailed information about the electron impact ionization process can be obtained from fully differential cross section measurements, where the outgoing electrons are detected in coincidence. We present experimental and theoretical fully differential cross sections for electron impact ionization of the 2s and 2p orbitals in neon, the 3s and 3p orbitals in argon, and the 5p orbital in xenon, performed at intermediate energies of the incident electron, between 100 and 150 eV. Previous measurements for ionization of argon indicated that there were significant challenges to theory in describing this process, prompting the current extended study of electron impact ionization in this kinematic regime, for different targets. Theoretical calculations have been performed using a distorted wave Born approximation calculation with the inclusion of the Gamow factor (DWBA-G), a hybrid DWBA-R matrix calculation and a convergent close-coupling (CCC) calculation. The agreement between theory and experiment is mixed and appears to be somewhat orbital dependent.

*Support from the Australian Research Council and the United States National Science Foundation is gratefully acknowledged.

11:30

QR2 5 Energy and angle dependent ionization cross sections

for C₆₀ by electron collision SATYENDRA PAL, NEERAJ KUMAR, *Janta Vedic College, Baraut, Baghpat, India* In the present study, we have extended and generalized the previously developed JK semi empirical method [1-2] for the calculation of energy and angle dependent ionization cross sections corresponding to the formation of singly charged ions C₆₀⁺, doubly charged ions C₆₀⁺² and triply charged ions C₆₀⁺³ in electron-C₆₀ collision. The cross sections are made as a function of angle (θ) and the secondary electron energy (W) at constant impact energy E=100 eV. The required oscillator strengths, the major input are used from the recent established experimental measurements of Jaensch and Kamke [3], Reinköster et al. [4] and Berkowitz [5]. [1] S. Pal, Phys.

Scr. 77 (2008) 055304. [2] S. Pal, P. Bhatt, *Chem. Phys.* 326 (2006) 428. [3] R. Jaensch, W. Kamke, *Mol. Mater.*, 13 (2000) 163. [4] A. Reinköster, S. Korica, G. Prümper, J. Viehhaus, K. Godehusen, O. Schwarzkopf, M. Mast, U. Becker, *J. Phys. B: At. Mol. Opt. Phys.*, 37 (2004) 2135. [5] Berkowitz, J., *J. Chem. Phys.* 111 (1999), 1446.

11:45

QR2 6 Total and Total ionization Cross sections for Silicon hydrides SiH_x (x=1-4) and Disilane on electron impact from 0.1 eV to 5 keV*

CHETAN LIMBACHIYA, *P.S. Science College, Kadi (382 715)* MINAXI VINODKUMAR, KIRTI KOROT, *V.P. Science College, V V Nagar* K.N. JOSHIPURA, *Dept. of Physics, S.P. University, V V Nagar* NIGEL MASON, *Dept. of Physics and Astronomy, Open University, MK76AA, UK* Silicon is an important and most widely used element in the semiconductor industry. Silicon hydrides and in particular Silane and Disilane are the most important constituents used frequently in the low temperature plasmas required in the fabrication of microelectronic devices and other semiconducting components. In this paper we report electron impact total cross sections from 0.1 eV to 5 keV for SiH_x (x=1-4) and Si₂H₆. We employed R-matrix method using Quantemol N[1] till 15 eV and spherical complex optical potential formalism (SCOP) [2-3] beyond 15 eV. We also report total ionization cross sections using our Complex Scattering Potential-ionization contribution (CSP-ic) [2,3] for these targets. [1] J. Tenynson, D.B. Brown, J. Munro I. Rozum, H. Varambha, N. Vinci *Journal of Physics: Conference Series* 86 (2007) 012001 [2] M. Vinodkumar, C. Limbachiya, K.N. Joshipura, K. Korot, *Eur. J. Phys. D.* (2008) DOI: 10.1140/epjd/e2008-00106-3 [3] M. Vinodkumar, C. Limbachiya, K.N. Joshipura, K. Korot, Nigel Mason *Int. J. Mass Spectrom* 273 (2008) 145.

*MVK & CGL thank UGC for Major & Minor projects.

SESSION QR3: HIGH PRESSURE GLOW DISCHARGES

Thursday Morning, 16 October 2008

Addison Room at 10:00

Masaru Hori, Nagoya University, Japan, presiding

10:00

QR3 1 Time resolved studies of an industrial scale APGD system processing polymer film*

WILLIAM GRAHAM, DAMIAN DELLA CROCE, LUCAS SCHAPER, *Centre for Plasma Physics, Queens University Belfast, Northern Ireland* ALAN HYNES, LIAM O'NEILL, *Dow Corning Plasma Solutions, Midleton, Ireland* Time-resolved electrical, light emission and imaging characterisation of an industrial scale (1800cm²) atmospheric pressure plasma system operated under conditions which optimise polymer film processing is reported. The electrical and emission behaviour generally associated with uniform discharges i.e. a single discharge event per applied voltage half cycle, is observed at low input (< 500W) powers. As the power and hence applied voltage is increased more, but similar duration, individual discharge events are observed per half cycle until, at > 900W, only about 25% of the applied voltage cycle is free of discharge production. Imaging of the inter-electrode gap shows that, at the peak of each discharge event, crossing the gap there is a uniform layer of emission close to the cathode then evidence of a dark layer and then

further emission but at much reduced intensity. This is the spatial structure associated with glow discharge behaviour. Results with static or moving polymer film in the gap, which are similar, will also be reported. The assistance of B. Twomey and D. Dowling (UC Dublin) is gratefully acknowledged.

*Supported by Dow Corning Plasma Solutions and UK EPSRC.

10:15

QR3 2 Imminent Glow Discharges in Air at Atmospheric Pressure Using Nanosecond Repetitively Pulsed Discharges*

DAVID PAI, DEANNA LACOSTE, CHRISTOPHE LAUX, *Laboratoire EM2C, CNRS UPR288, Ecole Centrale Paris* Many applications for atmospheric pressure air plasmas require non-thermal large-volume low-power plasmas with high chemical reactivity at low gas temperature. The Nanosecond Repetitively Pulsed (NRP) method can generate such plasmas for power budgets much lower than those of traditional generation methods. A diffuse non-thermal plasma regime in air at atmospheric pressure from 300-1000 K has been generated using the NRP method. The discharge develops through an initial streamer, followed by a return wave of potential redistribution. In addition, it is an "imminent" glow discharge, because the field is switched off before ion-electron emission occurs. Thus, the cathode fall of a glow discharge is not formed. Furthermore, at a given gas temperature, there is a minimum gap distance required for the existence of the diffuse regime. This is a result of the non-uniform electric field generated by the pin-pin geometry, creating strongly ionizing regions near the electrodes and a weakly ionizing region between the electrodes, which can inhibit the diffuse-to-filamentary regime transition. As the gas temperature is decreased, the field in the strongly ionizing regions must be increased to maintain sufficient ionization, and the gap distance must be increased for the weakly ionizing region to remain a buffer against the transition.

*This work was supported by the Agence Nationale de la Recherche IPER project.

10:30

QR3 3 Investigations of acustoplasmic phenomenon in air discharge GEVORG HARUTYUNYAN, ARTUR ARAMYAN, GEORGY GALECHYAN, This work is dedicated to the investigations of flashes, which occur in the air discharge under the influence of gas flows. This phenomenon is explained by the following way: making gas flow leads to raising the probability of ionization processes in the discharge. Due to these, the concentration of electrons increases and energy decreases. As a result increases speed of dissociation attachment of oxygen molecules. It is known that this process' probability has resonance origin depending on the electron energy (max. at 6.3 eV). As a result of these processes appear numerous high-excited Rydberg oxygen atoms. During atomic collisions, in the result of quenching atoms accumulate in lower energetic levels (4s, 4d, 3d and 3p), which brings to overpopulation on 3p level. Overcoming of overpopulation threshold leads to superluminescence radiation. In the other experiment, the atmosphere was radiated by acoustic waves. The investigations show that an increment of electromagnetic radiation in the optical and radio ranges was recorded. As a result, a new mechanism of the red sprites' formation can be given, which is conditional with acoustic waves.

10:45

QR3 4 Microwave Discharge in a Supersonic Flow of Simulated Martian Atmospheric Gas*

D.J. DRAKE, S. POPOVIC, L. VUSKOVIC, *Old Dominion University* Martian entry plasma can be considered a high-volume plasma reactor that is sustained by the dissipation of the spacecraft's kinetic energy. It was estimated that several kg of O₂ could be "harvested" during entry. However, the entry plasma parameters vary considerably depending on the spacecraft's trajectory. Probable range of plasma parameters was evaluated using the existing Martian atmospheric data and all recorded probe trajectories. Comparison to the existing simulation facilities is discussed. An alternative desk-top supersonic flow apparatus is devised for the study of aerothermodynamic and chemical properties of a simulated Martian atmospheric gas (SMAG). We performed detailed laboratory measurements of the excited-species populations in the supersonic flow of weakly ionized SMAG. A cylindrical cavity was used to sustain a discharge in SMAG in the pressure range of 100-600 Pa and a stationary acoustic shock wave was generated by an oblique solid body. Excited state populations of Ar and atomic oxygen were measured using absolute emission and absorption spectroscopy. Comparison was made in a model free flow and across the shock front. The gas and electron temperature were determined from the CO rotational spectra and Ar spectra, respectively.

*Supported by NASA LaRC and NASA MSFC.

11:00

QR3 5 Micro-Discharge Scaling and Development from Centimetres to Microns: DC and RF Breakdown and Discharge Characterization around the Paschen Minimum.

PAUL MAGUIRE, *NIBEC, University of Ulster* Joint talk with Z. Lj. Petrovic (Institute of Physics, Belgrade) Two aspects of micro discharges are addressed: The scaling of electrical characteristics and the properties of a recently developed RF micro discharge. We review attempts to measure voltage and current waveforms, Paschen curves and oscillation characteristics of dc and rf discharges from the macroscopic (cm) scale to micro discharges, considering pd values below, at and above the Paschen minimum. Conventional scaling (pd, E/N and jd[2]) are found to be valid for dimensions down to 100 microns, however anomalous Paschen curves are observed below this value and field emission and or long path breakdown are considered as possible explanations. We also present radial profiles estimates for sub mm discharges in an attempt to determine realistic local current densities. In order to explore fundamental discharge mechanisms at reduced scales, we have developed the first radio frequency micro-hollow cathode (RF-MHC) device. This operates stably, for many hours, in neon and in argon. We present measurements performed with a 50 micro metre diameter RF MHC neon discharge. Electron heating modes and information on the electron energy distribution were investigated through electrical and spectroscopic techniques. A number of discharge modes are observed and analysis points to the possibility of pendular electron heating at low voltages. Collaborators: D. Maric, N. Skoro, G. Malovic & M. Radmilovic-Radjenovic (Institute of Physics, Belgrade), C.M.O. Mahony (University of Ulster), WG Graham & T. Gans, (Queen's University Belfast).

11:30

QR3 6 Production of atomic oxygen in an atmospheric pressure arc in air and its implications for NO₂ generation* MATTHEW R. KING, CHRISTOPHER J. OLDHAM, JENNA R. PUCKETT, JEROME J. CUOMO, *Department of Materials Science and Engineering, NC State University* Given the complexities associated with air plasma chemistry, it is important to understand the formation mechanisms of common reaction products such as NO₂. Ground state atomic oxygen (OI) is found to be an indicator of NO₂ formation, as it has been observed that the availability of OI, determined from line emission at 777 nm, has a direct correlation to NO₂ production. In particular, we find a post-discharge reaction involves the consumption of OI for a two-fold increase in NO₂. This work investigates the parameters affecting OI generation in an atmospheric pressure arc in air. In order to fully understand the dynamics of this relationship, we have studied the effect of applied power, frequency, nitrogen to oxygen mixing ratio, and gas temperature on OI emission. The data is also compared to a theoretical kinetic model available in the literature that includes various ionic, neutral, and excited metastable species. This work has implications for all air-based plasma applications, given NO₂ is a ubiquitous, and toxic, byproduct of these discharges.

*This work was funded by the Dean's Office in the College of Engineering and the Department of Materials Science and Engineering

11:45

QR3 7 Multivariate analysis of an Industrial atmospheric pressure glow discharge VICTOR LAW, *Dublin City University* BARRY TWOMEY, JOHN TYNAN, *University College Dublin* NIALL O'CONNOR, *Dublin City University* DENIS DOWLING, *University College Dublin* STEPHEN DANIELS, *Dublin City University* VICTOR LAW TEAM, DENIS DOWLING TEAM, This paper explores the Multivariate Analysis (MVA) of the APGD electrical outputs (non-sinusoidal periodic voltage current waveforms and drive frequency). A Principle Component analysis (PCA) model is used to compress the electrical data for the generation a real-time loading plot. A Lissajous figure projection of the current and voltage waveforms is also used to identify system instabilities and micro-scale events. The purpose the PC-space and phase-space is to provide new coordinate systems where the surface treatment outcomes may be mapped directly. Visual information on the discharge uniformity is also overlaid to aid process interpretation. The complete data acquisition, data compression, and displays are performed in real-time using National Instruments LabVIEW 8.2 software. The results of the MVA demonstrates that a helium discharge, a helium discharges containing 1% oxygen and a helium discharge with hexamethyldisiloxane yields different loading plot scores which allow data-set separation and unique process identification.

SESSION RR1: MATERIAL PROCESSING I
Thursday Afternoon, 16 October 2008
Salon E at 13:30
P. Kothnur, Novellus Systems, Inc, presiding

13:30

RR1 1 Plasma Characterization of MPCVD Discharges for Nanocrystalline Diamond Deposition LEIGH WINFREY, STEVEN SHANNON, *NC State University* RICHARD CHROMIK, *McGill University* KATHRYN WAHL, *Naval Research Laboratory* ROBERT NEMANICH, *Arizona State University* MOHAMED BOURHAM, *NC State University* Carbon forms into many different allotropes that can be useful in deposition of thin films. These forms or phases vary in properties and performance, and the variations are largely due to bonding structure and chemical properties. These properties result from plasma chemistry and environment. This work correlates the plasma deposition environment with surface properties and friction performance of nanocrystalline diamond coatings in a microwave plasma discharge. The plasma characterization was carried out using optical emission spectroscopy of the discharge at various gas mixing ratios in both UV-VIS and VIS-NIR. Examination of the plasma parameters has shown radical and ion formation, which satisfies conditions needed for diamond deposition. Plasma number density and electron temperature vary with plasma composition, they range from $2-4 \times 10^{14} \text{ cm}^{-3}$ and 1-5 eV respectively.

13:45

RR1 2 Nano-particle manipulation using pulse RF discharges with amplitude modulation SHINYA IWASHITA, HIROSHI MIYATA, HIDEFUMI MATSUZAKI, KAZUNORI KOGA, MASAHARU SHIRATANI, *Kyushu University* We have proposed a novel nano-system construction method, which consists of production of nano-blocks and radicals (adhesives) in reactive plasmas, their transport towards a substrate, arrangement of nano-blocks on the substrate [1-3]. For the method, size of nano-blocks is controlled by the duration of pulse RF discharges [1] and their rapid transport towards a substrate is realized using pulse RF discharges with amplitude modulation (AM) of the discharge voltage [2, 3]. During the period of AM nano-blocks can be transported from their generation region near the powered electrode to a substrate at a velocity more than 67 cm/s, which is at least 6 times that after turning off the unmodulated discharges. Such rapid transport needs an asymmetric potential profile, in other words, a large voltage drop across the sheath near the powered electrode. We will report the experimental results and discuss the mechanism of the rapid transport in this presentation. [1] S. Nunomura, et al. *J. Appl. Phys.*, 99, 083302 (2006). [2] K. Koga, et al. *J. Phys. D*, 40, 2267 (2007). [3] M. Shiratani, et al. *Faraday Discuss.*, 138, 127 (2008).

14:00

RR1 3 GEC Student Award for Excellence Finalist: Plasma controlled adatom delivery and (re)distribution: enabling uninterrupted low temperature growth of ultra long vertically aligned carbon nanotubes EUGENE TAM, *The University of Sydney* KOSTYA OSTRIKOV, *CSIRO PLASMA NANOSCIENCE TEAM*, Vertically Aligned Single Wall Carbon Nanotubes (VASWCNTs) are of intense research interest, particularly in nanoelectronics. A major obstacle for VASWCNTs is the limited lengths in which they can be grown. The growth of surface bound VASWCNTs seems to halts after their maximum length is

reached, a phenomena that is commonly attributed to catalyst poisoning. In addition, VASWCNTs generally require very high temperatures and thus the growth of the VASWCNTs is usually performed by separate intermediate steps before attachment to any device. Some experiments have shown that it is possible to grow VASWCNTs at sub 500[r]C and all have been done in plasma environments. We present the results that uses a Monte-Carlo technique to elucidate how plasmas affect the growth of VASWCNTs by controlling the precursor trajectories, substrate heating and changing surface activation and desorption energies. Here we show the precursor distribution along the surface is the primary cause for the VASWCNT growth to slow down and under the same gaseous and substrate conditions, VASWCNTs have a growth rate up to an order of magnitude higher than their neutral counter parts in plasma environments and allow for the growth of longer VASWCNTs.

14:15

RR1 4 Thermal treatment influence on magnetoresistive properties of the MgF₂ - Co and MgF₂ - Permalloy films prepared by thermoelectron sustained vacuum discharge C.P. LUNGU, I. MUSTATA, A. ANGHEL, A.M. LUNGU, O. POMPILIAN, C. POROSNICU, C. TICOS, *National Institute for Laser, Plasma and Radiation Physics* V. KUNCSEK, G. SCHINTEIE, D. PREDOI, *National Institute for Material Physics* A thermoelectron sustained vacuum discharge (TSVD) method was found to be suitable for preparation of films with different relative content of Co in the MgF₂ insulating matrix. Co-MgF₂ and Permalloy-MgF₂ granular films presenting TMR effects were prepared by the simultaneous ignition of plasmas in Co and MgF₂ vapors, respectively. The relative concentrations of the two materials used for deposition depend on the distance between the substrate and the anodes. Morphological, structural and magnetic behaviors were analyzed in as prepared and annealed samples. The influence of the Co content on the magnetic and optical properties of the prepared films was analyzed, in correlation with tunneling magneto-resistance and Kerr effects, respectively. The tunneling magneto-resistance and Kerr effect were found maximal for 20-30% Co content.

14:30

RR1 5 High Aspect Ratio HBr Based Dry Etching of GaInAsP/InP for Nanoscale Photonic Couplers* NAHID SULTANA, WEI ZHOU, DUNCAN MACFARLANE, *The University of Texas at Dallas* Large scale integrated photonics demand nanoscale features that extend deeply into the III-V substrate to cover a propagating mode. The researchers discuss HBr etching of frustrated total internal reflection (FTIR) couplers with feature sizes of approximately 140nm wide by 20 μm long by 3 μm deep in InP. A variety of HBr based chemistries will be benchmarked against more traditional Chlorine based processes. Both FIB and EBL patterned features will be presented with aspect ratios greater than 30:1. Importantly, with HBr, the heterostructures can be etched through with reasonable smoothness at 165 degrees Celsius, and these are beneficial for reliable InP devices.

*This research was supported by DARPA.

14:45

RR1 6 Control of deposition profile of plasma CVD hard carbon films on substrates with trenches MASAHARU SHIRATANI, *Kyushu University, JST, CREST* JUN UMETSU, KAZUHIKO INOUE, TAKUYA NOMURA, HIDEFUMI MATSUZAKI, *Kyushu University* KAZUNORI KOGA, *Kyushu University, JST, CREST* YUICHI SETSUHARA, *Osaka University, JST, CREST* MAKOTO SEKINE, MASARU HORI, *Nagoya University, JST, CREST* We have realized sub-conformal, conformal and anisotropic deposition profiles of Cu in trenches by plasma CVD [1]. Here we report control of deposition profile of carbon films by plasma CVD. Experiments were performed using a H-assisted plasma CVD reactor in which a 28 MHz capacitively-coupled main discharge and a 13.56 MHz inductive-coupled discharge for an H atom source were sustained. Toluene diluted with H₂ was supplied at a flow rate of 90 sccm. The total pressure of reactor was 13 Pa. To study dependence of deposition rate on a ratio of ion flux to radical flux, substrates were covered with a piece of mesh of 10-50 mesh/inch at 1-5 mm above the substrates. Without a mesh the deposition rates at the top, bottom, and sidewall of a trench of the aspect ratio of 1.2 are 20.4, 16.3, and 3.57 nm/min, whereas the corresponding values are 11.7, 9.17, and 3.31 nm/min with a piece of mesh of 14 mesh/inch and 60.8% transparency, set 1 mm above the substrate. The deposition profile can be controlled by the ratio of ion flux to radical flux. [1] K. Takenaka, et al. *Pure Appl. Chem.* **77**, 391 (2005).

15:00

RR1 7 Plasma assisted deposition of metal fluorides for 193nm applications MARTIN BISCHOFF, MAIK SODE, DIETER GAEBLER, NORBERT KAISER, ANDREAS TUENNERMANN, *Fraunhofer IOF Jena* The ArF lithography technology requires a minimization of optical losses due to scattering and absorption. Consequently it is necessary to optimize the coating process of metal fluorides. The properties of metal fluoride thin films are mainly affected by the deposition methods, their parameters, and the vacuum conditions. Until now the best results were achieved by metal boat evaporation with high substrate temperature and without plasma assistance. In fact, it was demonstrated that the plasma assisted deposition process results in optical thin films with high packing density but the losses due to absorption were extremely high for deep and vacuum ultraviolet applications. This paper will demonstrate that most of the common metal fluorides can be deposited by electron beam evaporation with plasma assistance. In comparison to other deposition methods, the prepared thin films show low absorption in the VUV spectral range, high packing density, and less water content. The densification of the thin films was performed by a Leybold LION plasma source. As working gas, a variable mixture of fluorine and argon gas was chosen. To understand the deposition process and the interaction of the plasma with the deposition material, various characterization methods like plasma emission spectroscopy and ion current measurements were implemented.

SESSION RR2: LIGHTING PLASMAS

Thursday Afternoon, 16 October 2008

Salon A-D at 13:30

D. Leonhardt, Fusion UV Systems, Inc., presiding

Contributed Papers

13:30

RR2 1 Phase resolved investigation of the power balance of HID lamp electrodes from low to RF frequency operation

JENS REINELT, MICHAEL WESTERMEIER, JUERGEN MENTEL, PETER AWAKOWICZ, *Ruhr-University of Bochum, Germany* For HID lamps the electrode temperature is a very important parameter since it has a strong influence on the whole discharge. Also the power balance of the lamp is strongly depending on the electrode temperature. For the efficiency of the lamp it is very important to minimize the part of the input power P_{in} which is not transformed into visible light. This part mainly consists of the power input into the electrode plasma sheaths P_{sheath} which is in part dissipated by thermal radiation of the electrodes and in part by heat conduction to the lamp bulb. For dc operation an extensive investigation of these parameters can be found in literature. For ac operation these parameters change since now the heat capacity and the change of the polarity of the electrodes have to be considered. Shown are phase resolved measurements and calculations for various frequencies at the Bochum model lamp of the electrode temperature, the input power, the power loss of the electrodes and the electrode sheath voltage (ESV). Furthermore calculations of the cathode and anode fall voltage U_c and U_a are presented.

Invited Papers

14:00

RR2 3 Continuum Processes in High and Ultra High Pressure Lamps .*J.E. LAWLER, *University of Wisconsin*

The growing use of Ultra High Pressure (UHP) lamps for projection applications has motivated studies of thermal or LTE Hg plasmas in a peculiar region of parameter space. These UHP lamps, which are now commonly found in conference room projectors and large screen TVs, operate with Hg pressures > 200 bar, electron densities $\sim 1.0E18$ / cc, and power densities $> 1.0E5$ W/cc. Such lamps were developed to couple the maximum amount of light into small etendue LCD projection systems. Unlike most other plasmas in similar parts of parameter space, the plasmas in UHP lamps are steady-state. A greater variety of diagnostic techniques and more accurate measurements are possible in UHP lamp plasmas. Continuum processes are much more important in both the opacity and power balance of UHP lamps than they are in typical (< 20 bar) High Intensity Discharge (HID) lamps. Electron + Hg atom bremsstrahlung dominates ($\sim 90\%$) the near IR emission from UHP lamps [1]. Quasi-molecular absorption at > 200 bar yields substantial opacity and results in minimal UV emission from UHP lamps [2, 3]. There are additional physics issues in the 200 bar to 1 kbar range: e.g. (1) spectral line broadening of the few remaining Hg transitions including the breakdown of the single perturber approximation of line broadening theory, (2) free electron continuum processes including the breakdown of the binary collision approximation, and (3) the effect of strong coupling of the plasma on radiative processes. A more quantitative understanding of electron + Hg atom bremsstrahlung in UHP lamps has resulted in a better understanding of near IR losses from widely used, lower pressure metal-halide HID lamps. [1] Lawler JE, Koerber A, and Weichmann U 2005 J. Phys. D: Appl. Phys. 38, 3071. [2] Wharmby D 2008 J. Phys. D: Appl. Phys. in press. [3] Kato M, Kane J, and Lawler JE 2008 J. Phys. D: Appl. Phys. submitted.

*Supported by NSF CTS 0613277.

13:45

RR2 2 Barium transport in fluorescent lamps* F. SIGENEGER, K. RACKOW, D. UHRLANDT, J. EHLBECK, *INP Greifswald, Germany* G. LIEDER, *RLS-M, OSRAM GmbH, Munich, Germany* The transport of barium atoms and ions in the cathode region of fluorescent lamps driven at 25 kHz is studied experimentally and theoretically. The density of Ba atoms and ions have been measured time-resolved by laserinduced fluorescence at different distances from the spot center. Furthermore, the time-dependent cathode fall voltage was approximately determined using an improved band method. The model comprises the solution of the time-dependent particle balance equations of Ba and Ba^+ which include the Ba ionization as gain and loss terms, respectively. The ionization rate coefficient of Ba and the electron density are determined by solving the space-dependent electron Boltzmann equation in spherical geometry using the measured cathode fall voltage and the discharge current as input. Good agreement between the measured and calculated density profiles of barium atoms has been obtained. The results demonstrate the sensitive dependence of the Ba density profiles on the ionization which leads to a strong depletion of the Ba density in the cathode phase of the investigated electrode. The model yields the Ba flux from the cathode which limits the lifetime of the lamp.

*The work was supported by RLS-M, OSRAM GmbH, Munich.

Contributed Papers

14:30

RR2 4 Generation of Transition Probability Data: Can quantity and quality be balanced? J.J. CURRY, C. FROESE

FISHER, *NIST, Gaithersburg, USA* The possibility of truly predictive plasma modeling rests on the availability of large quantities of accurate atomic and molecular data. These include a variety of collision cross-sections and radiative transition data. An example of current interest concerns radiative transition probabilities for neutral Ce, an additive in highly-efficient metal-halide lamps. Transition probabilities have been measured for several hundred lines (Bisson et al., *JOSA B* **12**, 193, 1995 and Lawler et al., unpublished), but the number of observed and classified transitions in the range of 340 nm to 1 μm is in excess of 21,000 (Martin, unpublished). Since the prospect for measuring more than a thousand or so of these transitions is rather low, an important question is whether calculation can adequately fill the void. In this case, we are interested only in electric dipole transitions. Furthermore, we require only that the transition probabilities have an average accuracy of $\sim 20\%$. We will discuss our efforts to calculate a comprehensive set of transition probabilities for neutral Ce using the Cowan (*The Theory of Atomic Structure and Spectra*, 1981) and GRASP (Jönsson et al. *Comput. Phys. Commun.* **176**, 559-579, 2007) codes. We will also discuss our efforts to quantify the accuracy of the results.

14:45

RR2 5 Arguments for increased efficiency of Xe excimer DBDs by pulsed instead of sinusoidal excitation MARK PARAVIA,

KLAUS E. TRAMPERT, MICHAEL MEISSER, WOLFGANG HEERING, *Light Technology Institute, University Karlsruhe* Xenon excimer dielectric barrier discharges are used as VUV sources or as plane light sources with phosphor coating. The plasma efficiency of up to 65% [1] depends on the excitation waveform and rises by pulsed operation compared to sinusoidal excitation. However, loss processes and efficiency gain are not completely known. This is caused by the dielectric barrier prohibiting direct measurement of the plasma power. Here internal plasma power measurements, based on an analog method, are presented for sinusoidal and pulsed excitation. The plasma power can be separated into ignition power during ignition phase and glow phase after ignition. It can be shown that ignition power correlates with the VUV radiation. A comparison of ignition power and glow phase power shows that during ignition the generation of excited Xe atoms is very efficient whereas the glow phase is inefficient in production VUV radiation. Time resolved optical measurements of NIR line radiation of excited xenon atoms show that the discharge is supported during glow phase. Comparing sinusoidal and pulsed excitation, the efficiency gain can be explained by reduced glow phase losses. This is shown and explained experimentally using pulse excitation down to a pulse length of a few hundred ns. [1] Vollkammer, F.; Hitzschke L., WO94/23442, 1994

SESSION SR1: INDUCTIVELY AND CAPACITIVELY COUPLED PLASMAS

Thursday Afternoon, 16 October 2008

Salon E at 16:00

Greg Hebner, Sandia National Laboratories, Albuquerque, NM, presiding

16:00

SR1 1 3-Dimensional Modeling of Capacitively-Coupled Plasmas with Asymmetric Reactor Elements JASON KENNEY,

SHAHID RAUF, KEN COLLINS, *Applied Materials, Inc.* As plasma processing uniformity requirements grow more stringent, there is an increasing emphasis on the characterization of asymmetric reactor elements which may give rise to azimuthal non-uniformities. Experimental analysis of isolated components is difficult, however, providing impetus for the development of a three-dimensional fluid plasma model. In this model, charged species densities are computed by solving continuity equations for all species (using the drift-diffusion approximation) implicitly in time, in combination with the Poisson equation governing the electrostatic fields. The model also includes the full set of Maxwell equations in their potential formulation, Kirchhoff equations for the external circuit, electron temperature from the electron energy equation, and continuity equations for neutral species, along with non-uniform mesh generation. Using this model, we have investigated azimuthally asymmetric components (e.g., slit valve, off-axis plates, misaligned electrodes) with the potential to perturb the plasma density, ion flux, and electric fields and quantified the perturbations using Fourier analysis.

16:15

SR1 2 Comparison between fluid simulations and experiments in inductively-coupled Ar/Cl₂ plasmas EMILIE DESPIAU-

PUJO, *LPTP, Ecole Polytechnique, France* CORMAC S. CORR, *SP3, Australian National University* PASCAL CHABERT, *LPTP, Ecole Polytechnique, France* WILLIAM G. GRAHAM, FERNANDO G. MARRO, *Queen's University Belfast, Northern Ireland* DAVID B. GRAVES, *University of California, Berkeley, USA* Comparisons of 2D fluid simulations with experimental measurements of Ar/Cl₂ plasmas in a low pressure ICP reactor are reported. The electron density, negative ion fraction and Cl atom density are investigated for various conditions of Ar/Cl₂ ratio, gas pressure and applied RF power. Simulations show that the wall recombination coefficient of Cl atom (γ) is a key parameter of the model and that neutral densities are very sensitive to its variations. The best agreement between model and experiment is obtained for $\gamma=0.02$, which is much lower than the value predicted for stainless steel walls ($\gamma=0.6$). This is consistent with reactor wall contaminations classically observed in such discharges. The plasma electronegativity decreases with RF power and increases with Cl₂ content. At high pressure, the power absorption and distribution of charged particles become more localized below the quartz window. Although the experimental trends are well reproduced by the model, the calculated charged particle densities are systematically overestimated by a factor of 3-5. The reasons for this discrepancy are discussed in the paper.

16:30

SR1 3 Electron series resonance in an inductive ion etching reactor HYO-CHANG LEE, JIN-YOUNG BANG, CHIN-WOOK CHUNG, *Electrical Engineering, Hanyang University, Republic of Korea* The electron series resonance at an RF bias substrate was observed in a 13.56 MHz inductively coupled plasma (ICP). As ICP coil power increases, the impedance of the RF bias transits from a capacitive load to an inductive load. When bias voltages and discharge impedances reach minimum values, bias voltages and currents are in-phase at the transition. The transition can be understood as a series LC resonance between sheaths (capacitor) and plasma bulks (inductance due to electron inertia). This corresponds to the electron series resonance (ESR) observed in very high-frequency capacitive discharges, and a new ESR frequency is presented when sheath resistances are considered.

16:45

SR1 4 Electron and Ion Energy Distributions in Dual Frequency Capacitively Coupled Plasmas Considering Wave Effects* YANG YANG, MARK J. KUSHNER, *Iowa State University* Dual frequency, capacitively coupled plasma (DF-CCP) tools typically use a high frequency (tens to hundreds of MHz) to sustain the plasma and a low frequency (a few to 10 MHz) for ion acceleration onto the wafers. Achieving uniform, selective and anisotropic etching depends on one's ability to tailor electron energy distributions (EEDs) in the plasma and ion energy and angular distributions (IEADs) incident on wafers. With an increase in both the high frequency and the wafer size, electromagnetic wave effects must be considered that may produce radial variations in electron heating, effecting the spatial variations in EEDs; and in sheath voltages, that could effect the radial distribution of IEADs. To address these spatial variations, a generalized full Maxwell equation solver has been implemented in a 2-dimensional plasma hydrodynamics model. Using a variation of the Finite-Difference Time-Domain method, multiple frequencies can be resolved. Results will be discussed for the spatial dependence of IEADs and EEDs in DF-CCPs for low frequencies of ≤ 10 MHz and high frequencies up to 200 MHz; and gas pressure of < 10 s mTorr in electropositive and electronegative gas mixtures.

*Work supported by the Semiconductor Research Corp., Tokyo Electron and Applied Materials.

17:00

SR1 5 Separate control of ion flux and energy in capacitively coupled RF discharges via the Electrical Asymmetry Effect* JULIAN SCHULZE, *Ruhr University Bochum* ZOLTAN DONKO, *Hungarian Academy for Science* BRIAN HEIL, UWE CZARNETZKI, *Ruhr University Bochum* Recently a novel approach towards achieving separate control of ion flux and energy in capacitively coupled RF discharges based on the Electrical Asymmetry Effect (EAE) was proposed using fluid models. If the applied voltage waveform contains an even harmonic of its fundamental frequency, the sheaths will not be electrically symmetric. In order to balance electron and ion fluxes at each electrode a DC self bias develops. The self bias and, consequently, the ion energy can be controlled by tuning the phase between the two applied voltages. This technique works in geometrically symmetric and asymmetric discharges. Here the EAE is verified using a PIC simulation of a geometrically symmetric discharge. The self bias is found to be a nearly linear function of the phase angle. If the phase is changed, the ion flux stays constant within 5%, while the self bias reaches values of up to 80% of the applied voltage amplitude and the ion energy is changed by a factor of three. The EAE is investigated at different pressures and electrode gaps with focus on separate control of ion flux and energy.

*Funded by the DFG through SFB591 and GRK1051 and the Hungarian Scientific Research Fund.

17:15

SR1 6 The 2nd Harmonic ECR Microplasma in Narrow Closed Space for Low Pressure Conditions HIROSHI FUJIYAMA, AKIHIRO YUKISHIGE, KE YAN, MASANORI SHINOHARA, *Nagasaki University* TATSUYUKI NAKATANI, *Toyo Advanced Technology* Plasma generation in narrow closed space has been succeeded for the pressure of 0.01Torr and gap length of 500 μ m in xenon gas for the 2nd harmonic Electron Cyclotron Resonance (2nd harmonic ECR). Resonant confinement of electrons at the 2nd harmonic ECR leads to interesting micro plasma characteristics: the higher electron density, the lower plasma potential, the lower electron temperature and the effective power absorption against with the well-known ECR plasma. PIC-MC simulation of low pressure micro plasma supported such interesting plasma characteristics obtained by the experiments and simulations. In the experiments, it was found that the typical micro plasma characteristics: the higher electron density, the lower plasma potential, the lower electron temperature became remarkable. The ionization degree for the 2nd harmonic ECR plasma in the present research, showed about 10^{-3} by 2 order higher than that of PDP micro plasma.

SESSION SR2: ION ATOM/MOLECULE COLLISIONS II
 Thursday Afternoon, 16 October 2008; Salon A-D at 16:00
 T.J. Gay, University of Nebraska, presiding

Invited Papers

16:00

SR2 1 Ion-Impact Induced Ionization of Atoms and Molecules in Single-Pass Experiments and Storage Rings.

DANIEL FISCHER, *Max-Planck-Institut für Kernphysik, Heidelberg*

In the last decade cold target recoil ion momentum spectroscopy (COLTRIMS) and so-called Reaction Microscopes became standard tools to study the dynamics of atomic and molecular break-up processes. They enable to obtain a complete momentum analysis of all final state fragments produced in single collisions with electrons, ions, single photons, or with strong laser fields. In combination with ion storage rings, which provide excellent experimental conditions w.r.t beam intensities and emittances, they represent the ideal tool to obtain highly differential information on fundamental processes like ionization or charge transfer in ion-atom collisions. An overview on recent advances in collision studies in single-pass experiments at the tandem accelerator of the MPI in Heidelberg, at the ion storage ring CRYRING at MSL in Stockholm and the experimental storage ring ESR at the GSI in Darmstadt will be given. With the COLTRIMS setup implemented in CRYRING, single and double electron capture from hydrogen molecules in collisions with protons and He^{2+} -projectiles has been investigated. A variation in the total electron-transfer cross section as function of the molecular orientation has been observed which is attributed to interference in analogy to a Young-type double-slit scenario. Recently, for the first time a fully-equipped Reaction Microscope allowing the momentum-resolved detection of electrons in coincidence with recoil ions was operated in a storage ring, the ESR at GSI in Darmstadt. The results of the first experiments on target ionization and charge transfer in collisions between He, Ne, and Ar targets and highly charged projectiles ranging from 13 AMeV U^{92+} to 400 AMeV Ni^{28+} will be presented.

Contributed Papers

16:30

SR2 2 Fully Differential Cross Sections for Ionization of H_2 by 75 keV Proton Impact*

JASON ALEXANDER, AARON LAFORGE, MICHAEL SCHULZ, ZAAL MACHAVARIANI, RYAN HUPE, UTTAM CHOWDHURY, DON MADISON, *Missouri University of Science & Technology* MARCELO CIAPINA, *MPI Dresden* We have performed fully differential experimental and theoretical studies of single ionization of H_2 by 75 keV proton impact. In the scattering angle dependence of the measured cross sections for fixed electron energies pronounced structures were observed at relatively large angles. These structures are interpreted as an interference resulting from the two-center potential of the molecule. In our theoretical calculations such structures are only found if the interaction between the projectile and the nuclei of the molecule is incorporated. This suggests that the interference pattern originates mostly from indistinguishable diffraction of the projectile wave from the two centers rather than from the ejected electron wave. Furthermore, we found that the interference pattern is consistent with ionization being most likely for an orientation of the molecular axis perpendicular to the projectile beam axis at small scattering angles and parallel to the projectile beam axis at large angles. However, the preferred molecular orientation does

not depend sensitively on the ejected electron energy, which may explain that the observed structures are more pronounced in the scattering angle dependence than in the electron energy dependence.

*Work supported by NSF.

16:45

SR2 3 Four-Body Interactions in Excitation-Ionization

A.L. HARRIS, D.H. MADISON, *Missouri University of Science and Technology* S. BELLM, J. LOWER, E. WEIGOLD, *Australian National University* I. BRAY, D.V. FURSA, *Curtin University of Technology* K. BARTSCHAT, *Drake University* J. COLGAN, *Los Alamos National Laboratory* The process of electron impact excitation-ionization of helium has recently been of interest in order to better understand four body processes. Calculations of the 4 body distorted wave model (4DW) and the 2nd order R-matrix with pseudostates (DWB2-RMPS) model for this process show discrepancies when compared with absolute experiment. The original experimental measurements were presented as cross section ratios for ionization plus excitation relative to ionization without excitation. New cross-normalized experimental data now allow for a comparison of the individual triple-differential cross sections (TDCS) used in the ratios. These experimental results are compared with the 4DW and DWB2-RMPS models, allowing for more accurate investigation into the physics involved in the four body process.

17:00

SR2 4 Double ionization of helium by ion impact assessed using four-body Dalitz plots* MICHAEL SCHULZ, *Missouri University of Science & Technology* MARCELO CIAPPINA, *MPI Dresden* ROBERT MOSHAMMER, DANIEL FISCHER, JOACHIM ULLRICH, *MPI Heidelberg* TOM KIRCHNER, *TU Clausthal* We have performed experimental and theoretical studies of double ionization (DI) of helium by 6 MeV proton impact using a recently developed tool: four-particle Dalitz plots.¹ These plots are basically an extension of conventional Dalitz plots originally introduced in particle physics to analyze three-body fragmentation processes. DI represents a *four-body* fragmentation process and consequently an extra dimension needs to be incorporated. Four-

particle Dalitz plots are very powerful because they enable the representation of multiple differential cross sections as a function of all four fragments in a single spectrum without loss of any part of the total cross section. As a result, the relative importance of the various interactions between the fragments can be studied in great detail. Our results suggest that an uncorrelated DI mechanism, involving two independent interactions of the projectile with both electrons, is significantly more important than previously expected for such fast collisions.

*Work supported by NSF.

¹M. Schulz *et al.*, *J. Phys.* **B22**, 3091 (2007)

SESSION VF1: GLOWS

Friday Morning, 17 October 2008; Salon E at 8:00

R. Dussart, GREMI, CNRS/Universit'e d'Orl'eans, presiding

Invited Papers

8:00

VF1 1 Study of Planar Surface Wave Excited Plasma.CAIZHONG TIAN, *Tokyo Electron Ltd.*

The need for plasma processing has increased as miniaturization in semiconductor manufacturing goes ahead. In these processes, a large-diameter plasma source is required with respect to 300mm wafer size. A Radial Line Slot Antenna (RLSA) driven surface-wave-sustained plasma is a potential best candidate to various applications with respect to damage free process. Many researches focus on the control of plasma density and electron temperature in RLSA technique. However, the plasma stability and uniformity control are less implemented in the practice. In recent years, we study sheath formation and plasma behavior at the interface, where the surface wave propagate, by using electromagnetic particle-in-cell simulation techniques. The simulations include the effects of ionization, and allow us to study the buildup of plasma density associated with ionization in the presence of the large fields of the RF-enhanced sheath. Our results show both the mechanism of plasma generation and heating at the plasma dielectric interface and the strong effect on geometric design of dielectric. Various scenarios are of interest, and help us to design an optimal RLSA driven plasma source, where the plasma stability and uniformity are firmly sustained under the various process conditions. Plasma diagnosis is carried out to reveal the more essential difference in plasma behavior between our RLSA and a custom inductively coupled plasma (ICP) source.

Contributed Papers

8:30

VF1 2 Hybrid modelling of an ac-driven low-pressure He-Xe

lamp discharge DETLEF LOFFHAGEN, FLORIAN SIGENEGGER, *INP Greifswald, Felix-Hausdorff-Str. 2, 17489 Greifswald, Germany* The spatiotemporal evolution of the column plasma of an ac-driven glow discharge in He-Xe mixtures is analyzed by means of hybrid modelling. The theoretical description of the cylindrical, axially homogeneous discharge plasma is based on the coupled solution of hydrodynamic equations for the charge carriers and neutral species in the plasma, equations of the external electric discharge circuit for the determination of the axial electric field, the Poisson equation describing the behaviour of the radial space charge field and the time-dependent, radially inhomogeneous Boltzmann equation providing the transport and rate coefficients of the electrons. Results of the periodic behaviour of the plasma in a discharge tube with a diameter of 18 mm at a gas pressure of 2.5 Torr using a mixture of 98% helium and 2% xenon are discussed. Pronounced structural changes of the particle and flux densities of the different plasma components, the electric field components and the energy distribution of the electrons are found. In particular, the electron energy flux changes between a purely outward directed flux and a partly inward and outward directed one during the period. The comparison with experimental data of discharge voltage and current as well as excited state densities of xenon shows good agreement between calculated and measured data.

8:45

VF1 3 Role of metastable molecules and negative ions in dc and rf oxygen discharges GORDON K. GRUBERT, DETLEF LOFFHAGEN, FLORIAN SIGENEGGER, *INP Greifswald, Felix-Hausdorff-Str. 2, 17489 Greifswald, Germany* For various technological oxygen plasma applications it is supposed that the metastable molecules play a decisive role for the charge carrier production and consequently, the negative ions deform the electric

potential intensely. To analyze the influence of these species, a self-consistent theoretical description for an oxygen discharge between plane electrodes has been performed. A hydrodynamic approach including the continuity equations for the particle densities in addition with the drift-diffusion approximation for the fluxes of all relevant species coupled with Poisson's equation for the determination of the space-charge field has been adapted. The electronic transport and rate coefficients are determined by solving the stationary, spatially homogeneous electron Boltzmann equation in multiterm approximation. The pressure range from 10 to 100 Pa has been investigated for typical dc and rf discharge conditions. It was found that the metastable molecule densities are orders of magnitude smaller than expected and their spatial profiles are similar to diffusion profiles. Furthermore, the influence of the negative ions on the electric potential is found to be negligible. This work is supported by the Deutsche Forschungsgemeinschaft within SFB TR 24.

9:00

VF1 4 Scaling Relationship for Energetic Electron Beams

Propagating in Air* R.F. FERNSLER, S.P. SLINKER, S.G. LAMBRAKOS, *Naval Research Laboratory* Electron beams are the most efficient means for producing plasmas in air and other gases, and unlike discharges, beams ionize gas at rates almost directly proportional to the concentrations of the constituents. In addition, because the beam is responsible for ionization, the temperature of the plasma electrons (which far outnumber the beam electrons) is unusually low. The plasma potential and ion energies at adjoining surfaces are therefore low as well, properties that are important for certain applications. Electron beams are thus unique as a plasma source. Unfortunately, predicting the ionization generated by a beam over its entire range is difficult, and particle codes are usually used to do so. In this work scaling relationships for energy loss and scattering are combined with a particle code to construct a purely algebraic formulation capable of predicting the beam energy deposited in field-free, homogeneous air. This formulation is then combined with a simple fluid model to predict the

plasma density and temperature. By this means, plasmas generated in air can be predicted easily and algebraically at every point in space for beams having an initial energy of several keV or more. Similar models are possible in media other than air.

*Work supported by the Office of Naval Research.

9:15

VF1 5 Effect of Electron Energy Distribution Function on Global Model for High Power Microwave Breakdown at High Pressure* SANG KI NAM, JOHN VERBONCOEUR, *University of California Berkeley* The effect of a wide spectrum of reaction kinetics is very important in high power microwave (HPM) breakdown in molecular gases. However, it is not practical to investigate breakdown including detailed reaction kinetics using particle simulation due to the computational expense. Therefore, a fast volume-averaged global model was developed for the purpose of investigating the effect of reaction kinetics and plasma parameters for multiple species needed to model molecular gases. Since the global model is a fluid-based model, it requires specification of the electron energy distribution function (EEDF). Most global models assume a Maxwellian distribution for the EEDF. The electrons, however, are not in equilibrium unless the electron-electron collision is dominant. The assumption of a Maxwellian EEDF produces inaccurate reaction rate coefficients for the plasma discharge and results in incorrect plasma parameters especially at high pressure. We examine the effect of the EEDF on the global model and develop a method to find the proper approximation of the EEDF to improve fidelity of the prediction of the HPM breakdown at high pressure.

*AFOSR Cathodes and Breakdown MURI04 Grant No. FA9550-04-1-0369.

SESSION VF2: ELECTRON AND ION TRANSPORT IN GASES

Friday Morning, 17 October 2008

Salon A-D at 8:00

Rainer Johnsen, University of Pittsburgh, presiding

8:00

VF2 1 Variation of electron mobility with gas density ARDESHIR BAGHERI, *Imam Hossein University* The density (N) dependence of electron mobility (U) in various dense gases (H₂, N₂, O₂, CO₂ and rare gases) has been calculated. The multiple scattering of electron shifts its kinetic energy and it also changes the distribution function of electrons. This unified approach predicts both the positive (increasing) and negative (decreasing) effects. We have assessed the data on momentum transfer cross-sections by comparing the mobility at very low densities (NU)₀ with those of experimental values. The calculated ratio (NU)/(NU)₀ is compared with the observed values and other theoretical work. The Legler model which assumes constant cross-section is inadequate for predicting the observed density dependence. We obtain good agreement with available experimental work for all the atomic and molecular species studied here.

8:15

VF2 2 Direct Determination of He-O⁺ Interaction Potential from Gaseous Ion Mobility Data AMIR-HOSSEIN JALILI, NASER SEYED-MATIN, *Gas Research Division, Research Institute of Petroleum Industry, Tehran, Iran, P.O. Box: 14857* The analysis of charged particle transport in gases under the influence of electric fields has widespread applications in science and technology ranging from swarms experiments used to determine ion-neutral interaction cross-sections/potentials to plasma chemistry and atmospheric physics. In the last fifty years it has become possible to make accurate measurements of the mobility of trace amounts of ions through a neutral gas over a wide range of the ratio of electric field strength, E, to the neutral gas number density, N. In the 1970s the required theories has developed sufficiently to permit to obtain accurate information about ion-neutral potentials from analysis of such measurements. Here the direct inversion scheme of Viehland and co-workers is used to calculate the interaction potential of He-O⁺ from recently published gaseous ion mobility data for this system. The obtained potential (INVERT potential), which is in good agreement with the ab initio potential of Danailov and co-workers was employed to compute the ion mobility of O⁺ ion in He gas as a function of E/N ratio by the two temperature theory of Viehland and Mason. Results show that the INVERT potential reproduces the ion mobility within experimental accuracy.

8:30

VF2 3 Electron swarm coefficients for H₂O and H₂O-N₂* A.M. JUAREZ, *ICF-UNAM* E. BASURTO, J.L. HERNANDEZ-AVILA, *Universidad Autonoma Metropolitana-A, C.B.I.* J. DE URQUIJO, *ICF-UNAM* We have used a pulsed Townsend technique to measure the electron drift velocity v_e , the density normalized longitudinal diffusion coefficient ND_L , and effective ionization coefficient $(\alpha - \eta)/N$, in water vapour and water vapour-nitrogen mixtures over the density-reduced electric field range E/N , $16-650 \times 10^{-17} \text{ V cm}^2$. The v_e values are in good agreement with previous ones, while those for ND_L agree well with a previous calculation. The limiting value for E/N was found to be $E/N_{lim} = 137 \times 10^{-17} \text{ V cm}^2$. For $E/N < 70 \times 10^{-17} \text{ V cm}^2$, the v_e curves lie below that for pure N₂; however, the 10% H₂O-N₂ curve for v_e shows the trend for negative differential conductivity. The $(\alpha - \eta)/N$ curve for H₂O shows a shallow, negative minimum, in disagreement with a recent measurement using the steady-state Townsend technique. The H₂O-N₂ curves for $(\alpha - \eta)/N$ show a progressively smaller minima, together with a trend to lower values of $(\alpha - \eta)/N$ as the N₂ content in the mixture increases. This research aims to provide a complete set of self-consistent electron swarm parameters for the simulation of flue-gas discharges.

*This work was supported by Projects PAPIIT-UNAM IN 108508 and IN110907.

8:45

VF2 4 Modeling of positron thermalization in collisional traps ANA BANKOVIC, *Institute of Physics, Belgrade, Serbia* JOAN P. MARLER, *University of Aarhus, Aarhus, Denmark* GORDANA MALOVIC, *Institute of Physics, Belgrade, Serbia* STEPHEN J. BUCKMAN, *RSPHYSSE, Australian National University, Canberra, Australia* MILOVAN SUVAKOV, ZORAN LJ. PETROVIC, *Institute of Physics, Belgrade, Serbia* A Monte Carlo code has been used to follow the orbits of positrons thermalizing from approximately 10 eV down to very low energies. This technique is appropriate as positrons suffer only a very few collisions so their transport is fully non-hydrodynamic. We have

studied how the initial energy distribution of a moderated positron beam changes to a low energy, trapped, group of positrons, and which processes contribute to that. We followed how energy and momentum are dissipated in collisions, the thermalization time, the role of the magnetic field, the size of the Larmor radius and geometry of the trap, and how different abundances of gases in the mixture affect the result and other aspects of low energy positron traps. Most importantly in all cases we could sample the efficiency of thermalization by following the losses of positrons due to Ps formation. Complete sets of cross sections covering all major, number, momentum and energy balance processes were included for gases such as Ar, He, H₂, N₂ and N₂/CF₄ mixture. For example our results indicate thermalization times of $Nt = 2.51 \cdot 10^{17} \text{ sm}^{-3}$ for pure nitrogen and $1.41 \cdot 10^{16} \text{ sm}^{-3}$ for N₂/CF₄ mixture.

9:00

VF2 5 Complex interplay of collisional and RF electric/magnetic field effects for electron transport in gases* S. DUJKO, ARC CAMS, MPIT, JCU, Australia & Institute of Physics, Zemun, Serbia R.D. WHITE, K.F. NESS, R.E. ROBSON, ARC CAMS, MPIT, JCU, Australia Advancements in modern day technology associated with non-equilibrium low-temperature magnetized plasma discharges demand the most accurate modeling of the underlying transport processes involved. In this work, the non-equilibrium transport of electrons in gases under the influence of **E** and **B** fields is studied via a unified time-dependent multi term solution of the Boltzmann equation. We will focus on the time-dependent behavior of electron transport properties in ICP discharges where **E** and **B** are RF. We systematically investigate the explicit field effects including field to density ratios, field frequency to density ratio, field phases and field orientations. In addition we will highlight the explicit modification of transport coefficients brought about by attachment/ionization. A multitude of kinetic phenomena were observed that are generally inexplicable through the use of steady-state dc transport theory. Phenomena of significant note include the existence of transient negative diffusivity, time-resolved NDC and anomalous anisotropic diffusion. Most notably, a proposed new mechanism for collisional heating in ICPs has emerged.

*ARC Centres of Excellence program and the MNTR project 14102J

9:15

VF2 6 Experimental Investigation on the Boltzmann Relation for a Bi-Maxwellian Plasma JIN-YOUNG BANG, CHIN-WOOK CHUNG, *Electrical Engineering, Hanyang University, Republic of Korea* The Boltzmann relation is applied to the electron density distribution in plasmas. However, Maxwellian electron distributions are assumed. New Boltzmann relation with bi-Maxwellian electron distributions is derived from the fluid equation and compared with the experimental results in inductively coupled plasma. It is found that the spatial distribution of the electron density is governed by the effective electron temperature and that of the cold and hot electrons is governed by each electron temperature. The increase in the effective temperature around the plasma sheath interface is negligible, thus the effective temperature at the discharge center can be simply used as the temperature in the Boltzmann relation.

SESSION VF3: PLASMA BOUNDARIES

Friday Morning, 17 October 2008

Addison Room at 8:00

Raoul Franklin, The Open University, UK, presiding

8:00

VF3 1 Improvement of a multi-fluid plasma model for the near-cathode region in thermal plasmas* FRANK SCHARF, RALF PETER BRINKMANN, *Ruhr-Universitaet Bochum, Germany* To model and simulate High Intensity Discharge lamps, a proper model for the near-cathode region of thermal plasmas is necessary. Two such models have been presented by the groups around Benilov and Mentel, respectively.^{1,2,3} Both models yield good results for some conditions (defined mainly by differing collision rates), but also non-physical or no results for other conditions. A prominent indicator of the second case is the appearance of super-sonic neutrals. In this contribution a multi-fluid approach incorporating elements from both previous models is presented. In particular, the new model allows for both three body recombination and heavy particle inertia. It thus promises more accurate results over a wider range of physical parameters. Additionally, the new model features a new way to implement the physical boundary conditions numerically. Applying linearization techniques allows a direct, consistent implementation without having to resort to time-consuming shooting methods.¹M. S. Benilov et al., *Proc. GEC2004*, MT1.002²N. A. Almeida et al., *J. Phys. D: Appl. Phys.* **37** (2004) 3107³S. Lichtenberg et al., *J. Phys. D: Appl. Phys.* **38** (2005) 3112*Supported by the DFG within Graduiertenkolleg 1051

8:15

VF3 2 Presheaths are a useful concept; their role in establishing anisotropy at the sheath edge NOAH HERSHKOWITZ,* *Dept. Engineering Physics, UW-Madison, Madison, Wisconsin 53706* GREG SEVERN,† *Dept. Physics, USD, San Diego, California 92110* Presheaths provide ion acceleration to the Bohm velocity. Presheaths are a useful concept for collisionless and weakly collisional plasmas, but their nature and their effects on ions depend on the neutral pressure and the mechanisms of ion production. Presheaths depend on chamber geometry and ion-neutral collisions as the neutral pressure is increased, and cease to be interesting when the collision lengths become comparable to the sheath thickness. They are certainly complicated by the presence of more than one ion species, positive or negative; the question is by how much. At the lowest pressures they affect the spread in the parallel ion velocity distribution function (IVDF), which can be interpreted as the ion "temperature." At higher pressures ion-neutral collisions determine the perpendicular ion temperature as well. This talk will consider modifications to the parallel and perpendicular IVDFs (measured with respect to the normal to wafer surfaces) associated with the presence of presheaths, and will try to make sense of out of lots of apparently contradictory experimental results.

*work funded by DOE grant No. DE-FG02-97ER54437

†work funded by DOE grant No. DE-FG02-03ER54728.

8:30

VF3 3 Experimental studies of transverse metastable ion velocity distribution functions in the presheath of a weakly collisional argon plasma GREG SEVERN,* *Dept. Physics, USD, San Diego CA 92110* DONGSOO LEE, *Dept. Engineering Physics, UW-Madison, Madison, Wisconsin 53706* NOAH HERSHKOWITZ,† *Dept. Engineering Physics, UW-Madison, Madison, Wisconsin 53706* Laser-induced fluorescence (LIF) measurements made with a diode laser have measured the transverse metastable ion velocity distribution function profile near a negatively biased plate in a low temperature ($T_e < 1\text{ eV}$), low pressure ($p_0 < 1\text{ mTorr}$) dc multidipole argon discharge plasma. The metastable argon ions in the $3s^23p^4(3P)3d^4F_{7/2}$ state are found to be characterized by a Maxwellian temperature transverse to the direction normal to the plate. For a neutral pressure of 0.3mTorr, the transverse temperature increases along the presheath from 0.026 eV in the bulk plasma to 0.058 eV at the presheath sheath boundary. This result is compared with PIC code simulations¹ and experimental results² found in the literature.

*work funded by DOE grant No. DE-FG02-03ER54728

†work funded by DOE grant No. DE-FG02-97ER54437

¹A. Meige, *et al.*, *Phys. Plasmas*, 14, 032104 (2007)

²N. Claire, *et al.*, *Phys. Plasmas*, 13, 062103 (2006)

8:45

VF3 4 How is the Bohm criterion satisfied in plasmas with several positive ions MILES M. TURNER, DEREK D. MONAHAN, *Dublin City University, Ireland* Under most conditions, ions entering the sheath at the edge of a plasma satisfy the Bohm criterion. When there are several ions present, the Bohm criterion fails to uniquely determine the speeds with which the ions enter the sheath. Instead it prescribes a locus of possible solutions, and in general, we do not know which solution will be realized. In a generalization of the Tonks-Langmuir model, and in other cases where essentially all ions have the same mean free path, it has been shown that the realized solution is that each ion leaves the plasma with its own Bohm speed, which is to say, with the same kinetic energy. This seems intuitively reasonable, because in such cases one may assert that all the ions reaching the sheath edge have traversed the same potential drop. In this paper, we consider a model in which the ion elastic collision frequency is large compared with the ionization frequency. With this assumption, there is a region adjacent to the sheath where the ion fluxes approaching the sheath may be assumed to be constant, and in this region an analytical solution to the transport equations can be found in which the ion motion is mobility limited. For two ion species, this analytical solution is characterized by two dimensionless physical parameters, which are essentially the ratio of the ion fluxes and the ratio of the mean free paths. In this model, the sheath solution must match this bulk transport solution, and this requirement uniquely determines the manner in which the Bohm criterion is satisfied. In fact, one can realize any and every solution of the Bohm criterion by an appropriate choice of the dimensionless parameters.

9:00

VF3 5 Analytical expression for Child-Langmuir sheath edge around a corner T.E. SHERIDAN, *Ohio Northern University* An expression for the position of the sheath edge around a two-dimensional corner cathode with included angle θ_c has been discovered. This expression is valid in the Child-Langmuir approximation, i.e., $\phi_c \gg kT_e/e$, where $-\phi_c < 0$ is the cathode bias

and T_e is the electron temperature. In polar coordinates (r, θ) , the sheath edge is given by $(r/s_0)\sin[\pi\theta/(2\pi - \theta_c)] = [\pi/(2\pi - \theta_c)]$ where s_0 is the planar sheath width far from the corner. This result is verified by comparison with numerical solutions of Watterson [*J. Phys. D: Appl. Phys.* 22, 1300 (1989)] for a knife edge ($\theta_c = 0$) and a convex square corner ($\theta_c = \pi/2$). The observed agreement suggests that this expression is correct for all corner angles, both convex and concave.

9:15

VF3 6 Langmuir's paradox, wave-particle scattering, and the presheath* SCOTT BAALRUD, JAMES CALLEN, CHRIS HEGNA, *University of Wisconsin-Madison* Langmuir's paradox, perhaps the oldest unsolved mystery of gas discharge physics, is a measurement of anomalous electron scattering near plasma boundaries. In particular, a Maxwellian was reportedly measured much closer to the boundary than the mean free path for electron scattering in a stable plasma; here one should expect truncation of the distribution function corresponding to the sheath potential energy. In this paper we theoretically analyze the presheath region that is present in Langmuir paradox-relevant plasmas ($T_e \gg T_i$). It is shown that the ion-acoustic instability is present throughout the presheath causing amplification of the thermal fluctuations. A collision operator for the plasma kinetic equation including instabilities in a finite space-time domain is derived which shows that the electron collision frequency is dominated by wave-particle interactions in the presheath by up to 3 orders of magnitude. The collision operator satisfies the Boltzmann \mathcal{H} -theorem, so the only equilibrium is a Maxwellian which is achieved at a rate depending on collisionality. Wave-particle scattering shrinks the electron mean free path to within $\sim \text{cm}$ for these discharges showing that one should expect a Maxwellian at the location of the previously reported measurements.

*Supported by NSF GRFP and DoE Grant No. De-FG02-86ER53218.

SESSION WF1: PLASMA DIAGNOSTICS II

Friday Morning, 17 October 2008

Salon E at 10:00

M. Goeckner, The University of Texas at Dallas, presiding

10:00

WF1 1 Origin of electrical changes at plasma etching endpoints MARK SOBOLEWSKI, DAVID LAHR, *National Institute of Standards and Technology* Electrical signals are often used for endpoint detection in plasma etching, but the origins of the electrical changes observed at endpoint are not well understood. Such changes may indicate a difference in plasma electron density caused by changes in the gas-phase densities of etch products and reactants. Alternatively, changes in substrate electrical properties or surface properties (such as work function or secondary electron yields) may be involved. Investigation of these effects was carried out in an inductively coupled reactor equipped with rf bias and a wave cutoff probe, which allows small changes in plasma electron density to be measured with good accuracy and resolution. Simultaneous cutoff probe and electrical measurements were made during CF_4/Ar etches of SiO_2 films on Si substrates. Changes observed in the voltage, current, impedance and phase components at the rf bias frequency were related to, and fully explained by,

changes in electron density. The dc self-bias voltage and harmonic signals showed more complicated behavior. The results allow several conclusions to be drawn about the relative reliability of endpoints obtained from different electrical signals.

10:15

WF1 2 Photon-assisted Beam Probes for Low Temperature Plasmas ALVARO GARCIA DE GORORDO, GARY A. HALLOCK, *The University of Texas at Austin* The Heavy Ion Beam Probe (HIBP) diagnostic has successfully measured the electric potential in a number of major plasma devices in the fusion community. In contrast to a Langmuir probe, the HIBP measures the exact electric potential rather than the floating potential. It is also has the advantage of being a very nonperturbing diagnostic. We propose a new photon-assisted beam probe technique that would extend the HIBP type of diagnostics into the low temperature plasma regime. We expect this method to probe plasmas colder than 10 eV. The novelty of the proposed diagnostic is a VUV laser that ionizes the probing particle. Excimer lasers produce the pulsed VUV radiation needed. These new photo-ionization techniques can take an instantaneous one-dimensional potential measurement of a plasma and are ideal for nonmagnetized plasmas where continuous time resolution is not required, as in plasma processing of semiconductors. It should be noted that the variation of plasma conditions over a wafer surface causes a very problematic non uniformity in the resulting chips.

10:30

WF1 3 Negative Ion Densities and EEDFs in BCl_3/N_2 and BCl_3/SF_6 CCP Plasmas* BOGDAN PATHAK, JOHN ALEXANDER, KAREN NORDHEDEN, *Plasma Research Laboratory, University of Kansas* Previous work has shown that the addition of N_2 or SF_6 to BCl_3 plasmas results in an enhancement of the etch rate of GaAs. Langmuir probe measurements were performed to further investigate this enhancement. The energy distribution functions revealed an increase in negative ion density as N_2 or SF_6 were added to BCl_3 . The negative ion density reaches a maximum near 55% BCl_3 for N_2 mixtures and 40% BCl_3 for SF_6 mixtures. This increase is most likely due to dissociative attachment. The shape of the electron energy distribution function in BCl_3/N_2 mixtures remains relatively unchanged and there is a decrease in the average electron energy with increasing N_2 percentage. Energy transfer from nitrogen metastables appears to be responsible for the increased dissociation in BCl_3/N_2 mixtures. This contrasts with BCl_3/SF_6 mixtures in which the electron density rapidly decreases and the average electron energy sharply increases at low SF_6 percentages, indicating that electron attachment heating is responsible for the enhanced dissociation.

*This work was sponsored by the Air Force Office of Scientific Research (AFOSR)

10:45

WF1 4 Application of an RF Biased Langmuir Probe to Etch Reactor Chamber Matching, Fault Detection and Process Control DOUGLAS KEIL, JEAN-PAUL BOOTH, NEIL BENJAMIN, CHRIS THORGRIMSSON, MITCHELL BROOKS, MIKIO NAGAI, LUC ALBAREDE, JUNG KIM, *Lam Research Corporation* Semiconductor device manufacturing typically occurs in an environment of both increasing equipment costs and per unit sale price shrinkage. Profitability in such a conflicted economic environment depends critically on yield, throughput and cost-of-ownership. This has resulted in increasing interest in improved fault detection, process diagnosis, and advanced process

control. Achieving advances in these areas requires an integrated understanding of the basic physical principles driving the processes of interest and the realities of commercial manufacturing. Following this trend, this work examines the usefulness of an RF-biased planar Langmuir probe¹. This method delivers precise real-time (10 Hz) measurements of ion flux and tail weighted electron temperature. However, it is also mechanically non-intrusive, reliable and insensitive to contamination and deposition on the probe. Since the measured parameters are closely related to physical processes occurring at the wafer-plasma interface, significant improvements in process control, chamber matching and fault detection are achieved. Examples illustrating the improvements possible will be given. ¹J.P. Booth, N. St. J. Braithwaite, A. Goodyear and P. Barroy, *Rev.Sci.Inst.*, Vol.71, No.7, July 2000, pgs. 2722-2727.

11:00

WF1 5 Simultaneous determination of electron density and electron temperature in low-pressure plasmas using the Multipole Resonance Probe* MARTIN LAPKE, THOMAS MUSENBROCK, RALF PETER BRINKMANN, *Ruhr University Bochum* Plasma diagnostics is a highly developed science. In this contribution a diagnostic concept is proposed which enables simultaneous determination of electron density and electron temperature in low-pressure gas discharges, suitable for an industrial setting. The proposed method is robust, calibration free, and economical, and can be used for ideal and reactive plasmas alike. The diagnostic tool – the Multipole Resonance Probe [1] – is a radio-frequency driven probe of particular spherical design which is immersed in the plasma to excite a family of spatially bounded surface resonances. An analysis of the measured absorption spectrum provides information on the distribution of the plasma in the probe's vicinity, from which the values of electron density and electron temperature can be inferred. For an idealized case, the probe consists of two dielectrically shielded, conducting hemispheres which are symmetrically driven by an rf source. The excited resonances can be classified as multipole fields, which allows the analytical evaluation of the measured signal. [1] M. Lapke et al., submitted to *Appl. Phys. Lett.* (2008)

*The work is supported by the Deutsche Forschungsgemeinschaft and the Ruhr University Research School.

11:15

WF1 6 A direct measurement of the energy flux density in plasma surface interaction REMI DUSSART, ANNE-LISE THOMANN, NADJIB SEMMAR, LAURIANNE PICHON, LARBI BEDRA, JACKY MATHIAS, YVES TESSIER, PHILIPPE LEFAUCHEUX, *GREMI PLASMA SURFACE INTERACTION TEAM*, The energy flux transferred from a plasma to a surface is a key issue for materials processing (sputtering, etching . . .). We present direct measurements made with a Heat Flux Microsensor (HFM) in an Ar plasma interacting with the surface of the sensor. The HFM is a thermopile of about one thousand metal couples mounted in parallel. An Inductively Coupled Plasma in Argon was used to make the experiments. Langmuir probe and tuneable laser diode absorption measurements were carried out to estimate the contribution of ions, neutrals (conduction) and metastables. In order to evaluate the ability of the HFM to measure the part due to chemical reactions, a Si surface in contact with the HFM was submitted to an SF_6 plasma. The direct measurements are in good agreement with the estimation we made knowing the etch rate and the enthalpy of the reaction. Finally, tests were performed on a sputtering reactor. Additional energy flux provided by condensing atoms (Pt) was also measured.

11:30

WF1 7 Development of a compact, high energy electron beam source SCOTT WALTON, RICHARD FERNSLER, ROBERT MEGER, *Naval Research Laboratory* The US Naval Research Laboratory is developing a compact, high-energy electron beam source for welding and metal forming applications. The delivery of 1-2 kW over a small surface area is typically sufficient to melt thin metal rods. Thus, beam energies and currents in the range of 25 keV and 50 mA, with a spot size of about 3 mm, are required to deliver this level of power. In this work, we discuss the development of the electron beam source, which operates by extracting electrons from a discharge and then accelerating them to the required energy. To date, we have used a hollow cathode discharge to produce the electrons and a high-voltage wire mesh to accelerate them. We discuss the key attributes of operation and also the possibilities in using different sources and configurations to achieve the desired beam characteristics. This work was supported by the Office of Naval Research and NASA.

11:45

WF1 8 The motion of cathode spots of vacuum arc in removing oxide film on metal surface* ZONGQIAN SHI, SHENLI JIA, LIJUN WANG, QINGJUN YUAN, XIAOCHUAN SONG, *State Key Laboratory of Electrical Insulation and Power Equipment, Xi'an Jiaotong University* The motion of vacuum arc cathode spots has very important influence on the efficiency of removing oxide film on metal surface. In this paper, the characteristics of cathode spots motion are investigated experimentally. Experiments were conducted in a detachable vacuum chamber with AC (50Hz) arc current of 1kA (rms). A stainless steel plate covered by oxide layer was used as cathode. The motion of cathode spots during the descaling process was photographed by a high-speed digital camera with exposure time of 2ms. Experimental results indicate that the motion of cathode spots is influenced by the interaction among individual cathode jets and the position of anode as well as the surface condition.

*This work was supported by NCET (No. 06-0830).

SESSION WF2: RECOMBINATION AND ATTACHMENT
Friday Morning, 17 October 2008; Salon A-D at 10:00
A. Orel, University of California, Davis, presiding

Invited Papers

10:00

WF2 1 Cold electron collisions with atomic and molecular ions in merged beams: high-resolution collision spectroscopy in storage rings.

ANDREAS WOLF, *Max-Planck-Institut for Nuclear Physics, Heidelberg*

Down to the lowest collision energies, free electrons efficiently react with atomic and molecular cations. Atomic ions can bind the colliding electrons by the emission of photons (radiative and dielectronic recombination), while molecular ions are efficiently broken up by slow free electrons without an energy barrier (dissociative recombination). For most atomic and molecular species, the cross sections for recombination and other inelastic cross sections show important resonances reflecting the energetic positions as well as the autoionization and pre-dissociation of quasibound intermediate states formed in the electron collision. High resolution experiments revealing such resonances as well as the underlying atomic and molecular properties and the rich dynamics are performed with merged beams of ions and electrons in ion storage rings, using event-by-event counting and imaging methods. Recently, monochromatic electron impact energies down into the few-meV range have been realized by intense and cold merged electron beams from photocathode sources. Ion beam storage controls the internal vibrational and, to some extent, rotational state of the cation. Fast-beam multiparticle imaging is used to reconstruct the molecular fragmentation events and to monitor the initial ionic ro-vibrational state. Examples of recent measurements with multicharged atomic ions and with smaller molecules, from the hydrogen ions to di- and triatomic heavier species (such as CF^+ and CH_2^+) are presented.

Contributed Papers

10:30

WF2 2 Dissociative recombination of molecular ions in the plasma environment RAINER JOHNSEN, *University of Pittsburgh* The two broad categories of experimental methods that are used to determine rates and products of dissociative recombination, single-collision techniques (e.g. merged beams, storage rings) and plasma techniques (afterglows), sometimes give strikingly differing results, in particular in the case of some polyatomic ions. For instance, the afterglow recombination coefficient for H_3^+ is twice that found in storage rings. Water-cluster ions $H^+(H_2O)_n$ for $n=4$ seem to recombine about eight times faster in afterglows! Neither of the methods necessarily gives "wrong" results but it is

questionable if recombination in the plasma environment is truly a binary process or if third-body interactions play a role. Plasma modelers also face a problem: Should they prefer the recombination coefficients obtained by single-collision methods or those measured in plasmas that are closer to the intended application? Which recombination coefficient applies in the D-region of the ionosphere that is dominated by water clusters? I will critically examine possible three-body mechanisms (l-mixing of Rydberg electrons, complex stabilization by ambient molecules) and estimate the magnitude of their contributions. It appears that some proposed mechanisms seriously overestimate third-body effects unless complex lifetimes are much longer than is indicated by available theory.

10:45

WF2 3 C₂⁻ Formation By Resonant Dissociative Electron Attachment to Acetylene* S.T. CHOUROU, A.E. OREL, *Department of Applied Science, UC Davis* Experimental work on dissociative electron attachment (DEA) of acetylene shows a peak in the cross section at around 8.1 eV corresponding to the formation of C₂⁻ anions. It has been further predicted that these anion fragments result from the decay of a series of Feshbach resonant states with the configurations ²(π_u, 3s²), ²(π_u, 3s3pσ), ²(π_u, 3s3pπ) and ²(π_u, 3p²) between 7 and 9.5 eV. In this work, we perform electron scattering calculations using the Complex Kohn Variational Method to determine the positions and autoionization widths of the Feshbach resonances. We iterate this process for relevant geometries of the molecule to construct the multidimensional complex potential energy surfaces. In order to study the dissociation dynamics leading to the (C₂⁻ + H + H) and (C₂⁻ + H₂) rearrangements, we treat the system in 4D taking into account the stretching and bending of the two C-H bonds of C₂H₂ in an appropriate coordinate system. By computing the flux of the wavepacket into the decoupled asymptotic regions associated with these two rearrangements, we deduce the DEA cross section and compare it to available experimental results.

*We acknowledge support from the National Science Foundation under Grant No. PHY-05-55401 and the U. S. DOE Office of Basic Energy Science, Division of Chemical Science.

11:00

WF2 4 Plasma decay in Air and N₂:O₂:CO₂ mixtures at elevated gas temperatures NICKOLAY ALEKSANDROV, SVETLANA KINDUSHEVA, ILYA KOSAREV, *Moscow Institute of Physics and Technology* ANDREI STARIKOVSKII, *Drexel University* Plasma decay after a high-voltage nanosecond discharge has been studied experimentally and numerically behind an incident and reflected shock wave in high temperature (900 – 3000 K) air and N₂:O₂:CO₂ mixtures for pressures between 0.1 and 2 atm. Time-resolved electron density history was measured by a microwave interferometer for initial electron densities in the range (1-3) × 10¹² cm⁻³. It was shown that the electron density varies in the air afterglow in the "recombination manner," $1/n_e(t) = 1/n_e(0) + \alpha_{eff}t$, where α_{eff} is the effective electron-ion recombination coefficient. A numerical simulation was carried out to describe the temporal evolution of the densities of charged particles under the conditions considered. A good agreement was obtained between the calculated and the measured electron density histories in the air afterglow when taking into account electron attachment to O₂ to form O₂⁻ ions and electron detachment from them, as well as electron-ion and ion-ion recombination. In CO₂-containing mixtures, it was necessary to consider the formation of complex negative and positive ions. These ions were formed in three-body reactions; therefore, the rate of plasma decay increased with gas density.

11:15

WF2 5 Dissociative recombination of CF⁺* VALERY NGAS-SAM, A.E. OREL, *Engr Applied Science, Univ of California Davis* We present results from our recent studies of the dissociative recombination of the CF⁺ ion. Extensive calculations of energy positions and autoionization widths for the doubly excited

states of CF between the first and second ionization thresholds have been obtained from electron scattering calculations using the complex Kohn variational method, followed by calculations of the dissociative recombination process using the time dependent wave packet method. All dissociative states in each molecular symmetry, were included. The resonances leading to dissociation into the product channels will be discussed and the calculated cross sections will be reported and compared to available experiment.

*This work was supported by the U.S. DOE Office of Basic Energy Sciences, Division of Chemical Sciences and the National Science Foundation, PHY-05-55401.

11:30

WF2 6 Electron attachment to SF₆ at high temperatures* T.M. MILLER, J.F. FRIEDMAN, A.A. VIGGIANO, *Air Force Research Laboratory* J. TROE, *Universität Göttingen* We have recently reported flowing-afterglow Langmuir-probe experiments on electron attachment to SF₆, thermal electron detachment from SF₆⁻, and the pressure dependence of the processes involved, in the temperature range 300-670 K, including theoretical analysis of the possible outcomes of the electron-SF₆ interaction, with modeling of the data. One significant result of that work was the finding that the electron affinity of SF₆ is 1.20 ± 0.05 eV.¹ We have now extended the temperature range up to 1300 K. The electron attachment rate constant at 700 K is 1.7 × 10⁻⁷ cm³ s⁻¹ (yielding SF₅⁻ and SF₆⁻ product), and the thermal detachment rate constant for SF₆⁻ is 580 s⁻¹. F⁻ becomes a major ion product at 1000 K and above. We suspect that in this temperature range the SF₆ molecules are decomposing, because the SF₅⁻ ion product disappears above 1100 K, and only the F⁻ ion product remains. Further work must be carried out to determine the origin of the F⁻, whether from decomposition or a surface-ionization effect.

*Supported by AFOSR.

¹A. A. Viggiano et al., *J. Chem. Phys.* 127, 244303, (2007).

11:45

WF2 7 Thermal electron attachment to O₂, NO, N₂O, and Nucleobases EDWARD C. CHEN, EDWARD CHEN, *Baylor College of Medicine* CHEN COLLABORATION, New electron affinities and activation energies for thermal electron attachment for O₂, NO, N₂O and the nucleic acids are presented. These are (in eV): O₂, 1.07(1)/1.05(1); NO, 0.91(1); Guanine(G), 1.645(5); Adenine(A), 1.095(5); Cytosine(C); 1.041(5); Uracil(U) 1.000(5); and Thymine(T) 0.990(5) in agreement with literature values. The electron affinities for the nucleobases support that for Watson Crick AT, 1.40(10) eV and proposed mechanisms for electron conduction and radiation damage and repair and in DNA. Gas phase electron affinities from reduction potentials and voltage onsets for ESR spectra are: (in eV) [2,2] paracyclophane, -0.35(5); 3,3',5,5'-tetra-*t*-butylbiphenyl, -0.05(5); 4,4' di-*t*-butylbiphenyl, -0.02(5) 4,4-dimethylbiphenyl, -0.01(5); 2,3-dimethylnaphthalene, 0.09(5); acenaphthaene, 0.10(5) pyrimidine, 0.35(5); pyradazine, 0.49(5) pyrazine, 0.55(5); s-triazine, 0.64(5); as-triazine, 1.08(5); purine, 1.20(5); s-tetrazine, 1.84(5). Multiple excited state electron affinities including one for N₂O, 0.4(1) eV and activation energies are reported. These are examples of fundamental data that can be obtained from ion molecule reactions in plasmas.

SESSION WF3: COMPUTATIONAL METHODS FOR PLASMAS

Friday Morning, 17 October 2008; Addison Room at 10:00

J.P. Boeuf, LAPLACE, CNRS - University of Toulouse, presiding

*Invited Papers***10:00****WF3 1 Numerical Simulation on the Profile of Plasma and Radicals in Plasma Chambers.**IKUO SAWADA, *Tokyo Electron Limited*

With the dimensions of integrated circuit devices approaching less than 45nm regime, the control of uniformity of plasma and radicals in etching chamber becomes more and more important. In spite of many studies on the capacitively coupled plasma, there had been no matured one which can predict the plasma and radical profiles in a plasma chamber reasonably. Recently, I. Lee et al. [1] proposed a new model to predict the non-uniformity of radial power deposition caused by electromagnetic effects such as standing wave and skin effects. Y. Yang et al. [2] has proposed a coupled solution method between plasma fluid eqs. and Maxwell eqs. to consider both EM and electrostatic effects. In this report, we present some results on our methodology-mix to predict the profile of plasma and radicals comparing with the measured data. The non-uniformity of plasma and radicals are governed by many process and tool parameters like as pressure, gas species, gas flow-rate, frequency and power of RF, configuration of electrodes and wall, solid materials surrounding plasma and so on. From a physical standpoint of view, these parameters change the impedances of plasma or boundary materials and affect some non-linear phenomena among plasma, sheath and boundary materials. Considering these aspects, we developed a several kind of models and methods. One of them is the introduction of a new dimensionless parameter to predict the uniformity of plasma. One of the other is the hybrid method to predict the plasma and radicals profiles by using the two-dimensional numerical simulation models described above. Based on the chemical reaction database either developed by ourselves or obtained in the published papers, we've calculated the profiles of plasma and radicals and compared the calculated electron density profile with the measured one in a mass-production chamber in case of some gases to confirm the good accuracy of the calculation. [1] I. Lee et al. : Plasma Sources Sci. Technol. (17) 2008, p16 [2] Y. Yang et al. : Proceeding of IITC 2008

*Contributed Papers***10:30****WF3 2 Numerical Simulation of Feature Profile Evolution**

PAUL MOROZ, SONG YUN KANG, IKUO SAWADA, *Tokyo Electron Ltd.* During semiconductor processing in plasma reactors, interaction of plasma species with material surfaces results in competing mechanisms of etching and deposition, sometimes strongly depending on energy and angular distribution of incoming fluxes. We present results of feature profile simulations with a new Monte Carlo simulator written in a C++ environment that has a number of advantages. All plasma fluxes are modeled as incoming super-particles with energy and angle varied by a random number generator in correspondence with actual fluxes generated by the plasma code (HPEM[1]). The code also allows setting of incoming fluxes arbitrary to simulate various processes affecting etching and deposition. It runs in real time with iterations at specified time-step, allows consideration of arbitrary number of solid materials and gas species, convenient input of arbitrary initial geometry of the features, and convenient specification of chemistry models. [1] Y. Yang, M.J. Kushner, JVST A25, 1420 (2007).

10:45**WF3 3 Quantitative improvement in MD-based plasma etching simulator: Si etching by halogen-including plasmas**

HIROAKI OHTA, TATSUYA NAGAOKA, AKIRA IWAKAWA, KOJI ERIGUCHI, KOUICHI ONO, *Kyoto University* Classical molecular dynamics (MD) is widely used as a numerical technique to simulate interactions between chemically reactive plasmas and solid materials. Although many MD studies have been published, discussions on the accuracy, capability, and validity are still lacking. Here we focus on simulations of Si etch by HBr/Cl₂ plasmas because this is used in the state-of-art fabrication of gate structures or shallow trench isolators included in SRAMs. In this conference, recent progresses in our simulation technique are reported. First, a Stillinger-Weber-type interatomic potential for Si/H/Br systems was newly developed. Second, we modify its potential form adding a new term partially including multibody interactions, which enabled us to predict thicknesses of reaction layers more accurately. From the analysis of obtained etch yields for cases of Si etch by various ions such as Cl⁺, Cl₂⁺, Br, Br₂⁺, HBr⁺, and H⁺, a new scaling law, which is an extension of Steinbruechel's scaling, were derived. Third, simulations including both high-energy ions and low-energy neutral radicals with high neutral-to-ion flux ratio were performed. The distinct characteristics (monotonically decreasing yield curve as a function of incident angle) in realistic plasma conditions could be reproduced.

11:00

WF3 4 Finite volume formulation of low-temperature plasma equations and numerical solution in one dimension MIRKO VUKOVIC, *Tokyo Electron, U. S. Holdings* Differential transport equations for plasma are most commonly discretized using the finite difference formalism. More recently, discretizations based on the finite element method have also been used. An alternate method is the finite volume method which discretizes the integral conservation equations.¹ This method conserves flux across the

grid cell interfaces. In this presentation, we present the discretization of plasma transport equations based on the finite volume formalism. We will discuss the discretization of the drift-diffusion, momentum, and electron kinetic equations based on this formalism. A one-dimensional problem will be solved for several DC and time-dependent cases.

¹Numerical Heat Transfer and Fluid Flow, Suhas V. Patankar, McGraw-Hill, 1980.

Invited Papers

11:15

WF3 5 3-Dimensional Modeling of Capacitively and Inductively Coupled Plasma Etching Systems.
SHAHID RAUF, *Applied Materials, Inc.*

Low temperature plasmas are widely used for thin film etching during micro and nano-electronic device fabrication. Fluid and hybrid plasma models were developed 15-20 years ago to understand the fundamentals of these plasmas and plasma etching. These models have significantly evolved since then, and are now a major tool used for new plasma hardware design and problem resolution. Plasma etching is a complex physical phenomenon, where inter-coupled plasma, electromagnetic, fluid dynamics, and thermal effects all have a major influence. The next frontier in the evolution of fluid-based plasma models is where these models are able to self-consistently treat the inter-coupling of plasma physics with fluid dynamics, electromagnetics, heat transfer and magnetostatics. We describe one such model in this paper and illustrate its use in solving engineering problems of interest for next generation plasma etcher design. Our 3-dimensional plasma model includes the full set of Maxwell equations, transport equations for all charged and neutral species in the plasma, the Navier-Stokes equation for fluid flow, and Kirchhoff's equations for the lumped external circuit. This model also includes Monte Carlo based kinetic models for secondary electrons and stochastic heating, and can take account of plasma chemistry. This modeling formalism allows us to self-consistently treat the dynamics in commercial inductively and capacitively coupled plasma etching reactors with realistic plasma chemistries, magnetic fields, and reactor geometries. We are also able to investigate the influence of the distributed electromagnetic circuit at very high frequencies (VHF) on the plasma dynamics. The model is used to assess the impact of azimuthal asymmetries in plasma reactor design (e.g., off-center pump, 3D magnetic field, slit valve, flow restrictor) on plasma characteristics at frequencies from 2 – 180 MHz. With Jason Kenney, Ankur Agarwal, Ajit Balakrishna, Kallol Bera, and Ken Collins.

Contributed Papers

11:45

WF3 6 Prediction of SiO₂ etching profile under the presence of RIE-lag effect TAKASHI YAGISAWA, TOSHIKI MAKABE, *Keio University* As the size of ULSI elements shrinks further, functional design for a top-down plasma processing will be strongly required in order to predict and overcome many types of damages induced by plasma etching. The reactive ion etching (RIE) of high-aspect contact hole (HARC) or inter-layer dielectric (ILD) has been traditionally performed by fluorocarbon chemistry under the presence of high-energy ion bombardment in a two-frequency capacitively coupled plasma (2f-CCP) reactor. It is experimentally known as RIE-lag effect that the etching rate at the bottom decreases with increasing the aspect ratio of the pattern. The dependence of etch rate on the aspect ratio will be a crucial issue to be addressed in a top-down plasma nano-processing. In the present study, a feature profile evolution of SiO₂ trench pattern is predicted under competition among etching and polymer deposition by the level-set method. When the etch depth is small, the incident ions are reflected at the sidewall and focused in the center of the trench, resulting in a slight enhancement of the etch rate at the bottom. On the other hand, the geometrical shadowing effect which reduces both ions and radicals striking the bottom surface will be dominant at high aspect ratio. Dependence of RIE-lag on a biasing voltage will also be discussed.

SESSION XF1: MATERIAL PROCESSING II

Friday Afternoon, 17 October 2008

Salon E at 13:30

S.G. Walton, Naval Research Laboratory, presiding

13:30

XF1 1 Evaluation of Plasma Ashing Damages on Porous SiOCH Films by Measurement of H and N Radical Densities HIROSHI YAMAMOTO, KEIGO TAKEDA, MAKOTO SEKINE, MASARU HORI, *Nagoya University* The damage free plasma processes for Low dielectric constant (low-k) films are required for next generation ULSIs devices. Measurement of the radical densities which have a large impact on the damage generation in low-k film is important for clarification of plasma damage mechanism. We built up an *in situ* measuring system to evaluate the properties of low-k films and behavior of radicals. H₂/N₂ ashing plasma damages on porous SiOCH films have been investigated. The surface reactions were measured by using *in situ* Fourier transform infrared reflection absorption spectroscopy and spectroscopic ellipsometry. The H and N radical densities were measured by vacuum ultraviolet absorption spectroscopy. When the flow rate ratios of H₂/(H₂+N₂) for the plasma ashing were changed, the variation of damaged layer thickness agreed well with the H radical density in the plasma. From these result, damages on the porous SiOCH are probably determined by chemical reactions of H radicals which reduce the Si-CH₃ bonds and N radicals which have an effect of inhibition of the damages.

13:45

XF1 2 Threshold energy for plasma etching of high- k dielectric HfO_2 films in BCl_3 -containing plasmas YOSHINORI UEDA, KEISUKE NAKAMURA, HIROAKI KIYOKAMI, HIROAKI OHTA, KOJI ERIGUCHI, KOUICHI ONO, *Kyoto University* Plasma etching of high dielectric constant (k) materials is indispensable for fabricating of future high performance ULSIs. This paper presents the dependence of HfO_2 etch rate on incident ion energy onto a wafer stage, with emphasis being placed on the threshold energy for HfO_2 etching in BCl_3 -containing plasmas. Experiments were performed in both an electron cyclotron resonance (ECR) and an inductively coupled plasma (ICP) reactor by varying the rf bias power, indicating that the threshold in pure BCl_3 plasma was $E_{th} \approx 5\text{--}14$ eV, which is lower than the known $E_{th} \approx 26$ eV previously reported. In addition, the threshold was further lowered by adding O_2 to BCl_3 , where the HfO_2 etch rate was found to increase more significantly with increasing substrate temperature. These imply that the etching was chemically enhanced by O_2 addition to lower the threshold, probably because a small amount of added O_2 reduced the concentration of surface inhibitor species BCl_x and increased the concentration of atomic reactant Cl in the plasma [e.g., $2\text{BCl}_2 + \text{O} \rightarrow \text{BOCl} + \text{BCl} + 2\text{Cl}$]. We also investigated reactant and product species therein by using optical emission spectroscopy and quadrupole mass spectrometry, to discuss the etching mechanisms responsible for HfO_2 etching and their differences in ECR and ICP.

14:00

XF1 3 Etch Challenges Brought by the Metal Hardmask Approach for Advanced Contact Patterning with Fluorocarbon-based Plasma JEAN-FRANCOIS DE MARNEFFE, DANNY GOOSSENS, DENIS SHAMIRYAN, HERBERT STRUYF, WERNER BOULLART, *IMEC v.z.w. 75 Kapeldreef B-3001 Leuven, Belgium* In order to overcome patterning challenges brought by dimensional scaling and aggressive pitches, extreme ultraviolet (EUV) lithography has been recently pushed forward as a possible solution for IC manufacturing, allowing extended exposure latitude at sub-50nm dimensions. This work address the technological solutions used for contact holes patterning by means of EUV lithography. A metal hard-mask (MHM) approach has been selected, in order to combine the etching of high-aspect ratio features with thin EUV photoresist. The pre-metal dielectric stack covering the active fins was composed of 15nm Si_3N_4 as an etch-stop liner, covered by 240nm SiO_2 . The MHM was made of a 30nm TiN film on top of which was spun 20nm of organic underlayer and 100nm of EUV photoresist. This presentation will describe in details the various plasma processing issues and challenges met with this patterning strategy, for down to ~ 50 nm contact hole sizes: SiO_2 :TiN and SiO_2 : Si_3N_4 selectivities by means of fluorocarbon-based chemistries; loading effects; profile and mask undercut control with CCP plasma; residue cleaning.

14:15

XF1 4 Porous Low-k Material Etch For 32 nm and Beyond YIFENG ZHOU, QINGJUN ZHOU, RYAN PATZ, HAIRONG TANG, JEREMIAH PENDER, MICHAEL ARMACOST, *Applied Materials, Inc.* CATHERINE LABELLE, *Advanced Micro Devices* DAVID HORAK, *IBM Research* APPLIED MATERIALS, INC. TEAM, ADVANCED MICRO DEVICES TEAM, IBM RESEARCH TEAM, Porous low-k materials with $k \sim 2.2$ pose new challenges for plasma etch/strip damage, rough etch front/micro-trenching and via faceting are the top issues in ULK all-in-one etch. In this paper, low-k damage has been characterized for both etch and strip. The impacts of etch and strip on ULK etch and dependence of via faceting on plasma conditions and plug height have been studied. Process window of faceting control has also been discussed. It has been demonstrated that all-in-one etch and strip for via first approach can be extended to ULK (2.2) integration.

14:30

XF1 5 ABSTRACT WITHDRAWN

14:45

XF1 6 Control Capabilities of Low-Inductance-Antenna-Driven RF Plasmas for Low-Damage Processing of Polymers* YUICHI SETSUHARA, *Osaka Univ., JST, CREST* KOSUKE TAKENAKA, KEN CHO, *Osaka Univ.* AKINORI EBE, *EMD Corp.* MASAHARU SHIRATANI, *Kyushu Univ., JST, CREST* MAKOTO SEKINE, MASARU HORI, *Nagoya Univ., JST, CREST* Low-damage processing of polymers is of key importance for fabrication of next-generation devices including electronics on polymers, which require development of plasma sources with reduced plasma potential in order to control interface between the polymer substrate and functional films without suffering degradations due to ion bombardment. Furthermore, applications to polymer-based displays and photovoltaic devices require ultra-large area processes at high throughput. To meet these requirements, we have developed plasma processing technologies with low-inductance antenna (LIA) modules to sustain inductively-coupled RF plasmas. Ion energy distributions showed considerably suppressed ion energy as low as 3.8 eV. The polymer surfaces after plasma exposure were analyzed via hard x-ray photoelectron spectroscopy (HXPES) at SPring8 (National SOR facility in Japan), which exhibited nano-surface modification of polymer surface without suffering degradation of molecular structures underneath. Furthermore, plasma-enhanced deposition of silicon films showed low-temperature (200 deg.C) formation of micro-crystalline silicon films due to sufficiently reduced damage during deposition.

*JST, CREST, Global COE program (Material, Osaka Univ.)

15:00

XF1 7 Impact of Wafer Bias in an Inductively Coupled Plasma Reactor PRASHANTH KOTHNUR, ANANTH BHOJ, *Novellus Systems, Inc.* XIAOHUI YUAN, *Esgee Technologies Inc.* LAXMINARAYAN RAJA, *The University of Texas at Austin* Inductively Coupled Plasma (ICP) reactors such as the Novellus SPEED HDP-CVD product enable void-free dielectric deposition in high-aspect ratio trenches for microelectronics fabrication. The physical phenomena involves production of a high-density plasma by the inductive coils and charged species extraction and high-energy impact at the biased wafer surface. The talk will present a simulation study of an ICP discharge in a dome-shaped reactor with different bias voltage waveforms on the wafer surface. The waveforms considered include different shapes (e.g. sinusoidal, triangular) and pulsed bias waveforms. The distribution of species fluxes and Ion Energy Angular Distribution functions at the wafer will be presented. The study will use VizGlow, an unstructured, mixed-mesh plasma simulator. Simulations are performed in two steps. First, the power deposition due to the inductive coils is simulated to steady-state with the assumption of a quasi-neutral plasma with ambipolar transport of charged species in the presence of an unbiased surface. The simulation is subsequently continued in the self-consistent mode using the Poisson equation to determine the electric field in the vicinity of the surface. Secondary power deposition and plasma generation owing to the applied bias is simulated self-consistently.

15:15

XF1 8 The effect of plasmas on the equilibrium shapes of semi-conducting nanocrystals EUGENE TAM, *The University of Sydney* KOSTYA OSTRIKOV, *CSIRO PLASMA NANOSCIENCE TEAM*, Consumer needs drives the electronics market and as consumers require faster computers, chips are required to be miniaturized. There is a physical limit in MOSFETs can be scaled down and alternatives must be presented. Semi-conducting Nanowires (NWs) are a potential candidate in the production of logic gates. The production of NWs is an active research area and a recurring theme that occurs in this area is the fact that the growth conditions affect the morphology of the semi-conducting crystal. There are some papers in which the equilibrium shapes of semi-conducting nanocrystals under various growth conditions is discussed however, few mention the effects of charged surfaces or the presence of a charged fluid affecting the final outcome, despite the fact that plasmas are sometimes present to aid the fabrication of NWs. Here we present the results of our simulations which determine the equilibrium shape of ZnO nanocrystals in the presence of plasmas by considering the surface energy, surface stress and precursor distribution along the surface of the structure and attempt to determine what are the optimum conditions in which NWs can form.

SESSION XF2: CAPACITIVELY-COUPLED PLASMAS

Friday Afternoon, 17 October 2008; Salon A-D at 13:30

D. O'Connell, Queen's University Belfast, presiding

Invited Papers

13:30

XF2 1 Nonlinear Effects on Heating in Capacitive Discharges.*

THOMAS MUSSENBROCK, *Ruhr University Bochum*

In low-pressure capacitive RF discharges two mechanisms of electron heating are dominant: i) Ohmic heating due to electron-neutral collisions and ii) stochastic heating due to momentum transfer from the oscillating sheath. Numerous models have been proposed in order to study electron heating phenomena. However, these models do not account for non-sinusoidal RF currents due to self-excitation of the plasma series resonance. Recently, analytical and numerical calculations of both enhanced Ohmic electron heating and enhanced stochastic electron heating due to nonlinear series resonance excitation have been described. This paper discusses the phenomenon of resonance excitation induced by nonlinear plasma-sheath interaction in capacitive discharges and its effect on electron heating.

*The work is funded by the Deutsche Forschungsgemeinschaft DFG.

Contributed Papers

14:00

XF2 2 The RF Sheath, Nonlinearity and Stochastic heating: An extended analytical approach

MICHAEL KLICK, *Plasmatrix GmbH* For both proper modeling of RF discharges and model-based plasma diagnostics in RF discharges the analysis of the electron heating process is very important. At least at lower pressure, which now more used now in many industrial processes as in the semiconductor manufacturing, the stochastic heating is the dominant electron heating mechanism. The analytic model for the nonlinearity of the RF sheath is based on a series expansion of the

RF potential in the sheath which provides an parametric approach for the description of ion density distribution within the RF sheath. In contrast to established, analytical models, it is not restricted to a sinusoidal RF current. The electron dynamics is described by using the first three moments of the Boltzmann equation. In order to include also here nonlinear effects, harmonics in the RF current are considered as well. Finally the analytic results are discussed in comparison to experimental results of the electron collision rate for momentum transfer in RF discharges. For the comparison, the boundary condition of a sinusoidal RF voltage at the driven electrode is used.

14:15

XF2 3 Effects of Magnetic Field on Very High Frequency Capacitively Coupled Plasma KALLOL BERA, SHAHID RAUF, KEN COLLINS, *Applied Materials, Inc., Sunnyvale, CA* Both electromagnetic and electrostatic effects play important roles in determining the spatial plasma profile in very high frequency (VHF) plasma sources. We investigated the effect of magnetic field on plasma profile for different electromagnet coil configurations, pressure and plasma electronegativity. Our plasma model includes the full set of Maxwell equations. The equations governing the vector potential, A , are solved in the frequency domain for multiple harmonics. The tensor electron transport coefficients depend on the magnetic field. The coupled set of equations governing the scalar potential, and charged species are solved implicitly in time. Plasma simulation results show that radial component of magnetic field inhibits electron transport to the top and bottom electrodes, and modifies electron power deposition. The electron density increases near the wafer edge and decreases near the chamber center as the magnetic field is increased. The plasma current near the chamber center decreases reducing electromagnetic power deposition. The effects of magnetic field on the ion flux and energy have also been investigated.

14:30

XF2 4 Resonance heating of dual frequency capacitive discharges DENNIS ZIEGLER, THOMAS MUSSENBRÖCK, RALF PETER BRINKMANN, *Ruhr University Bochum* The dynamics of dual frequency capacitively coupled plasmas (2f-CCPs) is investigated using an approach that integrates theoretical insight and experimental data. Basis of the analysis is an extended version of a recently published model which casts the high frequency behavior of asymmetric 2f-CCPs in terms of a nonlinear second-order differential equation, or equivalently, a lumped element equivalent circuit [1]. The current work bases the choice of its model parameters on the data obtained by an actual 2f-CCP experiment conducted by Semmler et al. [2]. The analysis shows that the system is governed by a nonlinear interaction of the applied RF with the inner dynamics of the discharge, particularly with the collective oscillation mode known as the plasma series resonance (PSR). With respect to the power dissipation, two distinct paths can be identified which contribute in approximately equal parts. The first path is non-resonant and corresponds to the traditional picture of 2f-CCPs; the second path is resonant and identical with the mechanism of nonlinear electron resonance heating (NERH) proposed in [1,3]. [1] T. Mussenbrock, D. Ziegler, and R.P. Brinkmann, *Phys. Plasmas* 13, 083501 (2006) [2] E. Semmler, P. Awakowicz, and A. von Keudell, *Plasma Sources Sci. Technol.* 16, 839 (2007) [3] T.Mussenbrock and R.P. Brinkmann, *Appl. Phys. Lett.* 88, 151503 (2006).

14:45

XF2 5 Electrode Impedance Effect on Electron Density in a CCP Reactor YOHEI YAMAZAWA, *Tokyo Electron AT LTD.* The generation of harmonics is one of the major nonlinear phenomena in a capacitively coupled plasma. Recently, Mussenbrock and Brinkmann proposed nonlinear electron resonance heating (NERH) model that predict the enhanced Ohmic dissipation caused by the harmonics originated from the series resonance of the plasma bulk and the sheath[1]. In our previous study, we experimentally demonstrated the resonantly growth of the harmonics by tuning a variable capacitor attached to the electrode and clearly

shows that the electrode reactance must be taking into account in the series resonance condition.[2] Here, we focus on the change in electron density caused by the growth of the harmonics. We observed significant increases in electron density as the amplitude of the harmonics grows. We compared the influence of the growth in 3rd and 4th harmonics and found that 4th harmonic has smaller effect on electron density than that of 3rd harmonic has. [1] T.Mussenbrock and R.P. Brinkmann, *Appl. Phys. Lett.* 88, 151503, (2006) [2]Y. Yamazawa, M. Nakaya, M. Iwata and A. Shimizu *Jpn. J. Appl. Phys* 33 (2007) 4335.

15:00

XF2 6 Characteristics of Pulsed Capacitively Coupled Plasma Sources for Plasma Etching ANKUR AGARWAL, PHILLIP STOUT, SHAHID RAUF, KEN COLLINS, *Applied Materials, Inc.* Dielectric etching of high aspect ratio features is susceptible to plasma charging damage giving less than ideal profiles. Charging damage occurs due to charge trapping on sidewall polymer. Tapering and twisting of features can also occur due to randomness in ion/radical flux composition as feature dimensions approach only a few tens of nm. While neutral beam etching and UV photon bombardment help mitigate charging damage, pulsing of a multiple frequency capacitively coupled plasma (CCP) may also allow for control of charging damage if negatively charged species can be extracted from the plasma. Pulsed plasma operation of a multiple frequency CCP reactor in electronegative etching gases is computationally investigated using coupled plasma equipment – feature scale models. Results are compared to continuous plasma operation to assess the consequences on charging of features. Careful tailoring of pulsing at both source and bias frequencies enables negative charge acceleration in the features and helps negate charge buildup. Sustaining a steady pulsed plasma can however be complicated in strongly electronegative gas mixtures as the plasma may not re-ignite after power is turned-off.

15:15

XF2 7 A Parallelized 3D Particle-In-Cell Method With Magnetostatic Field Solver And Its Applications KUO-HSIEN HSU, YEN-SEN CHEN, *National Space Organization, Taiwan* MEN-ZAN BILL WU, JONG-SHINN WU, *National Chiao-Tung University, Taiwan* A parallelized 3D self-consistent electrostatic particle-in-cell finite element (PIC-FEM) code using an unstructured tetrahedral mesh was developed. For simulating some applications with external permanent magnet set, the distribution of the magnetostatic field usually also need to be considered and determined accurately. In this paper, we will firstly present the development of a 3D magnetostatic field solver with an unstructured mesh for the flexibility of modeling objects with complex geometry. The vector Poisson equation for magnetostatic field is formulated using the Galerkin nodal finite element method and the resulting matrix is solved by parallel conjugate gradient method. A parallel adaptive mesh refinement module is coupled to this solver for better resolution. Completed solver is then verified by simulating a permanent magnet array with results comparable to previous experimental observations and simulations. By taking the advantage of the same unstructured grid format of this solver, the developed PIC-FEM code could directly and easily read the magnetostatic field for particle simulation. In the upcoming conference, magnetron is simulated and presented for demonstrating the capability of this code.

Author Index

- A**
- Aanesland, Ane CT3 6,
GW1 3
- Abbate, Sara FTP1 44
- Abdallah, Joe BT1 4
- Abdoullin, Ildar FTP1 21
- Adamovich, Igor BT2 1,
GW3 4
- Adams, S.F. FTP1 12,
FTP1 38, FTP1 65
- Adaniya, Hidehito
FTP1 101
- Adesida, Ilesanmi PR1 3
- Agarwal, Ankur XF2 6
- Akashi, Haruaki MWP1 52
- Akatsuka, Hiroshi FTP1 24,
MWP1 14, MWP1 17
- Al-Hagan, Ola MWP1 7,
QR2 3
- Albarede, Luc WF1 4
- Aleksandrov, Nickolay
GW1 2, WF2 4
- Alexander, Jadon FTP1 109
- Alexander, Jason SR2 2
- Alexander, John WF1 3
- Alikhanov, A.I. MWP1 77
- Allan, Michael LW2 6
- Allegraud, Katia MWP1 55
- Altevogt, S. FTP1 100
- Alvarez, R. MWP1 41
- Alves, L.L. MWP1 41,
MWP1 42
- Amorim, Jayr MWP1 46
- Anderson, Tyler FTP1 62
- Anderson, W. Kyle ET1 6
- Anghel, A. RR1 4
- Aramaki, M. FTP1 68
- Aramyan, Artur QR3 3
- Armocost, Michael XF1 4
- Awakowicz, Peter
MWP1 43, MWP1 68,
MWP1 83, RR2 1
- Aziznia, Amin FTP1 61
- B**
- Baalrud, Scott VF3 6
- Baba, Kazuhiko PR3 4
- Babaeva, Natalia Yu.
CT3 1, FTP1 43
- Baby, A. MWP1 21
- Baeva, Margarita FTP1 25,
FTP1 26, FTP1 27,
FTP1 83
- Baghalha, Morteza FTP1 61
- Bagheri, Ardeshir VF2 1
- Bahrim, Cristian FTP1 108
- Bang, Jin-Young SR1 3,
VF2 6
- Bankovic, Ana VF2 4
- Barnat, Ed FTP1 59
- Bartschat, Klaus FTP1 89,
LW2 3, LW2 6, QR2 4,
SR2 3
- Basak, A.K. MWP1 3
- Basner, R. MWP1 80
- Basu, Anirban PR1 3
- Basurto, E. VF2 3
- Bauville, G. DT2 1
- Becker, Kurt FTP1 67,
MWP1 100
- Becker, Markus MWP1 58
- Bedra, Larbi WF1 6
- Begum, Asma LW1 1
- Belkacem, Ali FTP1 101
- Bellm, S. SR2 3
- Belostotskiy, Sergey CT1 4
- Belousov, Maxim FTP1 11
- Benedikt, Jan MWP1 76
- Benjamin, Neil WF1 4
- Bennani, Azzedine QR2 2
- Bentounes, Jounayd
MWP1 72
- Bera, Kallol XF2 3
- Berg, M.H. FTP1 100
- Bergner, Andre MWP1 65
- Bettega, M.H.F. MWP1 5
- Bhoj, Ananth LW1 8,
XF1 7
- Bienholz, Stefan MWP1 43,
MWP1 83
- Bing, D. FTP1 100
- Bischoff, Martin RR1 7
- Blessington, J.C. FTP1 65
- Boeuf, Jean-Pierre GW1 1
- Boffard, John B. FTP1 70
- Bogaerts, Annemie ET1 3,
MWP1 53, MWP1 76
- Bogdanov, Eugene FTP1 53
- Boisse-Laporte, C.
MWP1 41, MWP1 42
- Booth, Jean-Paul FTP1 39,
WF1 4
- Boullart, Werner XF1 3
- Bourdon, A. GW3 2
- Bourham, Mohamed RR1 1
- Bowman, Angela DT2 7
- Bozorgzadeh, Hamid Reza
FTP1 61
- Braithwaite, Nicholas
MWP1 91
- Brake, Mary L. FTP1 22
- Bravenec, Ronald
MWP1 59, MWP1 81
- Bray, I. LW2 5, MWP1 7,
QR2 4, SR2 3
- Brinkmann, R.P. FTP1 52
- Brinkmann, Ralf Peter
FTP1 33, MWP1 43,
MWP1 73, MWP1 83,
MWP1 84, MWP1 85,
MWP1 86, VF3 1, WF1 5,
XF2 4
- Broc, Alain FTP1 44
- Brok, Wouter ET1 3,
MWP1 53
- Brooks, Mitchell WF1 4
- Brown, Daniel B. FTP1 20
- Bruggeman, Peter
MWP1 54
- Bruzzese, John GW3 4
- Buckman, Stephen CT2 2,
FTP1 94, LW2 2, LW2 7,
VF2 4
- Buhr, H. FTP1 100
- Buzzi, Frank DT1 2
- C**
- Callen, James VF3 6
- Caradonna, Peter FTP1 94,
LW2 2
- Carrere, Marcel MWP1 72,
MWP1 74
- Cartry, Gilles DT1 1,
MWP1 72, MWP1 74
- Ceccato, Paul PR3 3
- Celestin, S. GW3 2
- Chabert, Pascal CT3 6,
GW1 3, MWP1 71, SR1 2
- Chae, Heeyeop FTP1 5,
FTP1 16
- Chang, Haegyoo FTP1 5
- Chatterjee, Barun MWP1 13
- Chen, Degui FTP1 29
- Chen, Edward WF2 7
- Chen, Edward C. WF2 7
- Chen, Francis F. CT3 5
- Chen, Lee MWP1 59,
MWP1 81
- Chen, Yen-Sen XF2 7
- Cheng, Qijin FTP1 14
- Chernyak, Valeriy PR3 5
- Chiavarini, Robert L. DT2 7
- Cho, Jin Hoon CT1 3,
DT2 5
- Cho, Ken XF1 6
- Choi, B. MWP1 89
- Choi, Ikjin FTP1 7,
FTP1 79
- Choi, Myung-Sun FTP1 73
- Chourou, S.T. WF2 3
- Chowdhury, Uttam SR2 2
- Chromik, Richard RR1 1
- Chua, Bishuang FTP1 14
- Chung, Chin-Wook FTP1 7,
FTP1 8, FTP1 9, FTP1 74,
FTP1 75, FTP1 76,
FTP1 79, SR1 3, VF2 6
- Chung, Kyu-Sun FTP1 71
- Churkin, Dmitry GW3 5
- Chwirot, Stanislaw LW2 4
- Ciappina, Marcelo
MWP1 9, SR2 2, SR2 4
- Clark, Robert W. MWP1 6
- Clifford-AzizKhan, Jane
DT2 4
- Colgan, J. BT1 4, SR2 3
- Collins, George CT1 3,
DT2 5, FTP1 31, FTP1 77
- Collins, Ken FTP1 85,
SR1 1, XF2 3, XF2 6
- Consoli, Angelo MWP1 76
- Corr, Cormac S. SR1 2
- Correa, Jorge MWP1 46
- Creemers, Joris MWP1 54
- Crintea, Dragos FTP1 69
- Cuomo, Jerome J. ET1 4,
LW1 2, MWP1 47, QR3 6
- Curry, J.J. RR2 4
- Curry, John LW1 3
- Czarnetzki, Uwe FTP1 69,
MWP1 18, MWP1 40,
MWP1 85, MWP1 86,
SR1 5
- D**
- da Costa, R.F. MWP1 5
- Dai, Ruicheng FTP1 29
- Daltrini, A.M. FTP1 6
- Daniels, Stephen FTP1 66,
MWP1 25, MWP1 27,
QR3 7
- Dasgupta, Arati MWP1 6
- Davis, Jack MWP1 6
- De Bie, Christophe ET1 3
- De Kuyper, Alec MWP1 54
- de Marneffe, Jean-Francois
XF1 3
- de Oliveira, E.M. MWP1 5
- de Urquijo, J. VF2 3
- Deconinck, Thomas CT1 6
- Delanty, Michael
MWP1 107
- Della Croce, Damian QR3 1
- Demidov, V.I. FTP1 38,
FTP1 65
- Den, Shoji FTP1 18,
MWP1 63, PR1 2
- Denysenko, Igor
MWP1 102

Despiau-Pujo, Emilie **SR1 2**
 Djordjevic, Antonije
 MWP1 15
 Djulgerova, R. FTP1 49
 Donko, Zoltan MWP1 86,
 SR1 5
 Donnelly, V. CT1 4, DT1 4,
 FTP1 72, MWP1 81
 Dorai, Rajesh ET2 4
 Dorf, Leonid **FTP1 85**
 Dorn, Alexander FTP1 99,
 MWP1 2, MWP1 7
 Doss, Natasha FTP1 20,
 PR1 4
 Dowling, Denis QR3 7
 Drake, D.J. **MWP1 93,**
QR3 4
 Dufour, Thierry **CT1 7**
 Dujko, S. **VF2 5**
 Dunaevsky, Alexander
MWP1 69
 Dussart, Remi CT1 7,
WF1 6
 Dziczek, Dariusz LW2 4

E

Ebe, Akinori XF1 6
 Economou, Demetre CT1 4,
 MWP1 81
 Eddine, N. FTP1 72
 Eden, J. Gary BT1 3,
 FTP1 62
 Ehlbeck, J. RR2 2
 Eismann, B. MWP1 38,
 MWP1 60
 Ellingboe, Albert R.
MWP1 26
 ElSaghir, Ahmed **FTP1 82**
 Endo, Hirotaka FTP1 17
 Ergler, Thorsten FTP1 91
 Eriguchi, Koji DT1 3,
 WF3 3, XF1 2
 Es-Sebbar, Et-Touhami
 MWP1 50
 Eshghabadi, Majid
 MWP1 28

F

Fadil, H. FTP1 100
 Feldman, Uri BT1 4
 Fernandez, Facundo DT2 2
 Fernandez, Sulmer
 MWP1 51
 Fernsler, Richard
 MWP1 36, **VF1 4**, WF1 7
 Ferreira, L.G. MWP1 5

Feuerstein, Bernold
 FTP1 88, FTP1 91
 Figus, Margaret FTP1 67
 Filippov, Anatoly MWP1 75
 Fischer, Daniel FTP1 110,
 MWP1 9, **SR2 1**, SR2 4
 Flitti, Aicha FTP1 42
 Fontes, Christopher BT1 4
 Foster, Lewis **PR2 2**
 Foster, Matt BT1 4
 Franke, Steffen FTP1 83
 Franklin, R.N. **ET2 1**
 Franz, Kai LW2 6
 Fridman, Alexander DT2 4
 Fridman, Gregory DT2 4
 Friedman, Gary DT2 4
 Friedman, J.F. WF2 6
 Froese, M. FTP1 100
 Froese Fisher, C. RR2 4
 Frolov, Oleksandr
 MWP1 20
 Fujii, Yosuke MWP1 98
 Fujiyama, Hiroshi **FTP1 35,**
SR1 6
 Fukuyama, K. FTP1 68
 Funk, Merritt MWP1 59,
 MWP1 81
 Fursa, D.V. **LW2 5**, QR2 4,
 SR2 3
 Fursa, Dmitry MWP1 7
 Furst, J.E. CT2 6
 Furuya, Kenji **PR1 5**

G

Gaebler, Dieter RR1 7
 Galechyan, Georgy QR3 3
 Galli, Federico **BT3 4**
 Ganguly, Biswa MWP1 39,
 MWP1 92
 Gans, Timo **BT1 1**,
 FTP1 78, MWP1 45
 Garcia, Gustavo LW2 7
 Garcia de Gorordo, Alvaro
WF1 2
 Gay, T.J. CT2 3, **CT2 6**
 Gherardi, Nicolas
MWP1 50
 Ghim(kim), Young-chul
MWP1 22
 Ghoranneviss, Mahmood
 MWP1 28
 Girault, Vincent MWP1 67
 Giuliani, John L. MWP1 6
 Gnybida, Mykhaylo
FTP1 47
 Godet, Ludovic ET2 4
 Goeckner, M. CT1 7,

FTP1 13, FTP1 64,
 MWP1 19, MWP1 35
 Gomes, Marcelo MWP1 46
 Goossens, Danny XF1 3
 Gorchakov, Sergey FTP1 25
 Gordon, Michael **QR1 2**
 Gorin, Vladimir **FTP1 54**
 Gorobets, Nikolay BT3 1
 Grafutin, Viktor I.
MWP1 77
 Graham, Bill FTP1 78
 Graham, William FTP1 6,
QR3 1, SR1 2
 Graves, David DT2 6,
 SR1 2
 Gregorio, J. **MWP1 41,**
MWP1 42
 Grubert, Gordon K. **VF1 3**
 Guaitella, O. **FTP1 60,**
 PR3 3
 Guarnieri, C. Richard
 ET1 4, MWP1 47
 Gudmundson, Jesse
MWP1 95
 Gudmundsson, Jon T.
CT3 3, FTP1 34,
FTP1 102
 Guha, J.D. **DT1 4**

H

Hagelaar, Gerjan MWP1 60,
 MWP1 71
 Hagmann, Siegbert
 FTP1 110
 Hallock, Gary A. WF1 2
 Hamaguchi, Satoshi
 MWP1 18, MWP1 40
 Han, In-Shik FTP1 16
 Hanaki, Hatsuyuki FTP1 2
 Haque, A.K.F. MWP1 3
 Harata, Akira PR1 5
 Hargreaves, L.R. QR2 4
 Harris, A.L. **MWP1 10,**
MWP1 11, **SR2 3**
 Harutyunyan, Gevorg
QR3 3
 Hasuo, Masahiro FTP1 108
 Hatakeyama, Rikizo PR3 4
 Havener, Charles **PR2 4**
 Hayashi, Toshio DT1 5
 Hayashi, Yuichiro **FTP1 3,**
 MWP1 23
 Heering, Wolfgang RR2 5
 Hegna, Chris VF3 6
 Heil, Brian MWP1 85,
 MWP1 86, SR1 5
 Helmersson, Ulf FTP1 34
 Hemke, Torben MWP1 84

Heneral, Andrij MWP1 64
 Hernandez-Avila, J.L.
 VF2 3
 Hershkowitz, Noah
 MWP1 22, MWP1 95,
VF3 2, VF3 3
 Hertlein, Marcus FTP1 101
 Higashijima, Yasuhiro
 MWP1 63, MWP1 109
 Hiramatsu, Mineo FTP1 18,
 PR1 2
 Hoffmann, J. FTP1 100
 Horak, David XF1 4
 Hori, Masaru DT1 5,
 FTP1 18, MWP1 63,
 MWP1 109, PR1 2, PR3 1,
 RR1 6, XF1 1, XF1 6
 Horikawa, Y. **LW1 6**
 Horner, Daniel **CT2 4,**
FTP1 90
 Hosch, Jimmy FTP1 64
 Hotop, Hartmut LW2 6
 Hsu, Kuo-Hsien XF2 7
 Huang, Shiyong FTP1 14
 Hupe, Ryan SR2 2
 Hwang, Kwang-Tae **FTP1 7**
 Hyde, Truell BT3 2, BT3 3,
 BT3 6, MWP1 61
 Hynes, Alan QR3 1

I

Ide, Akihiro PR1 5
 Inoue, Kazuhiko RR1 6
 Inui, Hiroto **PR3 1**
 Ionin, Andrey **GW3 6,**
MWP1 87
 Iqbal, Muhammad M.
MWP1 44
 Irie, Shoki DT1 3
 Isaenkov, Yuri BT2 5
 Iseki, Sachiko MWP1 109
 Isenberg, Christopher
 FTP1 69
 Ishijima, Tatsuo FTP1 17,
 PR3 2
 Itabashi, Hideyuki
 MWP1 99
 Ito, Masafumi MWP1 63,
 MWP1 109
 Ito, Toru **MWP1 24**
 Ito, Tsuyohito MWP1 18,
MWP1 40
 Itoh, Haruo **MWP1 48**
 Itoh, Hidenori MWP1 99
 Iwakawa, Akira WF3 3
 Iwashita, Shinya **MWP1 34,**
RR1 2

J

Jalili, Amir-Hossein **VF2 2**
 Jang, H. **MWP1 89**
 Jang, Sung-Ho **FTP1 8**,
FTP1 9, **FTP1 76**
 Jaroshevich, A.S. **FTP1 100**
 Jia, Shenli **FTP1 28**, **WF1 8**
 Jiao, C.Q. **FTP1 38**
 Johnsen, Rainer **MWP1 13**,
WF2 2
 Jolly, Jacques **CT3 6**,
FTP1 39
 Jones, Adric **FTP1 94**,
LW2 2
 Jordon-Thaden, B.
FTP1 100
 Joseph, Dwayne **FTP1 111**
 Joshi, Ravindra P.
MWP1 97
 Josphipura, K.N. **MWP1 4**,
QR2 6
 Juarez, A.M. **VF2 3**
 Jung, R.O. **FTP1 70**

K

Kadetov, Viktor **FTP1 69**
 Kaiser, Christian **QR2 3**
 Kaiser, Norbert **RR1 7**
 Kalghatgi, Sameer **DT2 4**
 Kane, J. **LW1 5**
 Kaneko, Toshiro **PR3 4**
 Kang, Song-Yun **PR1 4**,
WF3 2
 Kano, Hiroyuki **MWP1 63**,
MWP1 109, **PR3 1**
 Karahashi, Kazuhiro **PR1 1**
 Karakas, Erdinc **LW1 1**
 Kase, Ed **MWP1 59**
 Kasugai, Hiroki **FTP1 46**
 Kato, M. **LW1 5**
 Kavanagh, David **FTP1 66**,
MWP1 25
 Kawakami, Masato **PR1 4**
 KC, Utsav **GW1 5**
 Keil, Douglas **WF1 4**
 Keister, K. Ellen **BT1 3**
 Kelly, Crystal **DT2 4**
 Kelman, Volodymyr
FTP1 81, **MWP1 64**
 Kenney, Jason **SR1 1**
 Kersten, H. **MWP1 80**
 Kettlitz, Manfred **MWP1 66**
 Keville, Bernard **LW1 7**
 Khadilkar, Vaibhav
FTP1 108
 Khakoo, M.A. **CT2 5**,
MWP1 5

Kharchenko, Nadiia
FTP1 48
 Khare, R. **FTP1 72**
 Kheifets, A. **QR2 4**
 Kieckhafer, Alex **LW1 3**
 Kikuchi, Hirokazu **PR3 6**
 Kilcoyne, A.L.D. **CT2 6**
 Kim, Gon-Ho **FTP1 73**
 Kim, Gun-Ho **FTP1 9**,
FTP1 76
 Kim, Jin-Sung **FTP1 8**
 Kim, Jung **WF1 4**
 Kim, Kee-Hyun **FTP1 16**
 Kim, Robert **FTP1 5**
 Kimura, Takashi **FTP1 2**,
FTP1 46, **MWP1 79**
 Kinder, Ron **LW1 8**
 Kindusheva, Svetlana
GW1 2, **WF2 4**
 King, Matthew R. **ET1 4**,
LW1 2, **MWP1 47**, **QR3 6**
 Kirchner, Tom **MWP1 9**,
PR2 3, **SR2 4**
 Kittaka, Yusuke **MWP1 14**
 Kiyokami, Hiroaki **XF1 2**
 Klick, Michael **MWP1 84**,
XF2 2
 Klimachev, Yurii **GW3 6**
 Klosowski, Lukasz **LW2 4**
 Knake, Nikolas **CT1 1**
 Kobayashi, Kazunobu
MWP1 18, **MWP1 40**
 Kobayashi, Kazuto
MWP1 48
 Kochetov, Igor **GW3 6**
 Koepke, M.E. **FTP1 65**
 Koga, Kazunori **MWP1 34**,
RR1 2, **RR1 6**
 Kolacek, Karel **MWP1 20**
 Kolb, Juergen F. **DT2 7**,
MWP1 97
 Kolobov, Vladimir **CT3 2**
 Kondo, Shingo **FTP1 18**,
PR1 2
 Kong, Jay **BT3 2**
 Kono, A. **FTP1 68**
 Koo, Il Gyo **DT2 5**,
FTP1 31
 Korot, Kirti **MWP1 4**,
QR2 6
 Kortshagen, Uwe **BT3 4**
 Kosarev, Ilya **GW1 2**,
WF2 4
 Kothnur, Prashanth **LW1 8**,
XF1 7
 Kotkov, Andrey **GW3 6**
 Kozlov, Andrey **GW3 6**,
MWP1 87

Kramer, Nicolaas J.
MWP1 33
 Krantz, C. **FTP1 100**
 Krauss, Andreas **FTP1 110**
 Krivchenko, Viktor
FTP1 11
 Krstic, Predrag **GW2 3**
 Kudryavtsev, A.A. **FTP1 38**
 Kudryavtsev, Anatoly
FTP1 53
 Kuehnel, Kai-Uwe
FTP1 110
 Kulander, Kenneth **HW 1**
 Kumar, Neeraj **QR2 5**
 Kuncser, V. **RR1 4**
 Kurihara, K. **LW1 6**
 Kushner, Mark J. **CT3 1**,
FTP1 43, **SR1 4**

L

Labelle, Catherine **XF1 4**
 Lacoste, Deanna **QR3 2**
 Lacour, B. **DT2 1**
 LaForge, Aaron **FTP1 109**,
SR2 2
 Lahr, David **WF1 1**
 Lam, Cherk **FTP1 62**
 Lambrakos, S.G. **VF1 4**
 Land, Victor **BT3 3**
 Lange, Kyle **ET1 6**
 Lange, M. **FTP1 100**
 Lapiere, D. **FTP1 72**
 Lapke, Martin **WF1 5**
 Laroussi, Mounir **DT2 3**,
LW1 1
 Larsson, Petter **FTP1 34**
 Laux, Christophe **FTP1 44**,
QR3 2
 Law, Victor **QR3 7**
 Lawler, J.E. **LW1 5**, **RR2 3**
 Layet, Jean-Marc
MWP1 72, **MWP1 74**
 Lazovic, Sasa **MWP1 15**
 Lazzaroni, Claudia **CT1 2**
 Lebouvier, Alexandre
MWP1 33
 Lee, Dae-Sung **MWP1 108**
 Lee, Dongsoo **VF3 3**
 Lee, G. **MWP1 89**
 Lee, Hi-Deok **FTP1 16**
 Lee, Hyo-Chang **FTP1 74**,
SR1 3
 Lee, Jeong-Bong **CT1 7**
 Lee, Kyung-Hwan
MWP1 89
 Lee, Min-Hyong **FTP1 8**,
FTP1 74, **FTP1 75**
 Lee, Seok-Hwan **FTP1 73**

Lee, Sun **FTP1 101**
 Lee, Won-Mook **FTP1 16**
 Lee, Woong Moo **CT1 3**,
DT2 5
 Lee, Young-Kwang
FTP1 75
 Lefaucheux, Philippe
CT1 7, **WF1 6**
 Lempert, Walter **BT2 1**,
GW3 4
 Leonov, Sergey **BT2 5**
 Leprince, P. **MWP1 42**
 Leray, Gary **GW1 3**
 Leroy, O. **MWP1 42**
 Lestinsky, M. **FTP1 100**
 Levchenko, Igor
MWP1 104, **MWP1 106**,
MWP1 107
 Leys, Christophe **MWP1 54**
 Li, Rui **FTP1 29**
 Li, Xingwen **FTP1 29**
 Li, Yan-Ming **GW3 1**
 Liard, Laurent **CT3 6**
 Lichtenberg, Allan J. **ET2 2**
 Lieder, G. **RR2 2**
 Likhanskii, Alexandre
GW1 4, **MWP1 94**
 Lim, Chul-hyun **FTP1 41**
 Lima, M.A.P. **MWP1 5**
 Limbachiya, Chetan
MWP1 4, **QR2 6**
 Lin, Chun C. **FTP1 70**
 Lisovskiy, Valeriy
FTP1 39, **FTP1 48**
 Litaker, E. **CT2 6**
 Liu, N.Y. **GW3 2**
 LoCascio, Aaron **FTP1 50**,
FTP1 51
 Loch, Stuart **BT1 2**
 Lock, Evgeniya **MWP1 36**
 Loffhagen, Detlef **FTP1 47**,
MWP1 58, **MWP1 80**,
VF1 2, **VF1 3**
 Lohmann, B. **FTP1 94**,
QR2 4
 Long, Jidong **FTP1 14**
 Lopes, M.C.A. **CT2 5**,
MWP1 5
 Lopez, Jose **FTP1 67**,
MWP1 100
 Lower, J. **LW2 7**, **SR2 3**
 Lu, XinPei **MWP1 110**
 Luggenhoelscher, Dirk
FTP1 69, **MWP1 86**
 Lundie, D.T. **FTP1 58**
 Lundin, Daniel **FTP1 34**
 Lungu, A.M. **FTP1 84**,
RR1 4

Lungu, C.P. FTP1 84,
RR1 4

M

Ma, Jeffrey FTP1 62
Ma, Xinwen FTP1 110
MacFarlane, Duncan RR1 5
Macgearailt, Niall
MWP1 27
Machacek, J.R. CT2 6
Machavariani, Zaal SR2 2
Macheret, Sergey GW1 4,
MWP1 94
Maddern, Todd **QR1 3**
Madison, Don MWP1 7,
MWP1 10, MWP1 11,
QR2 3, SR2 2, SR2 3
Maguire, Paul MWP1 21,
QR3 5
Mahadevan, Shankar **BT2 4**
Mahony, C.M.O. MWP1 21
Makabe, Toshiaki FTP1 3,
FTP1 57, MWP1 23,
WF3 6
Makochekanwa, Casten
FTP1 94, LW2 2
Malovic, Gordana FTP1 49,
MWP1 15, VF2 4
Mandra, Monali CT1 7
Mao, Ming **MWP1 76**
Maric, D. FTP1 49
Marinov, D. FTP1 60
Marler, Joan P. VF2 4
Marode, E. GW3 2
Marro, Fernando G. SR1 2
Martens, Tom **ET1 3**,
MWP1 53
Martin, F. CT2 4, CT2 6
Martin, N.L.S. **QR2 1**
Masahiro, Horigome
MWP1 24
Maseberg, J.W. **CT2 3**
Mason, Nigel MWP1 4,
QR2 6
Massines, Françoise
MWP1 50
Mathias, Jacky WF1 6
Matsudaira, Yuto PR3 1
Matsukuma, Hiraku
FTP1 108
Matsuura, Haruaki FTP1 24,
MWP1 14, MWP1 17
Matsuzaki, Hidefumi
RR1 2, RR1 6
Matthews, Lorin BT3 2,
BT3 3, BT3 6, MWP1 61
McCurdy, C. William
CT2 4, FTP1 90

McEachran, Robert
FTP1 93, LW2 2
McKoy, V. MWP1 5
McLaughlin, K.W. CT2 6
McLoone, Shane MWP1 27
Meger, Robert WF1 7
Mehranfar, Mona
MWP1 28
Meige, Albert GW1 3,
MWP1 71
Meisser, Michael RR2 5
Mendes, M. FTP1 100
Mentel, Juergen MWP1 65,
MWP1 68, RR2 1
Merry, Walter FTP1 85
Mertmann, Philipp
MWP1 43, MWP1 83
Mihailov, V. FTP1 49
Miles, Richard GW3 3,
MWP1 94
Miller, T.M. **WF2 6**
Milosavljevic, Vladimir
MWP1 25, MWP1 26,
MWP1 27
Minakov, Pavel FTP1 11
Mitsuhashi, Hisahito
FTP1 57
Miyabe, Shungo CT2 4
Miyata, Hiroshi RR1 2
Miyazaki, Yasushi
MWP1 99
Mizuno, Kouichiro FTP1 19
Mo, Yun MWP1 24
Monahan, Derek D. **ET2 3**,
LW1 7, VF3 4
Mondal, Subhendu **LW2 7**
Moon, Chang Sung **DT1 5**
Moore, Cameron CT1 3,
DT2 5, FTP1 31, **FTP1 77**
Moore, Jon MWP1 91
Morales, Felipe CT2 4
Morgan, T.J. FTP1 6
Mori, Masahito DT1 3
Morishita, Satoshi
MWP1 23
Moroz, Paul **WF3 2**
Morshed, Mohammed
FTP1 66
Moshhammer, Robert
FTP1 91, FTP1 110,
MWP1 9, SR2 4
Moshkalev, S.A. FTP1 6
Mulders, Hjalmar
MWP1 67
Mungal, Godfrey **BT2 3**
Munro, James J. **FTP1 20**,
PR1 4

Muraoka, Katsunori
MWP1 98
Murray, Andrew QR2 3
Muse, J. CT2 5, MWP1 5
Mussenbrock, Thomas
MWP1 43, MWP1 83,
MWP1 84, MWP1 85,
MWP1 86, WF1 5, **XF2 1**,
XF2 4
Mustata, I. RR1 4

N

Nafarizal, N. **BT3 5**
Nagahara, Yoh FTP1 24
Nagai, Mikio WF1 4
Nagaoka, Tatsuya WF3 3
Nagorny, Vladimir **CT3 2**
Naidis, George FTP1 42
Najjari, Bennaceur
FTP1 110
Nakamura, Keisuke XF1 2
Nakatani, Tatsuyuki
FTP1 35, SR1 6
Nam, Sang Ki **FTP1 41**,
VF1 5
Napartovich, Anatoly
GW3 6
Naude, Nicolas MWP1 50
Nelson, Caleb **MWP1 35**
Nemanich, Robert RR1 1
Ness, K.F. VF2 5
Nezu, Atsushi FTP1 24,
MWP1 14, MWP1 17
Ngassam, Valery **WF2 5**
Niederhausen, Thomas
FTP1 87, FTP1 88,
FTP1 91
Niemi, Kari CT1 1,
FTP1 78, **MWP1 45**
Nikipelov, Andrei
MWP1 96
Nikitovic, Zeljka FTP1 98,
FTP1 104
Nishihara, Munetake
GW3 4
Nomura, Takuya RR1 6
Nordheden, Karen WF1 3
Novotny, Oldrich **FTP1 100**
Novotny, S. FTP1 100
Nudnova, Maryia **ET1 2**,
MWP1 96

O

O'Connell, Deborah
FTP1 78
O'Connor, Niall QR3 7
O'Neill, Liam QR3 1

Oberrath, J. **FTP1 52**
Oda, Akinori MWP1 52
Ogawa, Daisuke FTP1 13,
MWP1 19
Ohta, Hiroaki DT1 3,
WF3 3, XF1 2
Ohta, Takayuki **MWP1 63**,
MWP1 109
Okumura, Hiroshi PR1 5
Oldham, Christopher J.
ET1 4, LW1 2,
MWP1 47, QR3 6
Oliveira, Carlos MWP1 46
Olshevskii, Sergey PR3 5
Ono, Kouichi DT1 3,
WF3 3, XF1 2
Opaits, Dmitry GW1 4,
MWP1 94
Orel, A.E. WF2 3, WF2 5
Orlando, Thomas DT2 2
Orlov, D.A. FTP1 100
Osipov, Timur FTP1 101
Ostrikov, Kostya FTP1 14,
MWP1 102, MWP1 103,
MWP1 104, MWP1 105,
MWP1 106, MWP1 107,
RR1 3, XF1 8
Oukacine, Linda **ET1 5**
Overzet, Lawrence CT1 7,
FTP1 13, MWP1 19,
MWP1 35, MWP1 89

P

Packan, Denis FTP1 44
Pai, David **QR3 2**
Pal, Alexander **FTP1 11**,
MWP1 75
Pal, Satyendra **QR2 5**
Palacios, Alicia FTP1 90
Palmer, Richard E. **GW2 1**
Pancheshnyi, Sergey **ET1 1**,
FTP1 42, MWP1 38,
MWP1 60
Pankratova, Olga MWP1 32
Paramo, Jorge **DT1 7**
Paravia, Mark **RR2 5**
Park, Kun-Joo FTP1 5,
FTP1 16
Park, Sung-Jin **FTP1 62**
Pasko, V.P. GW3 2
Pathak, Bogdan **WF1 3**
Patoary, M.A.R. **MWP1 3**
Patz, Ryan XF1 4
Peacher, J.L. MWP1 10,
MWP1 11
Pedrow, Patrick **MWP1 51**
Pender, Jeremiah XF1 4
Peters, Raul DT1 7

- Peters, Silke MWP1 66
 Petrignani, A. FTP1 100
 Petrovic, Dragana ET1 3
 Petrovic, Zoran FTP1 49,
 FTP1 98, FTP1 104,
 MWP1 15, MWP1 31,
 VF2 4
 Pflueger, Thomas FTP1 99
 Phelps, Arthur **FTP1 105,**
FTP1 106
 Phillips, L. FTP1 15
 Pichon, Laurianne WF1 6
 Piejak, R.B. FTP1 6
 Pitchford, Leanne
 MWP1 38, MWP1 60
 Pitts, Marvin MWP1 51
 Piwinski, Mariusz LW2 4
 Pleskacz, Katarzyna LW2 4
 Podder, Nirmol **FTP1 50,**
 FTP1 51
 Pompilian, O. RR1 4
 Popovic, S. FTP1 15,
 MWP1 93, QR3 4
 Popugaev, S.M. FTP1 38
 Porosnicu, Cornel **FTP1 84,**
 RR1 4
 Predoi, D. RR1 4
 Price, Robert O. DT2 7
 Prokop'ev, Eugene P.
 MWP1 77
 Prukner, Vaclav MWP1 20,
 MWP1 56
 Prysiazhnevych, Iryna
 PR3 5
 Puac, Nevena MWP1 15
 Puckett, Jenna R. **LW1 2,**
 QR3 6
 Puech, V. DT2 1, MWP1 38
 Putney, Jeffrey L. BT1 3
- Q**
 Qiao, Ke **MWP1 61**
- R**
 Rackow, K. RR2 2
 Radjenovic, Branislav
 FTP1 40, **MWP1 31,**
 MWP1 90
 Radmilovic-Radjenovic,
 Marija **FTP1 40,**
 MWP1 31, MWP1 90
 Radovanov, Svetlana **ET2 4**
 Ragnoli, Emanuele
 MWP1 27
 Raimbault, Jean-Luc CT3 6,
 GW1 3
- Raja, Laxminarayan BT2 4,
 CT1 6, GW1 5, XF1 7
 Rakhimov, Alexander
 FTP1 11
 Rakitin, Aleksandr BT2 2
 Ramaswamy, Kartik
 FTP1 85
 Ramsayer, Chris LW1 4,
 MWP1 16
 Ranjan, Alok MWP1 81
 Ranson, Pierre CT1 7
 Raskovic, M. FTP1 15
 Rauf, Shahid SR1 1,
WF3 5, XF2 3, XF2 6
 Ravanat, J.L. DT2 1
 Razhev, Alexander **GW3 5**
 Razinkova, Tat'yane L.
 MWP1 77
 Rebic, Stojan MWP1 107
 Rees, J.A. **FTP1 58,**
FTP1 80
 Reinelt, Jens MWP1 68,
RR2 1
 Ren, XueGuang **FTP1 99,**
MWP1 2, MWP1 7
 Rescigno, Thomas **CT2 1,**
 CT2 4, FTP1 90
 Reuter, Stephan CT1 1
 Rhoton, Russell L. **FTP1 22**
 Rich, J. William GW3 4
 Rider, Amanda **MWP1 104**
 Rijke, Arij MWP1 67
 Ringwood, John MWP1 27
 Roark, Christine MWP1 59
 Robson, R.E. VF2 5
 Roquemore, Lane FTP1 51
 Roupassov, Dmiry
 MWP1 96
 Rousseau, A. CT1 2,
 FTP1 60, MWP1 55,
 PR3 3
 Rudek, Benedikt FTP1 101
 Rudenko, Artem FTP1 91
 Rulev, Oleg GW3 6
- S**
 Sadeghi, Nader CT1 2,
 CT1 4
 Sagbiev, Ilgizar **FTP1 21,**
MWP1 32
 Saha, Bidhan FTP1 111,
 MWP1 3
 Saito, Koya PR3 6
 Saito, Ryota PR3 2
 Sakai, Osamu **CT1 5,**
 MWP1 108
 Sakai, Yosuke MWP1 52
 Sakiyama, Yukinori **DT2 6**
- Sands, Brian **MWP1 39**
 Sant, Sanket MWP1 35
 Santos Sousa, J. **DT2 1,**
MWP1 38
 Sanz-Vicario, J.L. CT2 6
 Saraf, Iqbal **FTP1 13,**
 MWP1 19
 Sarra-Bournet, Christian
 MWP1 50
 Sasaki, K. BT3 5, LW1 6
 Sato, Kazunari FTP1 31,
 FTP1 77
 Satoh, Kohki **MWP1 99**
 Sawada, Ikuo **WF3 1,**
 WF3 2
 Schaper, Lucas QR3 1
 Scharf, Frank **MWP1 65,**
VF3 1
 Scharwitz, Christian FTP1 3
 Schiesko, Loic MWP1 72,
 MWP1 74
 Schinteie, G. RR1 4
 Schmidt, Jiri MWP1 20,
 MWP1 56
 Schmidt, Werner MWP1 58
 Schneidenbach, Hartmut
FTP1 83
 Schoenbach, Karl H. DT2 7,
 MWP1 97
 Schultz, David **PR2 1**
 Schulz, M. FTP1 109,
 FTP1 110, MWP1 9,
 MWP1 10, SR2 2, **SR2 4**
 Schulz-von der Gathen,
 Volker **CT1 1**
 Schulze, Julian **MWP1 86,**
SR1 5
 Scofield, J.D. FTP1 12
 Scott, Douglas **FTP1 31**
 Scully, Noah MWP1 97
 Segawa, Sumie PR1 4
 Segur, P. ET1 1, GW3 2
 Sekine, Makoto DT1 5,
 FTP1 18, PR1 2, RR1 6,
 XF1 1, XF1 6
 Seleznev, Leonid GW3 6,
 MWP1 87
 Self, Daniel FTP1 64
 Semak, Vladimir GW1 4
 Semmar, Nadjib WF1 6
 Sen, Vasily FTP1 11
 Senftleben, Arne FTP1 99,
 MWP1 7
 Setsuhara, Yuichi DT1 5,
 RR1 6, **XF1 6**
 Severn, Greg VF3 2, **VF3 3**
 Seyed-Matin, Naser
 FTP1 61, VF2 2
- Seymour, D.L. FTP1 58
 Shahjahan, M. MWP1 3
 Shamiryan, Denis XF1 3
 Shan, Yanguang **FTP1 30**
 Shannon, Steven FTP1 82,
 RR1 1
 Shapoval, Volodymyr
MWP1 101
 Sharafeev, Roustem
 FTP1 21
 Sharp, David MWP1 91
 Shen, Erica BT3 3
 Sheridan, T.E. **VF3 5**
 Sherrill, Manolo BT1 4
 Shi, Zongqian FTP1 28,
WF1 8
 Shibata, Tomohiko
 FTP1 24, **MWP1 17**
 Shimomura, Naoyuki
 MWP1 48
 Shinohara, Masanori
 FTP1 35, SR1 6
 Shiratani, Masaharu DT1 5,
 MWP1 34, RR1 2, **RR1 6,**
 XF1 6
 Shneider, Michail BT2 5
 Shneider, Mikhail GW1 4,
 GW3 3, MWP1 94
 Shornikov, A. FTP1 100
 Shpenik, Yuriy **FTP1 81,**
MWP1 64
 Sigenefer, F. MWP1 58,
 MWP1 66, **MWP1 80,**
RR2 2, VF1 2, VF1 3
 Sigurjonsson, Pall **FTP1 34**
 Silva, H. CT2 5, MWP1 5
 Simek, Milan **MWP1 20,**
MWP1 56
 Singh, Vikram ET2 4
 Sinitsyn, Dmitry GW3 6,
 MWP1 87
 Sirin, Fatih FTP1 33
 Sismanoglu, Bogos
MWP1 46
 Skoro, N. **FTP1 49**
 Slaughter, Daniel FTP1 94,
 LW2 2
 Slinker, S.P. VF1 4
 Smith, Bernard **BT3 6**
 Smithe, David MWP1 59
 Sobolewski, Mark **WF1 1**
 Sobota, Ana **MWP1 33**
 Sode, Maik RR1 7
 Solomenko, Olena PR3 5
 Song, Xiaochuan WF1 8
 Sorg, T. FTP1 100
 Sra, A. MWP1 89

- Srivastava, Mahesh
MWP1 103
- Stacey, Michael DT2 7
- Stafford, L. **FTP1 72**
- Stalder, Kenneth LW1 4,
MWP1 16
- Starikovskaya, Svetlana
GW1 2
- Starikovskii, Andrei **BT2 2**,
ET1 2, GW1 2,
MWP1 96, WF2 4
- Starostin, Andrey
MWP1 75
- Stauffer, Allan **FTP1 93**,
LW2 2
- Stepanovic, Olivera
FTP1 18, PR1 2
- Stevenson, M.A. QR2 4
- Stevenson, Mark FTP1 94
- Stoffels, Winfred
MWP1 33, MWP1 67
- Stojanovic, Vladimir
FTP1 98, **FTP1 104**
- Stoltz, Peter MWP1 59
- Stout, Phillip XF2 6
- Straus, Jaroslav MWP1 20
- Struyf, Herbert XF1 3
- Strzhemechny, Yuri DT1 7
- Stuetzel, J. FTP1 100
- Suetin, Nikolay FTP1 11
- Sugawara, Hirotake
FTP1 4, FTP1 19
- Sugiura, Hiroyasu PR3 2
- Sullivan, James FTP1 94,
LW2 2
- Sultana, Nahid **RR1 5**
- Sun, Lan DT2 2
- Sundararajan, Radha
MWP1 81
- Surko, C.M. **FTP1 95**,
FTP1 96
- Suske, Jan FTP1 110
- Sutton, Yvonne MWP1 91
- Suvakov, Milovan VF2 4
- Suzuki, Susumu MWP1 48
- Swanson, R. James DT2 7
- Symonds, Joshua **DT2 2**
- T**
- Tachibana, Kunihide
MWP1 108
- Tachibana, Yoshihiro
MWP1 63
- Takada, N. BT3 5
- Takanishi, Yudai FTP1 17
- Takashima, Seigo DT1 5
- Takeda, Keigo DT1 5,
XF1 1
- Takenaka, Kosuke XF1 6
- Takota, Naoki MWP1 63
- Talukder, M.R. MWP1 3
- Tam, Eugene FTP1 14,
MWP1 102, MWP1 104,
MWP1 105, **RR1 3**,
XF1 8
- Tamai, Yuji PR1 5
- Tanahashi, Hiroki
MWP1 79
- Tang, Hairong XF1 4
- Tatibouet, Jean-Michel
ET1 5
- Tatsumi, Tetsuya **QR1 1**
- Tennyson, Jonathan
FTP1 20, PR1 4
- Teranishi, Kenji MWP1 48
- Terashima, Kazuo PR3 6
- Tessier, Yves WF1 6
- Thamban, P.L. Stephan
FTP1 64
- Thomann, Anne-Lise
WF1 6
- Thorgrimsson, Chris WF1 4
- Thorsteinsson, Eythor Gisli
FTP1 102
- Thumm, Uwe **FTP1 87**,
FTP1 88, **FTP1 91**,
GW2 2
- Tian, Caizhong **VF1 1**
- Ticos, C. FTP1 84, RR1 4
- Ting, Yuk-Hong DT1 2
- Tolson, B.A. FTP1 12,
FTP1 65
- Tomai, Takaaki **PR3 6**
- Touzeau, M. DT2 1
- Toyoda, Hirotaka **FTP1 17**,
PR3 2
- Trampert, Klaus E. RR2 5
- Troe, J. WF2 6
- Tsendin, Lev FTP1 53
- Tsuda, Hirotaka **DT1 3**
- Tsyganov, Dzimtry ET1 1
- Tu, Jun-Ming MWP1 69
- Tuennermann, Andreas
RR1 7
- Turner, Miles M. ET2 3,
LW1 7, MWP1 44,
MWP1 82, **VF3 4**
- Twomey, Barry QR3 7
- Tynan, John QR3 7
- U**
- Uddi, Mruthunjaya BT2 1
- Uddin, M. Alfaz MWP1 3
- Ueda, Yoshinori **XF1 2**
- Uhrlandt, Dirk FTP1 25,
FTP1 26, FTP1 27,
FTP1 47, RR2 2
- Ullrich, Joachim FTP1 91,
FTP1 99, FTP1 110,
MWP1 2, MWP1 7,
MWP1 9, SR2 4
- Umetsu, Jun RR1 6
- Upadhyay, J. **FTP1 15**
- V**
- Vagin, Nikolay GW3 6
- Valente-Feliciano, A.M.
FTP1 15
- van Dijk, Jan ET1 3,
MWP1 53
- van Veldhuizen, Eddie M.
MWP1 33
- Varambhia, Hemal N.
FTP1 20
- Varella, M.T. do N.
MWP1 5
- Varghese, Philip GW1 5
- Vegh, Joseph **QR1 4**
- Verboncoeur, John
FTP1 41, VF1 5
- Vidmar, Robert **LW1 4**,
MWP1 16
- Viggiano, A.A. WF2 6
- Vinodkumar, Minaxi
MWP1 4, QR2 6
- Voitkiv, Alexander
FTP1 110
- Vozniy, Oleksiy **GW2 4**
- Vukovic, Mirko **WF3 4**
- Vural, Murat **FTP1 33**
- Vuskovic, L. FTP1 15,
MWP1 93, QR3 4
- W**
- Wagner, Clark J. BT1 3
- Wahl, Kathryn RR1 1
- Walton, Scott MWP1 36,
WF1 7
- Wang, Lijun **FTP1 28**,
WF1 8
- Ward, Arlen FTP1 77
- Waskoenig, Jochen
MWP1 45
- Weber, Thorsten FTP1 101
- Weigold, E. SR2 3
- Wendt, A.E. FTP1 70
- Wendt, Amy **DT1 2**
- Wendt, Martin FTP1 83,
MWP1 66
- Westermeier, Michael
MWP1 68, RR2 1
- White, R.D. VF2 5
- Whitmore, T.D. FTP1 58
- Williamson, J.M. **FTP1 12**
- Winfrey, Leigh **RR1 1**
- Winstead, C. MWP1 5
- Wisman, David **MWP1 92**
- Wolf, A. FTP1 100, **WF2 1**
- Woo, Hyun-Jong **FTP1 71**
- Wu, Jong-Shinn XF2 7
- Wu, Men-Zan Bill XF2 7
- X**
- Xiao, Shu MWP1 97
- Xu, Lin **MWP1 81**
- Xu, Shuyan FTP1 14
- Y**
- Yagisawa, Takashi
FTP1 57, **WF3 6**
- Yamagata, Yukihiko
MWP1 98
- Yamakawa, Koji FTP1 18,
PR1 2
- Yamamoto, Hiroshi **XF1 1**
- Yamauchi, Tatsuya
FTP1 19
- Yamazawa, Yohei **XF2 5**
- Yan, Ke FTP1 35, SR1 6
- Yang, D. MWP1 89
- Yang, Yang **SR1 4**
- Yasserian, Kioumars
MWP1 28
- Yatsenko, Andrey **BT3 1**
- Yegorenkov, Vladimir
FTP1 39, FTP1 48
- Yeom, Geun Young GW2 4
- Yoshida, Kazuyuki
FTP1 24, MWP1 17
- Yoshida, Naofumi PR3 1
- Young, J.A. FTP1 95,
FTP1 96
- Yousif Azooz, Aasim
MWP1 29
- Yuan, Qingjun WF1 8
- Yuan, Wei FTP1 28
- Yuan, Xiaohui XF1 7
- Yui, Hiroharu PR3 6
- Yukishige, Akihiro
FTP1 35, SR1 6
- Yurushev, Nikolay GW3 6
- Z**
- Zagorodny, Anatoly
MWP1 75
- Zaidi, Sohail MWP1 94
- Zapukhlyak, Myroslav
PR2 3

Zatsarinny, Oleg **FTP1 89**,
LW2 1, LW2 3, LW2 6
Zdunek, Krzysztof **CT3 4**
Zhang, Shaofeng **FTP1 110**

Zhang, Zhili GW3 3
Zheltoukhin, Victor
FTP1 21, MWP1 32
Zheng, Jie FTP1 62

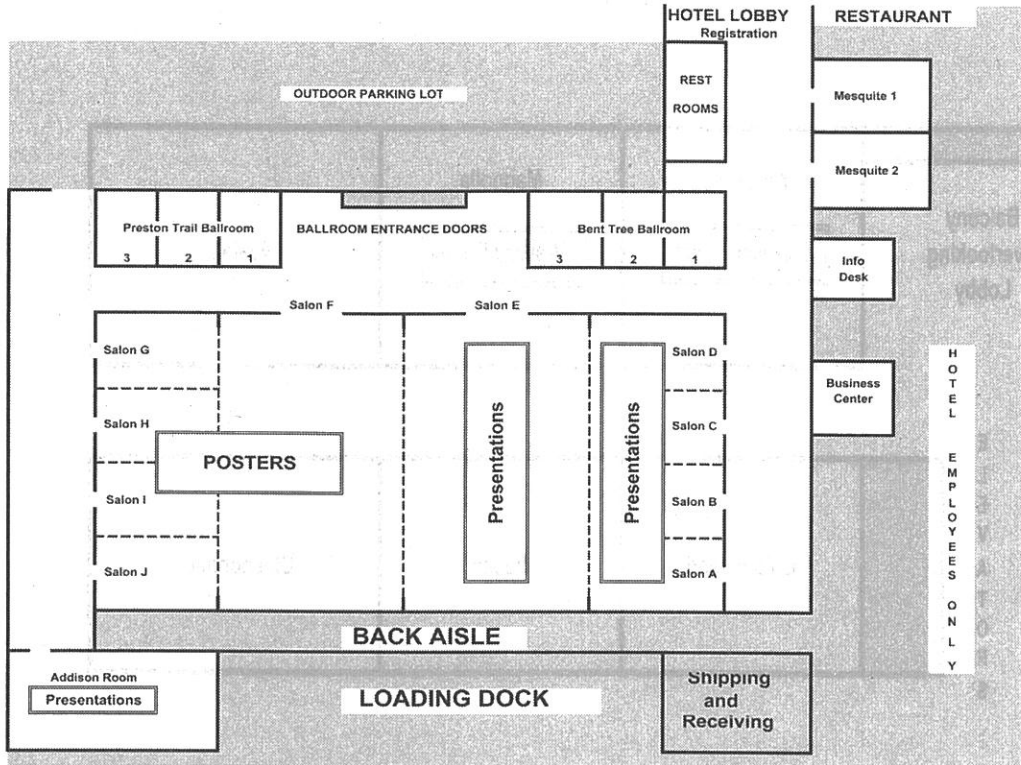
Zhmenyak, Yuriy FTP1 81,
MWP1 64
Zhou, Qingjun XF1 4
Zhou, Wei RR1 5

Zhou, Yifeng **XF1 4**
Zhu, WeiDong FTP1 67,
MWP1 100
Ziegler, Dennis **XF2 4**

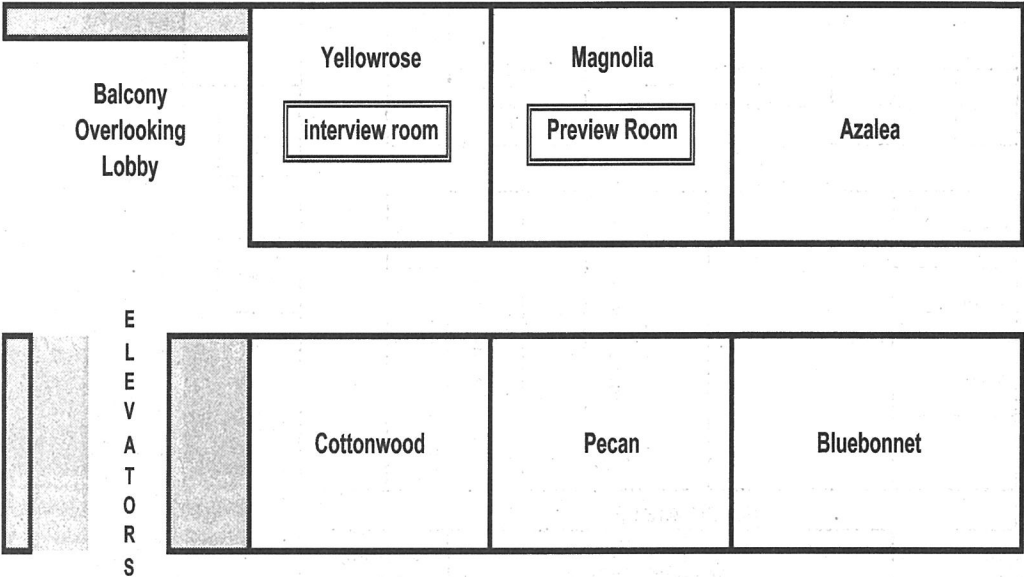
NOTES

Dallas-Addison Marriott Quorum by the Galleria

Dallas-Addison Marriott Quorum by the Galleria - Ground Level



Dallas-Addison Marriott Quorum by the Galleria
Mezzanine (2nd) Level



On the Cover: Pictures of CF₄ plasmas in the mGEC reactor at the University of Texas at Dallas for two different gaps between the ICP source (above) and the chuck (below). Photos courtesy of L. Overzet, M. Goeckner, E. Joseph and S. Sant.

Epitome of the 61st Gaseous Electronics Conference of the American Physical Society

19:00 MONDAY EVENING
13 OCTOBER 2008

AS Opening Reception
Poolside

8:00 TUESDAY MORNING
14 OCTOBER 2008

BT1 Collision Data For and From Plasma Applications
Timo Gans, Stuart Loch
Salon E

BT2 Plasma Aerodynamics and Propulsion I
Godfrey Mungal
Salon A-D

BT3 Dusty Plasmas
Addison Room

10:00 TUESDAY MORNING
14 OCTOBER 2008

CT1 Microhollow Cathode Discharges
Osamu Sakai
Salon E

CT2 Electron/Photon Interactions with Molecules
Thomas Rescigno, Stephen Buckman
Salon A-D

CT3 Magnetically-Enhanced and Related Plasmas
Jon T. Gudmundsson
Addison Room

13:30 TUESDAY AFTERNOON
14 OCTOBER 2008

DT1 Plasma-Surface Interactions
Gilles Cartry
Salon E

DT2 Biological and Emerging Applications of Plasma
Mounir Laroussi
Salon A-D

16:00 TUESDAY AFTERNOON
14 OCTOBER 2008

ET1 Dielectric Barrier Discharges and Displays
Salon E

ET2 Negative Ion Plasmas
R.N. Franklin, Allan J. Lichtenberg
Salon A-D

19:00 TUESDAY EVENING
14 OCTOBER 2008

FTP1 Poster Session I (19:00-21:30)
Salon F-J

8:00 WEDNESDAY MORNING
15 OCTOBER 2008

GW1 Plasma Aerodynamics and Propulsion II

Jean-Pierre Boeuf
Salon E

GW2 Charged Particle Surface Interactions
Richard E. Palmer, Uwe Thumm
Salon A-D

GW3 Lasers, Breakdowns and Sparks
Addison Room

10:00 WEDNESDAY MORNING
15 OCTOBER 2008

HW Allis Prize Lecture
Kenneth Kulander
Salon A-E

11:00 WEDNESDAY MORNING
15 OCTOBER 2008

JW Business Meeting
Salon A-E

12:00 WEDNESDAY NOON
15 OCTOBER 2008

KW General Committee Meeting
Bent Tree I-II

13:30 WEDNESDAY AFTERNOON
15 OCTOBER 2008 13:30

LW1 Plasma Diagnostics I
Salon E

LW2 Electron/Positron Atom Collisions
Oleg Zatsarinny
Salon A-D

16:00 WEDNESDAY AFTERNOON
15 OCTOBER 2008

MWP1 Poster Session II (16:00-18:30)
Salon F-J.

19:00 WEDNESDAY EVENING
15 OCTOBER 2008

NW Executive Committee Meeting
Bent Tree I-II

8:00 THURSDAY MORNING
16 OCTOBER 2008

PR1 Fluorocarbon Plasmas I
Kazuhiro Karahashi
Salon E

PR2 Ion Atom Collisions I
David Schultz, James Colgan
Salon A-D

PR3 High Pressure Discharges and Liquids
Addison Room

10:00 THURSDAY MORNING
16 OCTOBER 2008

QR1 Fluorocarbon Plasmas II
Tetsuya Tatsumi, Michael Gordon, Todd Madsen, Joseph Vegh
Salon E

QR2 Electron Impact Ionization of Atoms and Molecules
N.L.S. Martin, Azzedine Bennani

Salon A-D

QR3 High Pressure Glow Discharges
Paul Maguire
Addison Room

13:30 THURSDAY AFTERNOON
16 OCTOBER 2008

RR1 Material Processing I
Salon E

RR2 Lighting Plasmas
J.E. Lawler
Salon A-D

16:00 THURSDAY AFTERNOON
16 OCTOBER 2008

SR1 Inductively and Capacitively Coupled Plasmas
Salon E

SR2 Ion Atom/Molecule Collisions II
Daniel Fischer
Salon A-D

19:00 THURSDAY EVENING
16 OCTOBER 2008

TR Banquet
R. Heelis
Salon A-E

8:00 FRIDAY MORNING
17 OCTOBER 2008

VF1 Glows
Caizhong Tian
Salon E

VF2 Electron and Ion Transport in Gases
Salon A-D

VF3 Plasma Boundaries
Addison Room

10:00 FRIDAY MORNING
17 OCTOBER 2008

WF1 Plasma Diagnostics II
Salon E

WF2 Recombination and Attachment
Andreas Wolf
Salon A-D

WF3 Computational Methods for Plasmas
Ikuo Sawada, Shahid Rauf
Addison Room

13:30 FRIDAY AFTERNOON
17 OCTOBER 2008

XF1 Material Processing II
Salon E

XF2 Capacitively-Coupled Plasmas
Thomas Mussenbrock
Salon A-D



0003-0503(200810)53:10;1-Q